M.D. Klomp

Hybrid interaction of timber decks in movable bridges

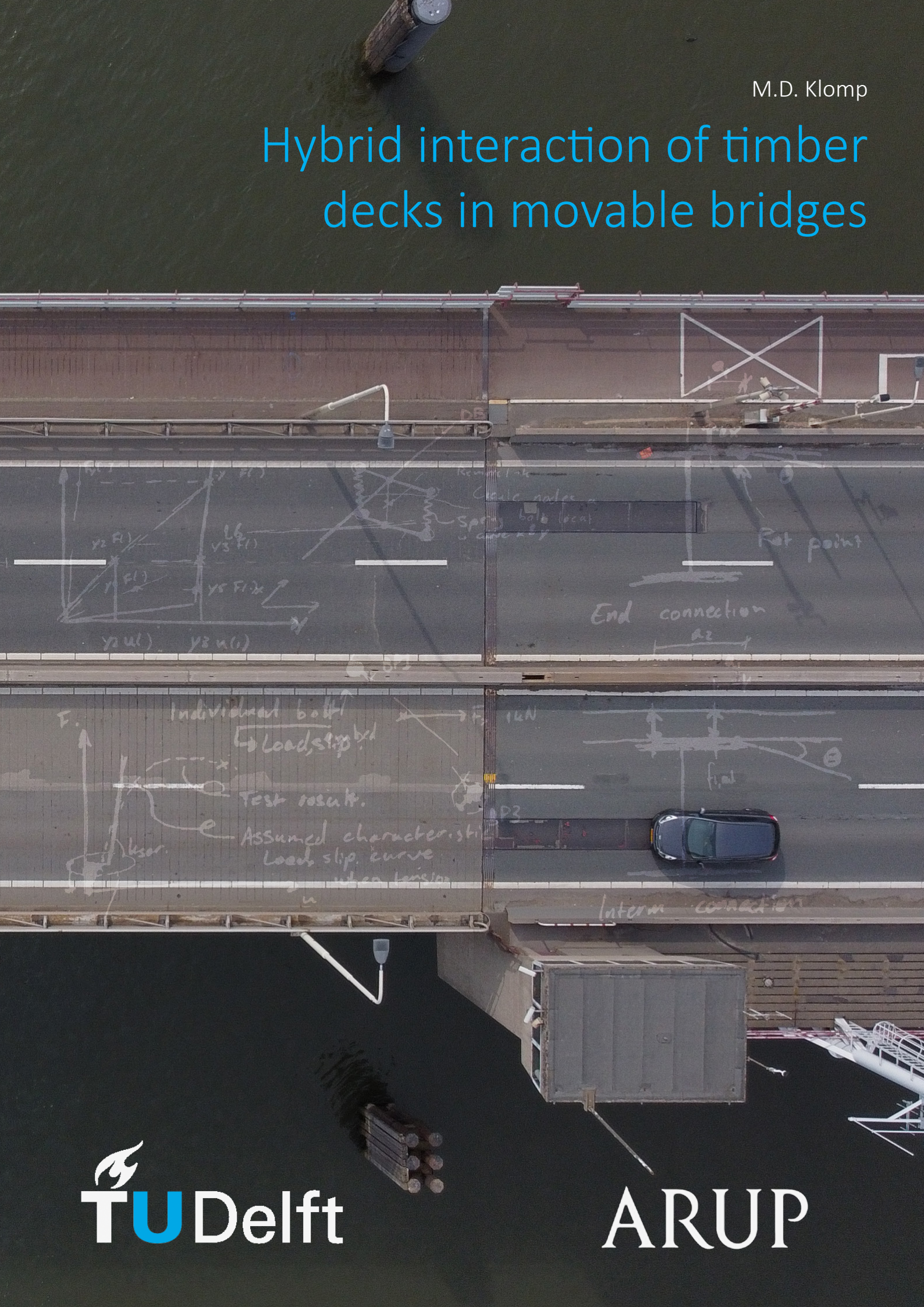

TU Delft

ARUP

Hybrid interaction of timber decks in movable bridges

by

Maureen Danique Klomp

To obtain the degree of Master of Science in Structural Engineering
at Delft University of Technology,
to be defended publicly on Thursday July 23rd, 2020 at 9:15.

Student number:	4371453
Project duration:	October 16, 2019 – July 23, 2020

Assessment Committee

Chairman:	Prof. dr. ir. J.W.G. Van De Kuilen,	Biobased Structures and Materials (TU Delft)
Daily supervisors:	Dr. M. Pavlovic,	Steel and Composite Structures (TU Delft)
	Dr. ir. G.J.P. Ravenshorst,	Biobased Structures and Materials (TU Delft)
	Ir. J.M. Houben,	Pavement Engineering (TU Delft)
	Ir. S. Joosten,	Senior Bridge Engineer (Arup)

TU Delft Delft University of Technology

Voor Lyn

Preface

This thesis report marks the end of my career as a student at TU Delft, but will also mark the start of my career as a structural engineer.

Before starting my thesis, what I knew about my topic was, it should be focused on engineering practice. I ended up researching timber decks in movable bridges, because of the current challenges that are faced in that regard. To do this, I was able to team up with Arup in the Amsterdam office. The relation between my topic and the current project on movable bridges, made it interesting and relevant to research.

For my master thesis research, I was able to rely on the help of my assessment committee. The diversity in expertise and view is something a have valued throughout my thesis. I would like to thank Jan-Willem van de Kuilen for being the chairman of my committee and his critical remarks regarding the combination of structural mechanics and timber in my research. Together with Geert Ravenshorst, my assumptions on timber properties, could become more specific. I am grateful to both of them for providing useful criticism during progress- and individual meetings.
Furthermore, I would like to thank Marko Pavlovic for his feedback on modelling and expertise on steel bridges. His remarks did not only help my research content, but skills on presentation as well.
I'd like to acknowledge the assistance of Lambert Houben for his administrative support throughout my research.
I am extremely grateful to Stijn Joosten as my daily supervisor at Arup. I would like to thank him for being my mentor during this thesis period and always being critical on my work. Being able to rely on the experience in bridge engineering of my supervisor, was a major help throughout this research project.

I also want to make a shout-out to all my colleagues at Arup. During my time as a graduate intern, I was able to develop various skills and had all the resources needed to successfully finish my thesis project. But more importantly, I was always able to ask for help within the team, felt part of the infrastructure group and appreciated their remarks and criticism to help me improve myself.

I would like to acknowledge some people who have especially helped my research. Fruzsina Csillag for keeping up with my questions on Finite Element modelling, Laetitia

Koning on discussing project specific and timber subjects and Mike, Tessa, Jan, Katinka and all others for their support on my thesis progress. Furthermore I would like to thank Roel Vernooij and Janwillem Breider for their help in scripting and modelling.

In six years as a student, I have not only obtained knowledge on civil engineering courses. Experiencing to cooperate, manage, plan tasks and improving soft skills in study associations, will help me in my future career. Therefore I am especially grateful to everyone at U-BASE and I would like to extend my special gratitude to Geert, Jose, Michelle, Knut and Lisa for their loyal support and friendship.

In the end, none of this would have been possible without the help of my friends, roommates and family. I want to extend my deepest gratitude to my parents for enabling me to graduate and always supporting me at everything.

Maureen Danique Klomp
Rotterdam, June 2020

Abstract

Highway traffic bridges have been subjected to increasing loads over the past decades. Some of the movable bridge leafs in these highway bridges were constructed in the 1960s and they are now close to the end of their intended life span. These bridge leafs were typically designed and executed with hardwood deck boards. In the initial design calculations, traffic loads were smaller, complex calculation by computer models did not yet exist. Therefore, some phenomena like for example fatigue and global hybrid interaction were never considered.

Since some movable highway bridges are now due to be re-assessed, there is a growing need to gain knowledge on the way timber decks are functioning within the movable bridge leaf. These bridge decks have sustained all loads throughout the years without significant damage, but we don't know whether these timber deck boards help the main load bearing steel structure as well. Or in other words; do the timber deck boards interact with the steel girders in the current situation?

In this research, the degree of hybrid interaction was measured in terms of the magnitude of the main girder deflection for the reference case of the Bridge across the Beneden Merwede. The main girder deflection for bolted connections, having a certain free slip and embedding stiffness, was determined by running a linear sequential secant stiffness analysis. This analysis approximates a physically non-linear analysis.

The maximum deflection of the main girder was compared to the maximum main girder deflections for no hybrid interaction versus full hybrid interaction.

The resulting global deflections from the Secant Stiffness Analysis have shown that practically no hybrid interaction can be found between the current deck and the steel structure. For retrofitting options, the level of hybrid interaction can be significant. An increasing or decreasing degree of hybrid interaction did not only change the forces and moments in the steel girders, but also had a considerable effect on the deck and its connections. There is a gain and a loss for every retrofitting option considered. Decision-making for retrofitting timber bridge decks should take multiple contradicting criteria into account. An optimisation could be necessary in order to take a well-advised decision.

Contents

Nomenclature

α_v	Factor for bolt class and shear plane location
γ_{M2}	Partial safety factor for bolt resistance
γ_M	Material imperfection factor
ρ_k	Characteristic value of the density (5th percentile)
ρ_{mean}	Mean value for the density
θ	Stochastic variable for u_{slip}, uniformly distributed
A_{eff}	Effective shear area of the deck beam
A_k	Effective shear area of the longitudinal girder
A_s	Bolt area at bolt thread
d	Diameter of the fastener
$E_{m,0,k}$	Characteristic value of the modulus of elasticity (5th percentile)
$E_{m,0,mean}$	Mean value for modulus of elasticity parallel to grain
$E_{m,90,mean}$	Mean value for the modulus of elasticity perpendicular to grain
$F_{ax,Rk}$	Withdrawal capacity of metal fastener
$f_{c,0,k}$	Characteristic compressive strength parallel to grain
$f_{c,90,k}$	Characteristic compressive strength perpendicular to grain
$f_{h,\alpha,k}$	Embedment strength at an angle α to the grain
$f_{h,k}$	Embedment strength
$f_{m,k}$	Characteristic bending strength
$f_{t,0,k}$	Characteristic tensile strength parallel to grain
$f_{t,90,k}$	Characteristic tensile strength perpendicular to grain

NOMENCLATURE

$F_{t,Rd}$	Tensile resistance of the bolt (design value)
f_{ub}	Ultimate tensile strength of the bolt (characteristic value)
$f_{v,k}$	Characteristic shear strength
$F_{v,Rd}$	Shear resistance of the bolt (design value)
$F_{v,Rk}$	Characteristic resistance per shear plane per fastener
f_{yb}	Yield strength of the bolt (characteristic value)
G	Shear modulus of the deck beam
G_k	Shear modulus of the longitudinal girder
G_{mean}	Mean value for the shear modulus
k_2	Factor for bolt head types
k_{90}	Correction factor for determining embedment strength at an angle α with the grain
k_{def}	Factor for creep and climate class
k_{eq}	Equivalent spring stiffness
K_{mod}	Modification factor for load duration and moisture content
$K_{r,ser}$	Rotational stiffness of a joint with n dowel-type fasteners
$K_{ser,fin}$	Final slip modulus
K_{ser}	Slip modulus
k_{sh}	Shear stiffness of the longitudinal girders
K_{slip}	Stiffness (close to zero) while connection is freely slipping (no friction or embedding)
K_u	Slip modulus ULS
L_k	Center-to-center distance of the cross girders
$M_{y,Rk}$	Characteristic value yield moment of metal fastener
R	Stochastic variable for u_{slip}, Weibull distributed
R_d	Design value for resistance property
r_j	Distance from rotation point to fastener
R_k	Characteristic value for resistance property
t_1	Thickness of the timber plate in failure mode calculations
u_{slip}	Assumed free slip value in load-, displacement curve

Definitions

To improve understanding of certain processes within the structural system, some coordinate system directions, schematic notations for support types and a list of terms and concepts are specified here with a short explanation.

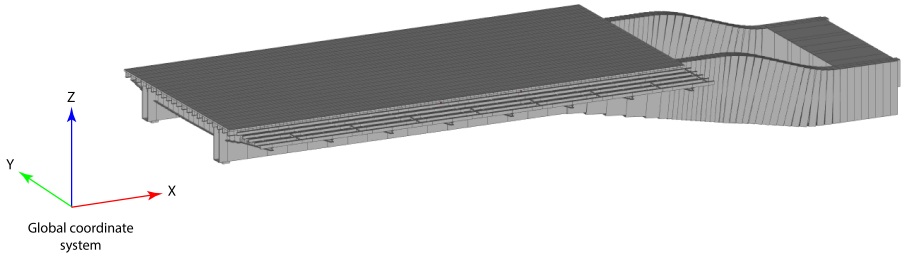

Figure 1: Global coordinate system of a movable bridge leaf

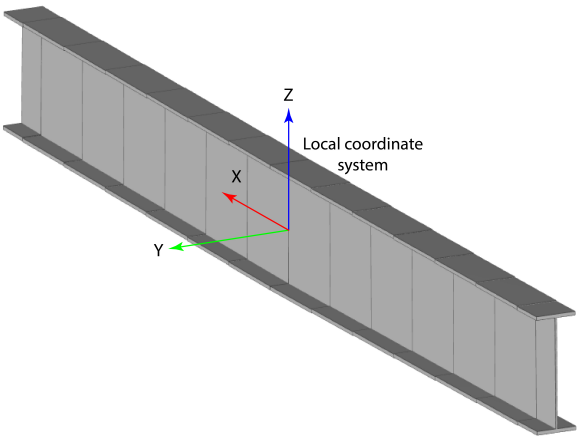

Figure 2: Example of a local coordinate system of an element, where the x-direction is always in the same direction as the longitudinal direction of the beam or spring element. Link elements are consistent with the global coordinate system.

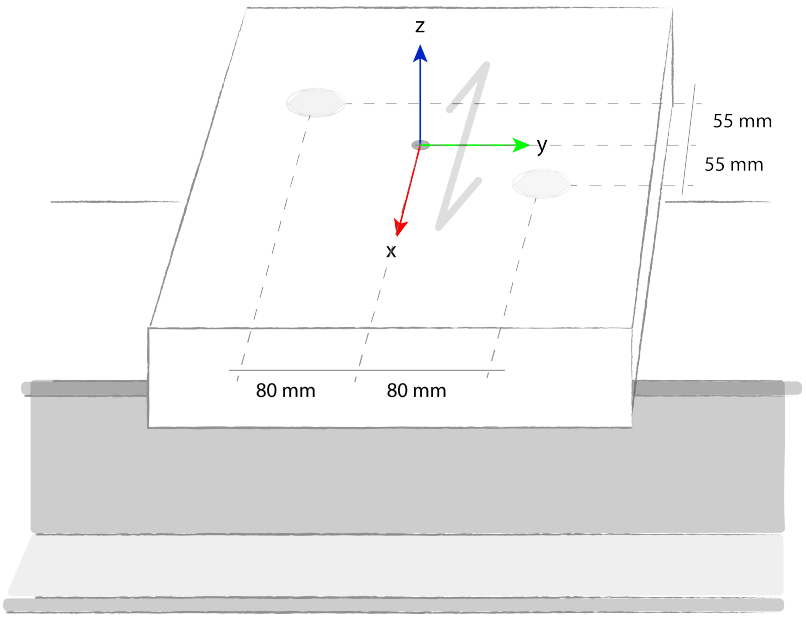

Figure 3: Local coordinate system of a deck joint including the grain angle direction

Symbols in plan view for supports

Symbol in plan view	x	y	
⬡	△	△	Pinned connection, all translational degrees of freedom restricted
◀⊕▶	△		Connection released in one direction and all rotations
⊕		△	Connection released in in-plane translational directions, only restrained in vertical (out-of-plane) direction

Table 1: Symbols in plan view for bearings in Eurocode 1337 [1]

List of terms and concepts

Back end	Part of the bridge leaf near the rotation point
Back post	(or: "achterhar") Bracing elements to provide support at cantilevering part of the bridge deck at the cross girder near the rotation point
BBM	Bridge across the Beneden Merwede

BP	Back Post
BR	Deck bracing
CG	Cross girders
CW	Counterweight
DB	Deck boards
Ekki	Same timber species as Azobé
End joints	Joints at both longitudinal ends of a timber deck board
FE	Finite Element
FEM	Finite Element Model
Front end	Part of the bridge leaf where the deck lifts off the supports when opening
Front post	(or: "voorhar") Bracing elements to provide support at cantilevering part of the bridge deck at the first cross girder (furthest from the counterweight)
Intermediate joints	All deck joints between deck board end joints
LG	Longitudinal girders
MG	Main girders
RBK	Richtlijnen Beoordeling Kunstwerken
Renovation	Strengthening certain structural elements within the bridge leaf (could also mean replacing certain elements within the bridge leaf)
Replacement	The full replacement of the bridge leaf
SG	Support girder
Slip modulus K_{ser}	Stiffness of dowel in timber while embedding

Part I
Introduction

Chapter 1

Introduction

Most often, highway bridges have been constructed in the 1960s, which means certain elements in the bridge are now, 50 years later, at the end of their intended life span. Replacing or renovating bridges is a common challenge nowadays in the Netherlands since traffic loads are ever increasing due to more traffic and heavier trucks.

Arup is currently assessing several movable bridge leafs on safety and serviceability, among which the movable part of the van Brienenoord bridge (2 movable parts), the Volkerak bridges (2 movable parts) and the Beneden Merwede bridge (1 movable part) on safety and serviceability. Assessments will include calculations to determine the most optimal solution in all bridge cases: renovation or replacement.

Here, the term 'replacement' is used to indicate the full replacement of the leaf and 'renovation' means strengthening of the structure. 'Renovation' can include replacing certain elements of the structure.

Currently, timber decks in movable bridges are assumed to offer no contribution to the main structure in the form of composite action, but they possibly do have an influence on its structural behaviour. Research into this topic is limited, but gaining this knowledge could prove useful to several (movable) bridges that are currently being assessed.

This chapter will start by defining the problem and relevance of this research. Hereafter, the research objectives and method will be discussed.

1.1 Problem statement

In the 1960s and 1970s, many of the current Dutch bridges have been constructed. The result is a major challenge in renovation- and replacement projects for now and the upcoming years. Some of these (movable) bridges have a timber bridge deck. These decks often experience issues like those that are mentioned in section 2.2. The current timber decks are assumed to offer no contribution to composite action. One of the main challenges for the use of timber decks, is that most of the hardwood properties are unknown or hard to determine.

The main problem with these timber decks right now is; uncertainty. Uncertainty which strength and stiffness parameters are valid to use, since tests and the Eurocode often differ.

Uncertainty regarding the possible decrease in structural performance of the hardwood and its connections over time (due to cyclic loading, environmental influences, etc.). So by having used these decks in infrastructure over decades, it can be concluded that they are still functional, but we don't exactly know how they work. Especially, how the timber decks interact with the steel girders below.

Researching the current hybrid interaction of the deck, can increase knowledge about the composite action of the deck in these types of bridges. It can help to make a more accurate assessment of the current structural behaviour in main elements and it can possibly help to propose an alternative to replace the current deck.
Increasing the knowledge on timber decks and its connections creates a better understanding of the level of hybrid interaction between the deck and the steel structure. This helps to more accurately estimate the change in current forces and moments in the cross- sections due to the presence of a timber deck.
This knowledge could change the decision-making regarding renovation or replacement of certain structural elements.

1.2 Relevance

So why is it important to gain this knowledge on timber decks? First of all, it is essential for the verification of the current structure to state whether the deck is still safe and whether it interacts with the steel structure. This could namely cause steel girders to be stressed less, while the deck and its connectors would have to sustain extra forces. Therefore, the obtained knowledge can cause a demand for the deck to be modelled differently, than is currently being done, since the distributions of forces is possibly different than we are assuming now. Thirdly, knowledge on the current hybrid interaction can support statements regarding future retrofitting solutions for (bascule) bridge decks.

In short, an increase of knowledge on (the hybrid interaction of) timber decks can influence:

- Current strength verifications of steel and timber elements
- Current modelling methods of the bridge deck and its connections
- Future decision making about retrofitting options for bridge decks

1.3 Objectives

The main objective of this research is...

"... to gain a better understanding of the hybrid interaction between timber decks and steel girders in a movable bridge leaf."

Improving knowledge of hybrid interaction between the timber deck and main steel structure, could possibly alter the verification results of different structural elements (i.e. the main girders, cross girders, longitudinal girders and the deck boards) of movable bascule bridge leafs built in the 1960s, when hybrid interaction is taken into account.

Additional to the main objective, the distribution of forces depending on the degree of hybrid interaction of the deck, will be investigated.

The degree of hybrid interaction will be measured by observing global deflection results in case of a load-, slip curve that is assigned to the deck connections. The theoretical background to the degree of hybrid interaction is given later in chapter 9.

1.3.1 Research questions

The deck- to- girder connection and the deck board type are expected to be the most influential factors for determining the degree of hybrid interaction between deck and girders.

To achieve the objectives stated before, some research questions have been established:

1. What is the typical load-, displacement behaviour of a timber deck- to- steel girder joint?
2. Comparing full hybrid interaction to no hybrid interaction, what are the positive and negative effects to the structural elements and the bridge leaf as a whole?
3. How do the assumed embedment and slip parameters influence the obtained degree of hybrid interaction of a bridge leaf?
4. How does the obtained degree of hybrid interaction relate to the maximum local shear forces in deck- to- girder connections?

Recommendations can be made regarding future designs of bridge decks in movable bridges. The additional question is:

- What can be recommended regarding retrofitting solutions of timber bridge decks considering the degree of hybrid interaction?

1.4 Method

In this research, the current degree of hybrid interaction of the deck will be researched. This will be done by reviewing the reference case of the Bridge across the Beneden Merwede (BBM). The non-linear behaviour of the deck connections and the deck board types are assumed to have the largest influence on the interaction of the deck with the steel structure. The load-, slip behavior of individual bolted connections and eventually a bolt group, is reviewed by a literature research and the relevant stiffness directions of the deck connections are found by analyzing the BBM beam model.
The non-linear load-, slip curves of connections are implemented in a FE model of the reference case. Due to the large number of elements in the bridge, a non-linear FE analysis is currently not possible. The alternative method to run a non-linear analysis linearly is the Secant Stiffness Method (SSM). The details of this method will be discussed in chapter 11, but the method is basically creating a secant stiffness for a previous result that is projected onto the assumed load-, displacement curves. The model that was used, is created in GSA and is analyzed through an API in python.

The global workflow of the API used for the Secant Stiffness Method is given in figure 1.1.

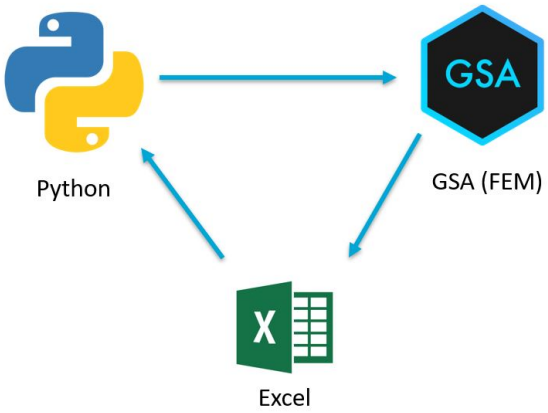

Figure 1.1: Workflow API used for SSM

To answer the first research question, a literature study has been done to the load-, slip behaviour of single-bolted connections from timber to steel. Hereafter, the bolt group behavior is determined by using the displacement method regarding the timber as a rigid body connected by springs. The result is a stiffness matrix that describes the theoretical relation between forces and moments versus displacements and rotations in a double-bolted connection.

Research questions 2 and 3 can be answered by reviewing the distributions of forces and moments when subjecting the structure to certain heavy load cases in a FE analysis. To compare the cases of full hybrid interaction and no hybrid interaction, the model is adapted and the influence of restraining deck joints in the relevant directions and applying a monolithic plate, are visible in the element results.

Research questions 4 and 5 can be answered by reviewing the results from the Secant Stiffness analysis using the load-, displacement curves for the deck connectors. Altering the main parameters of these load-, slip curves can highlight the possible spread in results for different assumptions.

1.5 Outline

This thesis report consists of 6 parts:

- Part I: Introduction
- Part II: Bolted steel- to- timber connections
- Part III: Loads and interaction
- Part IV: Analysis
- Part V: Results
- Part VI: Conclusions and recommendations

Part I offers an introduction into the research topic, the method used and the reference case that is being considered.

The literature review on connections and short study into the different relevant directions of deck joints, is given in part II.
The considered load cases and response of the bridge leaf structure to these loads locally and globally, are given in part III.
Part IV and part V respectively discuss the Secant Stiffness analysis and the results of the analysis.
The report is concluded by part VI, specifying conclusions and recommendations.

Chapter 2

Reference case

This thesis will focus on timber bridge decks in movable bridges. Movable highway bridges from the 1960s typically consist of main girders, cross girders, bracing elements, longitudinal girders and a timber bridge deck. Figure 2.1 shows these structural elements respectively from bottom to top. One of the challenges when designing a suitable bridge deck, is having a lightweight structure with sufficient strength and stability for intense road traffic. In the past, designers often chose a timber deck. These decks have certain advantages like fatigue resistance or sustainability and disadvantages such as water tightness or limited shear capacity. A movable bridge deck has to be lightweight to balance with the counterweight, driving mechanism and substructure.

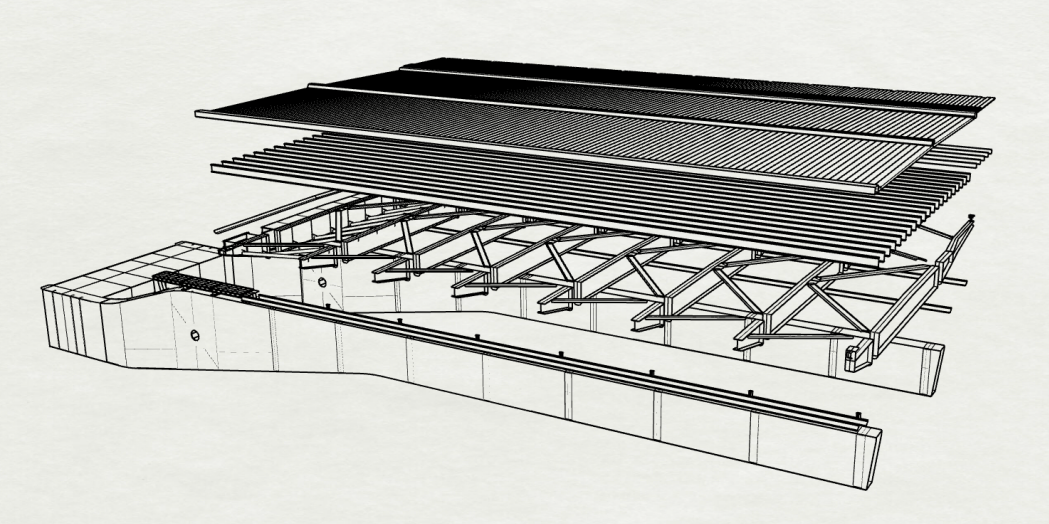

Figure 2.1: Structural element layers in a movable bridge leaf with a timber deck

In current movable bridge renovation projects, some problems like fatigue cracks in welded joints or weak axis bending in the steel girders, are observed. For some bridges, these problems are combined with other problems like corrosion due to contact with water and lack of inspection or maintenance. The bridge across the Beneden Merwede is one of these typical bridges and will be used as a case for this research.

2.1 About the bridge across the Beneden Merwede

The Beneden Merwede Bridge (BBM) opened in 1967 and in the 1970s, the bridge has been widened. The span of the movable part is 33,4 m and the width of the bridge is 20,27 m. The main load bearing structure consists of two hollow-section main girders with a spacing of 10,5 m and eight cross girders, having an intermediate distance of 4,4 m. On top of these girders, longitudinal girders are positioned at a 0,75 m distance of each other. All girders are made of structural steel. The current azobé deck forms the top layer with a 110 mm thickness.

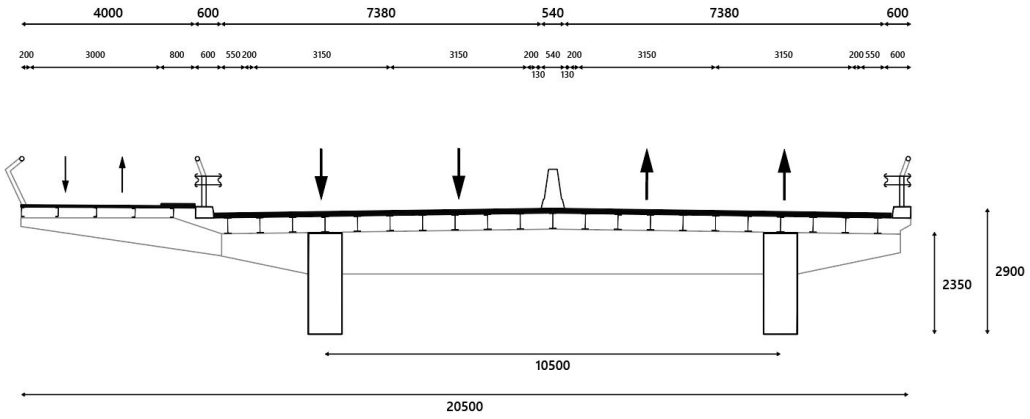

Figure 2.2: Transverse cross section of the Beneden Merwede Bridge including current traffic directions and dimensions

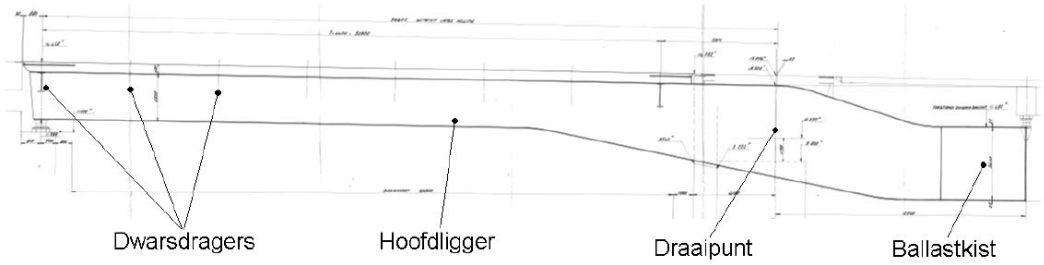

Figure 2.3: Original drawing of longitudinal cross section bascule bridge leaf Beneden Merwede Bridge

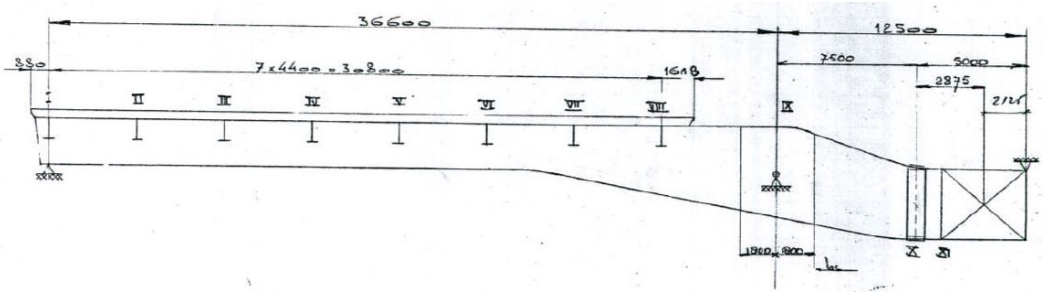

Figure 2.4: Definition of cross-girders in longitudinal direction

The schematic drawings of the cross sections (figures 2.2, 2.3 and 2.4) illustrate the components in the bridge leaf.

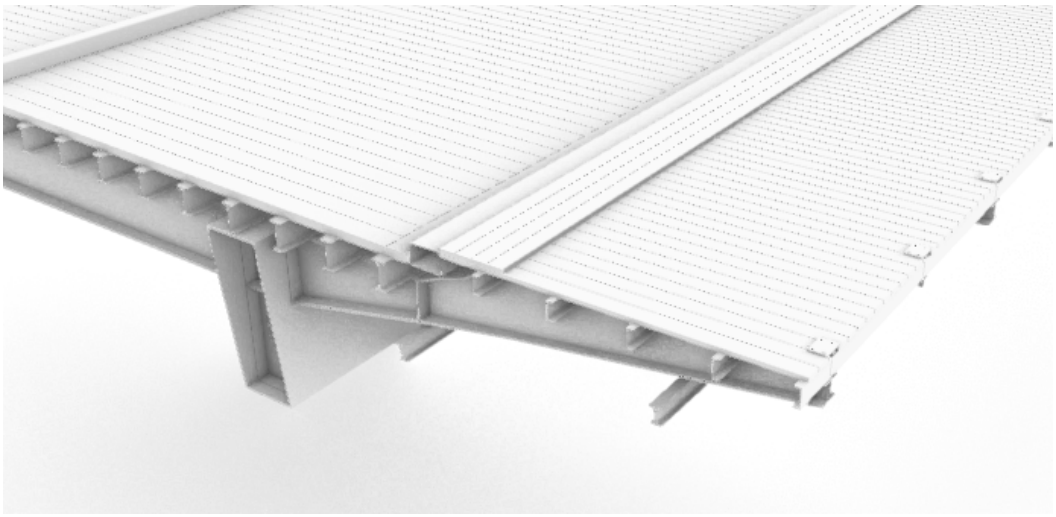

Figure 2.5: Close-up of a connection in the rendered model of the bridge leaf

Figure 2.5 shows a render of the bridge at the first cross girder to give an example of the connection between some of the girders and the extension that has been made to the cross girders for the bicycle lane.

The bridge is supported for the closed situation on both ends of the leaf at the main girder. Figure 2.6 shows a top view and front view of the supports for a closed situation of the bridge considering live loads.

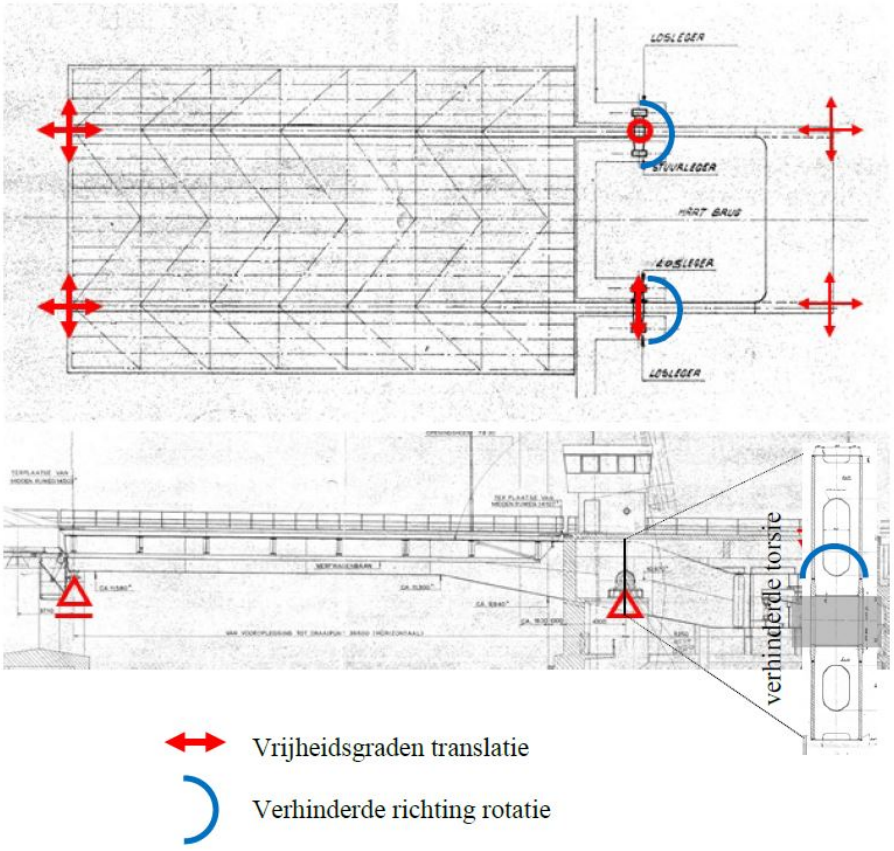

Figure 2.6: Supports of the bridge leaf in top- and front view for the closed situation in case of live loads

The technical drawing for the detail of the bolted deck-to-girder connection is shown in figure 2.7. Actual geometry of these connections (like the bolt clearance, geometry of the deck board or the position of the bolt) could deviate due to degradation, water intrusion or geometrical imperfection during production or execution.

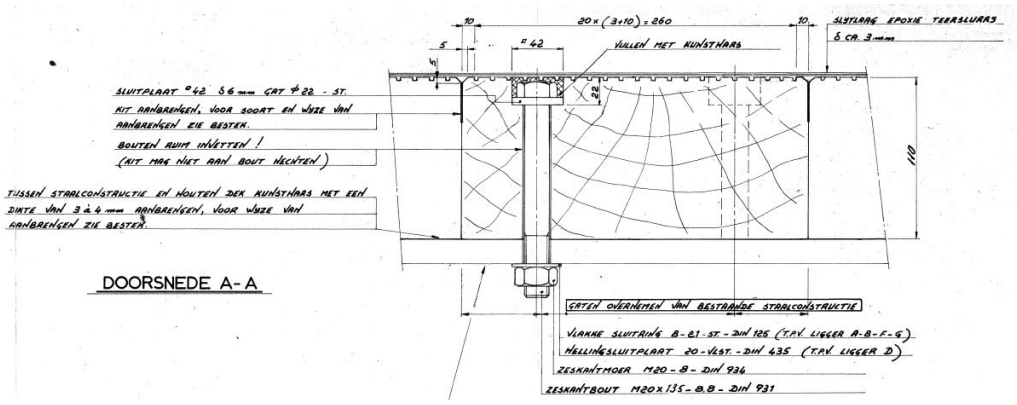

Figure 2.7: Geometry of the bolted deck- to- girder connection

The configuration of the deck boards in a top view is given in figure 2.8. Each deck board is connected by two bolts to a longitudinal girder on each side of its flanges. Every deck board is 3750 mm long and is connected to a longitudinal girder 6 times (so: every 750 mm).

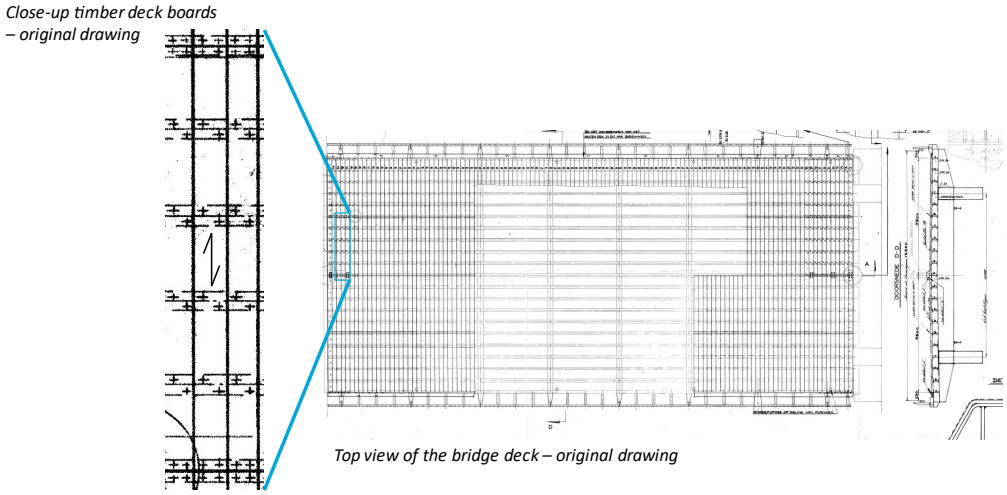

Figure 2.8: Top view deck boards in the BBM

2.1.1 Design verification

Previously, the method of verification of the bridge leaf structure was calculating from top to bottom. Loads were applied to the deck, distributed further to the longitudinal girders and so on. Hand calculations were sufficient, to distribute the forces and bending moments, directly from one girder to the one below. Fatigue calculations were not made. Generally, initial designs did not accurately account for complex calculations like fatigue and weak axis bending in steel girders.
Current verifications by engineering firms account for more complex calculations, allowed by computational modelling. The conventional method of assessment does not include

modelling the deck, but it can be done when considering the load spread. The deck will then only be connected in vertical direction, so the degrees of freedom are conservatively assumed.

In the 1960s, when this bridge was designed, traffic loads were far lower than nowadays. Previous verification of the deck board strength (section A.1) is quite similar to the current verification (section A.2). However, the shear strength unity check is satisfied for the verification by RWS (1960s) and is not satisfied in the current verification of the deck. Not only a different load had to be applied according to Eurocode, but partial safety factors have also been altered. Besides that, the method of calculating the acting bending moment and shear load is different.

So, if the shear strength capacity is exceeded according to these calculations, why didn't the deck fail already? This is because several safety factors have been taken into account. Additionally, the actual shear strength and the one given by the Eurocode differ significantly as will be discussed in chapter 3.

2.1.2 Current state of deck structure

After more than 50 years of usage, some of the steel components show signs of corrosion and the Azobé bridge deck is degrading at some parts of its surface. The timber has also been painted at the bottom, which is a poor choice. This way, water cannot escape the wood at the bottom and the timber will deteriorate in effect.

(a) Bottom side of the bascule leaf, showing the degradation of the steel and timber elements

(b) Detail of deck- to- longitudinal girder connection in its current state

Figure 2.9

All of the approximately 5000 bolts connecting the traffic deck and the longitudinal girders, have to be re-tightened annually. The bolts near the main girder (and the heaviest loaded lane) untighten most as an effect of cyclic loading. In case of bolt damage or pull-through of the bolt through the timber, respectively the bolts and/or timber deck boards should be replaced. It is unknown whether such replacements were made in this bridge.

2.2 Timber deck issues and requirements

The possibility of transverse shear failure in the deck boards is one of the problems of the deck according to verification results, but according to various researches, this should not be an immediate concern (see section 3.1). Other current problems are untightening of the

bolts, possible increase in clearances (holes and between deck boards), large weak axis bending in the steel girders, corrosion of the longitudinal girders and an undetermined degree of timber degradation over time. Figure 2.10 presents an overview of some of the problems, its consequences and thus the motivation for retrofitting the current deck.

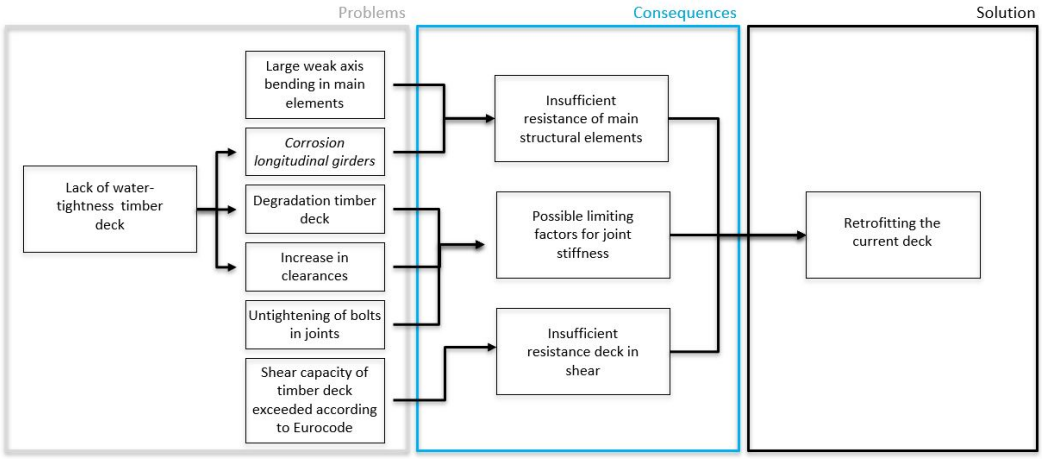

Figure 2.10: Motivation for retrofitting

Additional lifetime depends on the decision on replacement or renovation. For replacement, the additional lifetime will be 100 years, whereas renovation designs are commonly made for a lifespan of 30 years.

Azobé bridge decks have initially been chosen for its lightweight and high strength (in grain direction) properties. Timber is also sustainable and has a high resistance against fatigue compared to steel.

A bascule bridge deck has to satisfy certain requirements:

ULS:

- Unity check shear strength (τ)
- Unity check bending stresses (σ_m)
- Unity check combined bending and shear

SLS:

- In-plane deformations due to thermal expansion
- Deflection

Additional requirements:

- Lightweight ($\leq 181 kg/m^2$ including the longitudinal girders for BBM)
- Fatigue
- Durability
- Sustainability

- Deck wearing layer (friction)
- Watertightness
- Connectability

Chapter 3

Material properties

This chapter describes the material properties for the different structural elements in the bridge leaf. In figure 3.1 an exploded view is given of the different elements with their respective materials. The first section of this chapter will elaborate on the different mechanical properties for the timber deck and hereafter the properties for the steel bolts to connect them, will be discussed.

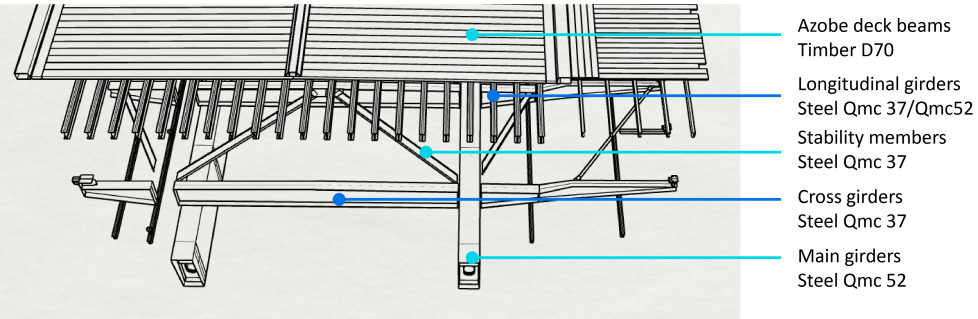

Figure 3.1: Exploded view illustrating the different types of materials in the movable bridge leaf

3.1 Deck boards

Azobé (Lophira alata) is a well-used material in structural applications in the Netherlands as lock doors, mooring posts or bridge decks. It has a high resistance against fungi (Class 1) and resistance to insects (Class D) (NEN-EN 350) [2]. Both the durability and sustainability of Azobé are an advantage to use it as a structural material (provided that sustainable forest management is guaranteed).

Material strength
The actual strength of timber species is generally defined by their origin location, moisture content and growth effects like knot ratio or grain angle [3].

$$R_d = k_{mod}\frac{R_k}{\gamma_M} \tag{3.1}$$

K_{mod} is the modification factor for load duration and moisture content and γ_M is the material imperfection factor [4]. Imperfection factor γ_M will be equal to 1,3 for both connections and sawn timber applications.

The knot ratio can also have an influence on the strength of a timber species, but in the case of Azobé, "knots are virtually non-existent, and the failure mode is generally based on grain deviation" (van de Kuilen, J. W. G., & Blass, H. J. (2004) [5]).

According to NEN-EN 1912 [6], Azobé as a species, is determined to be in strength class D70. Subsequently, NEN-EN 338 [7] specifies the corresponding properties like density, modulus of elasticity, shear strength and compressive- or tensile strength in parallel and transverse direction. Relevant material information is given in Table 3.1.

Material properties $[N/mm^2]$	**Bending strength** $(f_{m,k})$	**Tension parallel** $(f_{t,0,k})$	**Tension perp.** $(f_{t,90,k})$	**Compr. parallel** $(f_{c,0,k})$	**Compr. perp.** $(f_{c,90,k})$	**Shear strength** $(f_{v,k})$
Azobé (D70)	70	42	0,6	36	12,0	5,0

Table 3.1: Strength properties of Azobé (D70) according to NEN-EN 338.

A note has to be added to the shear strength $(f_{v,k})$ given by current regulations. Various researches [8] [9] have established a lower value for shear strength compared to the Eurocode through testing and subsequently, linear regression. NEN-EN 384 [10] states that the shear capacity of timber depends on its characteristic bending strength (equation 3.2).

$$f_{v,k} = min \begin{cases} 3.0 + 0.03 f_{m,k} \\ 5.0 \end{cases} \tag{3.2}$$

The shear capacity of 5 MPa in the Eurocode is based on the upper bound for softwood species and not on tests performed on hardwood species.
The shear capacity of hardwood species like Azobé is significantly larger in tests (and in reality) than the Eurocode values. This means that a ULS verification can result in unity check values well over 1, while in reality, the utilization ratio is much lower [8].

Species	spruce A	spruce B	azobé	massa-randuba	bilinga	oak	ash	beech
N	11	26	20	44	26	24	73	85
Characteristic shear strength $f_{v,k}$ (N/mm^2)	4.5	3.7	15.7	9.6	9.4	7.5	9.4	10.7
Characteristic density ρ_k (kg/m^3)	371	324	1022	948	719	654	553	650
Ratio ρ_k / $f_{v,k}$	82	87	65	100	76	87	59	61

Figure 3.2: Shear strength test results for different timber species [8].

Class	D18	D24	D27	D30	D35	D40	D45	D50	D55	D60	D65	D70	D75	D80
ρ_k	475	485	510	530	540	550	580	620	660	700	750	800	850	900
f_v EN-338	3.5	3.7	3.8	3.9	4.1	4.2	4.4	4.5	4.7	4.8	5	5	5	5
f_v-proposed	5.5	5.6	5.9	6.1	6.2	6.4	6.7	7.1	7.5	7.9	8.3	8.8	9.2	9.6

Figure 3.3: Current and proposed shear strength values for Eurocode EN-338 [8].

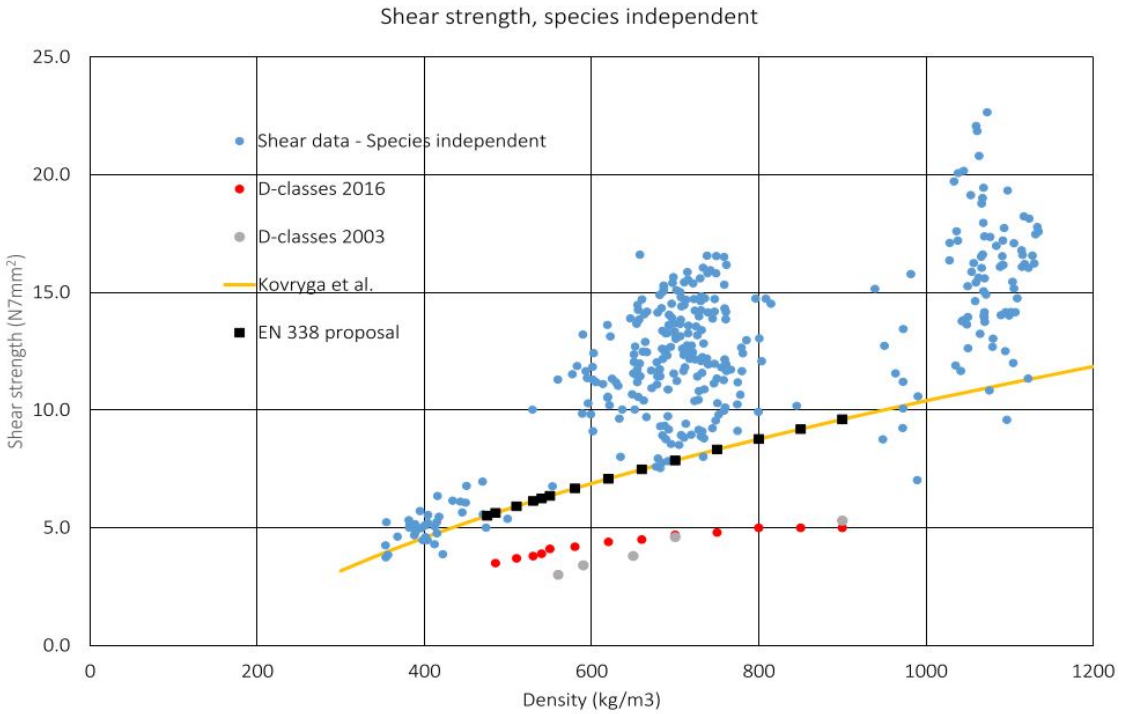

Figure 3.4: Graph showing current Eurocode values, tested values and proposed shear values for hardwoods in general [8].

Figure 3.2 shows the shear strength test results for different timber species. Azobé, in this case has a tested characteristic strength of 15.7 MPa, which is more than three times as large as the shear strength of 5 MPa given by the Eurocode [7] (figure 3.3). The graph in figure 3.4 visualizes the differences between the shear test data (independent of the species), the proposed values from testing and the current values stated by the Eurocode. The proposed value for the shear strength is 8.8 MPa for Azobé.

Material stiffness

The design value of the stiffness of sawn timber can be determined by using the mean value and applying the material factor ($E_d = \frac{E_{mean}}{\gamma_M}$). The characteristic values needed for stiffness and mean density can be found in the same part of NEN-EN 338 [7] as Azobé strength properties and are given in Table 3.2.

$E[kN/mm^2]$ & $\rho[kg/m^3]$	**MoE parallel** ($E_{m,0,mean}$)	**5% MoE parallel** ($E_{m,0,k}$)	**MoE perp.** ($E_{m,90,mean}$)	**Mean shear modulus** (G_{mean})	**5% Density** (ρ_k)	**Mean density** (ρ_{mean})
Azobé (D70)	20	16,8	1,33	1,25	800	960

Table 3.2: Stiffness properties and density of Azobé (D70) according to NEN-EN 338.

3.2 Bolts

For the reference case, bolts of type M20 8.8 (high strength steel bolt) were used to connect the deck to the longitudinal girders. Both the tensile resistance- and the shear resistance of the bolt depend on the bolt strength class and the cross-sectional area of the bolt [11]:

$$F_{t,Rd} = \frac{k_2 f_{ub} A_s}{\gamma_{M2}} \tag{3.3}$$

$$F_{v,Rd} = \frac{\alpha_v f_{ub} A}{\gamma_{M2}} \tag{3.4}$$

Boutklasse	**4.6**	**4.8**	**5.6**	**5.8**	**6.8**	**8.8**	**10.9**
f_{yb} (N/mm^2)	240	320	300	400	480	640	900
f_{ub} (N/mm^2)	400	400	500	500	600	800	1000

Figure 3.5: Bolt strength classes according to Eurocode

Part II
Bolted steel- to- timber connections

Chapter 4

Relevant stiffness directions

Every deck beam node has six degrees of freedom: translations in x, y and z, rotations xx, yy and zz (rotation xx for example, is a rotation around the local x-axis). The current method of modelling the deck connections is creating links with certain restraints and releases as is given in figure 4.1.

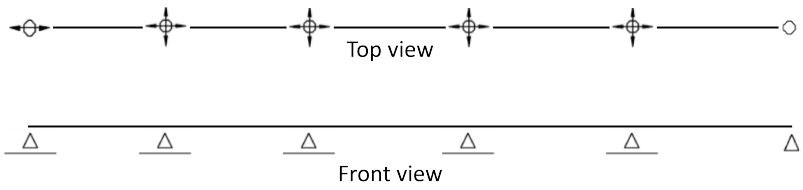

Figure 4.1: Current linkage of the deck in the BBM beam model

In this thesis research, the linkage of these deck joints will be adapted in order to investigate the influence of slipping joints on the degree of hybrid interaction of the current deck. It is therefore important to distinguish which degrees of freedom have an influence on the total deflection of the bridge leaf when restrained.

A short study was performed in order to find the maximum deflection of the main girder for each separate degree of freedom being restrained. Every joint in the full bridge leaf beam model is at least restrained in the vertical direction z, but can additionally be restrained in the other 5 directions. Figure 4.2 provides an overview regarding which individual directional restraints, result in which maximum deflections of the main girder for the vertical- and horizontal load case (for load case description, see chapter 7) for the model with beam deck elements.

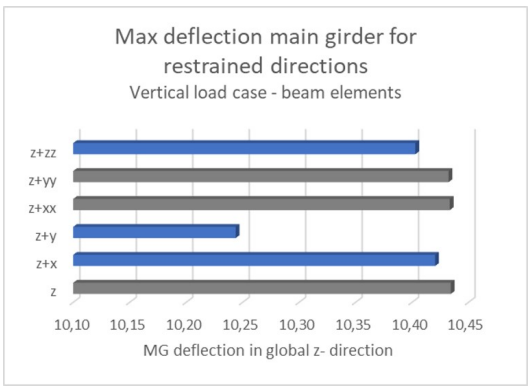

(a) Main girder displacements for vertical load case in case of beam elements for individually restrained degrees of freedom of the deck joints

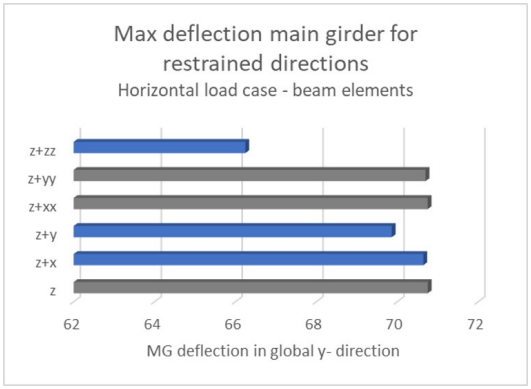

(b) Main girder displacements for horizontal load case in case of beam elements for individually restrained degrees of freedom of the deck joints

Figure 4.2

The same analyses for individual restraints can be performed for a monolithic deck plate as shell elements. These shell elements enable interaction between the elements, since the elements share their nodes, whereas for the beam elements this does not apply. Figure 4.3 displays the deflection results of the main girder for respectively the vertical- and horizontal load case, this time using shell deck elements.

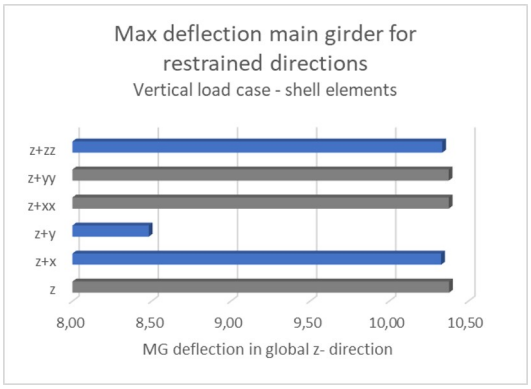

(a) Main girder displacements for vertical load case in case of shell elements for individually restrained degrees of freedom of the deck joints

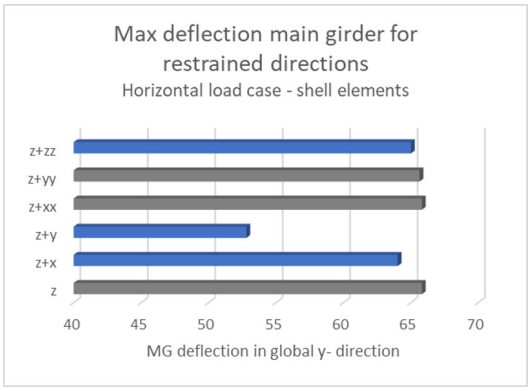

(b) Main girder displacements for horizontal load case in case of shell elements for individually restrained degrees of freedom of the deck joints

Figure 4.3

Judging by these graphs, restraining translational degree of freedom y, significantly decreases the total deflection of the bridge leaf for both load cases. The rotation around the vertical axis and the translation in x- direction also contribute, but in a lesser degree. Restraining rotations around the local y- and x- axis do not have a large effect on the maximum deflection results.

4.1 Conclusion

In this research, stiffnesses will be assigned to deck joints in the translational x- and y-directions and the rotation around the z- axis. The magnitude or distribution of rotational stiffnesses around the x- and y-axis are not relevant to pursue in this research.

Chapter 5

Theory of single- bolted connections

In this chapter, different stages of the expected load-, deformation behaviour of single-bolted connections will be described. The most influential factors for each stage of the curve will be specified and commented. The behaviour of an individual connector is mainly considered here and the theory will be the basis for the assumptions on the behaviour of deck- to- girder joints in chapter 6 and 10.

5.1 Load- deformation behaviour of an individual bolt

Timber- to- steel connections can have different types of failure mechanisms, but the load-deformation curve is generally shaped as in figure 5.1. The different stages can have a different shape, but when testing a joint to failure, these types of stages are expected to be observed.

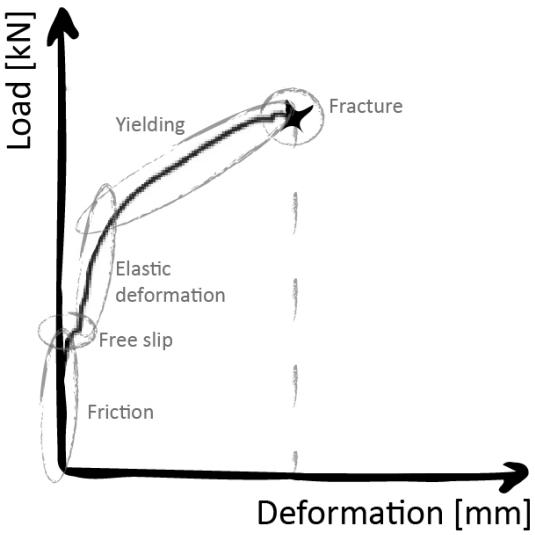

Figure 5.1: Typical load deformation stages for steel- to- timber connections. The displayed curve serves as an example and is obtained from bolted steel- to- LVL connection embedment tests by Hassanieh et al. [12]

The first stage will be friction, generally caused by pre- tensioning in the bolt. After this relatively stiff behaviour, the bolt can slip in the shaft and once it encounters the timber, elastic deformation sets in. Releasing the force here, will return the bolt to its deformed position just before the elastic deformation. When increasing the load further, the elastic capacity is exceeded, at a certain point and the ductile stage commences. Large permanent deformations will eventually lead to fracture.

In figures 5.2a and 5.2b, the elastic, plastic and fracture stages are clearly distinguishable. Especially the ductility (defined as the ratio of ultimate displacement over yield displacement), shows large differences for each of the specimen. The moisture content of the Azobé causes for a decrease in ductility and the point of yielding.

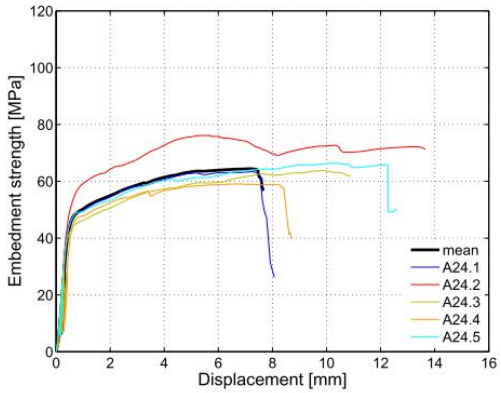

(a) Load-, slip graphs of embedment tests for 24mm HSS dowels in Azobé [13]

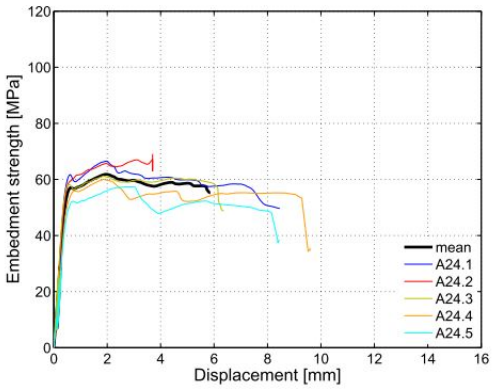

(b) Load-, slip graphs of embedment tests for 24mm HSS dowels in wet Azobé [13]

Figure 5.2

5.1.1 Friction

Timber can expand due to influences of moisture and temperature. This expansion or contraction can result in extra tension or relaxation respectively in the bolt. Several of these temperature or moisture cycles, can thus result in fatigue of the bolt and untightening. When the bolted connection loses its pre-loading, the friction component diminishes to a minimum and the slip phase initiates faster. The stiffness due to friction is relatively large, so losing that stiffness (by untightened bolts) in many of the deck connections will have a significant influence on the deck's system interaction.

According to research by Allan et al. [14] and Chesson et al. [15], a correlation appears to exist between the pretension loss over time and the hole size of a bolt or pin for steel- to-steel connections. Figure 5.3 shows the differences in pretension loss over time for different hole clearances in steel- to- steel connections. Such a correlation could exist for timber- to-steel connections as well, but this has not been investigated yet.

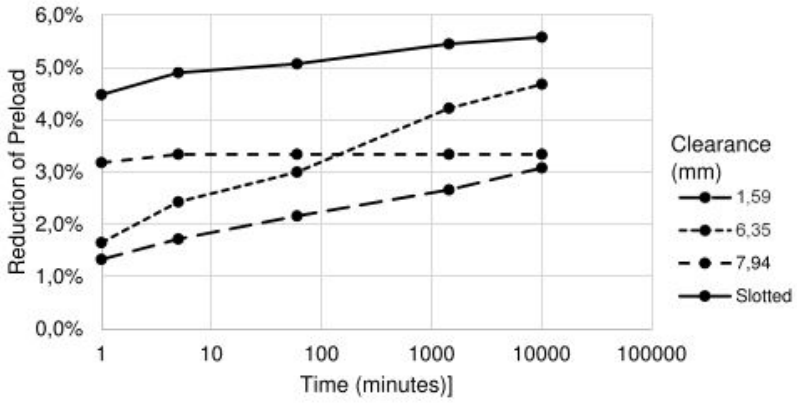

Figure 5.3: Loss of preload over time for different hole clearances in bolted steel- to- steel connections [14] [15]

The friction behaviour is dependant on a few parameters:

- Applied torque
- Time after applying torque
- Washer type
- Tension resistance of the bolt
- Crushing strength timber perpendicular to the grain
- Friction coefficient
- Timber expansion
- Hole clearance

5.1.2 Slip

The amount of slip, will mainly depend on the hole diameter, which determines the hole clearance. The magnitude of this slip is determined by the initial location of the bolt in its shaft, but the general rule will be that the slip is bounded by the physical limits of the shaft ($0 < u_{slip} < 2\Phi_{\Delta}$). Slip can be frictionless, but the interface can also still provide some friction, while slipping. If this is the case, the slip plateau will be slightly inclined, instead of fully horizontal.

Static friction between shear planes occurs when relatively small movements are considered. In general, for clean connection between wood and wet steel, a friction coefficient of 0.2 would be found. Dry surface conditions can increase this friction coefficient up to 0.6 [16].

So for the slip stage, the most important parameters are:

- Hole clearance
- Friction coefficient between Azobé and steel

5.1.3 Elastic deformation

The stage of elastic deformation is characterized by embedding of the bolt in the timber. The load-, deformation behaviour obtained from embedment tests can be relevant to review.

5.1.3.1 Embedment strength

Next to the yielding moment of a dowel- type fastener, embedment strength determines the failure load of a joint. The embedment strength is highly dependant on the density of the timber and the bolt diameter according to EC5 [4]. To determine the value for embedment strength empirically, the Eurocode has specified a test method [17]. An embedment test, requires the fastener not to bend at any point and the displacement of the dowel through the timber is similar to failure mode C.

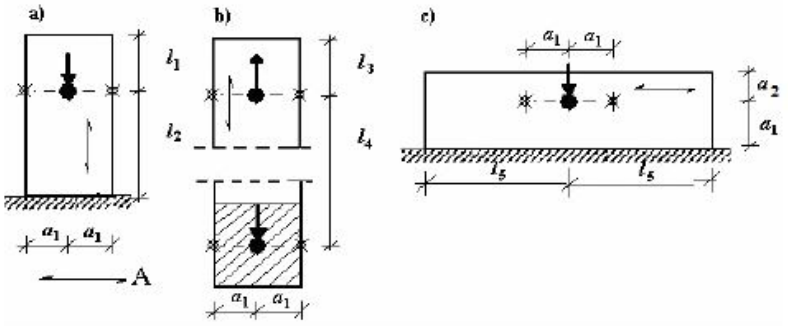

Figure 5.4: Embedment test set-ups [17]

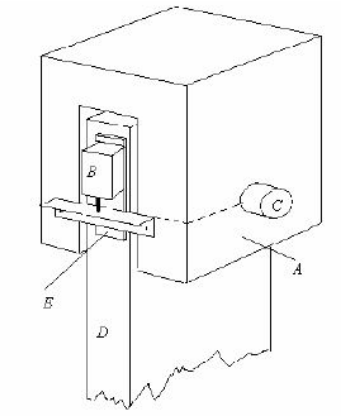

(a) Typical test set-up according to EN 383 [17]

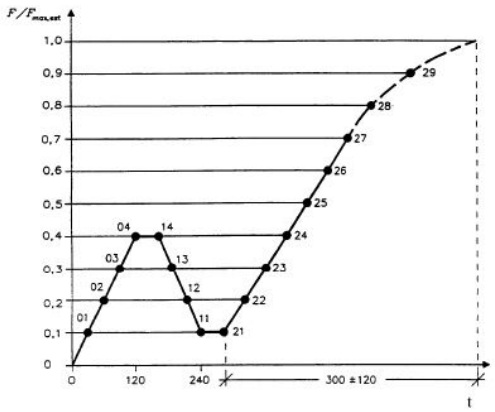

(b) Test loading procedure according to EN 383 [17]

Figure 5.5

Test procedures for embedment strength rely on the occurrence of the "uniform stress" in the timber. This can be induced by using relatively thick steel side plates in the apparatus. Embedment strength can be determined either by a tensile- or a compressive test set-up. No large difference was observed between these two methods according to L.R.J. Whale and I. Smith [18].

The embedment strength correlates to a few material- and environment dependant characteristics, such as the timber density, the bolt type, the bolt diameter and the relative

humidity.
In the results of recent research [19], these dependencies can be clearly observed. Using HSS dowels in mechanical joints generally results in a higher embedment strength, compared to mild steel dowels (figure 5.7). The same can be said for dry versus wet conditions. In dry conditions, the embedment strength is larger than in wet conditions (figure 5.7). Ductility is increased by using larger diameter dowels. A note that should be made regarding this graph is the limited amount of information on variation in results. The different graphs are plotted for one characteristic specimen and it offers no exact guarantees for the behaviour of other specimen.

Comparing different wood species in figure 5.6, higher density clearly enhances the embedding strength, but has no correlation with the ductility. The latter correlation is also supported by the formulas used in the Eurocode for embedding strength:

$$f_{h,k} = 0.082(1 - 0.01d)\rho_k \tag{5.1}$$

Whereas this equation might be accurate for softwoods, it is highly conservative for hardwood species and based on regression analysis of empirical data, a new formula was proposed [19]. Test results were adjusted for a 12% moisture content of the specimen, since it was observed that an increase of 1% in moisture content could lead to 2 % of strength decrease. The new relation shows less dependence on the dowel diameter and an increased value for the regression factor:

$$f_{h,k} = 0.095(1 - 0.0089d)\rho_k \tag{5.2}$$

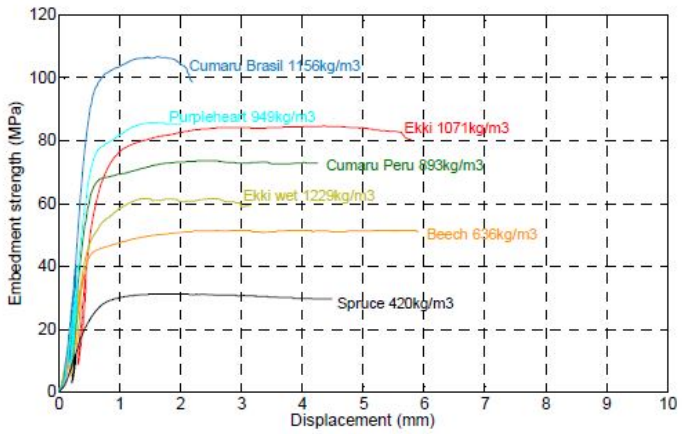

Figure 5.6: Mean load deformation curves for 12mm HSS dowels [19]

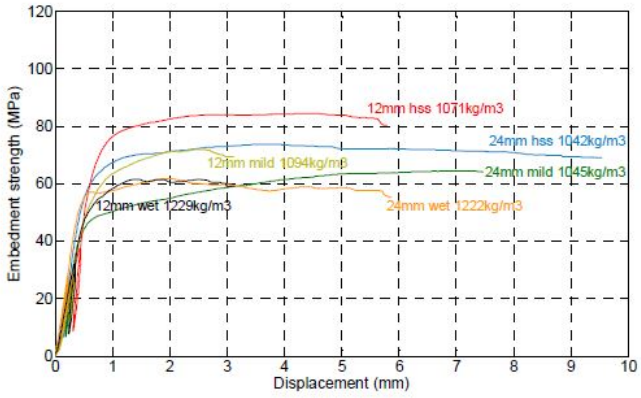

Figure 5: *Mean load-deformation curves, Ekki*

Figure 5.7: Mean load deformation curves for Ekki [19]

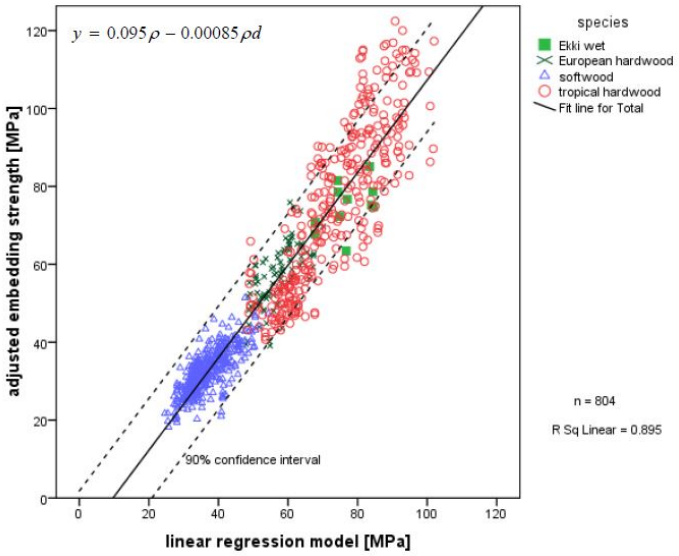

Figure 5.8: Linear regression model vs adjusted test results [19]

If the load is applied in an angle to the grain direction, the embedment strength formula should be corrected by a factor k_{90}. Applying this in the formula for $f_{h,\alpha,k}$, gives:

$$f_{h,\alpha,k} = \frac{f_{h,k}}{k_{90} * sin(\alpha)^2 + cos(\alpha)^2} \tag{5.3}$$

Where for hardwoods:

$$k_{90} = 0.09 + 0.015d \tag{5.4}$$

When applying cyclic loading to the test specimen for a bolted connection, stiffness rarely decreases after a certain amount of cycles. During the first few cycles the fastener densifies the timber around the bolt, so free deformation can keep increasing due to the ever increasing hole clearance. But when the fastener returns to touch the timber again, it encounters a stiffer material each time, until it crushes under a larger applied load. Figure 5.9 shows the load procedure and a characteristic response to both the initial load and cyclic loading [20].

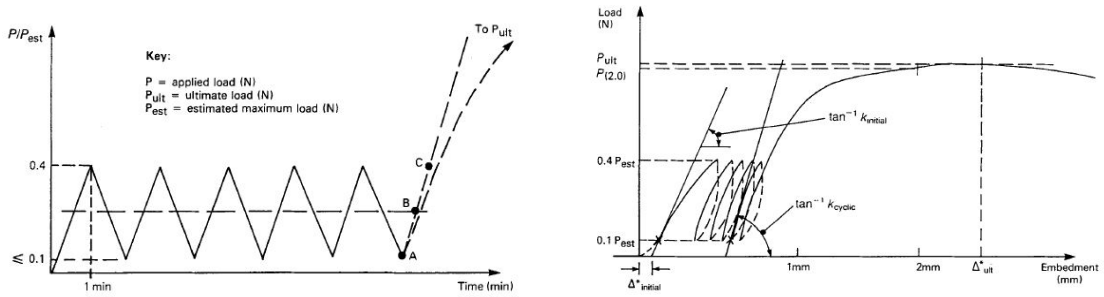

(a) Typical cyclic test load procedure [20]

(b) Response to cyclic test load [20]

Figure 5.9

5.1.3.2 Slip modulus

In the embedment stage, the stiffness is given by the parameter K_{ser} (= slip modulus). In the Eurocode the calculation of the slip modulus K_{ser} is given by a formula (equation 5.5) based on the mean density of the timber and the dowel diameter. This equation is valid for timber- to- timber connections. The slip modulus has to be multiplied by a factor 2 in case of a timber- to- steel connection.

$$K_{ser} = \frac{2 * \rho_m^{1.5} * d}{23} \tag{5.5}$$

The slip modulus K_{ser} would be expected to have a lower value when loaded perpendicular to its grain, since the material stiffness properties perpendicular to the grain are generally lower. However, the load spreads over a larger area when loaded perpendicular to the grain compared to a parallel loading. The Eurocode therefore, does not make any distinction between the slip modulus parallel- and perpendicular to the grain. Some other guidelines do, such as the Swiss code (SIA 265:2012) [21]. According to the Swiss Society of Engineers and Architects, the value for the slip modulus in the perpendicular direction could be 50% compared to the slip modulus in parallel to grain direction. Figure 5.10 shows a table from that code suggesting the difference in slip modulus value.

Load direction	Timber-to-timber Panel-to-timber	Steel-to-timber
Parallel to grain $K_{ser,0}$	$3 \cdot \rho_k^{0.5} \cdot d^{1.7}$	$6 \cdot \rho_k^{0.5} \cdot d^{1.7}$
Perpendicular to grain $K_{ser,90}$	$1.5 \cdot \rho_k^{0.5} \cdot d^{1.7}$	$3 \cdot \rho_k^{0.5} \cdot d^{1.7}$

Figure 5.10: Stiffness K_{ser} per shear plane per dowel according to the Swiss guidelines for timber structures [21].

The test protocol (figure 5.11) for determining the slip modulus is similar as for the embedment strength. The set-up for the tests is given in figure 5.12.
The weaknesses of the determination of K_{ser} through tests, are the estimated load carrying capacity F_{est} and the measuring locations. Estimating the load carrying capacity too high (especially for big specimens) can cause a joint to damage locally already at $0.4F_{est}$ during the tests. Furthermore, no protocol is specified to whether the measurement instruments should be placed in the rotation center of the joints or outside the joints [13].

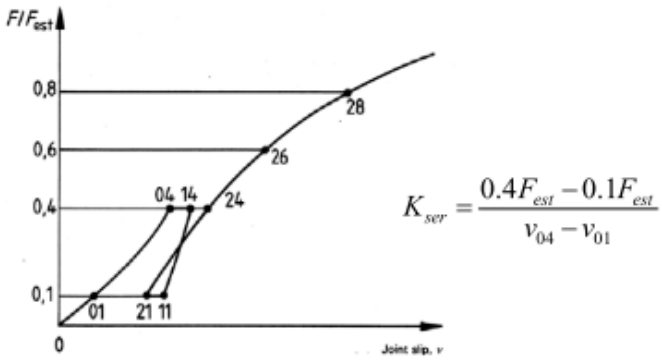

Figure 5.11: Test protocol to determine K_{ser} [13]

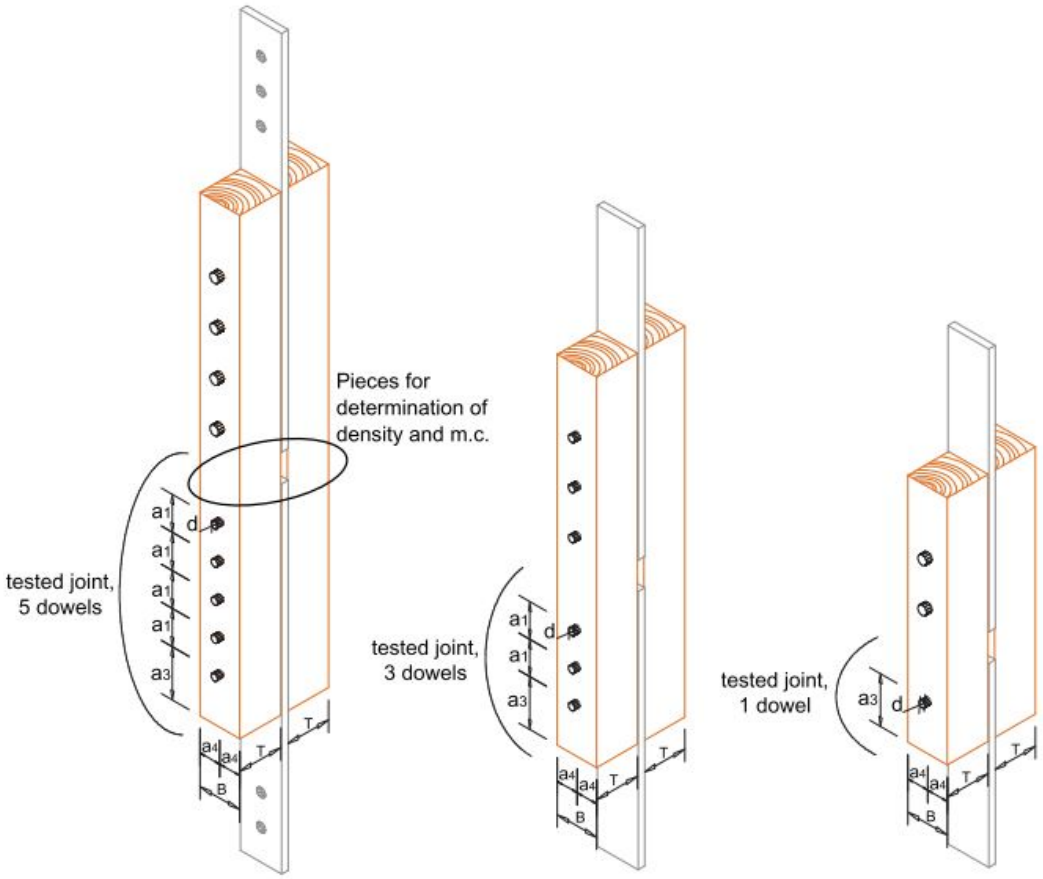

Figure 5.12: Test set-up to determine K_{ser} for respectively 5- bolted, 3- bolted and single- bolted joints [13]

In the research by Sandhaas [13], the slip modulus and the timber density are determined from tests. For two different dowel diameters, the slip modulus is calculated using the Eurocode equation 5.5. For each specimen the slip modulus according to the Eurocode formula versus the tested value are plotted in figures 5.13a and 5.13b. The dashed line represents the regression line of the results and the solid line shows where the calculated and the tested value would be the same (y=x).

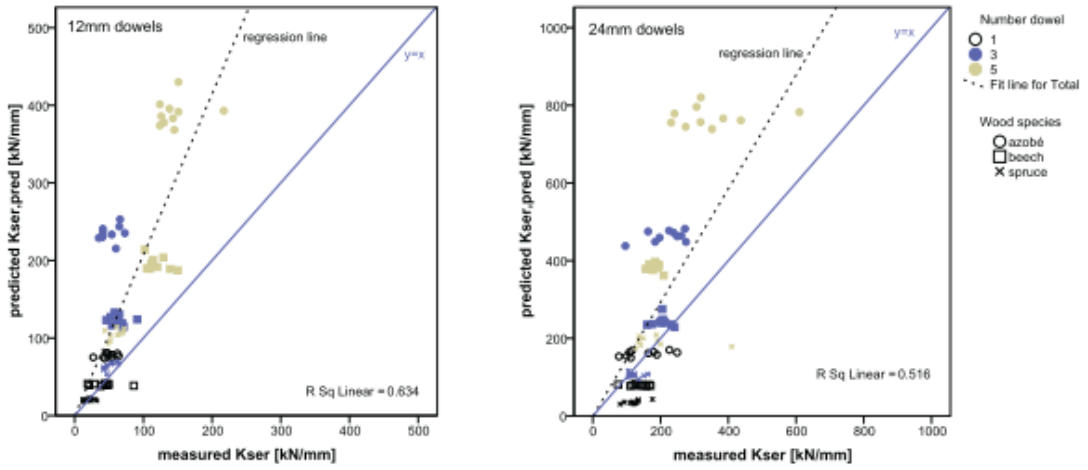

(a) Measured values versus calculated values of slip modulus K_{ser} for 12mm dowels [13]

(b) Measured values versus calculated values of slip modulus K_{ser} for 24mm dowels [13]

Figure 5.13

So, to summarise, the elastic deformation will thus be dependant on:

- Timber density
- Hardness of the bolt
- Bolt diameter
- Relative humidity
- Load cycles
- Angle of the load to the grain

5.1.4 Ductility and failure

During the ductile stage, many of the same parameters are of importance, as in the previous stage of elastic deformation. Ductility can be influenced by the anatomy (micro-structure) of the timber species and the bolt diameter [19]. The failure of the connection can be in the bolt or the timber and the type of failure can be analyzed by looking at the different failure modes.

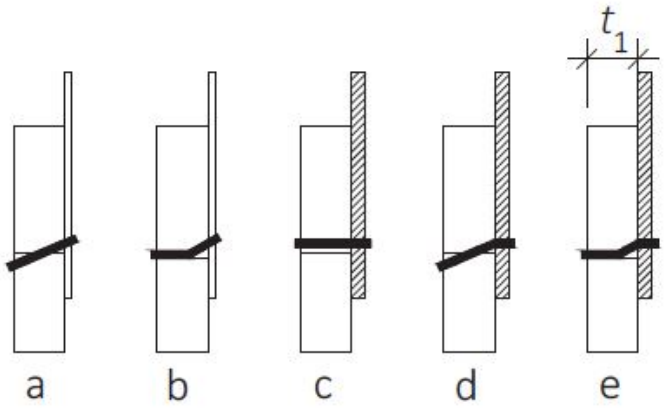

Figure 5.14: Possible failure modes for thin- and thick plated connections [4]

The load-bearing capacity of steel-to-timber connections, characterized by the possible failure modes, is related to the thickness of the steel plate (NEN-EN 1995-1-1) [4]. Load carrying capacity per bolt per shear plane for thin plated steel ($t \leq 0.5d$) is defined as:

$$F_{v,Rk} = min \begin{cases} 0,4 f_{h,k} t_1 d \\ 1,15\sqrt{2 M_{y,Rk} f_{h,k} d} + \frac{F_{ax,Rk}}{4} \end{cases} \tag{5.6}$$

And for thick plates ($t \geq d$):

$$F_{v,Rk} = min \begin{cases} f_{h,k} t_1 d \\ f_{h,k} t_1 d[\sqrt{2 + \frac{4 M_{y,Rk}}{f_{h,k} d t_1^2}} - 1] + \frac{F_{ax,Rk}}{4} \\ 2,3\sqrt{M_{y,Rk} f_{h,k} d} + \frac{F_{ax,Rk}}{4} \end{cases} \tag{5.7}$$

The characteristic yield moment of the bolt is equal to:

$$M_{y,Rk} = 0.3 f_{ub} d^{2.6} \tag{5.8}$$

The withdrawal capacity of a bolt is limited to 25% of the total bearing capacity $F_{v,Rk}$. To determine the withdrawal capacity, the minimum of the tensile strength of the bolt and the load bearing capacity of the washer (i.e. the compressive strength of timber under the washer, perpendicular to the grain).

The different failure modes can be identified by the formation of plastic hinges. Plastic hinges will form depending on the geometry of the fastener and ratio between fastener material strength and the embedment strength of the timber.
Interpolating between thin- and thick plated failure modes is necessary when the thickness of the steel plate is between 0.5d and d.

According to recent research [22], higher density tropical hardwood species are more likely to show signs of splitting than European hardwoods. Differences in failure types (e.g. splitting or consecutive buckling of the fibers) are a result of the difference in local properties of the timber species like the presence of rays or the length of the fibers [19].

The influence of oversized bolt holes on the failure load was investigated by T.L. Wilkinson in 1993 [23]. The result of his research was that the hole clearance has a negligible effect on the failure load. Deviations of the grain angle do have a small reductive influence on the failure load.

For the deck to girder joint, the most relevant parameters are described in chapter 3. Using the material properties of the timber and the bolt, "failure mode a" is most likely to occur in all possible load directions (relative to the grain). The steel top flange of the longitudinal girder is thus considered as a thin steel plate and the bolt is not expected to bend, only to rotate. See appendix C for the short calculation of possible failure modes in the timber deck for both parallel- and perpendicular- to- grain- direction.
So, the ductile and failure stage are characterized by:

- Angle deviation of the hole
- Timber anatomy
- Moisture content
- Bolt diameter

- Bolt hole clearance
- Hardness of the bolt

5.2 Conclusion

To verify the ultimate strength of a joint, different failure modes according to the Johanssen Model have to be considered related to either thick or thin plates. "Failure mode a" is most likely to occur for all load directions, which means that bending of the dowel is not to be expected for any magnitude of shear load considering these deck- to- girder connections.

Bolted joints do not have a linear response. Their individual behaviour is mainly dependant on the pretension in the bolt, the friction between the timber and steel plates, the bolt hole clearance and the embedment behaviour. The friction and the slip in the bolts are mostly dependant on the pretension, timber expansion and hole clearance. Inclusion of water or cyclic loading can affect the bolt hole clearance and the pretension. It can therefore be hard to accurately predict. The stage of elastic deformation (or embedding) can be predicted by reviewing the results from embedment tests on Azobé from C. Sandhaas [13] or by using the Eurocode formula including the test data for the timber density. Time-dependant effects on the slip modulus K_{ser} of hardwoods in bridges are currently unknown.

Chapter 6

Bolt group behaviour

6.1 Theoretical stiffness according to the Eurocode

Theoretically, the joint stiffness of a connection with multiple dowel-like fasteners, is relevant for calculating force or bending moment in the simple formulas of $F = K_{ser}u$ or $M = K_{r,ser}\omega$.

According to NEN-EN 1995-1-1 [4], the slip modulus K_{ser} for steel-to-timber connections is only determined by the fastener diameter d and the mean density ρ_m for the timber member (Eq. 10.1).

$$K_{ser} = \frac{2\rho_m^{1,5} d}{23} \tag{6.1}$$

Taking long term behaviour into account, the following formulas are relevant to determine respectively SLS and ULS values for the (rotational) joint stiffness.

$$k_{def,joint} = 2k_{def}$$

$$SLS : K_{ser,fin} = \frac{K_{ser}}{1 + k_{def,joint}}$$

$$ULS : K_{ser,fin} = \frac{K_{ser}}{1 + \psi_2 k_{def,joint}}$$

$$K_u = \frac{2}{3} K_{ser,fin}$$

Determining the value for rotational stiffness is according to formula 6.2:

$$K_{r,ser} = K_{ser} \sum_{j=1}^{n} r_j^2 \tag{6.2}$$

Equation 6.2 is based upon the theory as shown in the schematization in figure 6.1 for moment resisting joints [24].

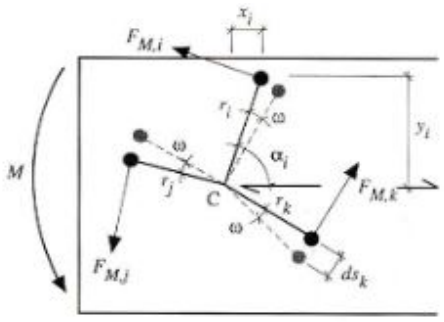

Figure 6.1: Theory of moment resisting joint with dowel-type stiffeners

6.2 Behaviour of a bolted deck connection

Since only the in- plane degrees of freedom are relevant to restrain according to the previous chapter, it is sufficient to model both bolts with two translational springs (in x- and y- direction). Figure 6.2 shows the locations of the bolts, the mid-node and illustrates the mesh size of the 2D elements.

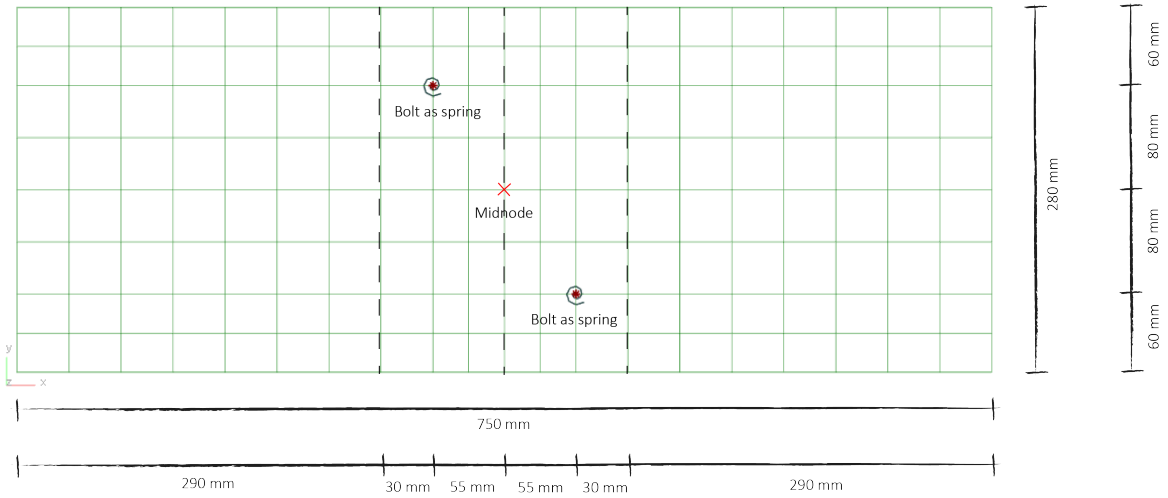

Figure 6.2: Geometry and dimensions of the modelled connection detail

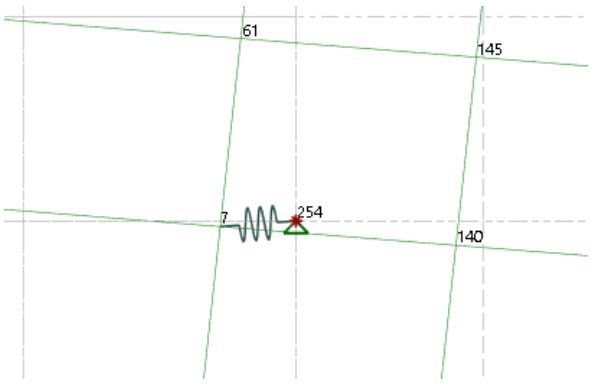

Figure 6.3: Detail of spring element restraining a 2D- timber element

One part of the deck board is considered here and the timber deck board is modelled as a

2D- shell element with mesh sizes. The bolts are modelled as spring elements. In figure 6.3, the spring element is displayed, but visually appears to have only a stiffness in the x-direction. The spring element, however, has a stiffness in both the x- and y- direction. The connected nodes have the same initial location. The mid node is the location where the load is applied and the deformations are also determined here.

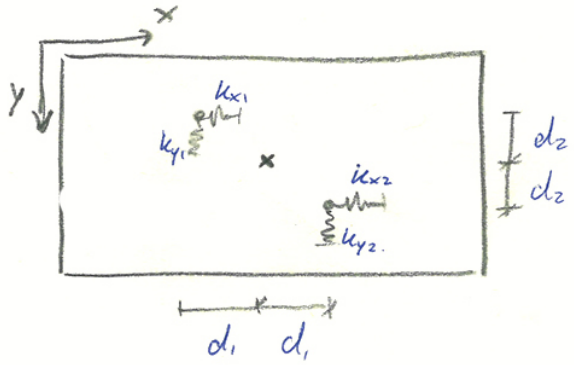

Figure 6.4: Schematic display of the local joint model to determine the stiffness matrix according to the displacement method

To verify this model, one can use the displacement method to find the stiffness matrix for a rigid body that is restrained by two springs in both nodes. The same geometry was used as in the GSA model. In appendix D, the method of determining the stiffness matrix, is given. The resulting stiffness matrix to the model schematized in figure 6.4 is given below.

$$\begin{bmatrix} k_{xx} & k_{xy} & k_{xzz} \\ k_{yx} & k_{yy} & k_{yzz} \\ k_{zzx} & k_{zzy} & k_{zzzz} \end{bmatrix} = \begin{bmatrix} k_{x1}+k_{x2} & 0 & d_2(k_{x1}-k_{x2}) \\ 0 & k_{y1}+k_{y2} & d_1(k_{y2}-k_{y1}) \\ d_2(k_{x1}-k_{x2}) & d_1(k_{y2}-k_{y1}) & d_2^2(k_{x1}+k_{x2})+d_1^2(k_{y1}+k_{y2}) \end{bmatrix}$$

Inserting values for the four springs and the distances d_1 and d_2, the local model (GSA) and the analytical method of using the stiffness matrix can be compared. For example, when a load in x- direction (F_x) of 10 kN is applied and the parameters as in table 6.2

k_{x1} =	30.000 N/mm
k_{y1} =	10.000 N/mm
k_{x2} =	10.000 N/mm
k_{y2} =	30.000 N/mm
d_1 =	55 mm
d_2 =	80 mm
F_x =	10 kN
F_y =	0 kN
M_{zz} =	0 kNm

The inverse stiffness matrix K^{-1} has to be used to calculate the displacement vector **u**.

$$u = K^{-1}F$$

The resulting displacement vector **u**, derived using the stiffness matrix, is:

$$\begin{bmatrix} u_x \\ u_y \\ \phi_{xy} \end{bmatrix} = \begin{bmatrix} 0,307mm \\ 0,039mm \\ 1,415 \cdot 10^{-3}rad \end{bmatrix}$$

Applying the same force and using the same linear stiffnesses in a GSA model as described before, will give the following result in the mid-node:

$$\begin{bmatrix} u_x \\ u_y \\ \phi_{xy} \end{bmatrix} = \begin{bmatrix} 0,3207mm \\ 0,037mm \\ 1,431 \cdot 10^{-3}rad \end{bmatrix}$$

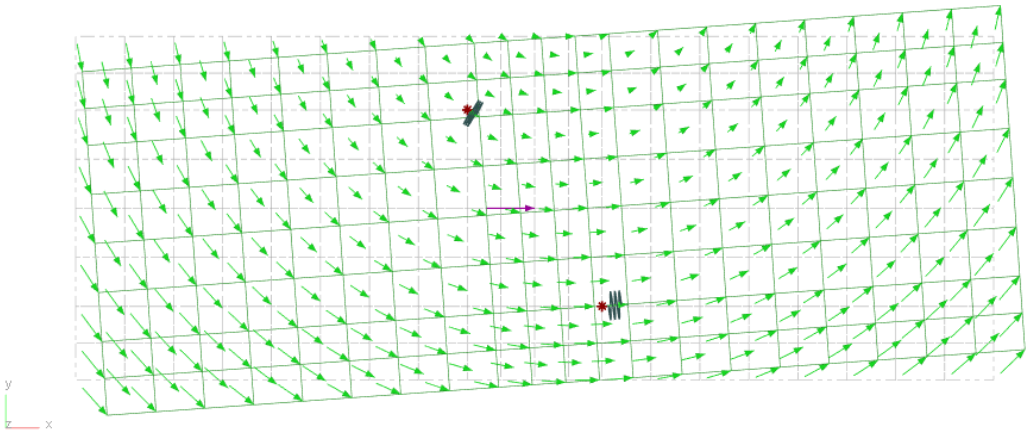

Figure 6.5: Resulting deformation of the GSA local model

Figure 6.5 shows the modelled results (GSA) in terms of displacements of the timber deck board.

The minor difference between these results can be explained by the type of element considered. The GSA model uses 2D- shell elements that can deform in the xy plane depending on the material's Young's modulus, thickness and Poisson's ratio. The displacement method regards the timber deck element as a rigid block. In other words: the distance between the bolts cannot change by exerting a force or moment on the mid-node, whereas for the GSA model and in reality, it can.

The mid node is not necessarily the same as the rotation point. The location of the rotation point depends on the relative stiffnesses of the springs in the loaded direction. Figure 6.5 shows an example of asymmetric spring stiffnesses, resulting in a rotation point outside the borders of the timber deck board.

6.3 Single- vs double spring for one deck board

In section 6.2, a (small) side effect could be observed for individual bolted connections in a single joint, having different load- displacement curves (or stiffnesses, as can be seen in the stiffness matrix for a rigid body). If one would opt for modelling the two bolted joint as one spring, this could be a factor to take into account. However, when a single joint is experiencing a large stiffness difference between the two bolts of that joint, effects could be limited by the surrounding joints of a single deck board, since the considered joint is restrained in some degree to rotate freely.

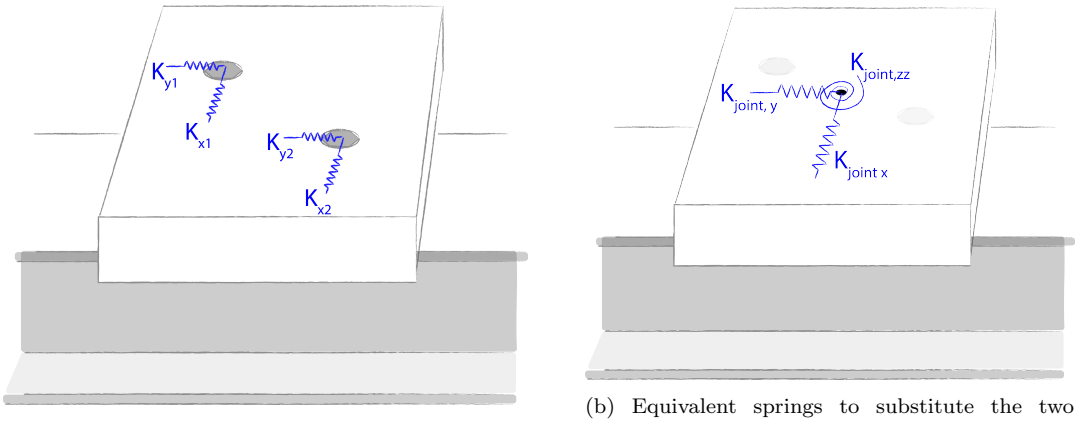

(a) Translational spring to represent stiffness in local x- and y- direction for each single bolted connection

(b) Equivalent springs to substitute the two translational non-linear springs for single- bolted connections

Figure 6.6

The effect of spring stiffness differences has not been explicitly researched in this thesis. The effect however is assumed to be small due to the presence of surrounding joints. Additionally, the differences in free slip stage length are often small, so possible secondary effects are limited and if present, short-lived.

6.4 Conclusion

According to the Eurocode, the rotational stiffness of a bolt group can be computed by multiplying the squared distance of the bolt to the rotation point with the slip modulus for every bolt. This relation is again found in the diagonal terms when using the displacement method to find a stiffness matrix.

The bolt group behaviour however is complex, even for two- bolted deck connections, since a translational force for can induce not only a displacement, but a small rotation as well, in case of a difference in stiffness between the bolts. Also, the rotation center is not at the location of the mid node when the spring stiffnesses are different for the bolts (see figure 6.5).

The results for the analytical model (determining the stiffness matrix) and the GSA model show similar results. However, modelling the deck boards as shell elements (and not as a rigid body or a beam element), results in generally larger deformations in the direction of the force or moment and some contraction due to the Poisson's ratio. This can be explained by the fact that 2D- elements can deform, depending on the material properties for D70 grade timber, that were assigned to the curved shell elements.

The secondary effects (off-diagonal terms in the stiffness matrix), are limited due to the surrounding joints and small difference in free slip, but these limiting effects have not been investigated in this research.

For this research, the off-diagonal terms of the stiffness matrix are not considered as effects when translating two bolts to one single spring (with two translational and a rotational stiffness). For the translational stiffnesses of the spring the two translational stiffnesses of the two individual bolts could be used, whereas the rotational spring stiffness is found by using the Eurocode formula (or the last diagonal term of the stiffness matrix).

Part III
Loads and interaction

Chapter 7

Load cases

For this research, only the most extreme load cases were considered to determine the current hybrid interaction. If the degree of hybrid interaction is already small for extreme load cases, considering smaller loads will lead to an even lesser degree of hybrid interaction. Therefore, large horizontal and vertical loads should be considered in this research first. If the current degree of hybrid interaction turns out to be large for extreme load cases, other load cases (with smaller magnitudes of forces) should be considered as well. This decision will be later reflected on in the discussion (chapter 13).

The vertical load case considered is a bridge full of trucks and the horizontal load is a static ship collision force.

7.1 Vertical load case

The most extreme vertical load would be a bridge full of trucks. In this case, it was assumed that both right lanes are occupied by 40 ton trucks of 16m long ($\approx 9kN/m^2$ distributed load). The left lanes in both directions are subjected to a distributed load of 2.5 kN/m^2 (ordinary lorries). The added bicycle lane is outside of the scope of this research and will thus not be subjected to any variable or permanent load.

The load is applied to the structure as a characteristic grid load (no safety factors included) on top of the deck boards. The characteristic value of the load has been used, since research is considered here, not a strength or stiffness verification. A transverse cross section of the traffic bridge leaf including the distributed truck loads, is given in figure 7.1.

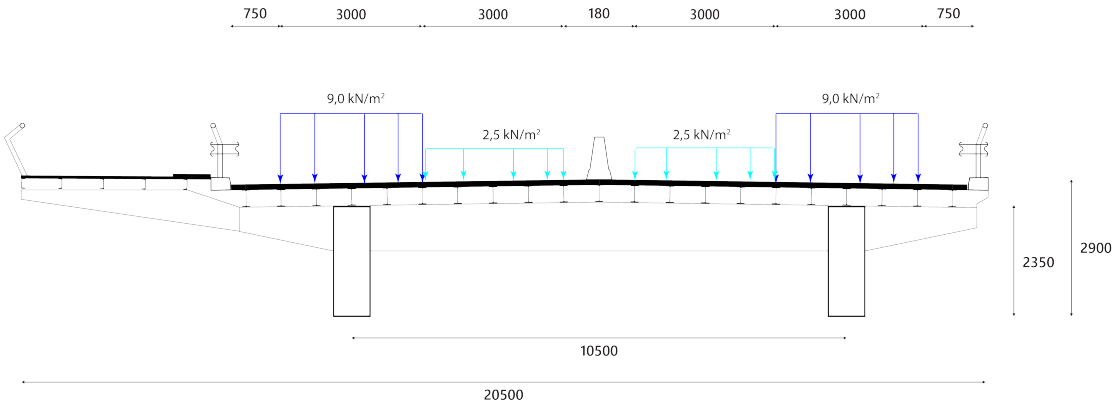

Figure 7.1: Vertical load case: bridge full of trucks (characteristic) ; cross section of the leaf

Figure 7.2 displays the total bridge leaf model in a 3D view with the applied grid loads.

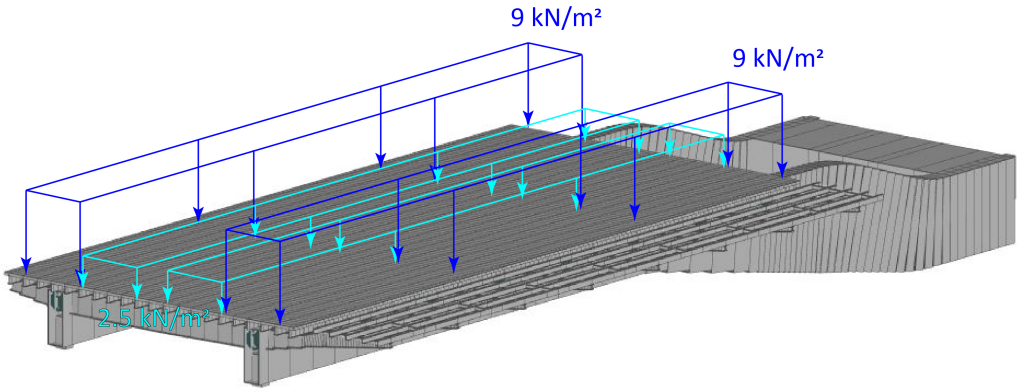

Figure 7.2: Vertical load case: bridge full of trucks (characteristic) ; 3D view model

For the analysis, the counterweight and supports consist of steel sections with no weight, whereas all other steel elements have their self-weight of 7850 kg/m^3 assigned to them. The weight of timber is 1050 kg/m^3 according to recent research into hardwood densities [5]. Dead loads of the structural elements are taken into account in the static linear analysis of the model.

7.2 Horizontal load case

Horizontal loads acting on the bridge leaf could be collision or braking forces for example. As an extreme horizontal load case, a collision force will be considered. Collision would be a large impact load and according to the Eurocode, one could interpret this load as a static patch load of 1 MN over an area of 3m x 0.25m [25]. In other projects, an advanced dynamic or probabilistic calculation for collision load verification could be requested depending on the type and height of the bridge, type of waterway, flow velocity, depth and type of the vessels and the energy dissipation behaviour of the bridge.

In the strength verification of the Beneden Merwede bridge, the 1MN indicative value for the collision force was used. This force value is a large simplification from energy dissipation and dynamic calculations.

The 1 MN patch load is applied to the right main girder (west side), divided amongst two beam nodes near the front support of the bridge leaf (figure 7.3). The collision load is applied as a characteristic load (i.e. no safety factors) and the dead load of the structural elements in the traffic bridge are taken into account (same as in section 7.1). Again, no load was applied to the added bicycle path.

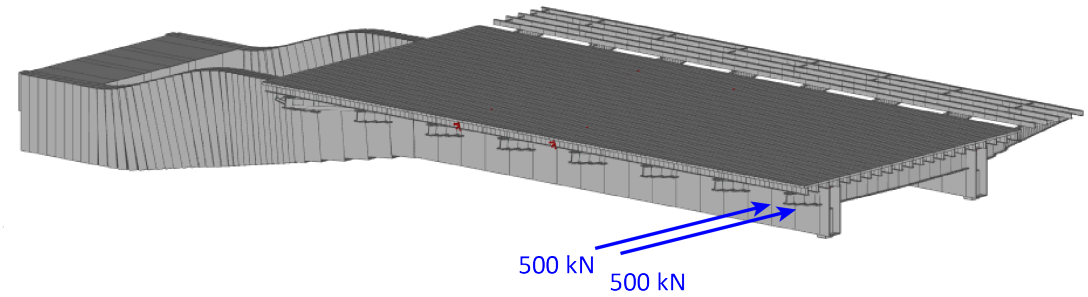

Figure 7.3: Horizontal load case: ship collision to right main girder (characteristic) ; 3D view model

Chapter 8

Lower and upper bound situation

The lower- and upper bound situations for this research can be defined as follows:

- In the **lower** bound situation, all connections are able to slip freely (or in this case: is assigned with a very low stiffness in the relevant directions x, y and zz) and deck boards are modelled according to the current situation
  - Bolted connections are assigned with a translational stiffness close to zero (100 N/mm)
  - Bolted connections are assigned with a rotational stiffness close to zero (10 Nmm/rad)
  - All deck boards are modelled as beams of 280 mm x 110 mm rectangular cross section that do not interact with each other
  - No plate action is achieved
- In the **upper** bound situation, all connections are restrained in the relevant directions x, y and zz. The deck is modelled as a monolithic plate of D70 timber, 110 mm thick.
  - Bolted connections are fully restrained in six degrees of freedom
  - The deck is modelled as a 110 mm thick timber plate

8.1 Vertical load case: bridge full of trucks

For the vertical load case, the difference in deflection between the lower- and the upper bound, is relatively small. However, this difference in deflection could still have a significant impact on the reduction of e.g. bending stresses in the steel main girders. In this chapter, the lower bound situation will be discussed first and later, the upper bound situation, including the expected load spread on a local and global level is being addressed.

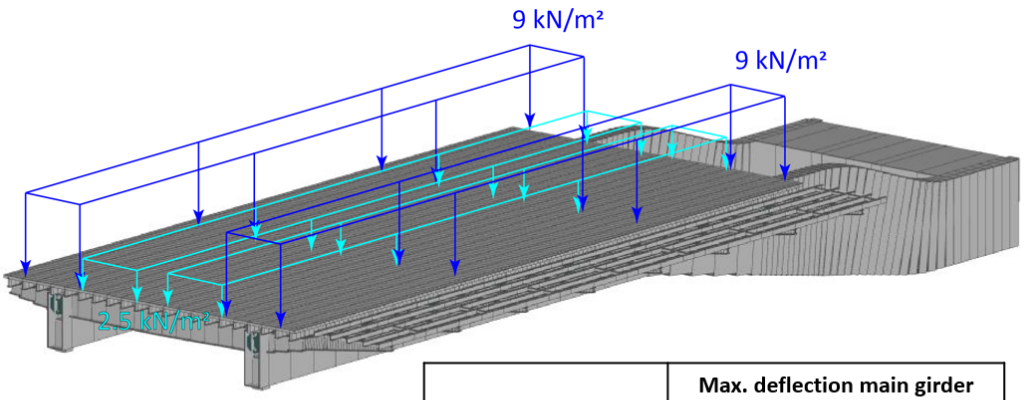

	Max. deflection main girder
Lower bound	10,43 mm
Upper bound	8,41 mm

Figure 8.1: Vertical load case including maximum main girder deflection values for the upper- and lower bound

8.1.1 Lower bound situation

In the lower bound situation, the deck boards all act separately from each other and the longitudinal girders below them. In fact, they only transfer the vertical forces directly downwards, but they can move (quite) freely in their horizontal global xy- plane. The types of restraints used in the current model, for a single deck board connected to six longitudinal girders, are given in figure 8.2. These restraints are similar to the deck-to-girder restraints in the lower bound situation.

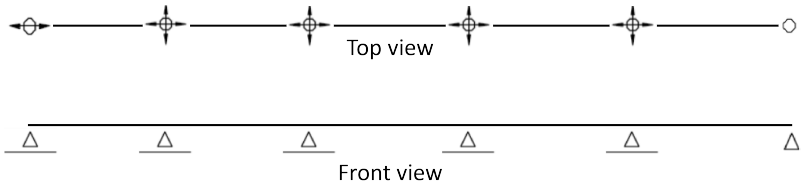

Figure 8.2: Modelled deck- to- girder restrained in current situation for strength verifications of the bridge leaf (similar to lower bound situation)

However, for the lower bound calculation, all connections have been replaced by springs and all their stiffnesses have been set to 100 N/mm, which is close to zero. The reason for this is to easily review whether a joint is expected to enter the elastic region, when a load-, slip curve is assumed. When the amount of slip in case of this low stiffness K_{slip} is larger than the free slip in the curve (or: F ¿ F_{slip}), the bolted connection is in the elastic region (or: embedding). See chapter 10 for information on assumed curves and parameters.

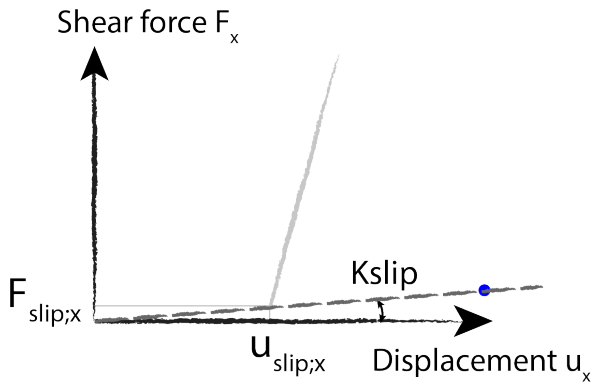

Figure 8.3: Result in x- direction for a joint in the embedding stage, given the used stiffness K_{slip} for the lower bound

Figure 8.3 shows a result of a joint that is presumably embedding considering the assumed curve and the low stiffness K_{slip}. A top view of all 2499 deck joints is given in figure 8.4a and figure 8.4b as colored dots. The black dots represent joints in the slipping stage and green dots are joints in the embedding stage.

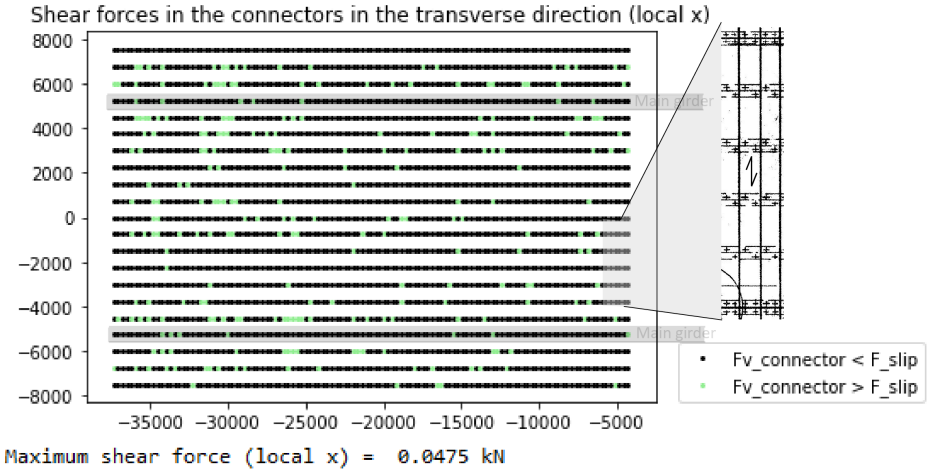

(a) Shear forces (local x- direction) in connections in case of the lower bound situation.

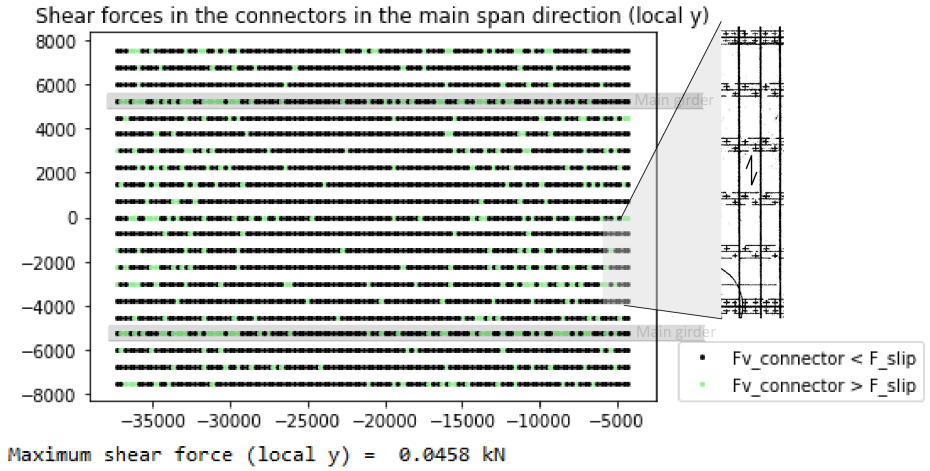

(b) Shear forces (local y- direction) in connections in case of the lower bound situation.

Figure 8.4

8.1.2 Upper bound situation

In the upper bound situation, all joints are considered to be rigid in all 6 directions. A visualization of a single deck board connected to six longitudinal girders, is given in figure 8.5.

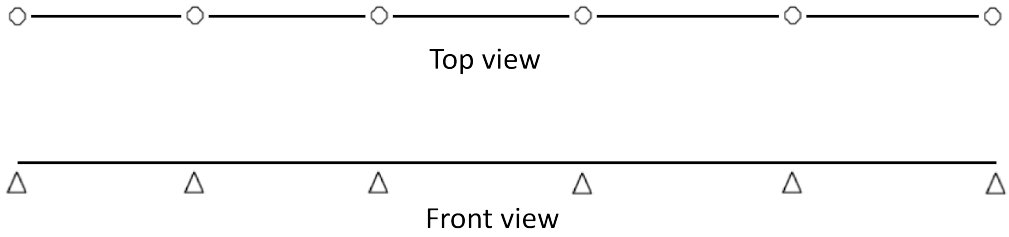

Figure 8.5: Restraints of deck- to- girder joints in upper bound situation

For the upper bound situation, all connectors are assumed to be in an "immediate embedding" stage. No slip is present and the individual deck boards are now replaced one single monolithic plate of 110 mm thickness. Figures 8.6a and 8.6b show the numerical values of the shear forces in the deck connections for the upper bound situation in both directions.

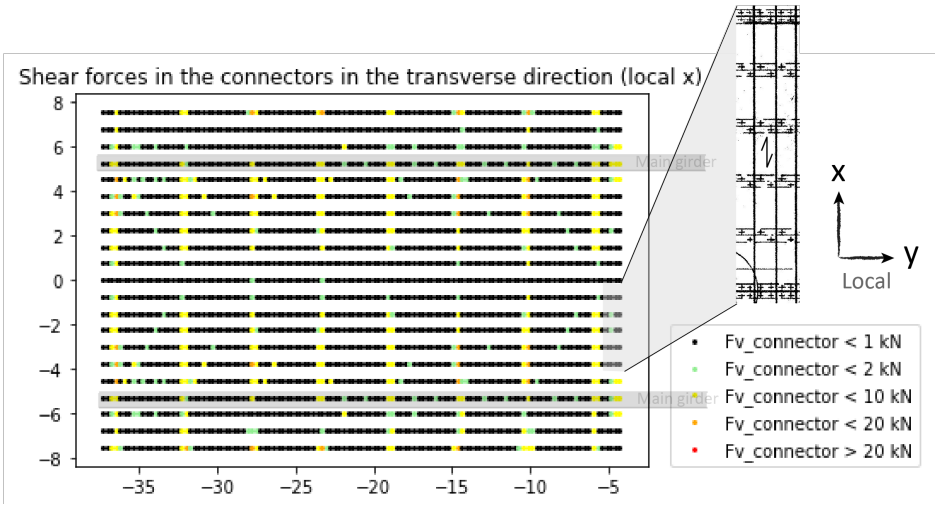

(a) Shear forces (local x- direction) in connections in case of the upper bound situation.

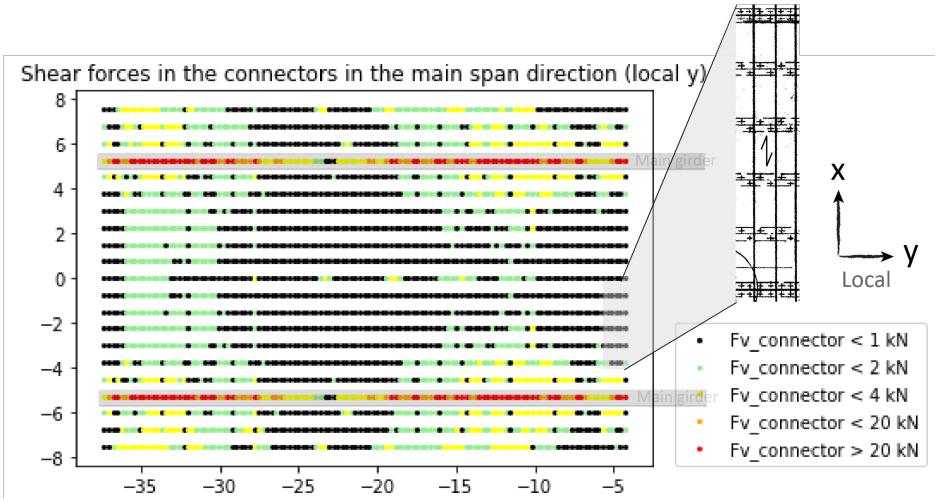

(b) Shear forces (local y- direction) in connections in case of the upper bound situation.

Figure 8.6

8.1.3 Lower- vs upper bound

Comparing the maximum deflection, shear forces, axial forces and bending moments in different structural elements, can quantify how much the steel girders can be relieved by reaching full hybrid interaction of the deck. In appendix G the positions of maximum forces, moments and deflections are given for different types of elements for the vertical load case. Table 8.1 shows these maximum values per element type and lower-/ upper bound situation. Additionally, the last column shows either the gain or the penalty of increasing the hybrid interaction to 100%. This is important to consider, since it quantifies the effect of hybrid interaction in the different structural elements.

$$\text{Gain of hybrid interaction } [\%] = (1 - \frac{\text{upper bound value}}{\text{lower bound value}}) \cdot 100\% \tag{8.1}$$

where:

$$0\% < \text{Gain of hybrid interaction} < 100\%$$

$$\text{Penalty of hybrid interaction } [\%] = (\frac{\text{upper bound value}}{\text{lower bound value}} - 1) \cdot 100\% \tag{8.2}$$

where:

$$0\% < \text{Penalty of hybrid interaction} < \infty\%$$

The gain of hybrid interaction is generally seen in terms of a decrease in forces, moments and deflections in the main girders, cross girders and bracing elements. The penalty of hybrid interaction, on the other hand, is generally found as an increase in forces in the deck, its connectors and the longitudinal girders. The gain and penalty of hybrid interaction can be expressed in two respective equations 8.1 and 8.2.

Structural elements	Lower bound max.	Upper bound max.	Gain / penalty of interaction
Deck boards			
Axial force compression (local x)	-0.059 kN	-19.87 kN	+ 33600%
Axial force tension (local x)	0.076 kN	13.84 kN	+ 18111%
Horizontal shear force (local y)	0.041 kN	21.13 kN	+ 51437%
Vertical shear force (local z)	3.04 kN	2.09 kN	- 32%
Board- to- board compression (global x)	0 kN	-81.59 kN	+ ∞%
Board- to- board tension (global x)	0 kN	50.33 kN	+ ∞%
Deck connections			
Shear force (local x)	0 kN	7.89 kN	+ ∞%
Shear force (local y)	0 kN	37.25 kN	+ ∞%
Bending (local zz)	0.2 kNm	1.2 kNm	+ 500%
Longitudinal girders			
Axial force (local x) compression	-224.56 kN	-153.39 kN	- 32 %
Axial force (local x) tension	157.39 kN	187.29 kN	+ 19%
Horizontal shear force (local y)	5.11 kN	20.66 kN	+ 300%
Vertical shear force (local z)	41.86 kN	40.10 kN	- 4%
Bending (local xx)	0.21 kNm	0.67 kNm	+ 219%
Bending (local yy)	18.32 kNm	12.81 kNm	- 30%
Bending (local zz)	2.96 kNm	2.57 kNm	- 13%
Cross girders			
Axial force (local x)	45.68 kN	91.04 kN	+ 99%
Horizontal shear force (local y)	-55.17 kN	-16.17 kN	- 71%
Vertical shear force (local z)	82.40 kN	66.88 kN	- 19%
Bending (local xx)	-0.72 kNm	-0.72	0%
Bending (local yy)	88.21 kNm	40.37 kNm	- 54%
Bending (local zz)	18.69 kNm	7.67 kN	- 59%
Deflection (global z)	10.95 mm	8.46 mm	- 23%
Stability members			
Axial force (local x)	-78.95 kN	-28.56 kN	- 64%
Horizontal shear force (local y)	17.08 kN	3.1 kN	- 82%
Vertical shear force (local z)	1.34 kN	1.23 kN	- 8%
Bending (local xx)	5.53 kNm	0.0027 kNm	- 100%
Bending (local yy)	14.04 kNm	2.00 kNm	- 86%
Bending (local zz)	-0.69 kNm	-0.62 kNm	- 10%
Main girders			
Axial force (local x)	745.04 kN	1333.68 kN	+ 79%
Horizontal shear force (local y)	12.98 kN	6.06 kN	- 53%
Vertical shear force (local z)	658.27 kN	635.60 kN	- 3%
Bending (local xx)	-82.46 kNm	-31.75 kNm	- 61%
Bending (local yy)	6044.00 kNm	5390.93 kNm	- 11%
Bending (local zz)	29.62 kNm	10.5285	- 64%
Deflection (global z)	10.43 mm	8.20 mm	- 21%

Table 8.1: Vertical load case: maximum/minimum forces, moments and deflections for structural elements in the upper- and lower bound situations

8.1.4 Global- and local responses to vertical loads

Observing an increased value of shear forces in the deck connectors (figures 8.6a and 8.6b), suggests an interaction between the deck and steel girders below it. To review how these forces develop, the global and local response to vertical loads are discussed here.

8.1.4.1 Global response

When the structural height is considered to consist of the main girders and the longitudinal girders (for global bending in longitudinal direction), the lower part of the main girder, will be in tension, while the upper part and the longitudinal girders will be subjected to compressive forces. The expected forces in the main- and longitudinal girders are schematized in figure 8.7 when subjected to a uniformly distributed load.

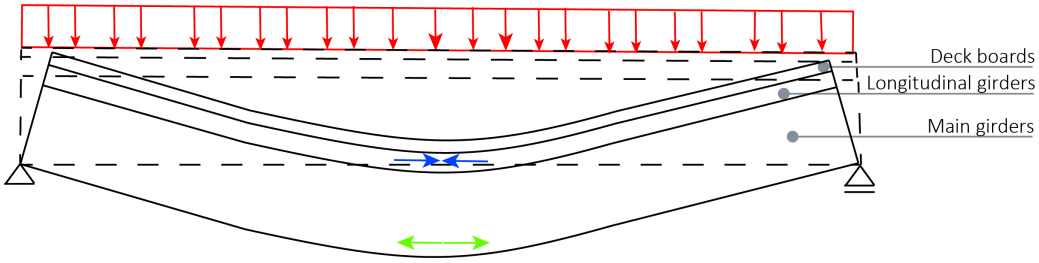

Figure 8.7: Schematization of the forces in the main- and longitudinal girders due to a uniformly distributed load

Since all connections are considered fully restrained in this case, some of the axial compression forces in the longitudinal girders, will be transferred via the joints to the deck as horizontal shear forces. In a case where the deck boards are in constant contact with each other, compressive forces can be taken by the deck as axial forces in the global x-direction (see figure G.5).

In figure 8.6b and G.5, the in-plane shear forces of the connectors and the deck, are localized around the main girders. Bending of the main girder will introduce axial forces in the longitudinal girders directly next to (and on top of) the main girders. For a uniformly distributed load, it could be expected that the deck joints located near the main- girders have to be able to withstand larger shear forces.

The same principle applies to bending in transverse direction, the cross- girders and deck beams bend together resulting in compressive forces in the deck. Since the deck joints are now fully restrained, larger normal forces will develop in the deck, between every connection. In the appendix, figures G.32a and G.2b present a comparison in axial forces in the deck beams for the lower- and upper bound situation.

8.1.4.2 Local response

One of the most simple cases to consider is one deck beam loaded by a vertical concentrated force 'F' on top of three longitudinal girders. These three longitudinal girders each span from cross girder to cross girder. Figure E.1 shows a sketch of this considered structure.

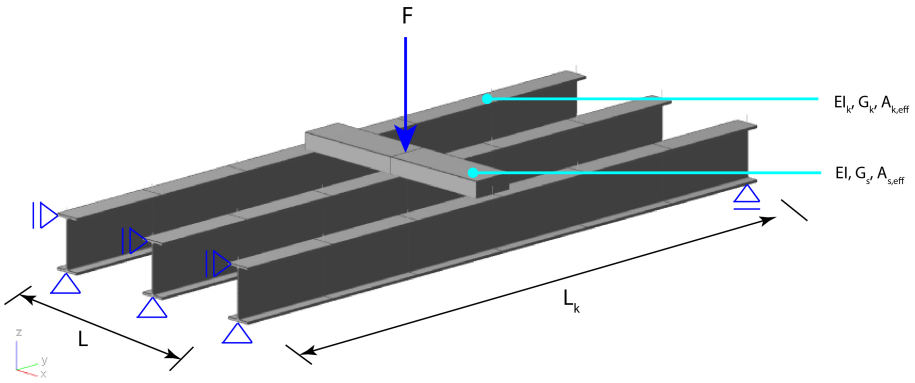

Figure 8.8: Sketch of three longitudinal girders with one deck beam loaded by a concentrated force 'F'

Every longitudinal girder can be replaced by a spring with the beam's bending- and shear stiffness assigned to it. Using these spring stiffnesses and the deck beam, reaction forces can be determined. This calculation and the assumptions are shown in appendix E. The maple sheets used for the analytical calculations are given in appendix F.

Considering the material- and geometrical properties of the deck beam and the longitudinal beams, will provide a solution as given in figure E.4a. The load spread, is visualized in a 3D view in figure E.6.

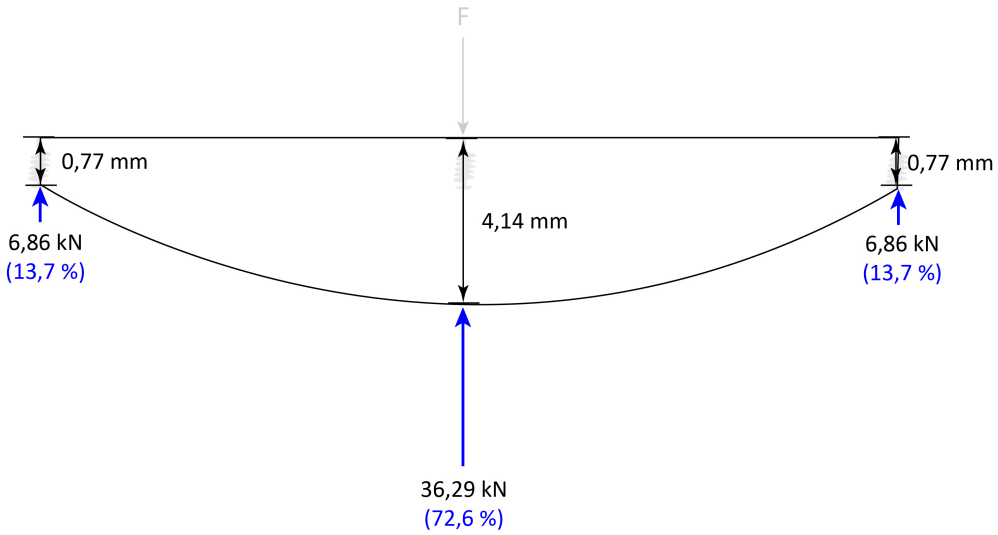

Figure 8.9: Resulting distribution of a concentrated load among three longitudinal girders

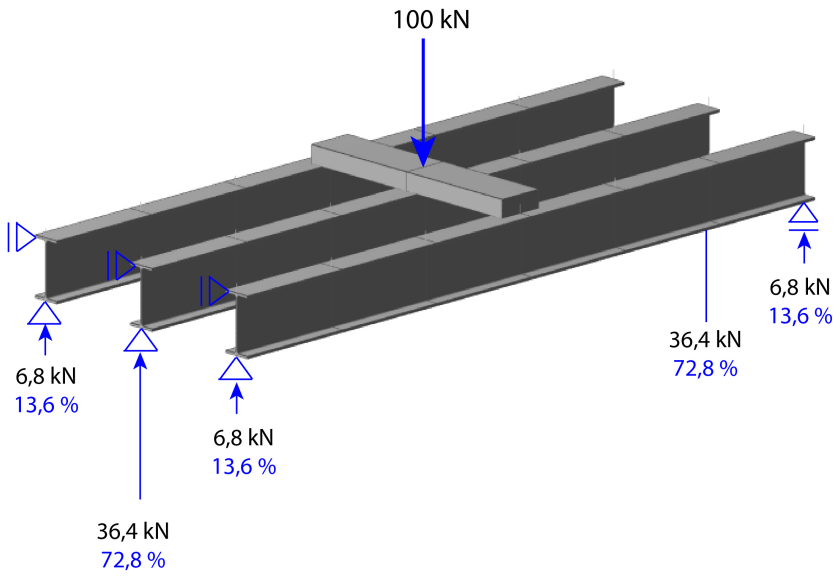

Figure 8.10: 3D view of resulting load spread

The influence of stiffnesses and spans

Increasing the spring stiffness of the longitudinal girders (either by decreasing the span, using a higher steel grade, a different cross section or a different support type of the longitudinal girders), will result in a different load spread. When these three "springs" get more stiff, a larger portion of the applied vertical load will distribute to the center girder. Figure E.7 presents a graph relating the percentage of load distributed to the center girder to the longitudinal girder span (c.t.c. distance of the cross girders).

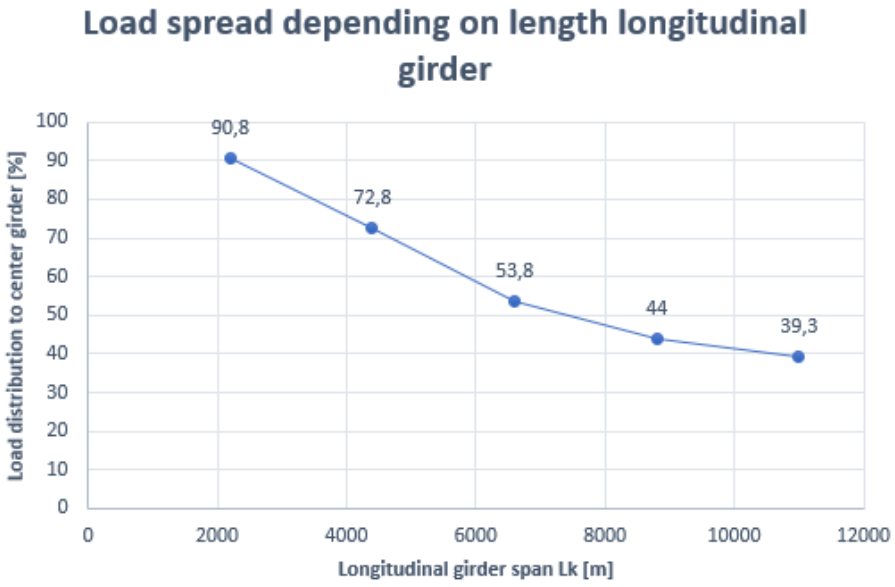

Figure 8.11: Relation between longitudinal girder span and portion of the load taken by the center girder

Similarly, if the loaded deck board is closer to one of the cross girders, the bending stiffness of the longitudinal girder increases and thus a larger portion of the load will distribute to the center girder. Considering a deck element to be closer to the supports up to the point

where the deck board is directly above the cross girder, means the full vertical force is then taken by the center girder support.

For the stiffness of the timber deck beams the opposite principle applies. For increasing stiffness of the deck beams, the load is spread more equally among the three girders. If one imagines the deck beam to be infinitely stiff, the beam would remain straight and all springs would deflect equally, resulting in equal reaction forces distributed to all three girders.

Load spread of a local wheel load

One deck field is in this case bounded by two adjacent cross- girders and the length of the deck beams (3750 mm) or: six consecutive longitudinal girders. Before, the cross girder- to-longitudinal girder connection was assumed to be a pinned connection, but in reality, their respective flanges have been welded together and their connection is thus assumed to be fairly rigid. Hence, a clamped support of the longitudinal girders on both ends is assumed.

This boundary condition will influence the load spread to the girders as was mentioned before. These clamped boundary conditions will increase the spring stiffness of the individual girders. As a result, the center girder will take more load. However, since there are now two loads applied and distributed, the center four girders all carry a substantial amount of load.

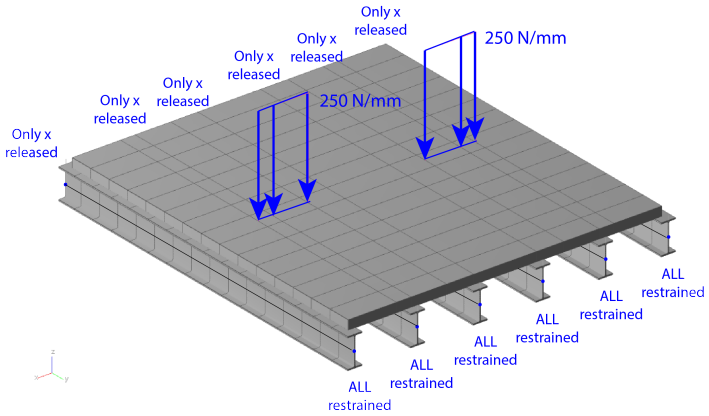

Figure 8.12: Loaded situation of one deck field with clamped connections to the cross girders

Figure E.11 illustrates the loaded situation of one "deck field" and in figure E.12, the response is shown in terms of reaction forces and deflection.

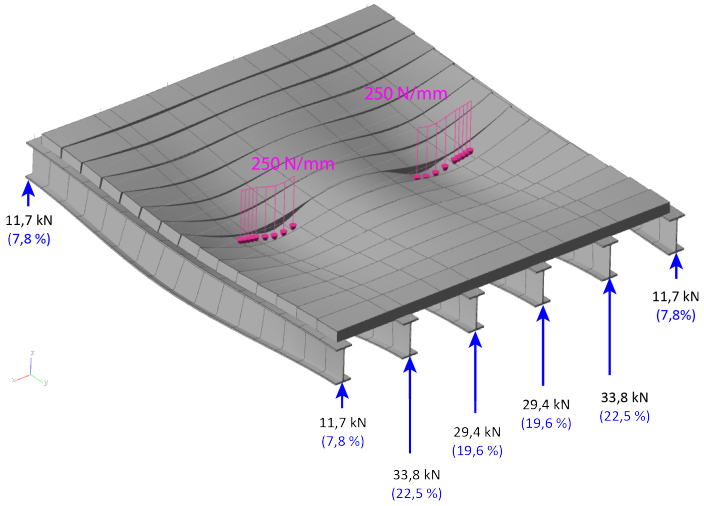

Figure 8.13: Response of one deck field to one heavy loaded axle (Q = 250 N/mm)

When one or two deck beams are loaded, the longitudinal girders will deform downwards as well as sidewards. The resulting forces in the deck boards, that are not directly loaded by the wheel, thus depend on the relative displacements of the longitudinal girders. A difference can be found between the results in the model and the actual behaviour of the girders (such as rotations and sidewards movement). These effects are due to the way linkage is modelled and it is further discussed in section 13.

8.1.4.3 Deck joint response

The static response of the joint to a vertical load is dependant on the normal- and shear forces in both the deck board and the longitudinal girder.

In section 8.1.4, the reduction of compressive axial forces in the longitudinal girders, is caused by the larger transverse stiffness of the deck joint. The joint will transfer part of the compressive forces to the deck, to which they will influence the in-plane shear present in the timber deck boards. Figure 8.14 shows how the fully restrained connection will transfer some of the axial compressive forces in the longitudinal girders to an in-plane shear force in the deck.

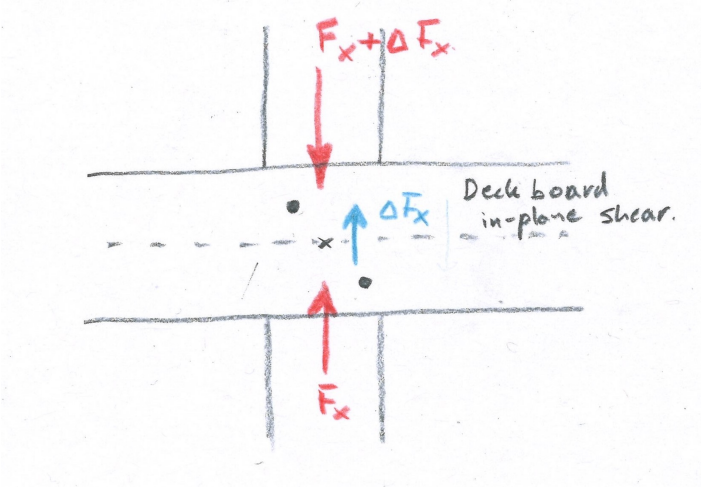

Figure 8.14: Sketch on how the fully restrained connection transfers part of the axial load in the longitudinal girders to the deck plate as a shear force

In terms of local behaviour, a wheel load between two longitudinal girders can cause the neighbouring bolted joints to be subjected to bending moments around the local y-axis as shown in figure 8.15. This bending moment will translate to tensile bolt forces i.e. pull-out of the bolt.

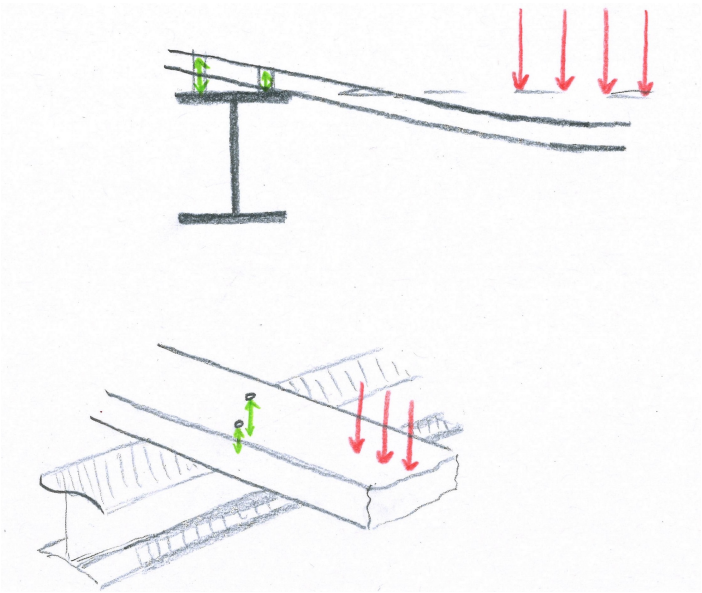

Figure 8.15: Sketch on how the fully restrained connection transfers vertical forces on the deck via bending moments in the joint to the longitudinal girder.

These asymmetrically exerted tensile bolt forces can cause local bending in the flanges, it can bend the web and the longitudinal girder cross section can rotate and translate as a whole. Figure 8.16 shows the possible deformation of the longitudinal girder due to the tensile forces in the bolts.

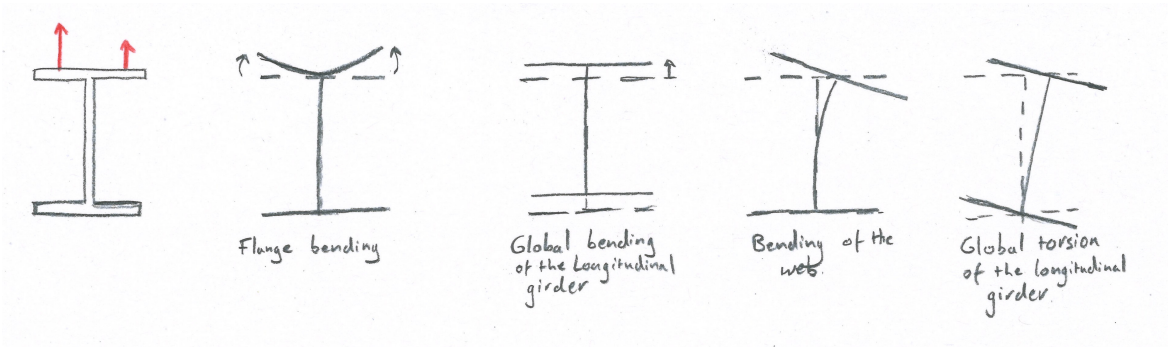

Figure 8.16: Response of the longitudinal girder to a bending moment in the deck joint due to a vertical wheel load on the deck.

So far, only static responses have been discussed. In reality however, a hysteretic response is expected due to cyclic loading of the bridge deck by passing traffic conform with e.g. the Foschi model [26]. The cyclic response can change the joint stiffness over time.

8.2 Horizontal load case: collision

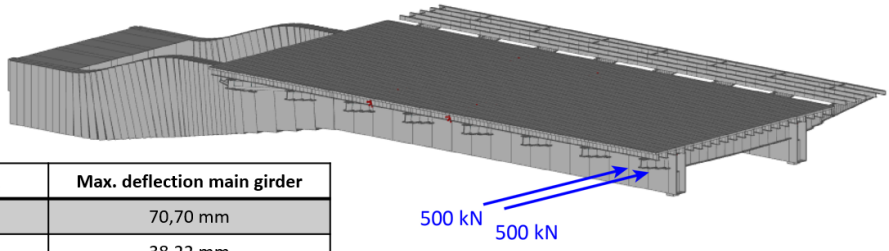

	Max. deflection main girder
Lower bound	70,70 mm
Upper bound	38,22 mm

Figure 8.17: Horizontal load case including maximum horizontal main girder deflection values for the upper- and lower bound

8.2.1 Lower bound situation

For the horizontal load case, the displacements in the connections for the current deck boards, with a low stiffness in the connectors (figure 8.3), are shown in figures 8.18a and 8.18b. For the vertical load case, connectors near both bridge leaf supports, are embedding (green dots) in the local y- direction (see figure 8.4b). Whereas for the horizontal load case, mainly connectors above the main girder near the rotation point are embedding in the y-direction.

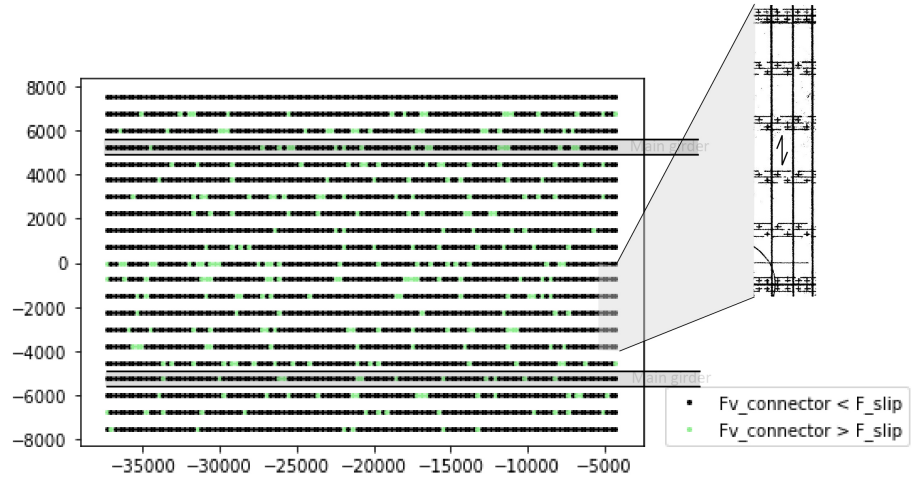

(a) Shear forces (local x- direction) in connections in case of the lower bound situation.

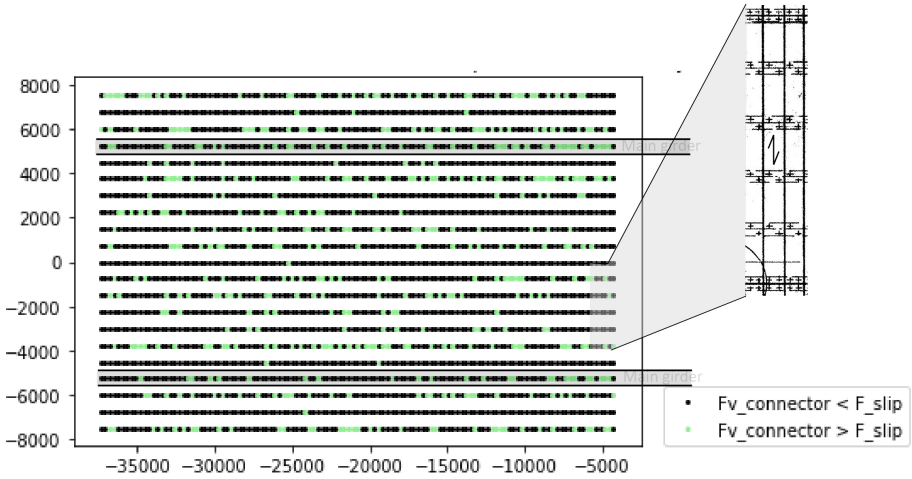

(b) Shear forces (local y- direction) in connections in case of the lower bound situation.

Figure 8.18

8.2.2 Upper bound situation

For the upper bound situation, the shear forces in the connections are given in figures 8.19a and 8.19b for both the local x- and y- directions. Large shear force values in deck connections will mainly be expected above the main girders near the rotation point of the bridge leaf.

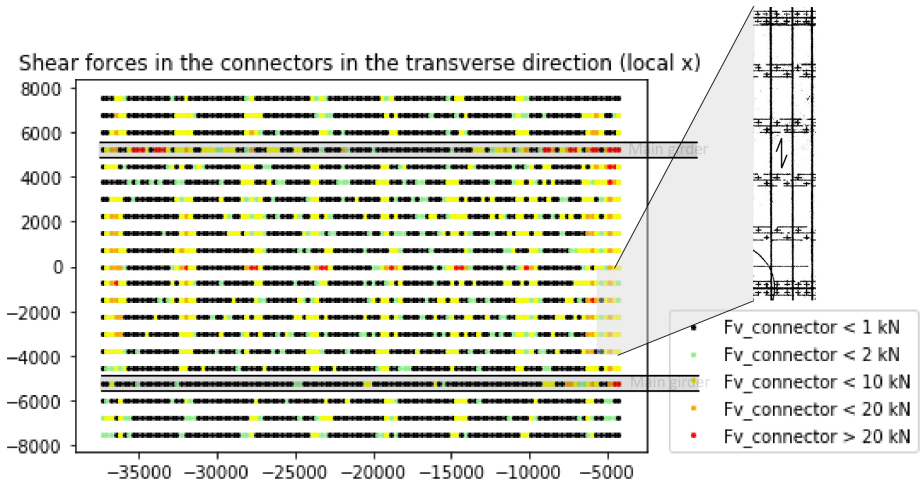

(a) Shear forces (local x- direction) in connections in case of the upper bound situation.

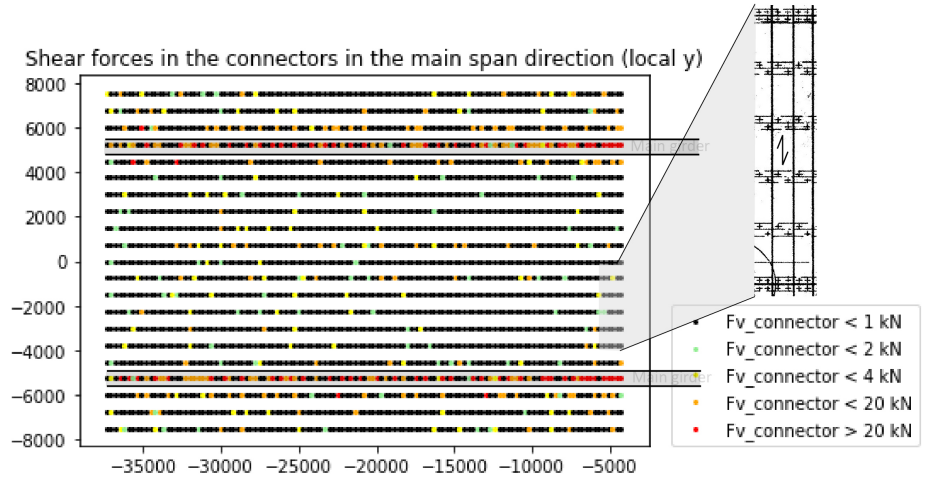

(b) Shear forces (local y- direction) in connections in case of the upper bound situation.

Figure 8.19

8.2.3 Lower- vs upper bound

Table 8.2 shows the difference of maximum forces, moments and deflections in the different structural elements.

Structural elements	Lower bound max.	Upper bound max.	Gain / penalty of interaction
Deck boards			
Axial force compression (local x)	-0.09 kN	-93.57 kN	+ 103867%
Axial force tension (local x)	0.09 kN	153.88 kN	+ 170878%
Horizontal shear force (local y)	0.08 kN	39.79 kN	+ 49638%
Vertical shear force (local z)	2.73 kN	30.76 kN	+ 1027%
Board- to- board compression (global x)	0 kN	-122.61 kN	+ ∞%
Board- to- board tension (global x)	0 kN	166.58 kN	+ ∞%
Deck connections			
Shear force (local x)	0 kN	130.39 kN	+ ∞%
Shear force (local y)	0 kN	88.48 kN	+ ∞%
Bending (local zz)	2.0 kNm	10.7 kNm	+ 400%
Longitudinal girders			
Axial force (local x)	194.72 kN	280.27 kN	+ 44%
Horizontal shear force (local y)	32.28 kN	194.40 kN	+ 502%
Vertical shear force (local z)	18.62 kN	54.93 kN	+ 195%
Bending (local yy)	1.27 kNm	21.25 kNm	+ 1573%
Bending (local zz)	25.86 kNm	21.02 kNm	- 19%
Cross girders			
Axial force (local x)	837.27 kN	713.18 kN	- 15%
Horizontal shear force (local y)	99.36 kN	59.67 kN	- 40%
Vertical shear force (local z)	96.69 kN	-147.93 kN	+ 53%
Bending (local xx)	1.39 kNm	0.41 kNm	- 71%
Bending (local yy)	-463.46 kNm	-549.14 kNm	+ 18%
Bending (local zz)	64.70 kNm	29.71 kNm	- 54%
Stability members			
Axial force (local x)	-824.90 kN	-68.56 kN	- 92%
Horizontal shear force (local y)	31.27 kN	7.83 kN	- 75%
Vertical shear force (local z)	7.06 kN	2.10 kN	- 70%
Main girders			
Axial force (local x)	2971.05 kN	3113.83 kN	+ 5%
Horizontal shear force (local y)	800.35 kN	815.65 kN	+ 2%
Vertical shear force (local z)	-358.38 kN	-261.96 kN	- 27%
Bending (local xx)	858.20 kNm	1525.23 kNm	+ 78%
Bending (local yy)	3421.06 kNm	2322.75 kNm	- 32%
Bending (local zz)	2801.68 kNm	2063.55 kNm	- 26%
Deflection (global y)	70.70 mm	38.22 mm	- 46%

Table 8.2: Horizontal load case: maximum/minimum forces, moments and deflections for structural elements in the upper- and lower bound situations

8.2.4 Responses to horizontal load

In response to a horizontal collision force, the main girders and cross girders are still able to rotate at the riveted connection in the weak direction (around the global z- axis). The bracing elements, together with the rotational stiffness of the cross girder- to- main girder connection, limit the rotation of the bridge leaf. Figure 8.20 shows a top view of the deformed main girders, cross girders and bracing elements under a static collision load of 1 MN. The case depicted is the lower bound situation. Comparison of the main-/cross girder grid to the perfect rectangle, shows the significant rotation in the main girder- to- cross girder connections.

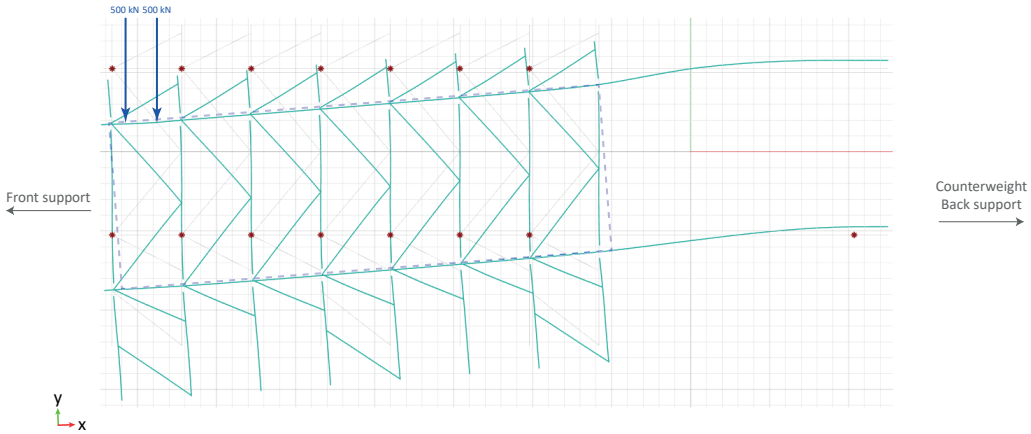

Figure 8.20: Lower bound response to a static collision force, showing the deformed main girders, cross girders and bracing elements

In case of the upper bound situation, a monolithic plate with deck connections restrained in all directions, limits the relative rotation between the cross- and main girders. When the total in-plane distortion of the structure is decreased, by the application of a monolithic deck plate, the full bridge leaf will have significantly less deformation in the global y-direction. However, on a local level, this will have an effect on the deck elements and joints. This can be seen in appendix G and table 8.2 highlighting the maximum forces and bending moments in the different structural elements for the upper- and lower bound situation. In general, the total deflection and forces/moments in the cross girders and stability members decrease, while forces in the deck and longitudinal girders significantly increase.

The largest difference to be observed in case of applying a monolithic plate as a deck, is the decrease in axial force in the stability members. In case of the lower bound for a static collision force, stability members are subjected to extremely large axial forces. For the upper bound these forces are taken mainly by the longitudinal girders and deck plate. The deck joints in this situation are also subjected to extremely large forces, as can be seen in figures 8.19a and 8.19b.

Chapter 9

Principle of hybrid interaction

In this chapter, it will be highlighted how hybrid interaction is quantified in other research. Hereafter, different approaches will be stated based on literature and finally, a short conclusion will be stated on which approach was chosen for this research.

9.1 Literature review

In literature, some examples can be found in terms of determining the degree of hybrid interaction (in case of slipping connectors).

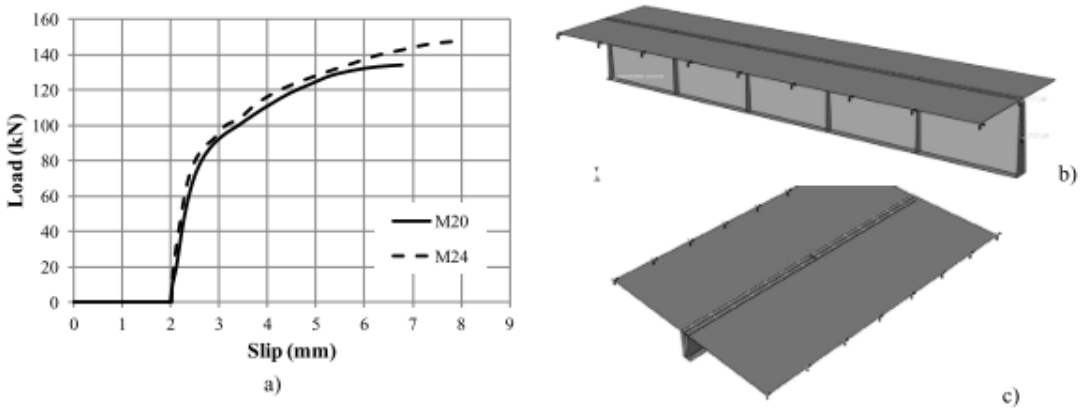

Figure 9.1: a) Non-linear curve and b) c) girder geometry of the ABAQUS FE model [27]

In a research published by Todorovic et al. [27], the hybrid interaction of a prefabricated steel- concrete composite bridge deck was analyzed by testing and FEA in case of slipping connectors. For a given geometry and standard shape of a load-, displacement curve (figure 9.1), the support reaction versus the deflection of the girder are plotted for different slip values (figure 9.2). The FEA was performed in ABAQUS.

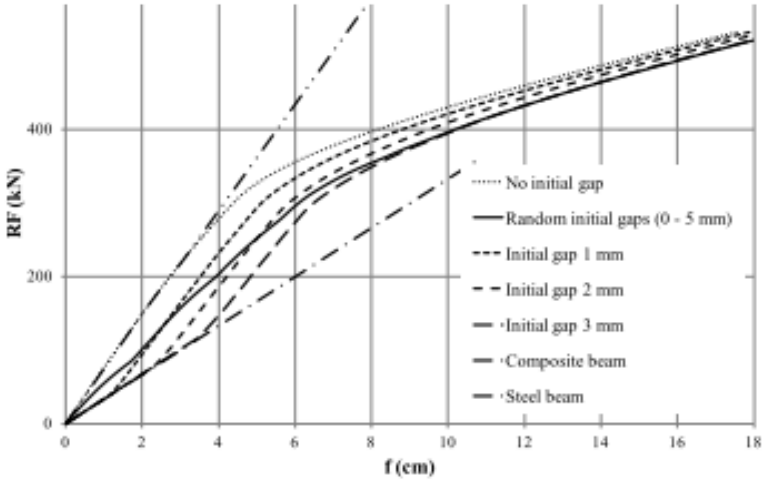

Figure 9.2: Support reaction vs girder deflection diagram for different slip values/distributions in case of a hybrid steel- concrete beam [27]

The hybrid interaction in this research is characterized by the amount of dead load 'q' [kN/m] applied to the girder, that is needed to overcome initial gaps in the connectors. A support reaction versus deflection relation presents the comparison for different distributions (e.g. uniform or random) of initial gap sizes.

In 2005, K.T. Park et al. [28] published a paper on the degree of composite action of a bolted GFRP bridge deck- to- steel girder system. Tests and FEA (in ABAQUS) have been performed for the composite system. Figure 9.3a and 9.3b respectively show the specimen shape and sensor attachment locations.

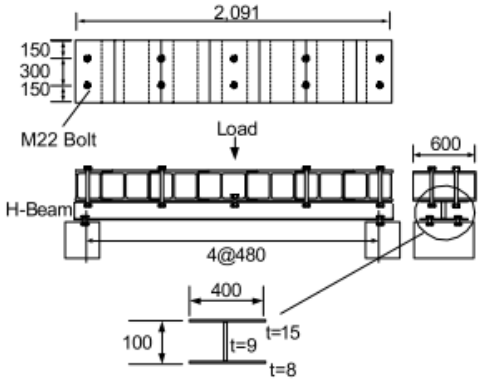

(a) Specimen shape and specification [28]

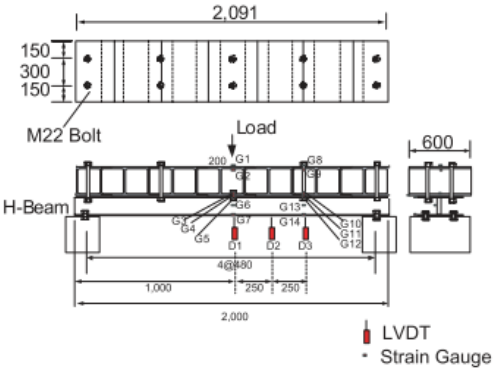

(b) Sensor attachment locations [28]

Figure 9.3

Figure 9.4 shows the method of modelling a bolted connection of the FRP deck and steel girder [28]. No initial slip is assumed to be present in the connectors. From the FEA, load-, displacement curves can be derived for the H-beam, the FRP deck and their combination by bolted connections every 48 cm (figure 9.5).

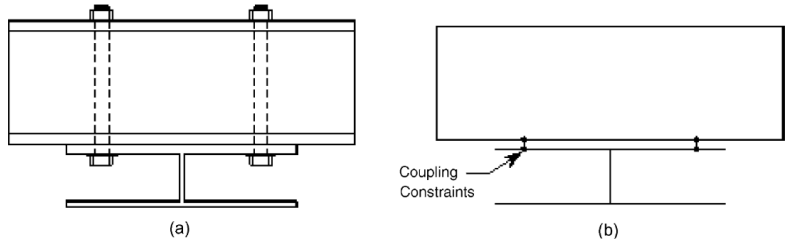

Figure 9.4: Method of modelling a bolted GFRP deck- to- steel girder connection [28]

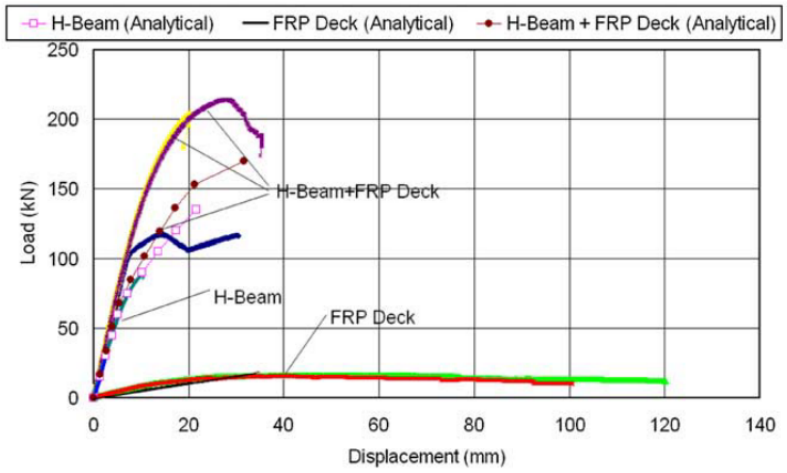

Figure 9.5: Load-, displacement curve [28]

Figure 9.6a specifies the behaviour characteristics of the FRP deck (compression, tension). This tension- compression can again be seen in the strain diagram of figure 9.6b (specimen BCG-1 as an example). The shift of the neutral axis, measured at a shear connector, for several specimen, relative to the upper bound and lower bound situation, are given in figure 9.7. The upper bound in this case will be the neutral axis position for full theoretical hybrid interaction between the FRP deck and the H-beam, whereas the lower bound is the neutral axis value for the use of just an H-beam.

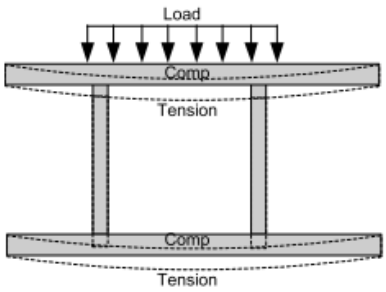

(a) Behaviour characteristics of FRP deck [28]

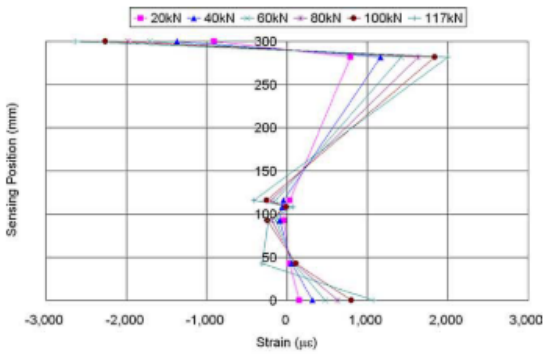

(b) Strain diagram for bolted GFRP- to- steel composite [28]

Figure 9.6

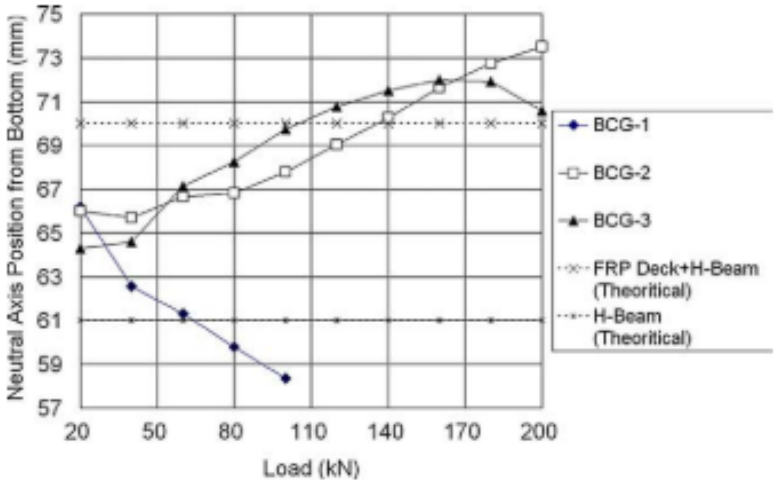

Figure 9.7: Comparison of neutral axis position for different specimen to calculate degree of composite action [28]

9.2 Different approaches

As stated before in the research of Park [28], one way would be to measure (or determine) the shift in neutral axis position for a simply supported beam. Another option would be to measure the difference in slip between the bottom of the deck and the top of the steel girder at connectors near the supports. For a simple case, e.g. having two beams on top of each other or a concrete deck atop of a steel girder over a certain span, these practices would suffice. However, a bascule bridge leaf, is more complex to analyse, due to its variety of structural elements present.

For a bridge leaf, having both longitudinal (main girders, longitudinal girders) and transverse elements (Cross girders, timber deck boards), measuring hybrid interaction in a single location by strain difference in a connector is challenging. An option would be to check what connectors are subjected to the largest shear forces in both the local x- and local y- directions. These connectors could then be evaluated in terms of relative slip between the top of the steel girder and the bottom of the timber deck board. However, when assigning distributed values for the load- displacement curve parameters of each joint in both directions, this discrete method is not accurate, since large differences could exist between nearby joints. In this case multiple connectors at locations where large shear is expected should be measured and compared.

Another approach, would be to determine the consequence of hybrid interaction: the total deflection of the structure and compare this to the upper- and lower limits. This will provide a percentage of hybrid interaction relative to the upper- and lower bounds. The total deflection in this case is assumed to be equal to the maximum total deflection of the main girders in the direction of the applied load case.

9.3 Conclusion

Common practice from literature would be to measure relative slip between the bottom of the deck and the top of the supporting girder, near the girders' supports.

However, in a traffic bridge leaf, measuring individual elements for their relative slip, will be insufficient when discussing hybrid interaction of the structural system (the bridge leaf) since individual connectors could have largely varying properties.
Therefore, it would be suitable for this research to compare the total deflection of the bridge by regarding the maximum total deflection of the main girders relative to the lower- and upper bounds for each load case. This method is not preferable when the considered girder for measurement deflects locally.

Part IV
Analysis

Chapter 10

Modelling description

In order to perform an iterative analysis (explained in chapter 11) to investigate the current degree of hybrid interactions, some assumptions have been made. The first topics to be discussed are choices and challenges regarding the used beam model (see also: appendix B). Hereafter, different assumptions for modelling the connections and the deck boards are explained, followed by a short conclusion.

10.1 Modelling the bridge leaf

This section will first shortly highlight the decisions made regarding the full bridge leaf model. Then the joint types and load cases applied will be discussed.

10.1.1 Full bridge leaf model

The bridge leaf of the Bridge across the Beneden Merwede is modelled in a finite element model. This model mainly consists of beam elements (1D) meaning that all nodes have three rotational degrees of freedom and three translational degrees of freedom. The FE program solves the equations in each node for both "Bernoulli" bending and "Timoshenko" shear deformation.

One of the advantages of using a beam model is the effectiveness. By running a linear analysis on a beam model, distributions of forces and moments can quickly be found for static load cases, even with a large number of elements. However, beam elements do not simulate plate action or through thickness behaviour. Another disadvantage is that a beam model is not able to simulate local bending of webs and flanges of girders, whereas a shell model can.

The beam element model described in appendix B of the existing bridge was made by Arup to simulate the forces in the elements and verify their strength, stability and stiffness. The model was used to make a recommendation on the safety of the bridge and whether to renovate or replace. For some connections separate local curved shell element models had to be made and were then translated into spring elements, having a rotational stiffness. For the strength verification of this bridge by Arup, the leaf was modelled in shell elements as well, but for this research the beam model is used.

10.1.2 Joint types

For further understanding of the bridge leaf structure, it is important to consider the way elements are connected to each other and how they were simplified in a verification model. Figure 10.1 shows a simplified perspective of a cross girder-to-main girder joint, but also displays the longitudinal girders and deck boards above it.

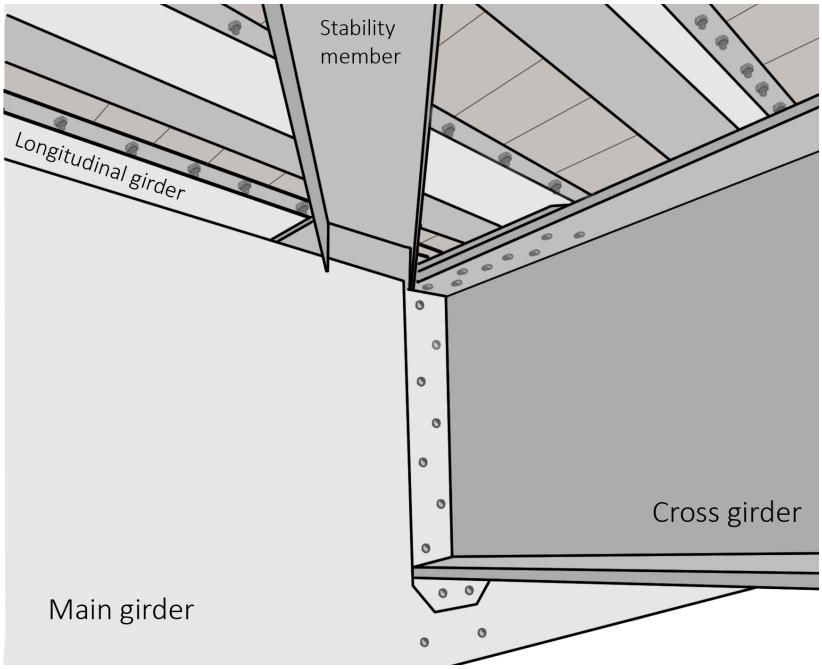

Figure 10.1: View of a cross girder- to- main girder connection location

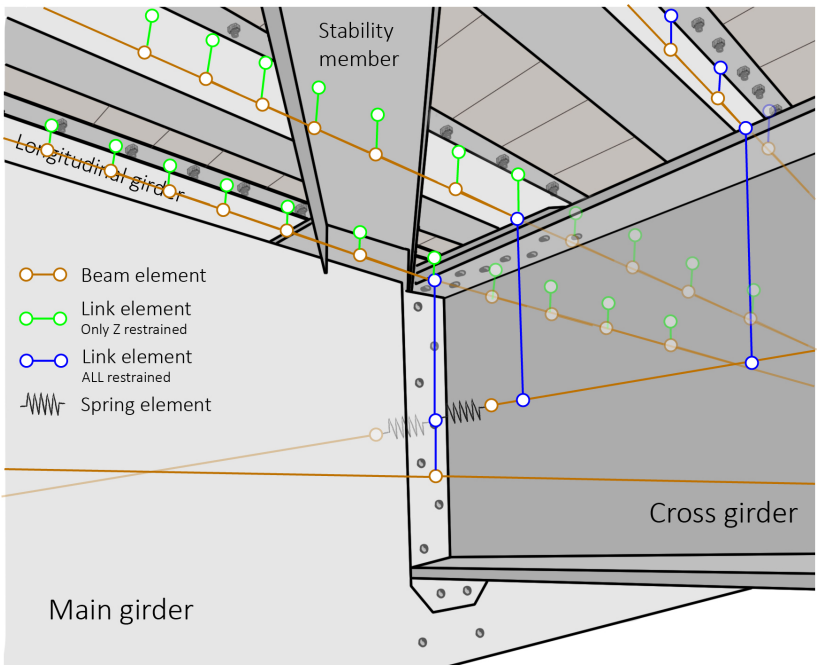

Figure 10.2: Perspective view of the way realized connections are currently modelled

For the verification model of the BBM in GSA (Finite Element program), beam, link and spring elements were used. Figure 10.2 shows the same perspective view as figure 10.1, but

additionally displays the type of elements used to create the beams and connections. For the sake of clarity in this figure, the deck beams have not been displayed as orange beam elements, but are present in the models to connect the other ends of the longitudinal girder- to- deck links (the uppermost nodes in figure 10.2).
Also, the stability member was not considered in this figure, to maintain a clear display of the other elements modelled. Stability members (or: bracing elements) are welded to the main- and cross girders. At every intersection of such a stability member with a longitudinal girder, they were welded together.

The beam ends have been connected by two bolts to one side of the longitudinal girder flange and are modelled by linking the two nodes and restraining all degrees of freedom. The intermediate beam- to- longitudinal girder connections are modelled by a linkage with a restraint in Z- direction only. The deck beams should not be able to slide off the girders and should therefore be restrained at both ends. The intermediate links should minimally have a restraint in Z- direction, which is the most conservative way to model the deck connections.

Secondly, the cross girder- to- longitudinal girder connection is assumed to be restrained in all directions, since the longitudinal girders are welded on top of them at all sides. The same can be said for the longitudinal girder directly above the main girder; they are welded together along their length. The model however, only links these two together by restraining all directions, at certain intervals at a distance of 5 deck elements.

Lastly, the cross girder- to- main girder connection is rather more complex. The welded end plate of the cross girder is connected by several rivets to the main girder. A local model of curved shell elements was made to determine the rotational and translational stiffness of the joint. These stiffnesses are input values for the girder- to- girder spring elements.

More information about the beam model and how all the elements were constructed and connected, can be found in appendix B and chapter 3. Figures B.31 and B.32 elaborate all the possible restraints, springs and releases for all types of connections.

10.1.3 Load cases

For the analysis of the hybrid interaction of this bridge, only extreme load cases were considered. The first load case would be a vertically distributed load representing a bridge full of trucks. The second load case would be a horizontal load on the main girder for ship collision. Chapter 7 specifies the basis of choosing the load cases and specifies the magnitude and distributions of the loads.

10.2 Assumptions for modelling deck connections

For the deck connections, it is key to first decide on the important stages in the load-, slip behaviour of a joint for this research. Consequently, two critical parameters determining the load-, slip curve will be discussed: slip modulus K_{ser} and the free slip.

10.2.1 Load-, displacement stages

Pretension loss can be quicker for larger hole clearances, as discussed in section 5.1.1. However, for these timber- to- steel connections, a nominal hole clearance (i.e. normal hole

size) is assumed. The period for pretension loss in timber bridge deck connections is currently unknown. Preferably, it should be researched by analyzing measurements of pretension force in bolts at different locations in an existing timber deck bridge. It is observed during annual inspection, that most bolts (for the BBM) are fully untightened, when re-applying a pretension force of 35 kN after one year. Especially the bolts in connections near the main girders, are completely loose, due to repetitive heavy traffic on those lanes.

For the generic case, it is assumed that no pretension is present in the bolted connections, so the load- displacement curve starts by a free slip plateau. It should however be mentioned that for a short period of time directly after re-tightening the bolts, a high initial stiffness is present. This will be mentioned when discussing the results of the iterations in chapter 12.

The free slip stiffness K_{slip} is close to zero, but has an assumed low value of 100 N/mm in this research. The amount of free slip in mm depends on certain assumptions, which are later discussed in section 10.2.3. The value of K_{slip} is solely based on convenience for modelling (stiffness cannot be zero) and friction of the steel- to- timber surface is not taken into account.
The elastic stage is characterized by the slip modulus (or: stiffness during embedding), which will, be explained later in section 10.2.2.

Plastic deformation (i.e. ductility of the joint) and the point of fracture will not be considered, since currently there are no signs of damage in either the bolt or the surrounding timber. If single-bolted steel-to-timber connections start to show shear forces in a range of 80 to 100 kN, one should consider to take the plastic deformation and fracture stage into account for the assumed load-, displacement curves.

The load-, displacement stages and main variables to be distinguished for the analysis using the secant stiffness method, are given in figure 10.3. The secant stiffness method adapts the secant stiffness for every iteration for the analysis based on the results from the previous iteration. The method is explained in chapter 11.

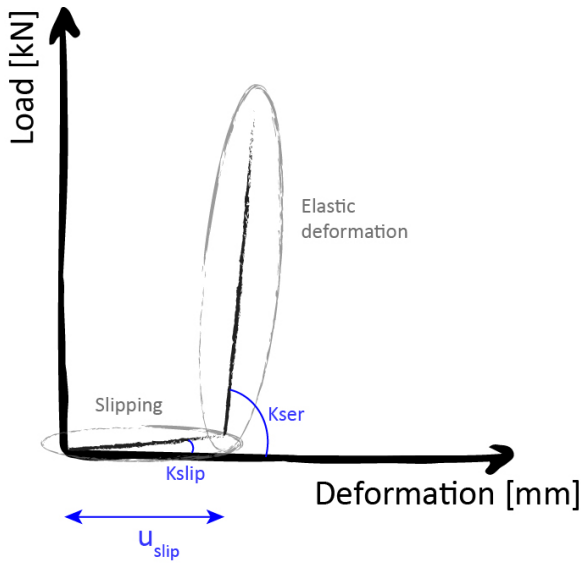

Figure 10.3: Assumed load-, displacement stages and variables

10.2.2 Slip modulus K_{ser}

In chapter 5, the slip modulus K_{ser} for a single bolted connection in Azobé is discussed. K_{ser} can either be obtained from test results or it can be calculated by a formula given in the Eurocode. Figures 5.13a and 5.13b from tests performed by Sandhaas [13], suggest a large similarity between test results and calculated values by the Eurocode equation using the tested mean density for a single dowel. A larger amount of dowels decreases the correlation between test results and Eurocode results.

The value for the slip modulus K_{ser} used for the rest of this research is calculated from the Eurocode formula using test values for the mean density of Azobé. The test values of the mean density for Azobé are clustered around 1050 kg/m^3. The mean value of K_{ser} for a single- bolted connection is calculated using equation 10.1.

$$K_{ser,\mu} = \frac{2 * \rho_m^{1.5} * d}{23} \tag{10.1}$$

Multiplication by a factor 2 is due the connection being a timber- to- steel connection, instead of timber- to- timber connection [4].

The standard deviation for the slip modulus is assumed to be 20%, since from tests [13], it appears standard deviations for the slip modulus in Azobé can be anywhere between 10% and 35%.

In section 5.1.3, different suggestions from both the Eurocode and the Swiss code are given for the use of the slip modulus K_{ser} in timber structures. For the continuation of this research, it has been assumed that the slip modulus is similar for any load direction relative to the grain, because of the difference in load spread for the deviating direction of the grain as was discussed earlier.

For the deck joints, the bending moment capacities around the vertical axis (global z) of intermediate- and end joints are different, since the configuration of the bolt group is different. Intermediate deck joints have a larger bending moment capacity around the z-axis since their lever arm is larger in comparison to the end deck joints. General equation 10.2 is used to calculate the rotational stiffness K_r for every joint.

$$K_r = \sum_{i=1}^{n} (K_{ser} * r_i^2) \tag{10.2}$$

10.2.2.1 Effective number of dowels for slip modulus K_{ser}

In order to translate the slip modulus of a single- bolted connection into a combined slip modulus for the deck joints, an effective number of dowels could be implemented. However, the research of Sandhaas [13] investigated the effective number of dowels by testing Azobé joint with respectively 3 and 5 dowels. For both of the test results for joint strength for 3 and 5 dowels, the effective number of 24mm dowels for Azobé was found to be equal to the number of dowels. This same effective number of dowels can also be used to calculate the combined slip modulus of the joint. In other words; for connections in Azobé with 20mm HSS bolts, the slip modulus can be multiplied by the number of dowels, in this case two, to obtain the slip modulus of the deck joint in both directions (local x and y).

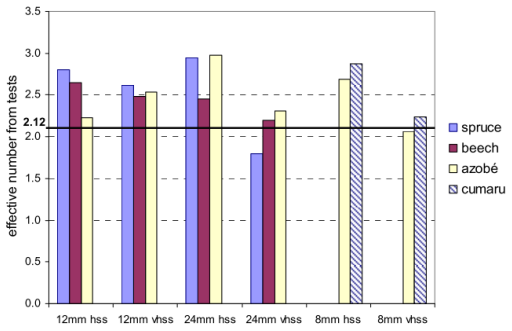

(a) Effective number of fasteners for strength of joint series with 3 dowels [13]

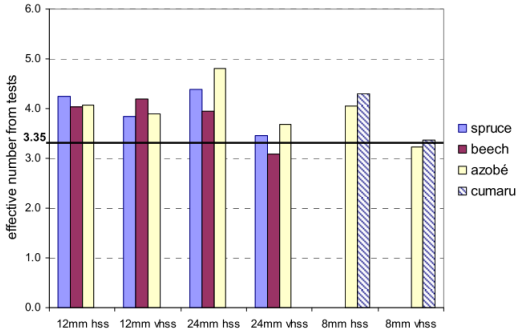

(b) Effective number of fasteners for strength of joint series with 5 dowels [13]

Figure 10.4

10.2.2.2 Distribution for slip modulus K_{ser} of two- bolted joint

Figure 10.5 shows the assumed distribution for slip modulus K_{ser} as will later be used in the analysis discussed in chapter 11. The curve fits the histogram of drawn values and the vertical line highlights the expected (or: mean) value.

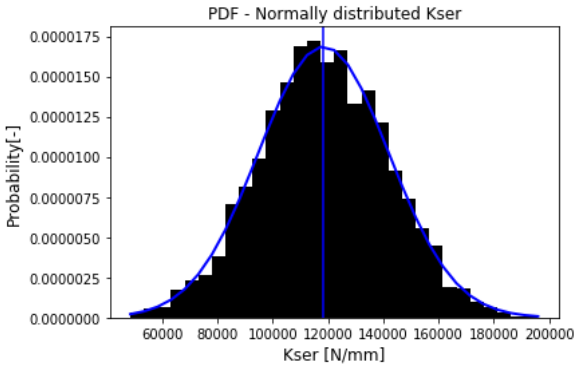

Figure 10.5: Slip modulus K_{ser} distribution for double bolted deck joint used for the static linear secant stiffness analysis

10.2.3 Free slip u_{slip}

The hole clearance (c_0) for bolts in the deck- to- girder joint are assumed to be 2mm, as specified in the original technical drawings. That means the value is within the nominal clearance limits for round holes (i.e. 2 mm clearance for 20 mm bolts, so no oversized holes are assumed).

Theoretically, a total slip of twice the hole clearance can occur for this steel- to- timber connection, but according to test results [29], slip deformations are often limited to the hole clearance value. In this case, that would mean, slip values would be inbetween 0 and 2 mm for a single bolted connection subjected to shear loading. The assumed free slip value is equal to the displacement from the bolts' initial position in the shaft to the point of embedding.

Contrary, to a normal distribution, the Weibull distribution has one closed interval at 0. This is preferable since the absolute slip value for bolted connections should always be

larger than 0. The expected slip value should be close to half the hole clearance and the maximum slip is equal to the specified clearance.

The absolute value for free slip is limited to the hole clearance c_0. Since the bolt hole is circular, a maximum free slip in the local x- direction cannot result in a maximum slip in y- direction as well. That is impossible when regarding the hole shape (see figure 10.6 for an example). To correlate u_{slip} in both directions, two stochastic variables have been used to draw values within the clearance limits.

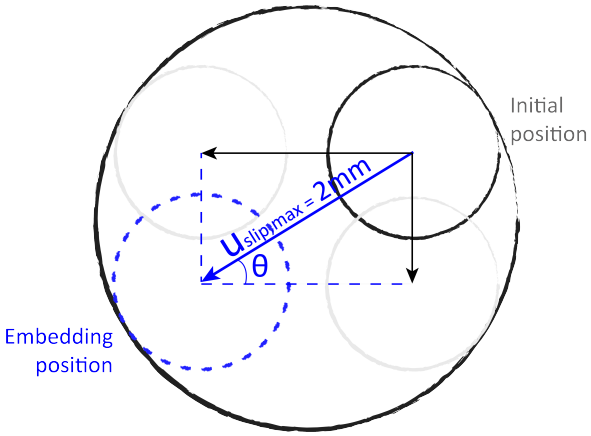

Figure 10.6: Example for the correlation between the free slip value in the x- and y- direction in terms of possible bolt positions

The stochastic variables that characterize the free slip values in both directions are θ and R. Figure 10.7a shows distribution types for the variables and figure 10.7b shows the correlation between $u_{slip,x}$ and $u_{slip,y}$. The free slip in respective x- and y- directions can be calculated by using the geometric equations stated in the figure.

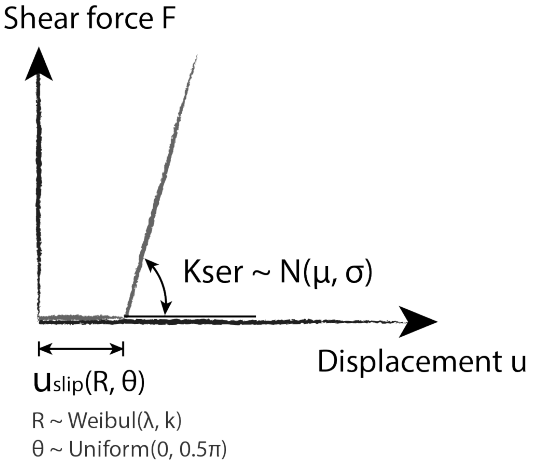

(a) Load-, displacement curve including distributions for stochastic variables

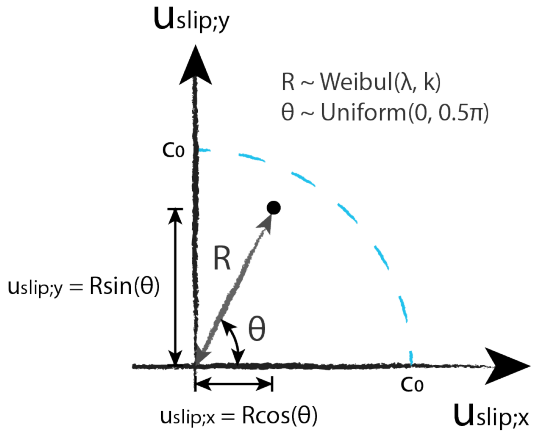

(b) Correlation between $u_{slip,x}$ and $u_{slip,y}$

Figure 10.7

The angle θ is uniformly distributed from 0 to 0.5π, since absolute values for the free slip are to be obtained. Slip factor R is Weibull distributed with an assumed shape factor k = 2 and a scale factor $\lambda = 0.8$. This results in a distribution of slip values within the bounds of 0 and 2 mm, while the event that the slip is equal to the maximum of 2 mm is highly

unlikely. Figure 10.8 shows the Weibull distribution including values. The blue curve displays the Weibull function and it properly fits to the histogram of drawn values. The vertical blue line shows the expected value ($\lambda = 0.8$).

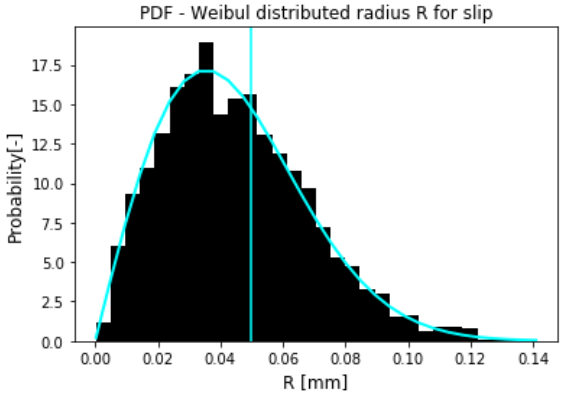

Figure 10.8: Weibull distribution of slip parameter R ($\lambda = 0.8$; k = 2)

As can be seen in figure 10.9a, the variable R is Weibull distributed. The values of this distribution can be drawn from this distribution for angles 0 to 0.5π. Figure 10.9b sketches a possible scatter plot of drawn u_{slip} values. These positive values for both $u_{slip,x}$ and $u_{slip,y}$ are used to construct the assumed load-, displacement curves.

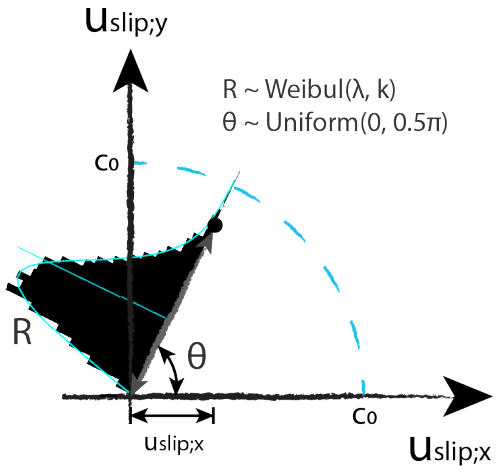

(a) Weibull distributed value R

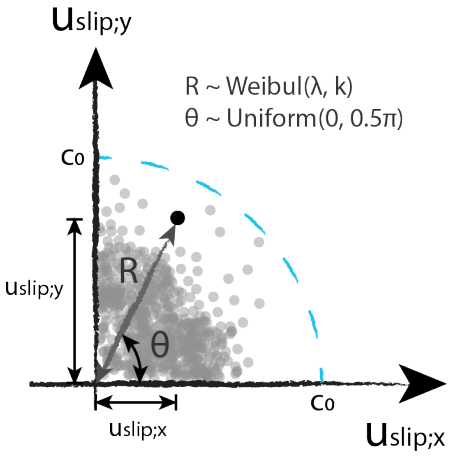

(b) Scatter plot with drawn values using the distributions R and θ

Figure 10.9

The established curve will be similar in the compressive- and tensile zone (point symmetric at the origin). However, in reality, there should also be a correlation between the tensile- and compressive zone. If, for one specific joint, an extremely large u_{slip} value is drawn from the distributions (e.g. close to c_0) for tension, the bolted connections should directly embed for compression.
But for the static linear secant stiffness analysis, this does not matter, since every joint is either in the compressive- or tensile zone and it does not change sign during the iterations. When considering cyclic/dynamic loading, the load-, displacement curve cannot be similar for the tensile and compressive zone (unless the initial position of the bolts is exactly at the center of the bolt shaft).

A deck joint with two bolts, can still result in a combined slip equal to c_0, if both bolts slip maximally for one direction. However, it is highly unlikely. Therefore the Weibull distribution was chosen such that the most likely value for u_{slip} is around 0.8mm and the shape factor allows a maximum slip of 2mm with a very low probability.

10.3 Assumptions for deck boards

For the deck boards, no board- to- board interaction was assumed, since the clearance between the deck boards is currently large (estimate: 5-10mm). The deck boards should be able to deform significantly in order to make contact. These large local bending deformations will not be induced by the specified extreme load cases. The contact could occur momentarily for extreme braking, since individual deck boards can be pushed to the adjacent one for a split second. These local effects are expected to be so small, they will not influence the global hybrid interaction. If the deck boards would be in contact anytime, the board- to- board interaction should be taken into account. For the current bridge that is not the case.

Since the deck boards are relatively narrow (280mm), the current deck is modelled using beam elements. When applying wider deck boards (e.g. double the width) more connections are made to one deck board and local stresses become larger. Therefore, it should be minded that deck boards can be regarded as beams for the analysis of the current situation, but for wider deck boards or plates, shell elements should be considered for the deck.

10.4 Conclusion

Two load-, displacement curves (local x- and y direction) should be generated for each deck joint. The free slip is considered to be correlated for both directions and the slip modulus is assumed to be similar for both directions. The key statistical distributions that are used as input for the load-, displacement curves in the secant stiffness analysis are given in figures 10.5 and 10.8. They respectively represent slip modulus K_{ser} and slip magnitude parameter "R".

Some of the assumptions for the slip modulus and the free slip values have large uncertainties. For example the wide range of standard deviations for K_{ser} and the Weibull distribution of slip parameter "R" are relatively uncertain. It is discussed later in chapters 12 and 13, whether these assumptions can have large effects on the total deflection of the bridge leaf.

Chapter 11

Analysis of current hybrid interaction

Since a great number of connectors has to be taken into account for this research, analyzing the complete bridge leaf structure non-linearly is time consuming. In this chapter, an alternative method is suggested to approximate the assumed non-linear curves for bolted connections by using a linear analysis. This method will be explained in section 11.1. The method will be verified in a simplified beam model to compare the non-linear analysis and the iterative linear secant stiffness method. The python script that was used to run the Secant Stiffness analysis, is given in Appendix J.

11.1 Iterative linear secant stiffness method

For a large amount of deck joints, it is hard to run a non-linear analysis. Even when the deck joints are all modelled by linear springs, analyzing the full bridge leaf with all its elements is challenging, especially for large loads.
Therefore, it was preferred to use a static linear analysis. However, this type of analysis presented another challenge. If load-, displacement curves are assumed for all deck joints (springs), how to approximate the non-linear curve and when does it converge to a feasible solution?

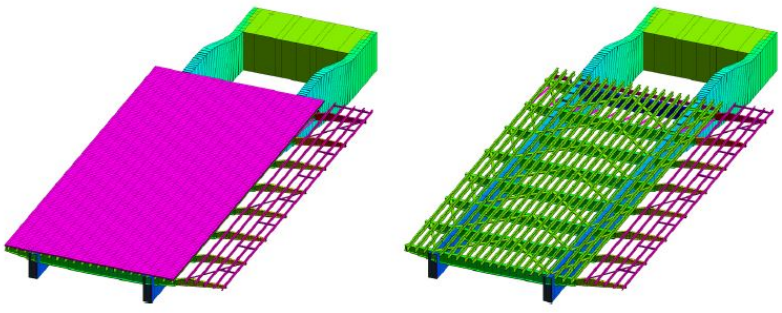

Figure 11.1: GSA beam model for the movable part of the BBM

The first step to the analysis is adapting/creating the (beam) model of the full bridge leaf (Figure 11.1 and Appendix B). All elements and connections are made in a FE program (like Oasys GSA) and the deck joints are constructed by creating small springs. In order to properly read the results of relative displacement between the bottom of the deck boards and the top flanges of the longitudinal girder, extra nodes and links had to be created.

Figure 11.2a schematically shows the constructed deck connections including all links, extra nodes and the spring. In Figure 11.2b, the elements of the deck joint in the GSA model, are given.

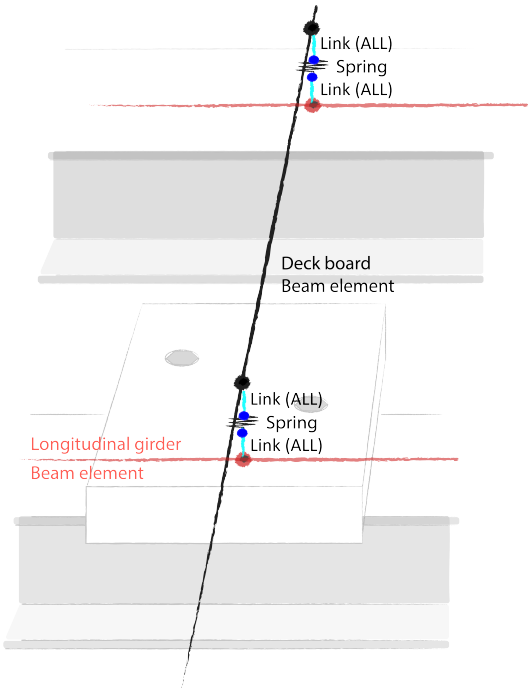

(a) Schematic representation of the deck- to- girder joint in a FE model

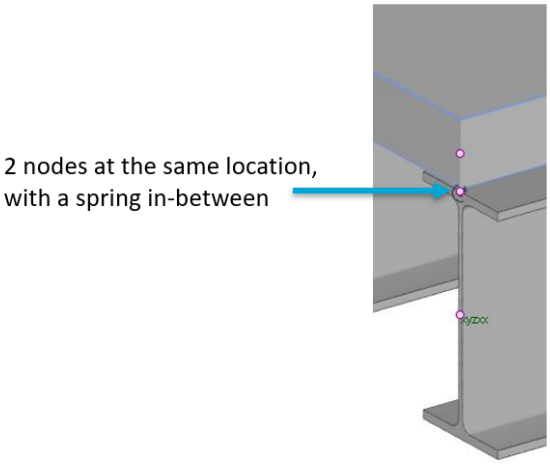

(b) Deck- to- girder joint elements in GSA model

Figure 11.2

After creating a deck- to- girder linkage in the model, the initial linear stiffness should be set to $K_{slip} = 100$ N/mm and the linear rotation stiffness to $K_{slip,r} = 10$ kNm/rad (both relatively small) to simulate a maximum slip as the initial step. The stiffness cannot be set to zero, since the model cannot analyze a spring stiffness of zero. The results after this first iteration are equal to the lower bound results. Figure 11.3 shows the assumed load-, displacement curve for a certain joint in local x- direction and the result after the first iteration with the stiffness K_{slip} and rotational stiffness $K_{slip,r}$.

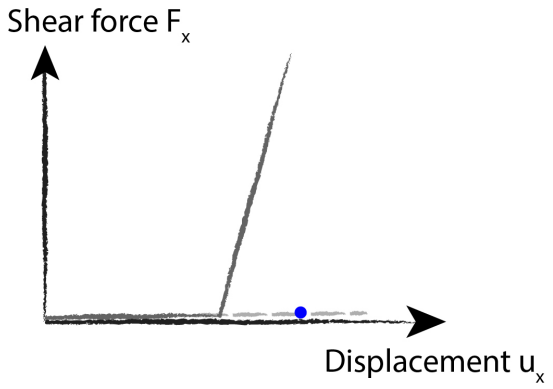

Figure 11.3: Result for joint "i" in direction x for assigned stiffness K_{slip}

Apparently, this exemplary joint should be in the embedding stage, not the slip stage. The result is not on the assumed load-, displacement curve and should be projected onto it

horizontally. Figure 11.4 shows the projection of the first iteration result onto the assumed curve. The dashed line crossing the origin and the projected result should be the new linear stiffness for the next iteration for this joint in the x- direction.

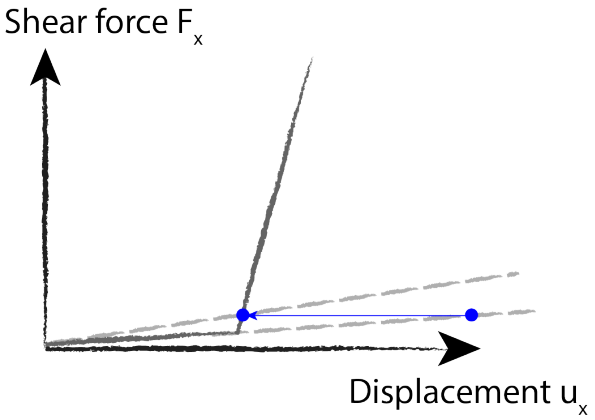

Figure 11.4: Result for joint "i" in direction x for assigned stiffness K_{slip} and projected result to the load-, displacement curve

Running the linear analysis for the full structure with adapted stiffnesses and again and again projecting the results to the curve, will result into results that get closer and closer to the assumed curve. Also, the total deflection of the bridge should stabilize after a certain number of iterations.

Therefore, a global- and local convergence criterion could be set. The global criterion is set to be 0.001 mm, meaning that whenever the difference in deflection of the main girders between iterations is equal to, or smaller than 0.001 mm, the analysis can be considered to have converged. Figure 11.5 displays an example of global convergence in a graph, having the iteration number on the horizontal axis and the main girder deflection on the vertical axis.

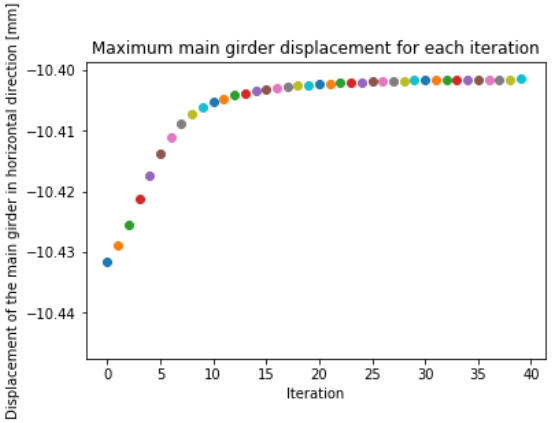

Figure 11.5: Example of global convergence; iteration number vs deflection of the main girder

The local convergence criterion is not a strict number for force or displacement, but should be a second check to see whether random deck joints have converged close to the assumed load-, displacement curve. This can be done by reviewing the analysis results and projected results as a scatter plot (see figure 11.6a) for random joints). Figure 11.6b shows an example of the shear force in y- direction for a certain joint "i" after each iteration. The

local convergence criterion is a second check for convergence.

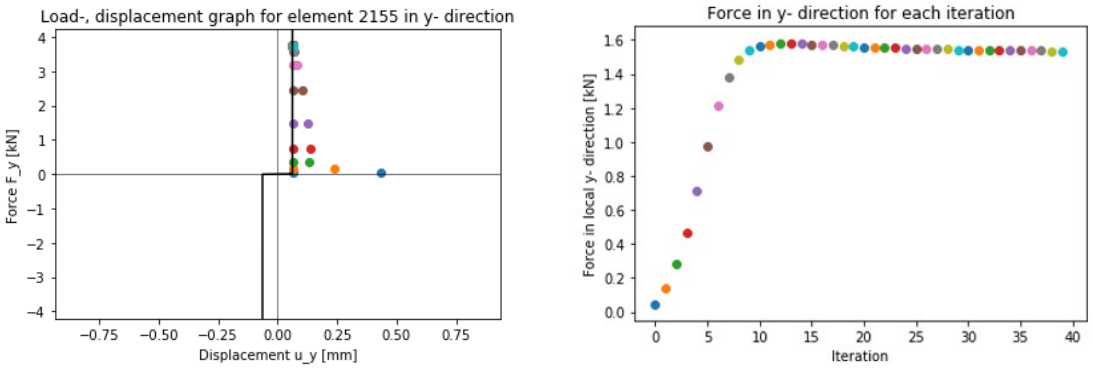

(a) Example of local convergence; iteration number vs shear force in y- direction for a certain joint 'i'

(b) Example of shear force values in the local y-direction for a certain joint "i" after every iteration

Figure 11.6

To summarize, the iterative method can be visualized as in figure 11.7.

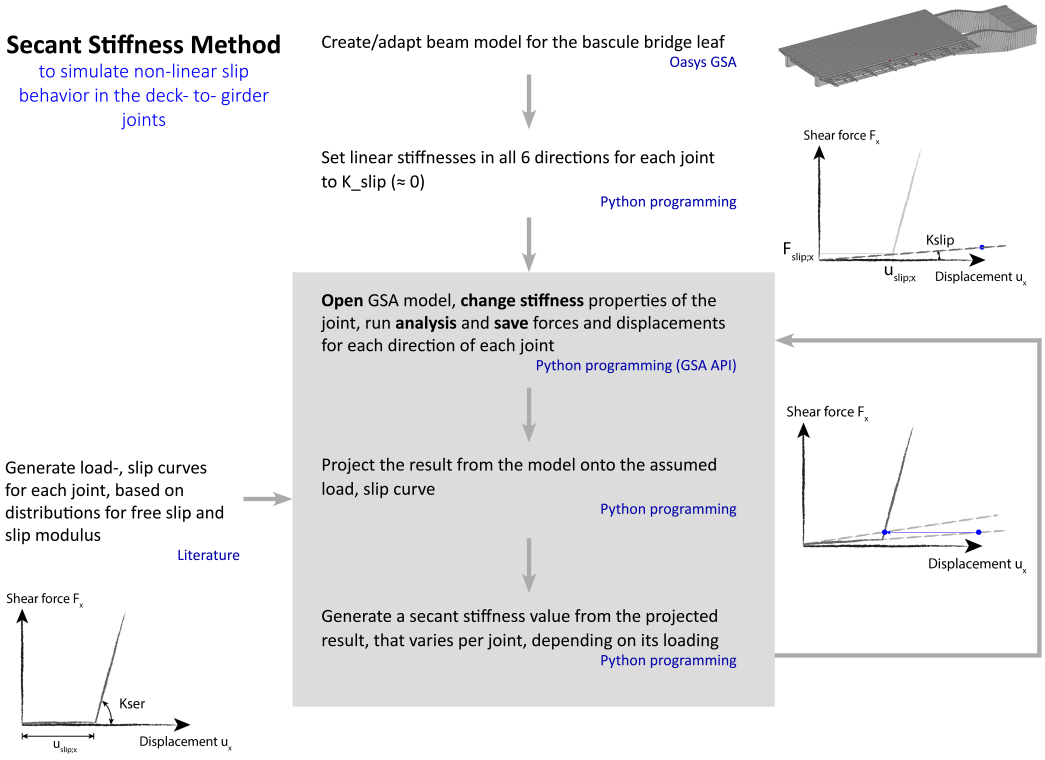

Figure 11.7: Flowchart of the static linear secant stiffness method (using GSA and python)

11.2 Validity of the secant stiffness method

Does the iterative method for a repetitive linear static analysis provide the same result as a non-linear model? To verify the Secant Stiffness Method (SSM), a comparison has been

made between a non-linear analysis and a secant stiffness analysis for the same simple model, with only a few connections to be analyzed.

First, the non-linear analysis, performed in GSA will be discussed. Hereafter, the results of the linear secant stiffness analysis will be provided. In the end, both results will be compared to conclude why the linear secant stiffness analysis is a valid alternative for a non-linear analysis.

11.2.1 Non-linear analysis (in Oasys GSA)

Using load-, displacement curves to characterize the stiffness of deck joints, generally leads to the use of a non-linear analysis. Especially the use of a physically non-linear analysis is common practise when analyzing non-linear curves.
Generally, during a non-linear analysis, load increments are applied at every step. This load increment can either be specified to be automatic or manual. At every load increment, the calculation of stresses should lead to a difference between adjacent elements that is smaller than the specified tolerances to reach convergence. For small stiffnesses in the joints, finding a stable result could be challenging. As many joints start slipping, instability of the structure will occur. This effect will be enlarged as geometrical non-linearity is taken into account as well.
Geometrical non-linearity updates the geometry and deformed shape of the structure after each load step, causing the load to be applied on deformed and displaced elements.

The non-linear model to validate the performance of the Secant Stiffness Model, has a simple configuration. Two IPE330 beams have been modelled above each other, being connected at every meter. The total span of the simply supported hybrid beam is 10 meters (figure 11.8). The numbers in brackets highlight the element numbers of the springs (or: joints).

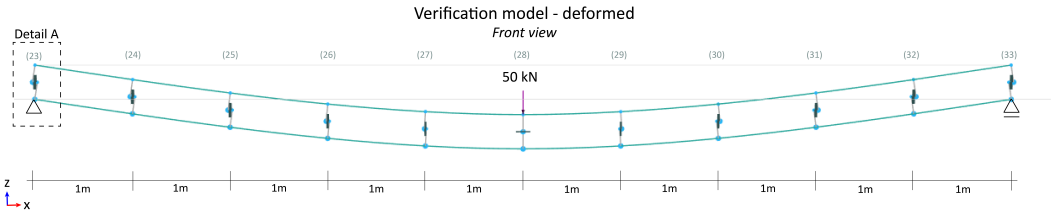

Figure 11.8: Geometry and elements of the verification model including spring element IDs

No torsional rotation is allowed by the supports at both ends of the beams. The geometrical and material properties of the two identical girders have been highlighted in appendix H. Detail A is identical to how the deck connections in the full model have been modelled (by links and a zero-length spring between the link ends). Figure 11.9 highlights the undeformed situation of detail A, including the lengths of the links.

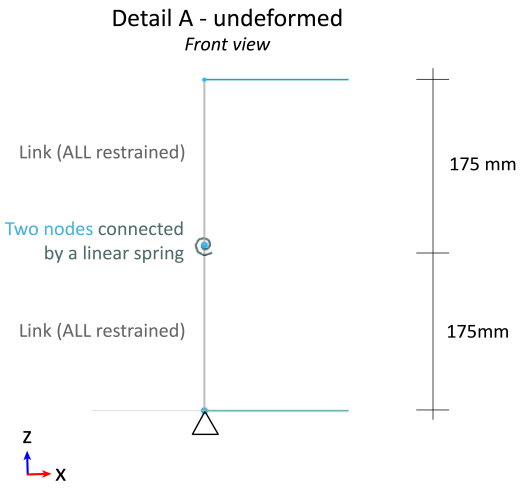

Figure 11.9: Geometry and configuration of a modelled connection (Detail A)

The spring stiffness properties are the same for every connection. The string for the spring property is given in figure 11.10. The material curve that is specified for the stiffness in the x- direction, is shown in figure 11.11.

Property	Name	Colour	Type	x		y		z		xx		yy		zz	
				Spring Curve	Stiffness	Spring Curve	Stiffness	Spring Curve	Stiffness	Spring Curve	Stiffness	Spring Curve	Stiffness	Spring Curve	Stiffness
					[N/mm]		[N/mm]		[N/mm]		[Nmm/rad]		[Nmm/rad]		[Nmm/rad]
Defaults	Spring prop. #		Axial	Linear	0	Linear	0	Linear	0	Linear	0	Linear	0	Linear	0
1	Joint	...	General	1 : Material C	0	Linear	1e+09	Linear	1e+09	Linear	1e+09	Linear	1e+09	Linear	1e+09

Figure 11.10: Spring stiffness properties in the non-linear model

	Displacement [mm]	Force [N]
1	-2	-5000
2	-1	-100
3	0	0
4	1	100
5	2	5000
6		
7		
8		
9		
10		
11		
12		
13		
14		
15		

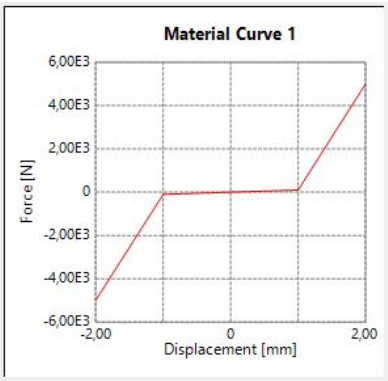

Figure 11.11: Assumed material curve (or: load-, slip curve) as input for the non-linear stiffness in x-direction

In the simple non-linear model to verify the validity of using secant stiffness method, only physical non-linearity has been taken into account. In this case, an implicit solver (GsRelax) has been used. Automatic load increments have been used and the analysis was force- controlled.

11.2.2 Static linear secant stiffness analysis (in Oasys GSA using Python programming)

The model for the Secant Stiffness Method (SSM) is identical to the non-linear model, except now, every spring element has its own property (meaning eleven strings for the

spring properties are created instead of just one, see figure 11.12). The reason for this, is every individual connector stiffness has to be adapted through the API in apython script.

Property	Name	Colour	Type	x		y		z		xx		yy		zz	
				Spring Curve	Stiffness	Spring Curve	Stiffness	Spring Curve	Stiffness	Spring Curve	Stiffness	Spring Curve	Stiffness	Spring Curve	Stiffness
					[N/mm]		[N/mm]		[N/mm]		[Nmm/rad]		[Nmm/rad]		[Nmm/rad]
Defaults	Spring prop. #		Axial	Linear	0	Linear	0	Linear	0	Linear	0	Linear	0	Linear	0
1	1	...	General	Linear	4e+04	Linear	1e+09	Linear	1e+09	Linear	1e+09	Linear	1e+09	Linear	1e+09
2	2	...	General	Linear	4e+04	Linear	1e+09	Linear	1e+09	Linear	1e+09	Linear	1e+09	Linear	1e+09
3	3	...	General	Linear	4e+04	Linear	1e+09	Linear	1e+09	Linear	1e+09	Linear	1e+09	Linear	1e+09
4	4	...	General	Linear	4e+04	Linear	1e+09	Linear	1e+09	Linear	1e+09	Linear	1e+09	Linear	1e+09
5	5	...	General	Linear	4e+04	Linear	1e+09	Linear	1e+09	Linear	1e+09	Linear	1e+09	Linear	1e+09
6	6	...	General	Linear	4e+04	Linear	1e+09	Linear	1e+09	Linear	1e+09	Linear	1e+09	Linear	1e+09
7	7	...	General	Linear	4e+04	Linear	1e+09	Linear	1e+09	Linear	1e+09	Linear	1e+09	Linear	1e+09
8	8	...	General	Linear	4e+04	Linear	1e+09	Linear	1e+09	Linear	1e+09	Linear	1e+09	Linear	1e+09
9	9	...	General	Linear	4e+04	Linear	1e+09	Linear	1e+09	Linear	1e+09	Linear	1e+09	Linear	1e+09
10	10	...	General	Linear	4e+04	Linear	1e+09	Linear	1e+09	Linear	1e+09	Linear	1e+09	Linear	1e+09
11	11	...	General	Linear	4e+04	Linear	1e+09	Linear	1e+09	Linear	1e+09	Linear	1e+09	Linear	1e+09

Figure 11.12: Spring stiffness properties in the SSM model

The same material curve has been assumed as for the non-linear model, but this will be specified and evaluated in python, not in GSA. Appendix H shows the python script used to run the SSM verification model by adapting the linear spring stiffness each iteration.

11.2.3 Differences between non-linear and SSM method

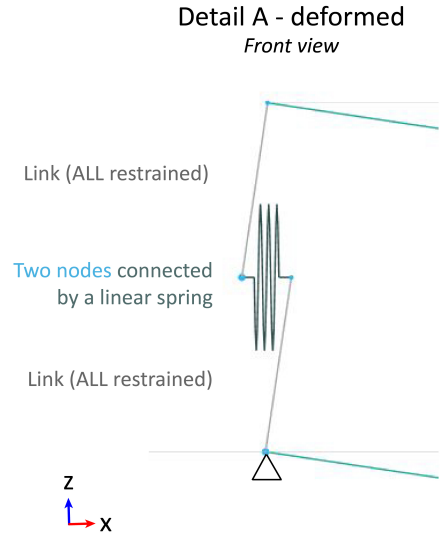

Figure 11.13: Deformation of modelled connection (detail A)

Results between the non-linear method and Secant Stiffness Method are generated for a concentrated load of 50 kN at mid-span of the beam. The joints deform in a way similar to what is shown in figure 11.13.

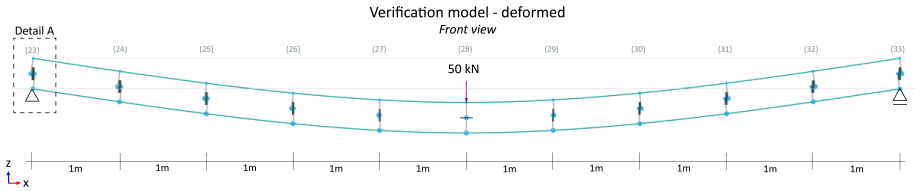

Figure 11.14: Geometry and elements of the verification model including spring element IDs

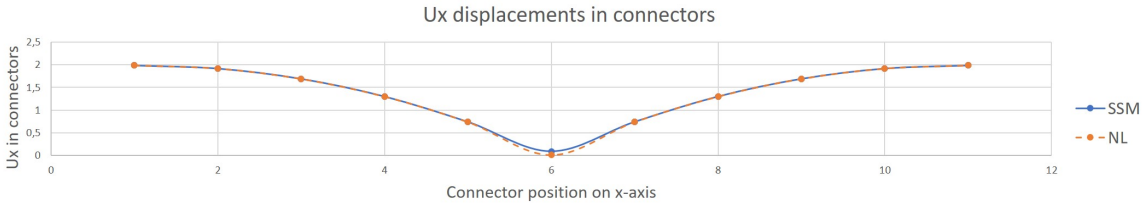

Figure 11.15: Comparison of non-linear- and SSM analysis results for elongation of shear connections (U_x)

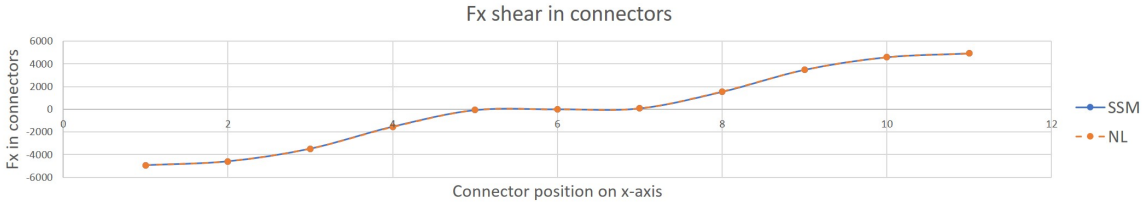

Figure 11.16: Comparison of non-linear- and SSM analysis results for shear force in connections (F_x)

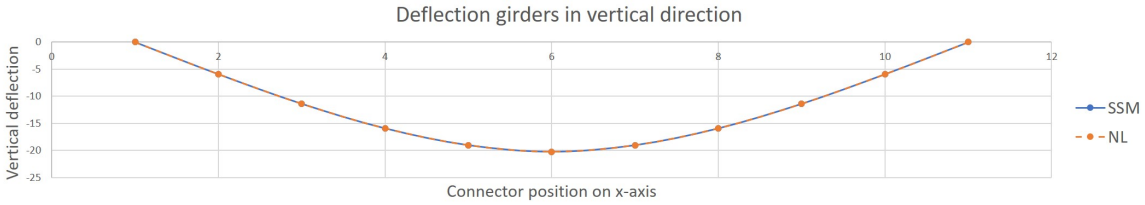

Figure 11.17: Comparison of non-linear- and SSM analysis results for total deflection of girders

The elongation in the spring (or: Ux) and the force in each spring, is compared for both methods in figure 11.15. The corresponding forces in the springs are shown in figure 11.16. Figure 11.17 compares both methods in terms of resulting deflection of the beams. The deflection values are obtained from the U_z data of the connectors (see figures H.13 and H.14, in appendix H).

The difference in results are marginal and therefore according to this short study, an iterative secant stiffness analysis would be equally accurate as the non-linear method to analyse partial hybrid interaction by non-linear shear connectors.

Further information on the SSM model, the non-linear model and the results can be found in appendix H.

11.3 Conclusion

It is important to investigate for a simple model, whether the secant stiffness analysis would be as accurate as the non-linear method. By performing a short study, shear connector forces, connector displacements and total deflection of the beam match for both methods. Therefore, for a model, consisting of a larger number of elements (such as the BBM bridge leaf), the iterative secant stiffness method could prove just as accurate and less time consuming compared to the use of a non-linear analysis.

Part V
Results

Chapter 12

Results

This chapter will highlight the results of the linear secant stiffness analysis that was discussed in chapter 11, based on the assumptions in chapter 10. Hereafter, the importance of the assumptions that were made and the different seeds will be highlighted. In the end, the hybrid interaction results in case of special situations, like directly after re-tightening the bolts or retrofitting the deck by a monolithic plate, will be discussed.

12.1 Expected current hybrid interaction

As discussed in chapter 10, the expected values of the load-, slip parameters (stochastic variables), were assumed to be 0.8 mm for the free slip and 118400 N/mm embedment stiffness for the bolt group.
This section shows the expected results for the current situation for both a vertical- and horizontal load case.

12.1.1 Vertical load case

The boxplot in figure 12.1a shows the main girder displacement results of 10 analyses for the parameters $\lambda = 0.8$ mm and $\mu = 118400$ N/mm. The shape factor of the u_{slip} Weibull distribution is always 2 and the standard deviation of the K_{ser} normal distribution is always 0.2μ, unless stated otherwise.

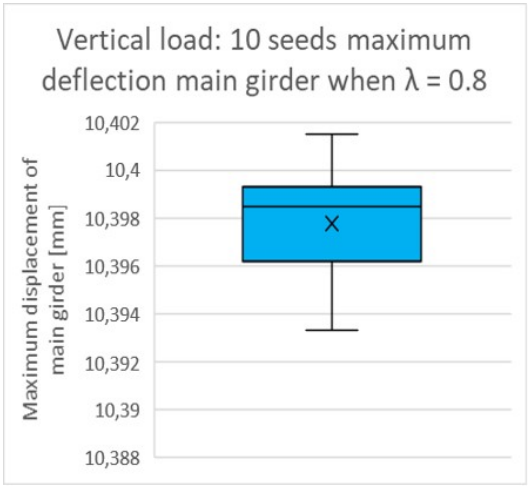

(a) Vertical load case: maximum deflection main girders for the current situation (λ = 0.8 mm and μ = 118400 N/mm connectors, timber deck boards 280 mm wide) for 10 different SSM analyses of 40 iterations

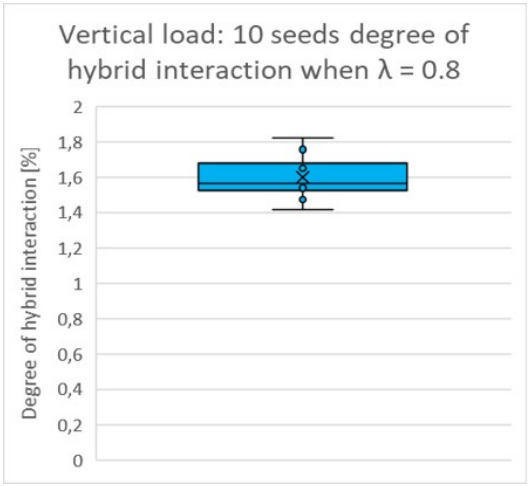

(b) Vertical load case: degree of hybrid interaction for the current situation (λ = 0.8 mm and μ = 118400 N/mm connectors, timber deck boards 280 mm wide) for 10 different SSM analyses of 40 iterations

Figure 12.1

The vertical main girder displacement results are compared to the lower- and upper bound values for the main girder deflection according to the simple equation 12.1.1. The degree of hybrid interaction is the difference between the lower bound deflection and the resulting deflection from the performed analysis, divided by the difference in lower- and upper bound deflection.

$$\text{Degree of Hybrid Interaction } [\%] = \frac{w_{lowerbound} - w_{SSManalysis}}{w_{lowerbound} - w_{upperbound}} * 100\% \tag{12.1}$$

Figure 12.1b shows a boxplot of the degree of hybrid interaction relative to the upper- and lower bounds for the vertical load case in the case of distributed slipping in the connectors and individual timber deck boards. The degree of hybrid interaction for the current situation, when the bridge leaf is subjected to an extreme vertical truck load, is expected to be close to 1.5% based on the assumptions and performed analysis.

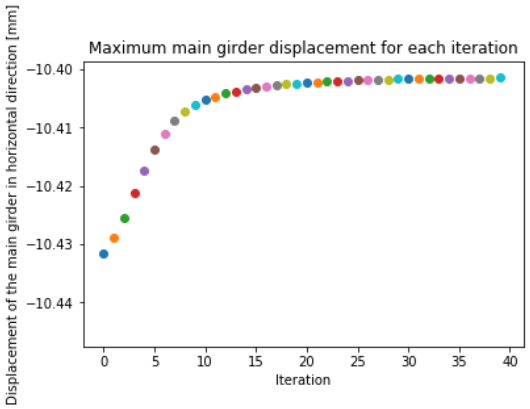

Figure 12.2: Global convergence shown as maximum main girder deflection over a number of 40 iterations

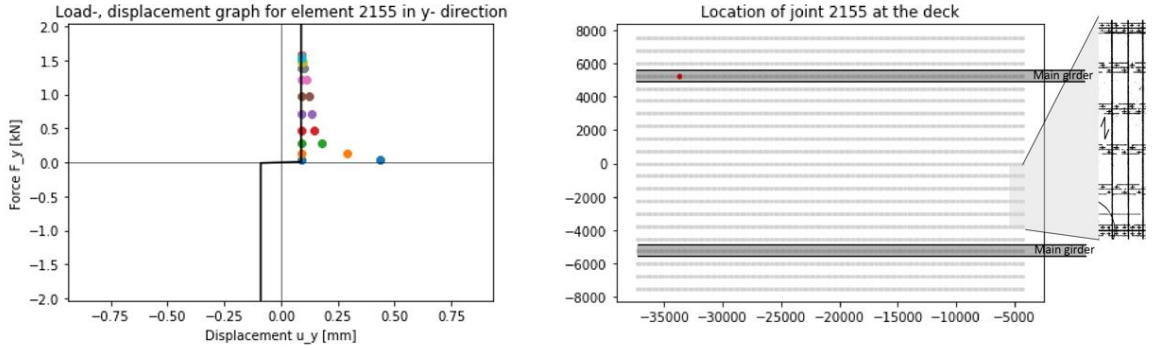

Figure 12.3: Local convergence for one of the connections directly above the main girder, that is in the embedment stage (when $\lambda = 0.8$ mm and $\mu = 118400$ N/mm). The location of the connection in the deck is given as a red dot in the top view of the deck connections

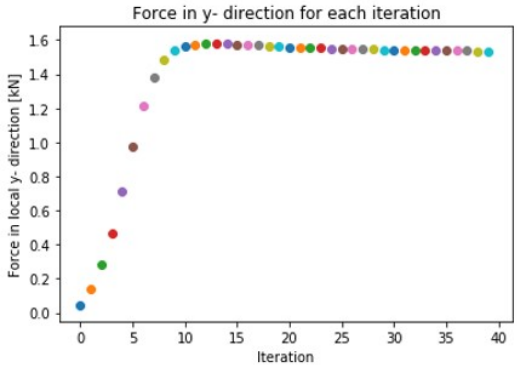

Figure 12.4: Local convergence of shear force in y- direction for one of the connections directly above the main girder, that is in the embedment stage (when $\lambda = 0.8$ mm and $\mu = 118400$ N/mm).

On a global level, the analysis should converge to a stable result and this is checked by presenting the maximum main girder deflections over 40 iterations (figure 12.2). Figures 12.3 and 12.4 show the local convergence of the load-, slip results over the length of an analysis of 40 iterations in a connection above the main girder. After 40 iterations, the linear SSM analysis is considered to be converged in any case for the assumed load-, slip parameters.

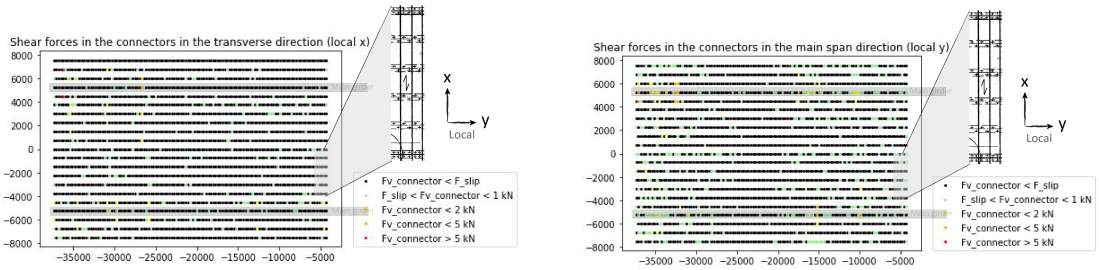

(a) Top view of shear force in local x- direction of connectors (when $\lambda = 0.8$ mm and $\mu = 118400$ N/mm)

(b) Top view of shear force in local y- direction of connectors (when $\lambda = 0.8$ mm and $\mu = 118400$ N/mm)

Figure 12.5

Figures 12.7a and 12.7b respectively show the shear forces in the local x- and y- directions for the connectors in a top view. The local x- direction of the connection equals the

transverse direction of the bridge leaf, whereas forces in the local y- direction run parallel to the main span of the bridge leaf.

The maximum shear force in the connections can differ per seed. The effect of seeds on connector shear forces and maximum deflection of the main girder is discussed in section 12.2.

12.1.2 Horizontal load case

For the horizontal load case, the same types of results can be generated. Figures 12.6a and 12.6b respectively show the maximum main girder deflection and the degree of hybrid interaction of the deck given the assumed expected values for u_{slip} and K_{ser}.

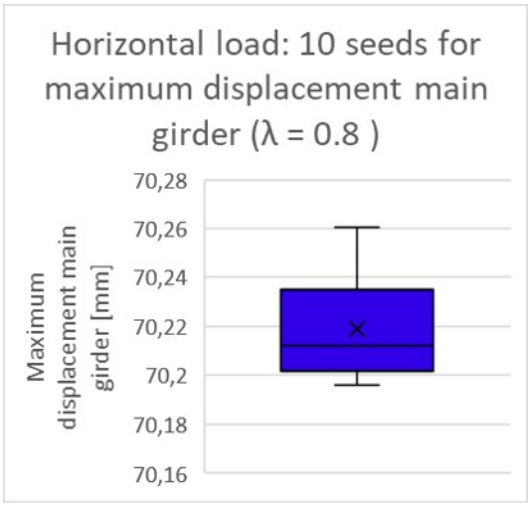

(a) Horizontal load case: maximum deflection main girders for the current situation (λ = 0.8 mm and μ = 118400 N/mm connectors, timber deck boards 280 mm wide) for 10 different SSM analyses of 40 iterations

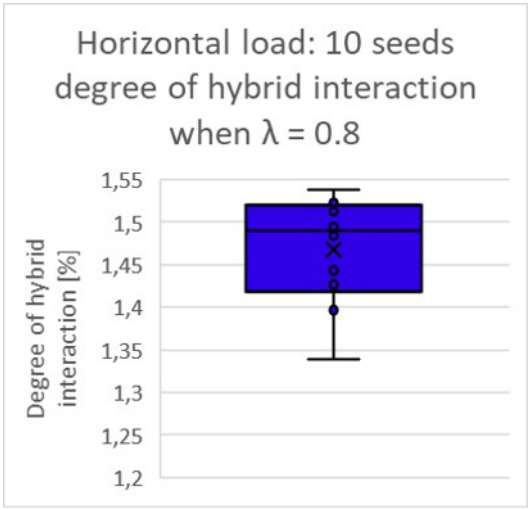

(b) Horizontal load case: degree of hybrid interaction for the current situation (λ = 0.8 mm and μ = 118400 N/mm connectors, timber deck boards 280 mm wide) for 10 different SSM analyses of 40 iterations

Figure 12.6

The current degree of hybrid interaction of the timber deck for this static collision force of 1 MN is expected to be approximately 1%. The maximum shear forces in the deck for the assumed load-, slip curve parameters, do not exceed 25 kN in case of a ship collision in the current situation. The magnitude of shear forces after 40 iterations have been plotted by dots in a top view in figures 12.7a and 12.7b. For both directions, shear forces in most connectors remain below 2 kN.

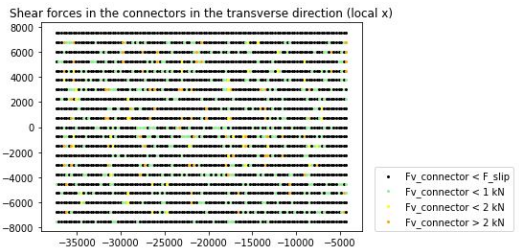

(a) Horizontal load: top view of shear force in local x- direction of connectors (when λ = 0.8 mm and μ = 118400 N/mm)

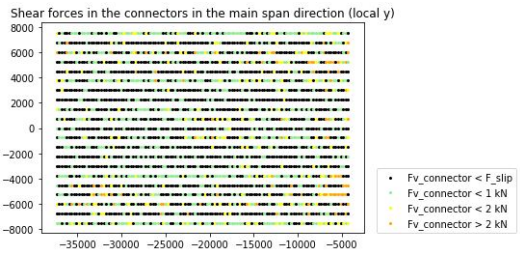

(b) Horizontal load: top view of shear force in local y- direction of connectors (when λ = 0.8 mm and μ = 118400 N/mm)

Figure 12.7

Figures on typical global- and local convergence for these analyses are given in appendix I.

Besides considering the degree of hybrid interaction and the maximum shear forces in the connectors, one should remark the effects of hybrid interaction in terms of gain or penalty. This was earlier defined in equations 8.1 and 8.2. Figure 12.8 highlights the gain and penalty for some of the most important phenomena in girders and deck boards. It is clear that since the current degree of hybrid interaction is low, its effects are equally insignificant.

Maximum deflections, forces and moments in specific elements for both load cases	Lower bound • 280 mm wide deck boards • Infinite slip in bolts	Current situation* • 280 mm wide deck boards • Slipping bolts: λ = 0.8 mm		Upper bound • Monolithic deck plate • No-slip bolts: λ = 0 mm	
		Vertical load case			
- Deflection **main girder**	○ 10.43 mm	↓ 0.3 %	10.40 mm	↓ 21.4 %	8.20 mm
- Myy **main girder**	○ 6044 kNm	↓ 0.1 %	6035 kNm	↓ 10.8 %	5391 kNm
- Mzz **main-cross girder**	○ 29.62 kNm	↓ 0.1 %	29.6 kNm	↓ 64.6 %	10.5 kNm
- Horizontal shear force **deck**	○ 0 kN	↑ ∞%	2.2 kN	↑ ∞ %	21.1 kN
- **Deck** board to board	○ 0 kN	○ 0 %	0 kN	↑ ∞ %	-81.6 kN
		Horizontal load case			
- Deflection **main girder**	○ 70.70 mm	↓ 0.7 %	70.20 mm	↓ 46.0 %	38.22 mm
- Mzz **main-cross girder**	○ 2802 kNm	↓ 0.4 %	2792 kNm	↓ 26.3 %	2064 kNm
- Axial force **bracing**	○ -824.9 kN	↓ 0.3 %	-822.1 kN	↓ 91.7 %	-68.6 kN
- Horizontal shear force **deck**	○ 0 kN	↑ ∞ %	7.4 kN	↑ ∞ %	39.8 kN
- **Deck** board to board	○ 0 kN	○ 0 %	0 kN	↑ ∞ %	166.6 kN

* Small differences can exist for the current situation since the results change slightly for different seeds

Figure 12.8: Effects of hybrid interaction in terms of gain and penalty for the current situation and the upper bound situation

12.2 Importance of assumptions and seeds

The assumptions on expected values for the stochastic variables u_{slip} and K_{ser} are relatively uncertain. This section will discuss the influence of altering these load-, slip curve parameters. Meanwhile it will address the influence of using different distributions each analysis (seeds).

12.2.1 Vertical load case

For the vertical load case, the influence of the assumed slip distribution and slip modulus will be examined. The spread in results due to different seeds, will be discussed as well.

12.2.1.1 Influence of assumed slip distribution

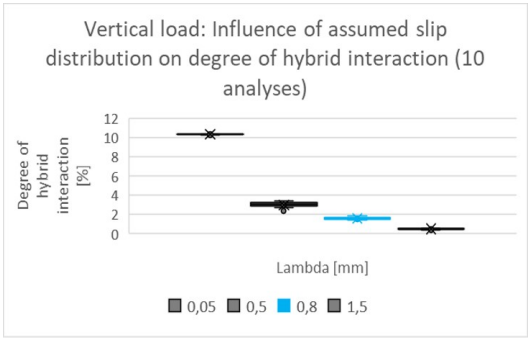

(a) Boxplots of 10 analyses per slip parameter λ for the current timber deck boards, based on maximum vertical deflection of the main girder

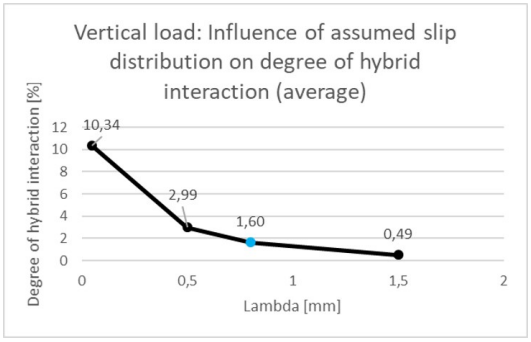

(b) Average of 10 analyses per slip parameter λ for the current timber deck boards, based on maximum vertical deflection of the main girder

Figure 12.9

Regarding the results for the maximum deflection of the main girder, it appears, for multiple seeds, the spread in results will not be large. Figure 12.9a shows the degree of hybrid interaction in boxplots for 10 different analyses run per value of λ (size factor or expected value for Weibull distribution "R"). The average values of these degree- of- hybrid interaction- spread results are given in figure 12.9b. The trend shows a small decrease of hybrid interaction when connections are slipping more and an increase in interaction when connections slip less. The blue results represent the most likely value of $\lambda = 0.8$ mm.

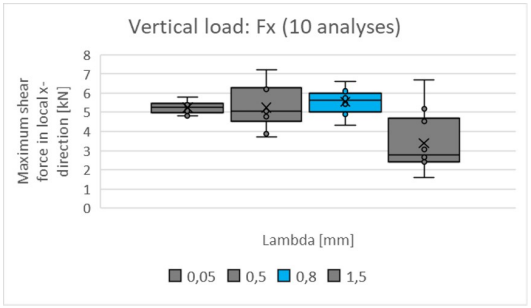

(a) Boxplots maximum shear force (Fx) in connections of 10 analyses per slip parameter λ for the current timber deck boards

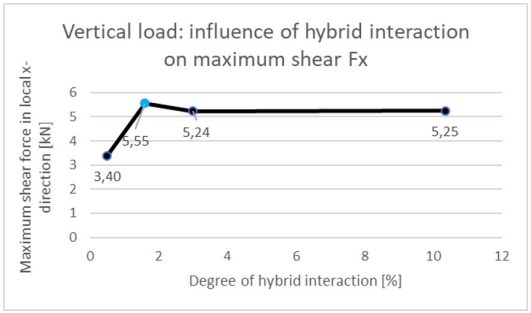

(b) Average of maximum shear force (Fx) in connectors of 10 analyses per slip parameter λ for the current timber deck boards

Figure 12.10

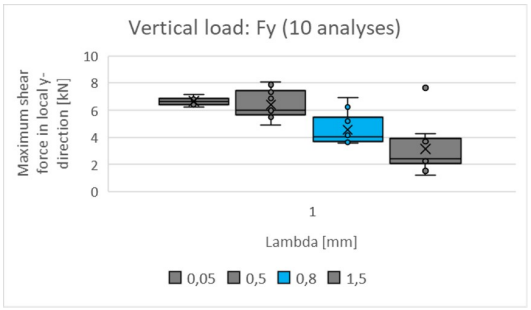

(a) Boxplots maximum shear force (Fy) in connections of 10 analyses per slip parameter λ for the current timber deck boards

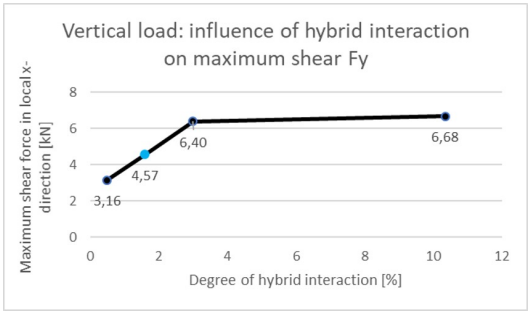

(b) Average of maximum shear force (Fy) in connectors of 10 analyses per slip parameter λ for the current timber deck boards

Figure 12.11

Figures 12.10a, 12.10b, 12.11a and 12.11b show the results for maximum shear forces in the connections related to the expected slip value λ. For the vertical load case, these results show that there is a small correlation between the assumed slip and the maximum shear forces in the connections. When connections slip more, maximum shear forces in both directions, decrease and for less slip, vice versa.
The spread in results is more significant than for the deflection of the main girder. This is to be expected since the overall response does not change much when some connectors increase or decrease in slip on a total number of 2499 connections.
For the shear forces however, seeds could have an effect. To give an example; when connections at key positions (e.g. directly above the main girder near the support for Fy) are assigned with a larger slip value for example, their force after n iterations will be lower. Either the maximum shear force is still found in the same connection (although lower) or the maximum shear will be found at another connection, which is at a less important position. Consequently, the maximum shear force over all connections would be lower.
From figures 12.10a and 12.11a, it can be observed that the spread in results becomes slightly smaller when the connections slip less ($\lambda = 0.05$ mm).

12.2.1.2 Influence of slip modulus

The influence of the slip modulus K_{ser} (or: embedding stiffness) will be discussed in this section for two different situations: $\lambda = 0.05$ mm and $\lambda = 0.8$ mm. In other words, analyses results for different values of K_{ser} are plotted for almost no slip in the connections ($\lambda = 0.05$ mm) and the expected slip distribution ($\lambda = 0.8$ mm). These results are the degree of hybrid interaction, based on the maximum deflection of the main girder and the maximum shear forces in the local x- and y- direction.

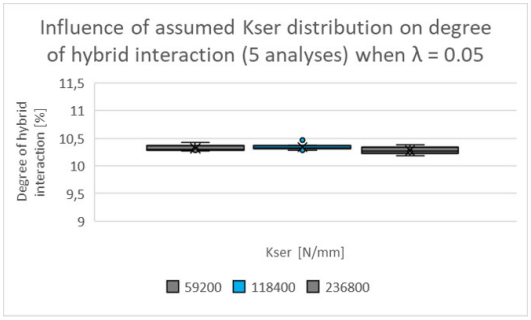

(a) Degree of hybrid interaction depending on the slip modulus K_{ser} for $\lambda = 0.05$ mm

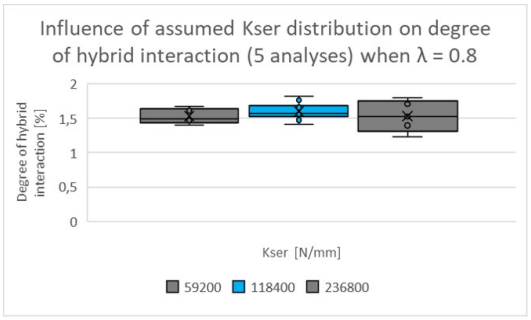

(b) Degree of hybrid interaction depending on the slip modulus K_{ser} for $\lambda = 0.8$ mm

Figure 12.12

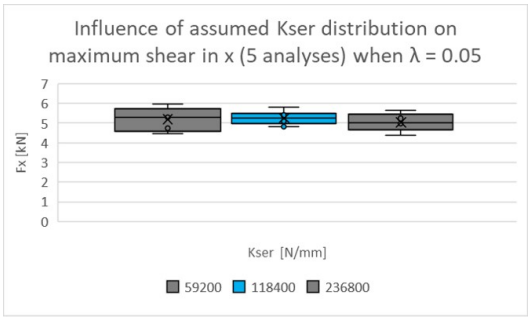

(a) Maximum shear force Fx depending on the slip modulus K_{ser} for $\lambda = 0.05$ mm

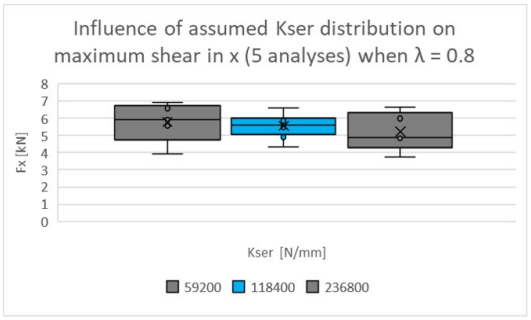

(b) Maximum shear force Fx depending on the slip modulus K_{ser} for $\lambda = 0.8$ mm

Figure 12.13

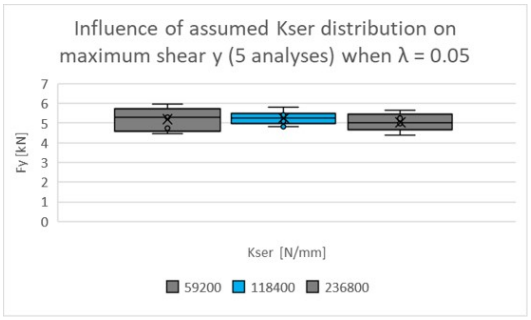

(a) Maximum shear force Fy depending on the slip modulus K_{ser} for $\lambda = 0.05$ mm

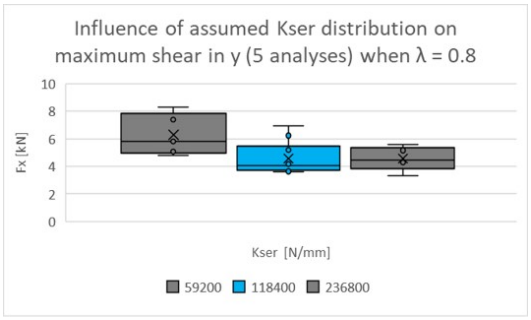

(b) Maximum shear force Fy depending on the slip modulus K_{ser} for $\lambda = 0.8$ mm

Figure 12.14

When considering the results for hybrid interaction (figures 12.12a and 12.12b) or maximum shear force (figures 12.13a, 12.13b, 12.14a and 12.14b), no real relation can be found, either in terms of magnitude or spread for different slip modulus values. This is true for both slip values λ.

12.2.2 Horizontal load case

The influence of the assumed slip distributions for a horizontal load case is discussed here in terms of results for the degree of hybrid interaction and maximum shear in the

connections. The influence of slip modulus K_{ser} is assumed to be negligible for the horizontal load case as well as for the vertical load case discussed earlier.

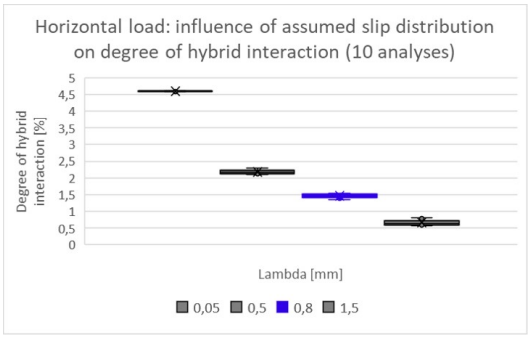

(a) Boxplots of 10 analyses per slip parameter λ for the current timber deck boards, based on maximum horizontal deflection of the main girder

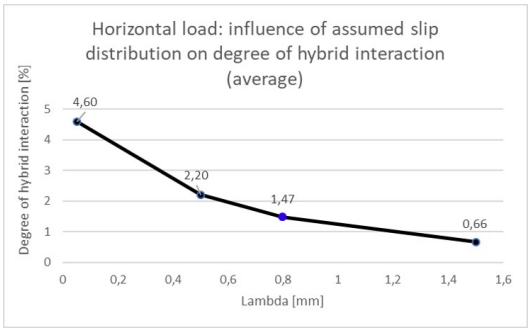

(b) Average of 10 analyses per slip parameter λ for the current timber deck boards, based on maximum horizontal deflection of the main girder

Figure 12.15

For the horizontal load case, the expected degree of hybrid interaction is affected by different slip values in the deck connections. Similarly to the vertical load case, the degree of hybrid interaction increases as the slip in the connectors decrease. For the collision force however, the difference between the upper- and lower bound in terms of horizontal deflection of the main girder, is larger than for the vertical load case. Even for low slip connectors, still a low (4.6 %) percentage of hybrid interaction is achieved for the current deck boards. For the horizontal load case, the distortion of the main- to- cross girder is not (significantly) influenced by the in-plane action of the deck when using the current individual boards, that are not in contact with each other.

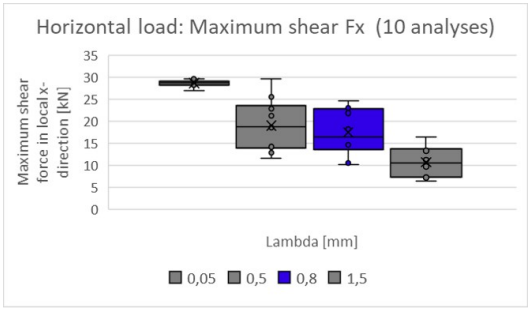

(a) Boxplots maximum shear force (Fx) in connections of 10 analyses per slip parameter λ for the current timber deck boards

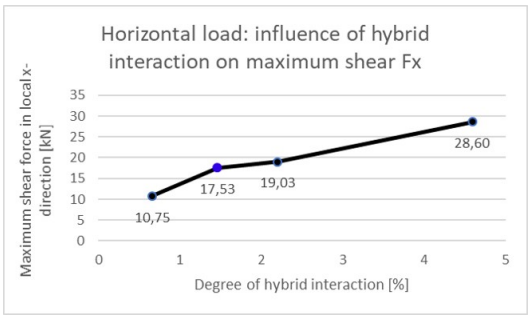

(b) Average of maximum shear force (Fx) in connectors of 10 analyses per slip parameter λ for the current timber deck boards

Figure 12.16

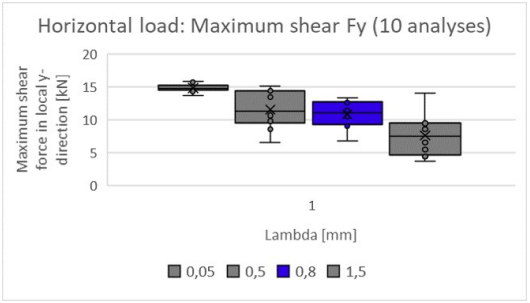

(a) Boxplots maximum shear force (Fy) in connections of 10 analyses per slip parameter λ for the current timber deck boards

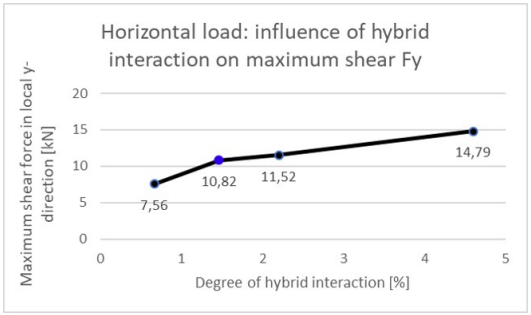

(b) Average of maximum shear force (Fy) in connections of 10 analyses per slip parameter λ for the current timber deck boards

Figure 12.17

Figures 12.16a and 12.17a show the resulting shear forces (in both directions) out of 10 analyses per value for λ in boxplots. Considering their average values in figures 12.16b and 12.17b, again it can be observed that the maximum shear in the connectors slightly increases for a larger degree of hybrid interaction (i.e. less slip in the connectors).

12.3 Hybrid interaction directly after re-tightening bolts

For the current situation, it is important to distinguish two situations: directly after re-tightening the bolts and the rest of the year when they are untightened. In previous sections, the results were discussed for different slip values in the connections. Directly after re-tightening the bolts in the deck connections, a pretension will be present in the bolts. In this small time period, the load slip curves of the connections will generally resemble the one given in figure 12.18. Over time, the pretension stage will eventually shorten to zero and the bolts are untightened.
Why is it important to consider such a situation? First of all, it should be investigated whether large shear forces act upon the connection in such a case for the current structure. Secondly, for future applications, it is important to know what the application of low- slip connectors would mean for the deck interaction and the forces imposed on the deck and its connection. Little research has been performed to low-slip connectors in timber-to-steel connections. Some of these alternatives could involve locking- or spring washers. Other options could be injecting bolts as is currently being researched for steel-to-steel and steel-to-concrete connections.

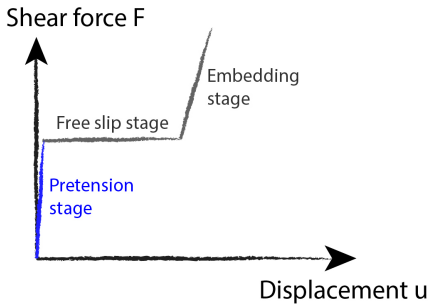

Figure 12.18: General load-, slip curve stages just after re-tightening the bolts in the deck joints

The pretension stage is generally characterized by a high (elastic) stiffness. For the current deck boards, it is not likely that any connection will surpass the pretension stage just after

re-tightening the bolts. Namely, each bolt is pretensioned with a force of approximately 35 kN (70 kN combined for double- bolted connections) and the maximum shear force present in the connectors for no (or limited) slip (when $\lambda = 0.05$ mm), is about 30 kN.

In figures 12.19a and 12.19b, the resulting main girder deflections and obtained degree of hybrid interaction have been plotted after 10 analyses for the vertical load case when (most) connectors do not slip ($\lambda = 0.05$ mm). Figures 12.20a and 12.20b show the same results, but for the horizontal load case.

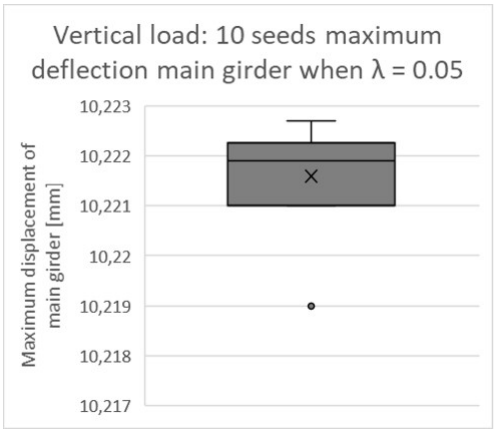

(a) Vertical load case: maximum deflection main girders for the current situation ($\lambda = 0.05$ mm and $\mu = 118400$ N/mm connectors, timber deck boards 280 mm wide) for 10 different SSM analyses of 40 iterations

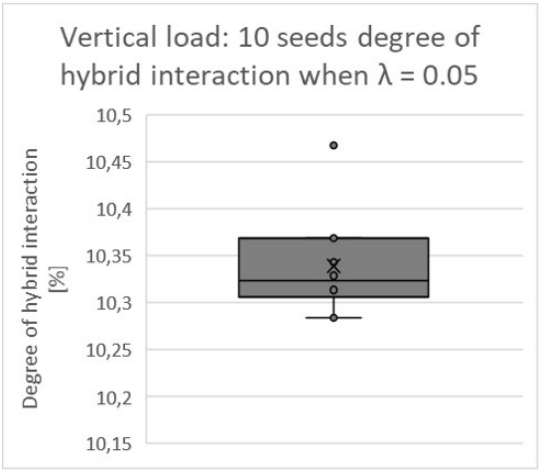

(b) Vertical load case: degree of hybrid interaction for the current situation ($\lambda = 0.05$ mm and $\mu = 118400$ N/mm connectors, timber deck boards 280 mm wide) for 10 different SSM analyses of 40 iterations

Figure 12.19

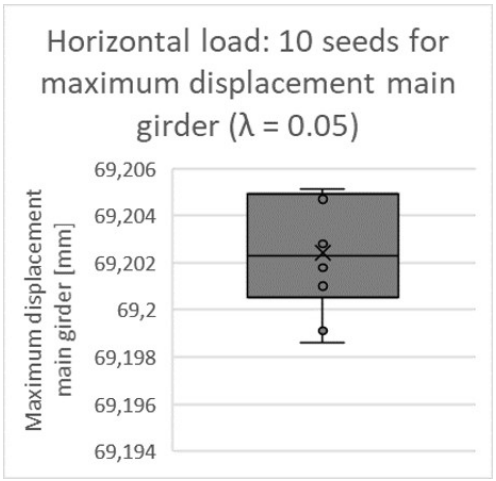

(a) Horizontal load case: maximum deflection main girders for the current situation ($\lambda = 0.05$ mm and $\mu = 118400$ N/mm connectors, timber deck boards 280 mm wide) for 10 different SSM analyses of 40 iterations

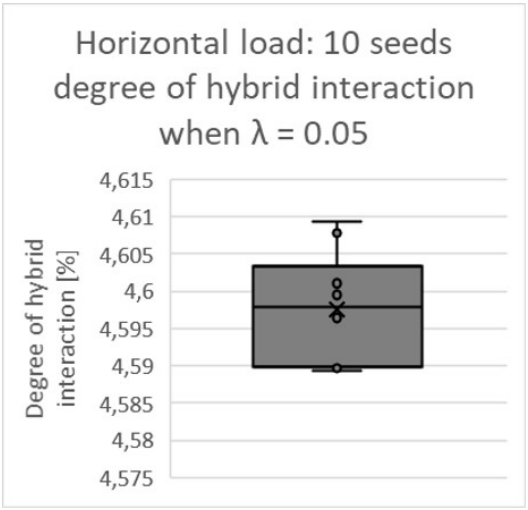

(b) Horizontal load case: degree of hybrid interaction for the current situation ($\lambda = 0.05$ mm and $\mu = 118400$ N/mm connectors, timber deck boards 280 mm wide) for 10 different SSM analyses of 40 iterations

Figure 12.20

For both load cases, just after re-tightening the bolts, the degree of hybrid interaction does not significantly increase when the current individual deck boards are considered. This also

means that applying low-slip connectors in the future while using the same timber deck boards on the bridge as currently, will not increase the degree of hybrid interaction of the deck significantly.

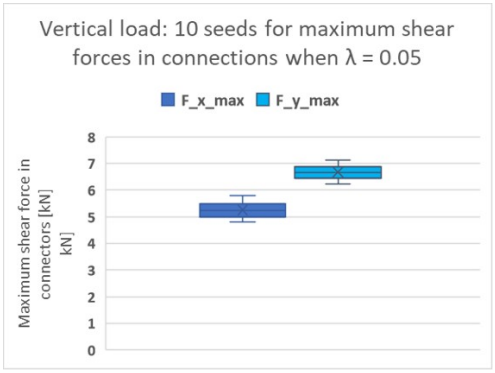

(a) Vertical load case: maximum shear forces in deck connections when high initial stiffness in the connection (or: $\lambda = 0.05$ mm) and current deck boards are considered

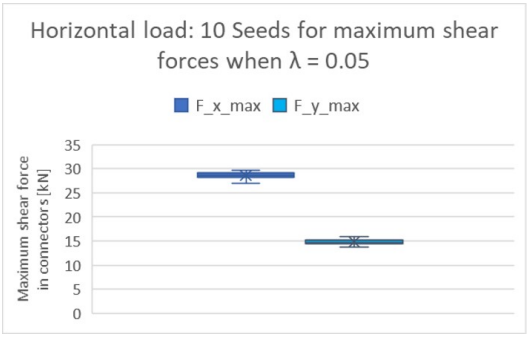

(b) Horizontal load case: maximum shear forces in deck connections when high initial stiffness in the connection (or: $\lambda = 0.05$ mm) and current deck boards are considered

Figure 12.21

The maximum shear forces in the deck connections for both load cases remain below 35 kN, so all connections will remain in the pre-stressing stage in case the re-tightened situation is discussed. For the current situation, the maximum shear forces in connectors (and subsequently the deck boards), are still relatively small for any load case, even when connections are not slipping or just have been re-tightened.

12.4 Possible effects of applying a monolithic deck plate

What would happen to the degree of hybrid interaction of the deck and the steel structure when deck boards no longer act individually, but the boards are replaced by one single monolithic plate?
The same (SSM) analysis can be performed when the individual deck boards (modelled as beams) are replaced by a monolithic plate in a grid of shell elements, again with a thickness of 110 mm and the material properties of D70 timber. The spring stiffnesses of the deck elements will again be adapted every iteration depending on their amount of slip relative to the assumed load-, slip curve. For the vertical load case, figures 12.22a and 12.22b show the shear forces in the connections in case of applying a monolithic deck plate.

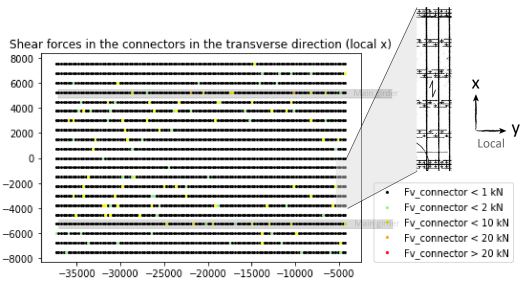

(a) Vertical load case: shear forces (Fx) in deck- to-girder joints (top view) when connectors are slipping ($\lambda = 0.8$ mm) and a monolithic deck plate is applied

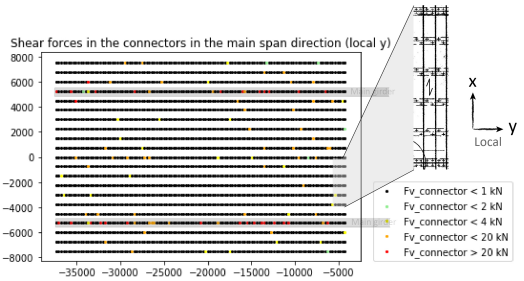

(b) Vertical load case: shear forces (Fy) in deck- to-girder joints (top view) when connectors are slipping ($\lambda = 0.8$ mm) and a monolithic deck plate is applied

Figure 12.22

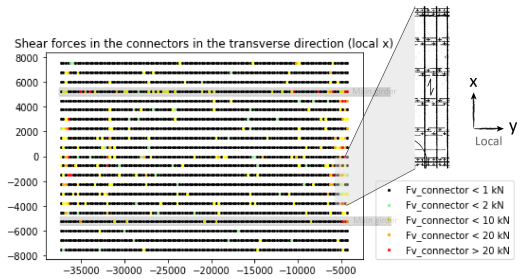

(a) Horizontal load case: shear forces (Fx) in deck- to-girder joints (top view) when connectors are slipping ($\lambda = 0.8$ mm) and a monolithic deck plate is applied

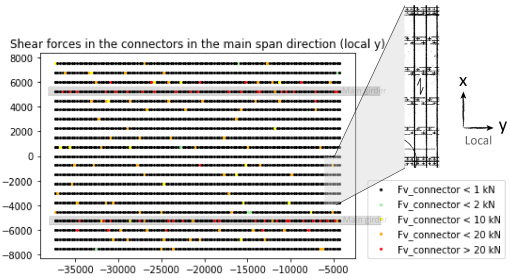

(b) Horizontal load case: shear forces (Fy) in deck- to-girder joints (top view) when connectors are slipping ($\lambda = 0.8$ mm) and a monolithic deck plate is applied

Figure 12.23

For the horizontal load case, it can be seen that shear forces concentrate above the main girders near the rotation point (figures 12.23a and 12.23b). For the monolithic plate, the amount of slip in the connections could have an influence as well. The degree of hybrid interaction per slip value λ for the vertical load case, is given in figure 12.24a. For the horizontal load case, figure 12.24b shows the same relation based on 5 analyses per slip value λ. For both load cases, the expected relation is found where less slip in the connectors leads to a larger degree of hybrid interaction. For the 5 analysis per slip value, the spread in results is generally small and becomes even smaller as the slip decreases. In case of the application of a monolithic plate, but with the current connectors, for the vertical- and the horizontal load case a respective 82% and 94% hybrid interaction of the deck can be found.

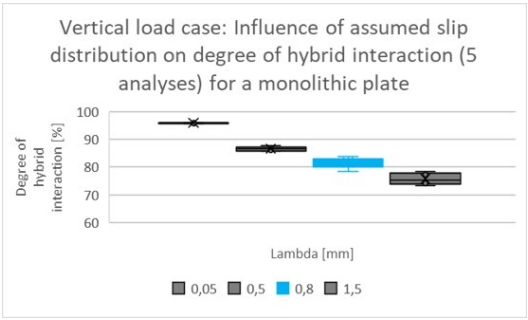

(a) Vertical load case: influence of assumed slip distribution for connections on the degree of hybrid interaction in case of applying a monolithic plate

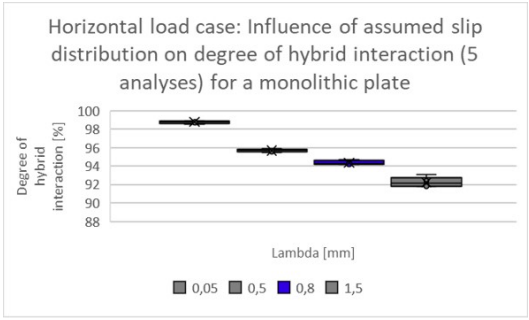

(b) Horizontal load case: influence of assumed slip distribution for connections on the degree of hybrid interaction in case of applying a monolithic plate

Figure 12.24

The relation between the degree of hybrid interaction and the maximum shear forces in the maximum connectors is remarkable (figures 12.25a and 12.25b). As the degree of hybrid interaction increases (for less slip in connectors), the maximum shear force in the longitudinal (local y) direction decreases. This relation was completely opposite when applying individual deck boards. In the case of individual deck boards, the maximum shear force increased as the deck was increasingly interacting with the structure, so deck connectors would all be subjected to larger shear forces as well.
For a deck plate, less slip in the connectors and more interaction means a better spread of shear forces among all connectors. This leads to smaller peak forces and more connections that are activated.

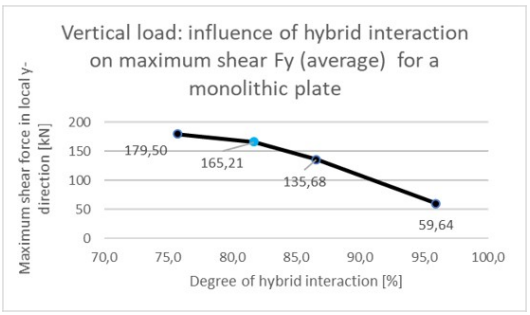

(a) Vertical load case: relation between the degree of hybrid interaction and the maximum shear force in longitudinal direction (Fy) for the application of a monolithic plate

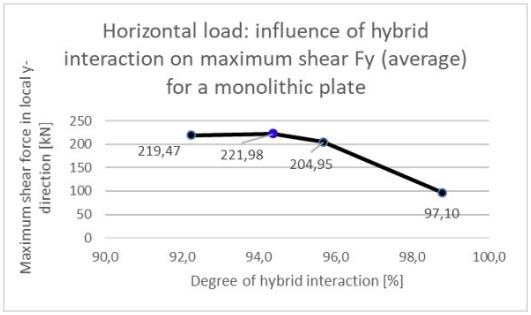

(b) Horizontal load case: relation between the degree of hybrid interaction and the maximum shear force in longitudinal direction (Fy) for application of a monolithic plate

Figure 12.25

To see this difference in activated connectors, the shear forces in the connectors in local y-direction are presented in top deck view graphs comparing large slip ($\lambda = 1.5$mm) to no slip ($\lambda = 0.05$mm). In figures 12.26a and 12.26b it can indeed be seen that for the vertical load case, less slip in all connectors, cause more connections to activate and contribute to hybrid interaction. Having a better spread of the shear forces among all connections, leads to smaller peak forces as can also be seen for the horizontal load case in figures 12.27a and 12.27b.

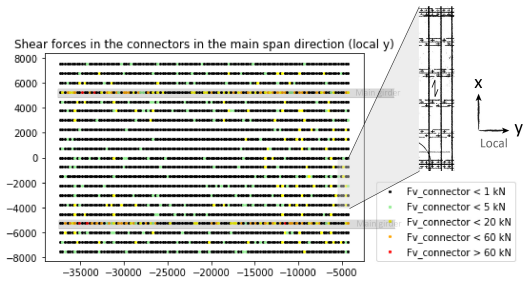

(a) Vertical load case: shear forces (Fy) in deck-to- girder joints (top view) when connectors are not slipping ($\lambda = 0.05$ mm) and a monolithic deck plate is applied. Maximum shear force is **59.6 kN**.

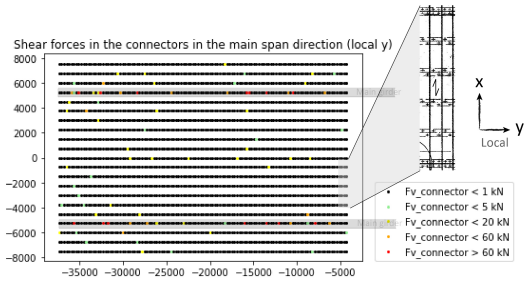

(b) Vertical load case: shear forces (Fy) in deck- to-girder joints (top view) when connectors are slipping ($\lambda = 1.5$ mm) and a monolithic deck plate is applied. Maximum shear force is **180.8 kN**.

Figure 12.26

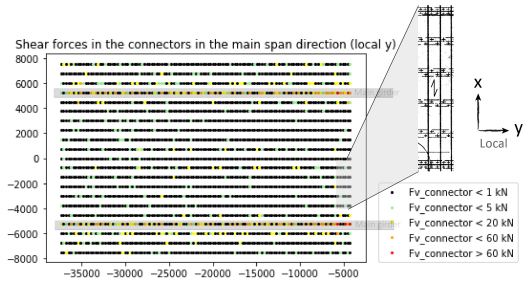

(a) Horizontal load case: shear forces (Fy) in deck-to- girder joints (top view) when connectors are not slipping ($\lambda = 0.05$ mm) and a monolithic deck plate is applied. Maximum shear force is **95.0 kN**.

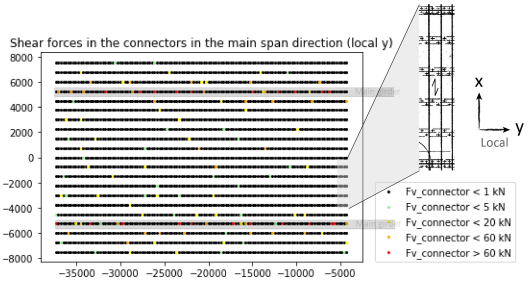

(b) Horizontal load case: shear forces (Fy) in deck- to-girder joints (top view) when connectors are slipping ($\lambda = 1.5$ mm) and a monolithic deck plate is applied. Maximum shear force is **157.6 kN**.

Figure 12.27

See appendix I for more SSM analyses result graphs.

The results for the monolithic plate are an important starting point when considering to replace the current deck boards by wider boards or place them in a different configuration (diagonal for example). The feasibility of creating a monolithic plate in timber largely depends on the glueability of the specific timber and its failure mechanisms. Currently no research was performed to the possible application of (hardwood) CLT or glulam panels in highway bridges. Another possibility for retrofitting the deck boards would be to replace them by stress laminated timber [30] or to place them in an diagonal configuration.

Chapter 13

Discussion

13.1 Load cases

For this research two heavy static load cases were chosen. After reviewing the results, subjecting the current structure to smaller (vertical) loads will not suddenly increase the degree of hybrid interaction. So when the current degree of hybrid is concerned, choosing smaller loads is not necessary. However for verification when connectors retain their pretension or wider deck boards are used, it could be useful to review for example a single truck passing the bridge leaf.

13.2 Load-, slip parameters

From the results it can clearly be observed that the slip modulus does not have an influence on the degree of hybrid interaction, whereas the slip does. The slip in the connections also has an influence on the shear force magnitude in the connections. For the current deck boards SSM results have shown that for a decreasing amount of slip in the connections, the degree of hybrid interaction can be up to about 10% for the vertical load case and 4% for the horizontal load case. The spread in results generally decreases for less slip in the connectors.
However, in this research the distribution of slip among all connectors was randomly done. But are the hole clearances completely independent at each location? In reality, no, they have some dependency, but timber is a largely in-homogeneous material and the drilled holes can have a slight offset at every location. Added to that is the complicated process of shrinkage or expansion of the timber due to temperature fluctuations. These parameters are more likely to influence the location of the bolt in the hole. If the material and the preparation of both the timber boards and the steel girders would be perfect, the bolt hole clearance of each bolt would be dependant on the material curve of its neighbouring connectors. In reality such a process is never perfect.
Material curves are assumed to be fully independent for this research, but there could still be a little dependency to their neighbouring spring elements. Temperature effects have also not been taken into account. Sometimes the temperature fluctuations could introduce some small pretension in the bolts (when the timber and/or steel is expanding) causing initial stiffness before slipping.
The slip modulus of all six connections to a deck board should be similar in theory, since the slip modulus is based on the density of the timber and the dowel diameter. This was not assumed in the analysis. However, the slip modulus does not have a significant influence on the current degree of hybrid interaction or the maximum shear forces, so this choice won't have any influence on possible conclusions.

The results in case of a pretension present in the bolts, is considered to be similar to the situation where $lambda = 0.05$ mm, so practically no slip present in all deck connections. For the static ship collision force, maximum shear forces in the bolts can exceed the pretension limit, so the connection starts slipping and embeds. This is not expected to have a large influence as only a few connections might be slipping and the degree of hybrid interaction might be a bit lower than the 4% that is obtained currently.

13.3 SSM analyses

The number of analyses performed for the current bridge leaf structure (280x110 mm deck boards as beams) is 10 per value of λ. For the investigation of the slip modulus influence and the degree of hybrid interaction when applying a monolithic plate, 5 analyses were performed. Ideally, for every parameter, about 30 analysis should be performed. However, due to the computation time of the SSM analysis, only a limited amount of analyses were performed. These results are not expected to change, since the spread in results is relatively small already for 5 analyses and increasing the number to 10 didn't change the spread or the average result much.
Convergence is obtained earlier for less slip in the connectors (about 5 iterations for the current structure). In general, all analyses have converged both locally and globally after about 25 iterations. Still, for every analysis, 40 iterations have been preformed.
Geometrical non-linearity not taken into account for SSM, every analysis is static linear and every iteration starts by using the initial position of all structural elements in the bridge leaf. Both the SSM- and the non-linear method represent an approximation of reality and interpretation of modelling results is therefore essential.

13.4 Modelling challenges

Rotation for certain girders or beams in the model is not always reliable. The linkage that is created in the FE model can induce an additional translation/rotation of a linked girder or beam, where there shouldn't be any. Figure 13.1 shows the effect of modelling. The blue dots represent the center nodes that are connected by a link (presented by a black dashed line). Due to bending, the distance between the deck nodes should decrease and therefore the longitudinal girders also move inwards. In the model, the longitudinal girder will rotate along with the rotation of the deck beam, since their rotations are linked. This rotation of the link causes the longitudinal girder to move outwards.

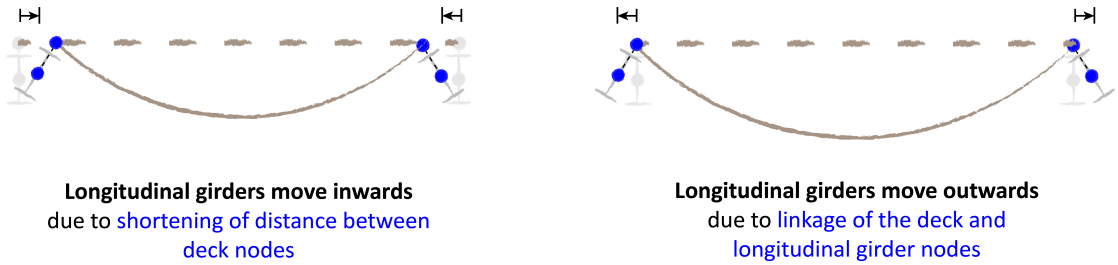

Figure 13.1: Longitudinal girder respectively moving inwards and outwards due to modelling effects when the deck beam is subjected to bending.

Another of the beam model disadvantages, is the inability to simulate local bending in webs and/or flanges of a girder. The possible rotations, translations and local bending of a

longitudinal girder were previously given in figure 8.16. For the current degree of hybrid interaction these local bending effects are not expected to have a large influence.

13.5 Retrofitting options

The general options for retrofitting comprise alterations to the deck boards and/or changes to the connectors. The first option is retaining the current situation. The second option would be to replace the connectors while preserving the current deck boards. Option number three would be to re-use the current bolts, but replace the deck boards. Lastly, both the deck boards and the deck connectors can be replaced.

Current situation	No-slip bolts	Wider deck boards	Upper bound
• 280 mm wide deck boards • Slipping bolts: λ = 0.8 mm	• 280 mm wide deck boards • No-slip bolts: λ = 0 mm	• > 280 mm wide deck boards • Slipping bolts: λ = 0.8 mm	• Monolithic deck plate • No-slip bolts: λ = 0 mm
- *No reduction* forces/moments in steel girders due to lack of deck interaction	○ *Small reduction* forces/moments in steel girders due to small deck interaction	+ *Large reduction* forces/moments in steel girders due to large deck interaction	+ *Large reduction* forces/moments in steel girders due to large deck interaction
- Annual re-tightening of bolts necessary	+ Annual re-tightening of bolts *not* necessary	- Annual re-tightening of bolts necessary	+ Annual re-tightening of bolts *not* necessary
+ *No progressive collapse* if deck fails	+ *No progressive collapse* if deck fails	- *Progressive collapse* if deck fails	- *Progressive collapse* if deck fails
+ Easy to model and local verifications of deck or connectors are unnecessary	+ Easy to model and local verifications of deck or connectors are unnecessary	- Harder to model and local verifications of deck and connectors is necessary	- Harder to model and local verifications of deck and connectors is necessary

Figure 13.2: (Dis)advantages of each retrofitting option for timber decks in movable bridges.

For all of these four general options, some different aspects can be considered in terms of pros and cons. Figure 13.2 shows the pros and cons for each option. The first aspect is about the positive effects of increased hybrid interaction and the second one is about bolt-specific maintenance. The third aspect addresses whether the deck should be considered to be part of the main load-bearing structure. The last point is about complexity of modelling and whether local verifications of the deck joints are necessary.

Judging by these different pros and cons, no option is perfect on all aspects. The choice for a certain option depends on the demands for the bridge leaf and the deck by the client.

Part VI
Conclusions and recommendations

Chapter 14

Conclusions and recommendations

This chapter summarizes the conclusions from this research and states the recommendations for future research. These conclusions and recommendations are applicable to bridges with similar elements and spans to those of the Beneden Merwede Bridge.

14.1 Conclusions

This research focused on gaining a better understanding of the hybrid interaction between timber decks and steel girders in a movable bridge leaf. To this end, the load-, slip curves in the bolted connections have been considered. To analyze the global interaction of the deck, a linear Secant Stiffness analysis was used. The influences of the assumed parameters have been reviewed and possible alternatives assessed in terms of hybrid interaction. The degree of hybrid interaction has previously been defined as the degree to which the timber deck interacts with the steel structure. In this research the level of hybrid interaction was measured in terms of the main girder deflection relative to no hybrid interaction and full interaction.

The effect of hybrid interaction can be can be either expressed in terms of gain or penalty. The penalty is the increase of forces or moments in structural elements as an effect of increased hybrid interaction. Th gain of hybrid interaction is defined as a reduction in forces, moments or deflections. The gain is generally found in the main girders, cross girders and bracing elements. Meanwhile the penalty of hybrid interaction is generally observed in the deck and longitudinal girders (see tables 8.1 and 8.2).

Reflecting on the objectives stated in section 1.3, the main conclusion of this research can be stated:

- **Current degree of hybrid interaction**
  The current degree of hybrid interaction is close to 1% for both a bridge full of trucks and ship collision. This result is based on the assumed free slip- and slip modulus distributions, which are discussed in chapter 10. The result was obtained through a beam model of the bridge on which an iterative linear secant stiffness method has been used. The low degree of hybrid interaction furthermore presents an insignificant effect in terms of gain and penalty of hybrid interaction.

The main conclusion is based on the secondary conclusions:

- **Influence of deck joint slip and slip modulus on hybrid interaction**
  An increased amount of slip in the connections has a negative influence on the degree of hybrid interaction between the deck and the steel structure. The influence of connector slip is smaller for the horizontal force than the vertical load case.
  The slip modulus (or: stiffness in the embedding stage) does not influence the degree of hybrid interaction or maximum shear force magnitude for any amount of slip in the connectors.

- **Degree of hybrid interaction vs maximum shear force in connections**
  For the current deck boards, the relation between the amount of hybrid interaction and the maximum shear force in the deck is positive in general. In other words, as the degree of hybrid interaction is larger, larger maximum shear forces can be found. As the deck will attract more force as a whole, connections at key locations (e.g. above the main girder for Fy in case of vertical load) will have to sustain larger shear forces.

- **Re-tightening the bolts**
  After annual re-tightening of the bolts, the degree of hybrid interaction increases from 1.6% to 10.3% for the vertical load case and from 1.5% to 4.6% in case of a static collision force. The maximum shear forces for the vertical load case, remain below 10.5 kN, meaning all connections will be in the pretension stage (as friction coefficient $\mu = 0.3$ for steel- to- timber joints and a pretension force of 35 kN is applied to each bolt). The maximum shear forces in case of collision can be as high as 30 kN, so failure of the connection is unlikely. However, this does mean some shear connections are loaded past the pretension stage, will slip freely and embed. This effect for collision was not taken into account in the analysis (all connectors were assumed to remain in the pretension stage), but this would lead to an even smaller degree of hybrid interaction than 4.6%.

- **(Dis)advantages of full hybrid interaction**
  An increased degree of hybrid interaction can change the distribution of forces in the main load-bearing structure. Especially for the main girders and cross girders, the forces, bending moments and deflections can significantly change. The gain of hybrid interaction in maximum main girder deflection would be about 21% for the vertical load case and 46% for the horizontal load case. Besides this, the largest possible gain of hybrid interaction will be the 92% decrease in axial force in the bracing elements for a horizontal collision force.
  However, this gain of hybrid interaction is coherent with a penalty. More hybrid interaction means the longitudinal girders are more rigidly connected to the main girders, resulting in large shear forces in the deck. Shear forces exceeded the capacity according to Eurocode checks for vertical shear already. This means that utilization ratios of the deck in shear according to standards will worsen if a horizontal shear load is added. However, this is inaccurate, since the shear capacity of hardwoods is heavily underestimated in the Eurocode. The capacity for D70 timber can be over three times as large in experiments. This should be revised in the Eurocode. Another negative effect is the increased shear force in the connectors. Current bolted connections are not designed to sustain large shear forces. In this case, the deck connections also start to act as part of the main load- bearing structure. For the current deck boards, the shear forces in the deck connections can go up to 130 kN (parallel to the grain) for the horizontal load case. In case of applying a monolithic plate and slipping connectors concentration of shear forces can even raise the shear up to 222 kN (perpendicular to the grain), again for the horizontal load. Both shear

forces are far beyond the shear capacity of the current joints, which is about 83 kN parallel to the grain and 72 kN perpendicular to the grain.
If the degree of hybrid interaction is included in the assessment, the performance of the main load-bearing structure depends on the functioning of the deck and its connections. Progressive collapse can be the result of deck failure. This is another disadvantage of full hybrid interaction.

- **Static response**
  The static response of the structure can be divided into a global- and a local response. For the vertical load case, the global response is the total bending of the bridge leaf, leading to tension at the bottom of the main girders and compression in the top of the main girders and in the longitudinal girders. For the current situation, the individual deck boards will not transfer compression forces from board to board. However, when applying a monolithic plate, the plate will be in axial compression. For a collision force, the rotational stiffnesses around the vertical axis for joints, including the deck connections, provide extra resistance to the horizontal collision force. Stability members, longitudinal girders and the deck can all increase the in-plane action to decrease distortion and to decrease the bending moment in the main girder. Replacing the individual deck boards by a plate would allow for the deck to take more shear and aid to the global resistance of the bridge leaf.
  On a local level, the flow of normal forces from the longitudinal girders to the deck boards, depends on the load-, slip curve of the bolted connections. Instant embedding will increase the shear forces in most connections and deck boards.

14.2 Recommendations

Recommendations have been subdivided into three categories: research, engineering and retrofitting.

14.2.1 Research recommendations

The research recommendations mainly highlight the uncertainties in assumptions for this research. This section highlights how researching these uncertainties further, can improve the understanding of hybrid interaction, both in the current situation as well as in the future decision-making on retrofitting.

Current situation

- **Free slip in shear connectors**
  The current degree of hybrid interaction is mainly influenced by the magnitude of slip in the bolted connections. Now, an estimate was made for the distribution of slip magnitudes in all connections and the slip values are randomly distributed for all 2499 bolted connections. The slip magnitude depends on the hole size and the position of the bolt in the hole. Both are relatively uncertain and the hole size can vary depending on different factors like manufacturing tolerances, cyclic loading, moisture and timber deterioration. Investigating the amount of slip in the bolted connections helps to provide a more accurate number for the degree of hybrid interaction and its effects.

- **Pretension loss over time**

Another unknown for the current situation is the pretension loss in the bolts over time. Directly after the annual re-tightening of the bolts, the degree of hybrid interaction is the maximum of what is to be expected in the structure over time. Gradually the bolts will untighten and the pretension loss relates directly to the decrease of hybrid interaction of the deck. To be able to accurately predict the degree of hybrid interaction of the deck at any time during the year, it is desirable to gain more knowledge on pretension loss for timber-to-steel connections.

Retrofitting

- **No-slip connectors**
  When the deck boards are replaced by wider boards or placed in a different configuration, the degree of hybrid interaction can result in a main girder deflection gain of 21% for the vertical load case and 46% for the horizontal load case. For the current deck boards, no additional capacity of the joints would be required, but when applying wider deck boards the shear capacity of the joints can be insufficient for no slip in the connections. The shear capacity of the joint parallel to the grain should be larger than 130 kN and larger than 88.5 kN perpendicular to the grain. An investigation into the performance of alternative connectors that do not slip can help recommend feasible options for retrofitting.
  The shear connectors should not only be tested for the magnitude of the failure load, but also the load-, slip curves should be investigated for multiple specimen.

- **Deck board width**
  The degree of hybrid interaction and the effects of specific alternatives like widening the deck boards by a factor 2, placing the deck boards in a diagonal configuration or stress laminated timber, have not been researched in this thesis. The feasibility of these alternatives for highway bridges have not been investigated yet either. In order to recommend the most optimal option for each movable bridge, this could prove valuable to investigate.

- **Material properties timber**
  Based on various researches, the shear capacity of hardwoods is a value that should be changed in the Eurocode. Therefore, accurate strength verification of a hardwood deck is difficult. If the deck would be part of the load- bearing structure for increased hybrid interaction between the deck and the steel structure, local strength checks of the deck become even more important. However, the time- dependant behavior of timber properties in existing structures is uncertain. Additional testing on currently used timber deck boards could reduce uncertainties regarding (time- dependant) hardwood material properties, such as the shear capacity.

14.2.2 Modelling recommendations

The modelling recommendations mainly focus on what can be recommended regarding the current practice in verification. The current practice in verification of a movable bridge assumes the timber deck only transfers vertical forces. Subsequently, no hybrid interaction is present between the timber deck and the steel girders. Is the current method of verification sufficient in this situation and should the hybrid interaction of the deck be taken into account when the deck is retrofitted with different deck boards and/or different connectors?

- **Current situation**

The degree of hybrid interaction is low for both of the considered static load cases. Directly after re-tightening of the bolts, the hybrid interaction increases a little (from 1.5% to 10.3% for vertical and 4.6% for horizontal loads), but its effects can still be assumed to be insignificant. It could therefore be stated that the current degree of hybrid interaction has no influence on the strength verifications of the structural elements. No alterations have to be made to the current method of verification, except for the use of an adapted shear capacity value for D70 hardwoods from the Eurocode.

- **Retrofitting**
  Only if the deck boards are replaced by a different deck type (e.g. wider boards, different configuration, stress laminated panel, etc.), it is necessary to reconsider the current practice of verification. Changing only the connector type, using the current deck boards, will not significantly increase the degree of hybrid interaction. If the interaction of the deck with the steel girders, is insignificant, the current practice is sufficient.

14.2.3 Retrofitting recommendations

In general four options can be considered for the deck. The first one is preserving the current deck boards and connections. If deck boards or bolts fail, replace them for new ones. The second option would be to just replace the bolts in the deck by a new connector type, preferably having less or no slip. The third option would be keeping the bolts but changing the deck board size, configuration, material or type. The last option would comprise both the deck boards and the connections to be replaced. The advantages and disadvantages of all options have previously been stated in figure 13.2.

- **Preserving the current deck**
  In the current situation, the degree of hybrid interaction is insignificant, so the forces, moments and deflections will be similar to the lower bound situation. The problem of untightening bolts remains an issue in this case.
  On the other hand, the current verification of the bridge is simpler as the deck will not be regarded as part of the main load-bearing structure. Currently, structural safety does not depend on the performance of the deck. Safety factors are therefore smaller than they would be when the deck is part of the main load-bearing structure. Furthermore, the deck-to-girder joint does not need a local strength verification, as the deck joints are not subjected to any significant forces or moments. Also, for the verification, no additional shear forces have to be considered in the deck boards based on the low degree of hybrid interaction.
  Additionally replacement of the deck boards and connections is relatively simple.

- **Changing the connections**
  When applying no-slip connectors, but still using the same deck boards, the effects of deck interaction are still relatively small. It can be assumed that the timber deck does not interact with the steel girders. The deck is not a part of the main load-bearing structure, so deck board failure will not lead to progressive collapse. Besides, replacing the bolts in the deck joints by no-slip connectors, will remove the need to re-tighten the bolts annually.

- **Changing the deck boards**
  The degree of hybrid interaction when retrofitting only the deck boards, can differ largely per option. Different options should still be investigated in order to give a

well-considered advice. In this research, replacing the deck by a monolithic plate and using the current bolts has been investigated. The degree of hybrid interaction that can be obtained in that case is respectively 82% and 94% for the vertical- and horizontal load case.
The use of wider deck boards or panels, generally leads to a significant increase in hybrid interaction, thus also to its corresponding penalty and gain. The gain in maximum main girder deflection is 15.8% for the vertical load and 43.4% for the horizontal load. Meanwhile the maximum shear force in the deck connections (when using the current bolts) increases from zero to 165 kN and 222 kN for respectively the vertical- and horizontal load case.
Alternatives for retrofitting the deck to act more as a plate, can include placing the deck boards in a diagonal orientation across the longitudinal girders or the use of stress laminated timber. Also, the use of hardwood CLT has not been researched for infrastructural applications. These alternatives pose interesting challenges to further investigate.

- **Retrofitting deck and its connections**
  Replacing both the deck and its connections will require a reassessment of the entire bridge leaf, since the effects of the deck interaction are large and should be accounted for. The deck interacts with the steel girders in a major way and should therefore be considered to be part of the main load-bearing system.

There is no such thing as a single best option on all accounts. For future decision-making on retrofitting timber decks, the options all have their advantages and disadvantages.
It is recommended to chose either the second or the fourth option as the use of connections that slip have a disadvantage compared to their no-slip counterpart: annual re-tightening. Comparing the option of only no-slip bolts versus the upper bound option, the most important difference is whether the deck should be part of the main load- bearing structure. Mainly in a case where the main girders, cross girders and bracing elements are over-utilized for a static collision force and this horizontal load case is considered to be a governing factor in decision-making, the last option should be considered as a suitable retrofitting solution.

Bibliography

[1] NEN-EN-1337-1. Nen-en 1337-1 structural bearings - part 1: General design rules. Nen-en, Koninklijk Nederlands Normalisatie-Instituut, Delft, The Netherlands, 2000.

[2] NEN-EN-350. Nen-en 350 durability of wood and wood-based products - testing and classification of the durability to biological agents of wood and wood-based materials. Nen-en, Koninklijk Nederlands Normalisatie-Instituut, Delft, The Netherlands, 2016.

[3] H.J. Blass and C. Sandhaas. *Timber Engineering - Principles for design*. 2017.

[4] NEN-EN-1995. Nen-en 1995-1-1 eurocode 5 design of timber structures - part 1-1: General - common rules and rules for buildings. Nen-en, Koninklijk Nederlands Normalisatie-Instituut, Delft, The Netherlands, 2005.

[5] J. W. G. van de Kuilen and H. J. Blass. Mechanical properties of azobé. *Holz als Roh- und Werkstoff*, 63:1–10, 2004.

[6] NEN-EN-1912. Nen-en 1912 structural timber - strength classes - assignment of visual grades and species. Nen-en, Koninklijk Nederlands Normalisatie-Instituut, Delft, The Netherlands, 2012.

[7] NEN-EN-338. Nen-en 338 structural timber - strength classes. Nen-en, Koninklijk Nederlands Normalisatie-Instituut, Delft, The Netherlands, 2016.

[8] J.W.G. Van de Kuilen, W. Gard, G. Ravenshorst, V. Antonelli, and A. Kovryga. Shear strength values for soft- and hardwoods. In *CIB -W18*, 2017.

[9] Geert Ravenshorst, N. Gamper, Jan Willem G Van De Kuilen, and Peter de Vries. Determination of the shear strength of tropical hardwood timber. In J. Eberhardsteiner, W. Winter, A. Fadai, and M. Pöll, editors, *WCTE 2016 - World Conference on Timber Engineering*, pages 677–684. Vienna University of Technoclogy, 2016.

[10] NEN-EN-384. Nen-en 384 structural timber - determination of characteristic values of mechanical properties and density. Nen-en, Koninklijk Nederlands Normalisatie-Instituut, Delft, The Netherlands, 2018.

[11] NEN-EN-1993-1-8. Nen-en 1993 design of steel structures - part 1-8: Design of joints. Nen-en, Koninklijk Nederlands Normalisatie-Instituut, Delft, The Netherlands, 2011.

[12] A. Hassanieh, H.R. Valipour, and M.A. Bradford. Experimental and analytical behaviour of steel-timber composite connections. *Construction and Building Materials*, 118:63 – 75, 2016.

[13] Carmen Sandhaas. Mechanical behaviour of timber joints with slotted-in steel plates. 06 2012.

[14] R.N. Allan and J.W. Fisher. Behavior of bolted joints with oversize or slotted holes. *Fritz Engineering Laboratory Report No. 318.3*, 1967.

[15] E. Chesson and W.H. Munse. Studies of the behavior of high-strength bolts and bolted joints. *University of Illinois, Urbana*, 1965.

[16] Friction and friction coefficients for various materials.

[17] NEN-EN-383. Nen-en 383: 2007 test methods - determination of embedment strength and foundation values for dowel type fasteners. Nen-en, Koninklijk Nederlands Normalisatie-Instituut, Delft, The Netherlands, 2007.

[18] L.R.J. Whale and I. Smith. The influence of orientation of mechanical joints on their mechanical behaviour. *CIB-W18 Paper No. 18-7-2*, 1985.

[19] C. Sandhaas, G. J. P. Ravenshorst, H. J. Blass, and J. W. G. van de Kuilen. Embedment tests parallel-to-grain and ductility aspects using various wood species. *European Journal of Wood and Wood Products*, 71(5):599–608, Sep 2013.

[20] L. R. J. Whale and I. Smith. A method for measuring the embedding characteristics of wood and wood-based materials. *Materials and Structures*, 22(6):403–410, Nov 1989.

[21] SIA. Sia 265:2012 timber structures. Sia, Swiss Society of Engineers and Architects, Zurich, Switzerland, 2012.

[22] J. Ehlbeck and H. Werner. Traffähigkeit von laubholzverbindungen mit stabförmigen verbindungsmitteln. *Forschungsbericht Versuchanstalt für Stahl, Holz und Steine*, 1992.

[23] T.L. Wilkinson. Bolted connection strength and bolt hole size. Technical report, United States Department of Agriculture, United States, 1993.

[24] P. de Vries. Lecture slides joints 3 - october 17th, 2017. Lecture material, TU Delft, Delft, The Netherlands, 2017.

[25] NEN-EN-1991-1-7. Eurocode 1: Actions on structures - part 1-7: General actions - accidental actions. Nen-en, Koninklijk Nederlands Normalisatie-Instituut, Delft, The Netherlands, 2015.

[26] Ricardo O Foschi. Determining embedment response parameters from connector tests. *... . of Civil Engineering & Dept. of ...*, pages 3–8, 2000.

[27] Marija Todorović, Saša Kovačević, Marko Pavlović, Milan Spremić, and Zlatko Marković. BEHAVIOUR OF PREFABRICATED STEEL-CONCRETE COMPOSITE BRIDGE DECKS with grouped headed studs and bolted shear connectors. 2014.

[28] Ki Tae Park, Sang Hyo Kim, Young Ho Lee, and Yoon Koog Hwang. Degree of composite action verification of bolted GFRP bridge deck-to-girder connection system. *Composite Structures*, 72(3):393–400, 2006.

[29] RCSC Committee. RCSC Specification for Structural Joints Using High-Strength Bolts. 2014(April), 2014.

[30] M.G. Oliva, A.G. Dimakis, A.M. Ritter, and R.L. Tuomi. Stress-laminated wood bridge decks - experimental and analytical evaluations. 1990.

[31] NEN-EN 1991-2. Nen-en 1991-2 belastingen op constructies - deel 2: Verkeersbelastingen op bruggen. Nen-en, Koninklijk Nederlands Normalisatie-Instituut, Delft, The Netherlands, 2015.

Appendices

Appendix A

Verification calculation deck

A.1 Verification calculation deck 1965 (Rijkswaterstaat)

Verification deck 1965 (Rijkswaterstaat)

$tf := 1000kg$

Class 60 vehicle: 20 tf

Wheel load:

$$\frac{20tf}{4} = 5 \cdot tf$$

$P_w := 5tf \cdot g = 49.033 \cdot kN$

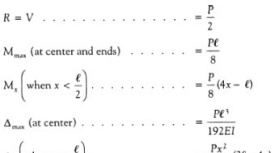

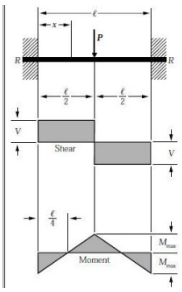

$b_{f.IPE36} := 170mm$

$b_{f.INP32} := 131 \cdot mm$

$L_{deck} := 750 \cdot mm$

$$L := L_{deck} - \left(\frac{b_{f.IPE36}}{2} + \frac{b_{f.INP32}}{2} \right) = 599 \cdot mm$$

$L_M := 2 \cdot L - 250mm = 949 \cdot mm$

Bending stress:

$$M := \frac{1}{8} \cdot P_w \cdot \left(L_M \right) = 5.817 \cdot kN \cdot m$$

Reduced thickness deck, because of small side notches in Azobe boards:

$t_{deck.red} := 105mm$

$b_{deck} := 280mm$

$$W_b := \frac{1}{6} \cdot b_{deck} \cdot t_{deck.red}^{2} = 5.145 \times 10^{5} \cdot mm^{3}$$

$$\sigma := \frac{M}{W_b} = 11.305 \cdot \frac{N}{mm^2}$$

$\sigma_b := 25 \frac{N}{mm^2}$ $\quad \frac{\sigma}{\sigma_b} = 0.452$ $\quad UC < 1$

Shear stress:

$$D_{max} := \frac{P_w \cdot \frac{L_M}{2}}{L} = 38.809 \cdot kN$$

$$\tau_{max} := \frac{3}{2} \cdot \frac{D_{max}}{b_{deck} \cdot t_{deck.red}} = 1.98 \cdot \frac{N}{mm^2}$$

$\tau_b := 2 \frac{N}{mm^2}$ $\quad \frac{\tau_{max}}{\tau_b} = 0.99$ $\quad UC < 1$

A.2 Verification calculation deck 2019 (Arup)

Verification deck 2019 (Arup)

$a := 5mm$

$h_{deck} := 110mm$

$h_{deck.red} := h_{deck} - a = 105 \cdot mm$

$w_{deck} := 280mm$

$w_{wheel} := 350mm$

Notches

$h_n := 10mm$

$w_n := 20mm$

Single axle inbetween longitudinal girders (BM2):

$Q_{\alpha.k.axle} := 400kN$

$Q_{\alpha.k.wheel} := \frac{Q_{\alpha.k.axle}}{2} = 200 \cdot kN$

$Q_{\alpha.k.beam} := \frac{w_{deck}}{w_{wheel}} \cdot Q_{\alpha.k.wheel} = 160 \cdot kN$

$\beta_Q := 1.0$

$\gamma_{Q1.traffic} := 1.25$

$\gamma_{Q1.sw} := 1.15$

$Q_d := \beta_Q \cdot Q_{\alpha.k.beam} \cdot \gamma_{Q1.traffic} = 200 \cdot kN$

$\rho_{Azobe} := 960 \frac{kg}{m^3}$

$g = 9.807 \frac{m}{s^2}$

$A := w_{deck} \cdot h_{deck.red} - 2 \cdot (w_n \cdot h_n) = 2.9 \times 10^4 \cdot mm^2$

$q_{sw.Azobe} := A \cdot \rho_{Azobe} \cdot g = 0.273 \cdot \frac{kN}{m}$

$$p_{sw.wear} := 0.16 \frac{kN}{m^2}$$

$$q_{sw.wear} := p_{sw.wear} \cdot w_{deck} = 0.045 \cdot \frac{kN}{m}$$

$$q_{sw} := q_{sw.Azobe} + q_{sw.wear} = 0.318 \cdot \frac{kN}{m}$$

Self weight can be neglected for strength verification

Azobe [D70]

$$f_{m.k} := 70 \frac{N}{mm^2} \qquad E_{m.0.mean} := 20 \frac{N}{mm^2}$$

$$f_{t.0.k} := 42 \frac{N}{mm^2} \qquad E_{m.0.k} := 16.8 \frac{N}{mm^2}$$

$$f_{c.90.k} := 12 \frac{N}{mm^2} \qquad G_{mean} := 1.25 \frac{N}{mm^2}$$

$$f_{v.k} := 5 \frac{N}{mm^2} \qquad k_{mod} := 0.7$$

Solid timber, climate class 1 NEN-EN 1995-1-1

$$\gamma_M := 1.3$$

Bending stress check

$$q_{traffic.d} := \frac{Q_d}{L} = 333.611 \cdot \frac{kN}{m}$$

Verification using two spans instead of five (conservative assumption and neglectable difference in bending moment value):

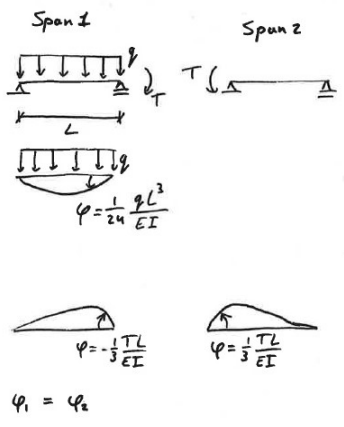

Continuous beam

$$\varphi_1 = \varphi_2$$

$$\frac{1}{24}\frac{qL^3}{EI} - \frac{1}{3}\frac{TL}{EI} = \frac{1}{3}\frac{TL}{EI}$$

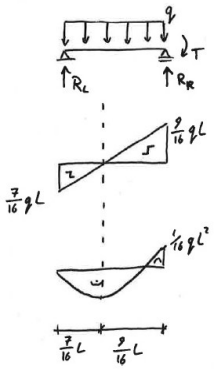

$$T_{mid} := \frac{1}{16} \cdot q_{traffic.d} \cdot L^2$$

$$R_R := \frac{\left(\frac{1}{2} \cdot q_{traffic.d} \cdot L^2 + \frac{1}{16} \cdot q_{traffic.d} \cdot L^2 \right)}{L}$$

$$R_L := \frac{7}{16} \cdot q_{traffic.d} \cdot L$$

$$M_{Ed.max} := \left(\frac{7}{16} L \right)^2 q_{traffic.d} - \frac{1}{2} \cdot \left(\frac{7}{16} L \right)^2 q_{traffic.d}$$

$$M_{Ed.max} := \frac{49 \cdot L^2 \cdot q_{traffic.d}}{512} = 11.475 \cdot kN \cdot m$$

$$I_{yy} := \frac{1}{12} \cdot w_{deck} \cdot h_{deck.red}^3 - 2 \cdot \left(\frac{1}{12} \cdot w_n \cdot h_n^3 \right) = 2.701 \times 10^7 \cdot mm^4$$

$$\sigma_{m.y.d} := \frac{M_{Ed.max} \cdot \frac{1}{2} \cdot h_{deck.red}}{I_{yy}} = 22.306 \cdot \frac{N}{mm^2}$$

$$UC_M := \frac{\sigma_{m.y.d}}{k_{mod} \cdot \frac{f_{m.k}}{\gamma_M}} = 0.592$$

Shear stress check

$$V_{Ed} := \frac{9}{16} \cdot Q_d = 112.5 \cdot kN$$

$$\tau := \frac{3}{2} \cdot \frac{V_{Ed}}{A} = 5.819 \cdot \frac{N}{mm^2}$$

$$UC_V := \frac{\tau}{k_{mod} \cdot \frac{f_{v.k}}{\gamma_M}} = 2.16$$

Unity Check for shear strength is larger than 1.0

Requirements for the timber deck are not fullfilled when verifying shear stresses according to Eurocode.

Appendix B

Global model description

This appendix will describe the utilized global Finite Element Model used for generating forces, moments and displacements necessary for the calculation of the degree of hybrid interaction of the bridge leaf. This global beam model was developed and validated by Arup to recalculate the static strength and fatigue capacity of the Bridge across the Beneden Merwede. All rights of figures and tables in this chapter are reserved to Arup bv. The geometry of all modelled elements, is based on drawings from the archive of technical drawings provided by Rijkswaterstaat for this project.

This global model (figure B.1) uses only beam elements for the girders and deck boards, each with their own assigned material properties and specified cross- section geometry. For the connection between the main- and cross girder, a rotation spring has been applied to model the riveted joint. This will be discussed later in this chapter.

First, the geometry of all different structural elements will be discussed. Hereafter, the connections and links will be discussed as adapted in the FE model. The support type of the structure is described and finally the material properties are stated.

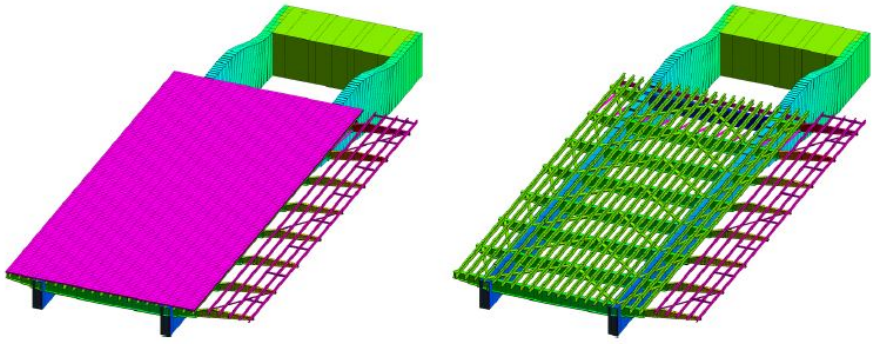

Figure B.1: Overview modelled structure bridge leaf (Arup bv)

B.1 Geometry

The geometry of the main girders, cross girders, the longitudinal girders, counterweight, deck bracing, back post, support girders and the timber deck beams are given here. The expanded part of the leaf for cyclists, is included in the global model, but is disregarded in this research, so its geometry is not specified here.

The measurements given in figure B.2 are used to create a grid. In reality, the left side of the girder to the rotation point, is rotated 1 °to the horizontal. This has not been taken into account in the model.

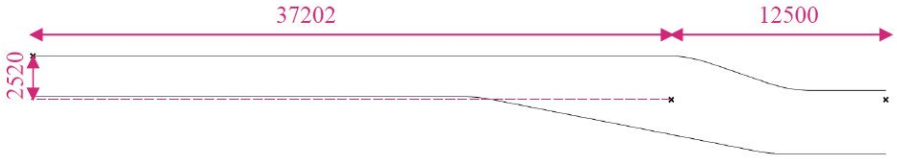

Figure B.2: Global measurements main girders (Arup bv)

B.1.1 Main girders (MG)

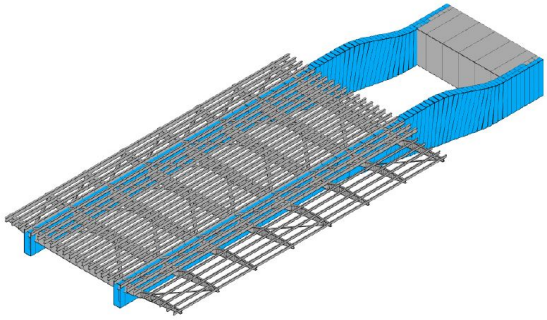

Figure B.3: Main girders (Arup bv)

Figure B.3 shows the main girders. The complex outer measurements of the course of the main girders are given by the distances and radius in figures B.2 and B.5.

Figure B.4: Outer measurements of the main girders (Arup bv)

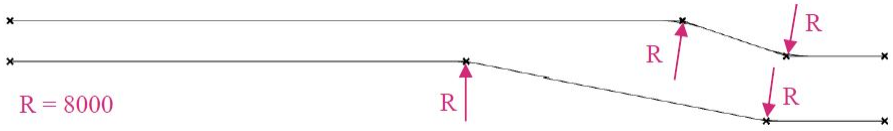

Figure B.5: Transition of lines of the main girders (Arup bv)

The shape of the center line given in figure B.6 is derived from the previously mentioned measurements. Nodes are located at the ends of cross girders, the rotation point and the connection to the counterweight. The mesh was created between the nodes.

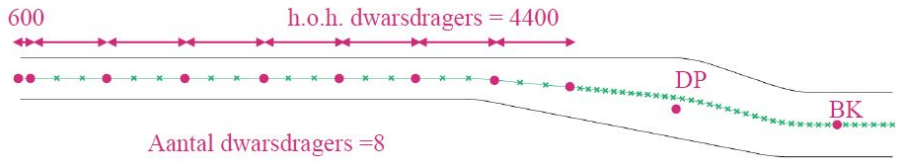

Figure B.6: Center lines of the main girders (Arup bv)

The heights for the elements (figure B.7) are determined at the center of the elements (between the nodes).

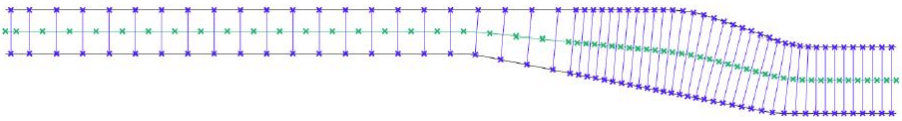

Figure B.7: Cross-sectional height of the main girders (Arup bv)

The cross- sectional properties of the main girder are given in figure B.8. The height of the cross- section and the thickness of the web plate vary over the length of the main girder.

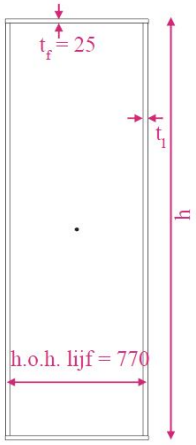

Figure B.8: Cross- sectional properties of the main girders (Arup bv)

Figure B.9 and B.10 respectively show the variation in thickness of the webs and the variation in sizes of the cross- section for the main girders.

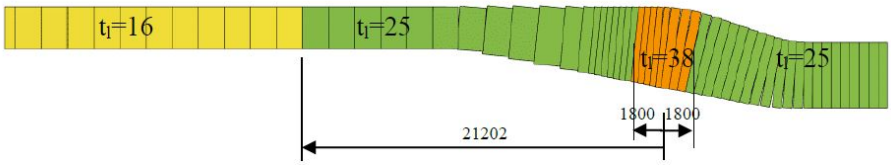

Figure B.9: Variation in web thickness over the length of the main girders (Arup bv)

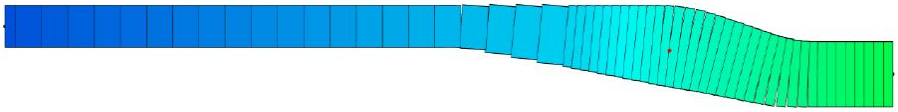

Figure B.10: Variation in size of the cross- section of the main girders (Arup bv)

B.1.2 Cross girders (CG)

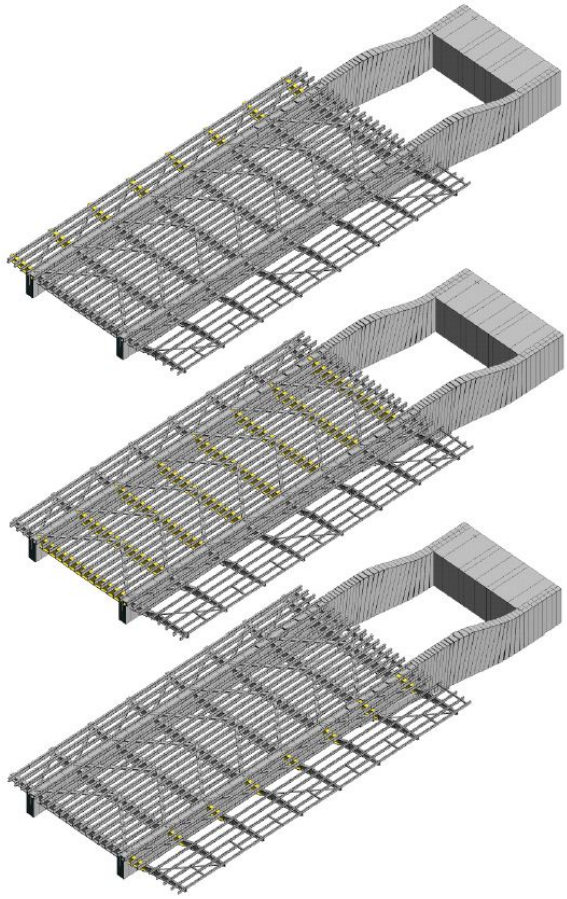

Figure B.11: Cross girders, consisting (top to bottom) of a right console (CR), a center cross girder (MDD) and a left console (CL) (Arup bv)

Figure B.11 shows the eight cross girders in the beam model. Each cross girder consists of a left console (CL), a center cross girder (CCG) and a right console (CR). The parameters of the main measurements of the cross girders are given in figure B.12. The values of these measurements and cross- sectional properties are given in figures B.13 and B.14. A distinction was made between the properties of cross girder 1 to 7 and cross girder 8 (closest to the counterweight).

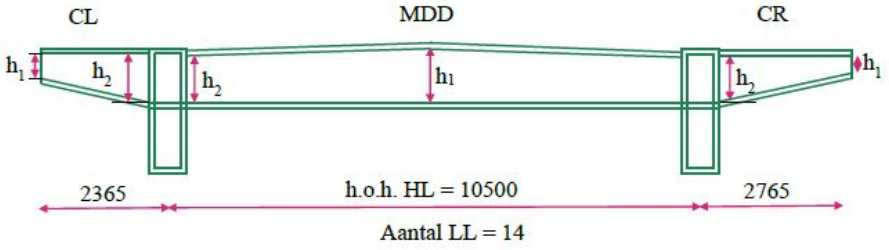

Figure B.12: Measurements of the cross girders (Arup bv) MDD = CCG (Center Cross Girder)

	DD(1) → DD(n-1)		DD8	
	h_1 [mm]	h_2 [mm]	h_1 [mm]	h_2 [mm]
CL	475,2	920	504,2	1120
CR	400	920	400	1120
MDD	1000	931	1200	1131

Figure B.13: Cross- sectional properties of the cross girders (Arup bv) MDD = CCG (Center Cross Girder)

	DD(1) → DD(7)			DD(8)			
	b_f [mm]	t_f [mm]	t_l [mm]	b_f [mm]	t_f [mm]	t_l [mm]	
CL	350	30	14	350	30	14	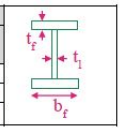
CR	350	30	14	350	30	14	
MDD	350	30	14	350	30	14	

Figure B.14: Cross- sectional properties of the cross girders (Arup bv) MDD = CCG (Center Cross Girder)

Figure B.15 shows a front view of the cross girder, as modelled in GSA.

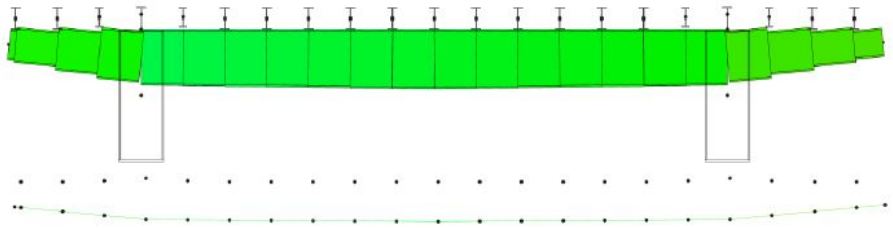

Figure B.15: Front view of the model of the cross girders in GSA (Arup bv)

B.1.3 Longitudinal girders (LG)

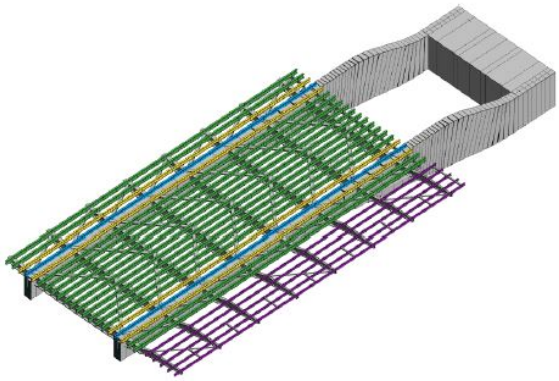

Figure B.16: Longitudinal girders (Arup bv)

Figure B.16 shows the longitudinal cross girders in the bridge leaf. Different types of profiles have been used in this bridge leaf for the longitudinal girders and these are shown in figure B.17.

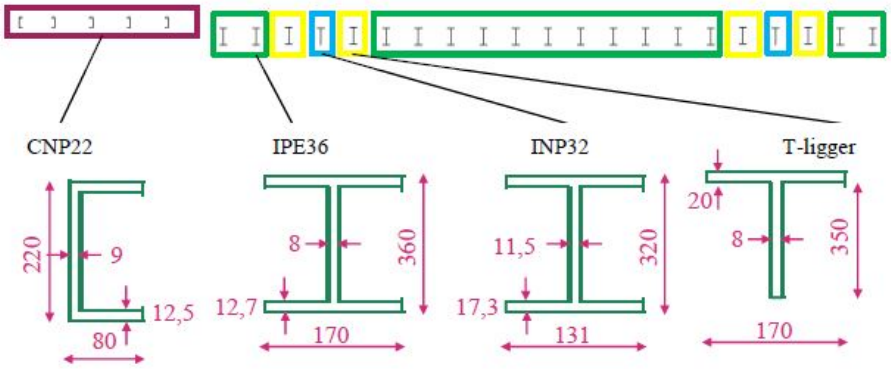

Figure B.17: Cross- sectional properties of the longitudinal girders (Arup bv)

The longitudinal girders cantilever on both ends over the cross girders as depicted in figure B.18.

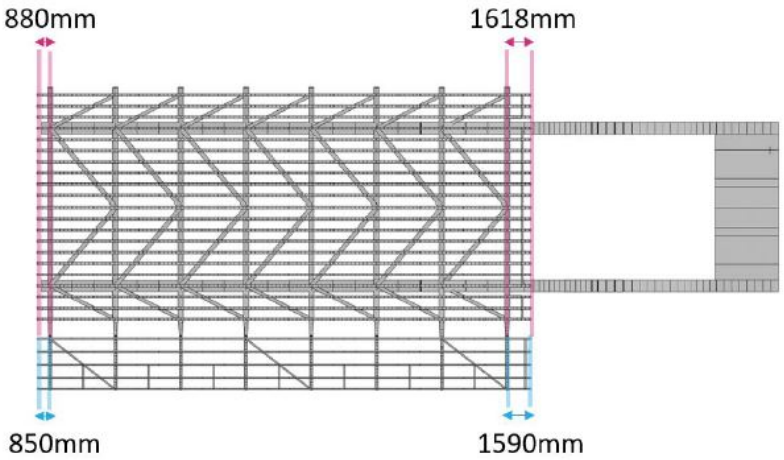

Figure B.18: Cantilever distance of longitudinal girders (Arup bv)

B.1.4 Counterweight (CW)

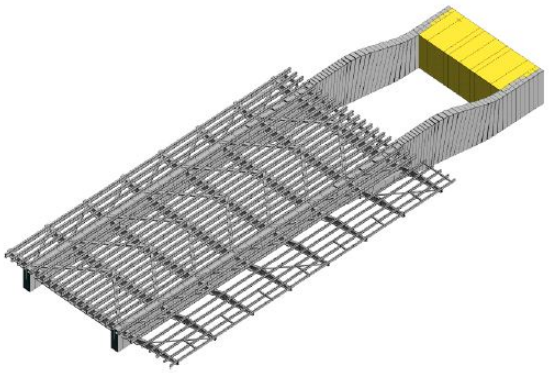

Figure B.19: Counterweight of bascule bridge leaf (Arup bv)

Figure B.19 shows the counterweight of this bascule bridge leaf. Nodes are modelled at the gravity centers of different weight portions within the counterweight. Stiff support elements connect them to the counterweight as can be seen in figure B.20.

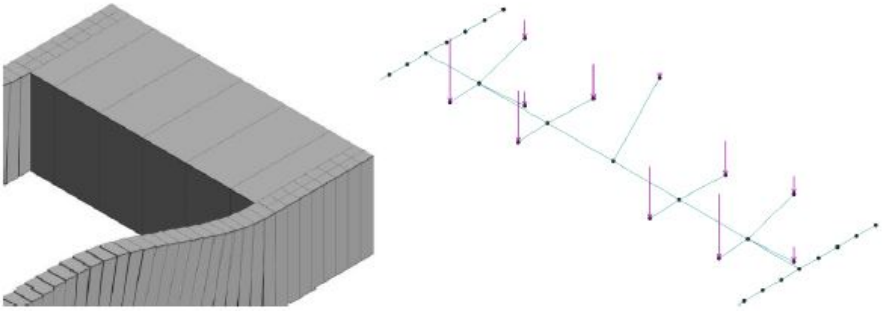

Figure B.20: Supportive elements to the counterweight (Arup bv)

In reality, the counterweight has three vertical web plates of 25 mm thickness, but this has been simplified to a hollow tubular section with two web plates, having a thickness of 32,5 mm as is shown in figure B.21.

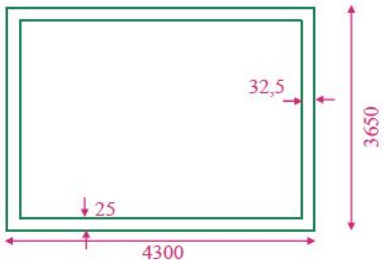

Figure B.21: Cross- sectional properties of counterweight (Arup bv)

B.1.5 Deck bracing (BR)

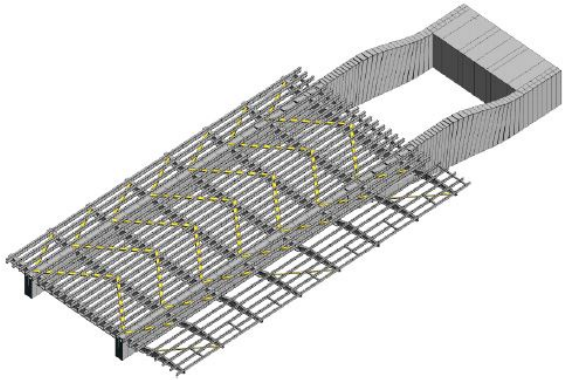

Figure B.22: Deck bracing (Arup bv)

Figure B.22 shows the deck bracing (or: stability member) of the bascule bridge leaf. The cross- sectional properties are given in figure B.23.

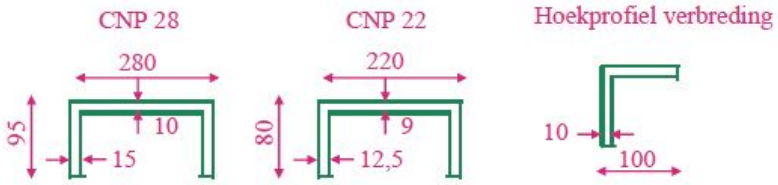

Figure B.23: Cross- sectional properties of the deck bracing (Arup bv)

B.1.6 Back post (BP)

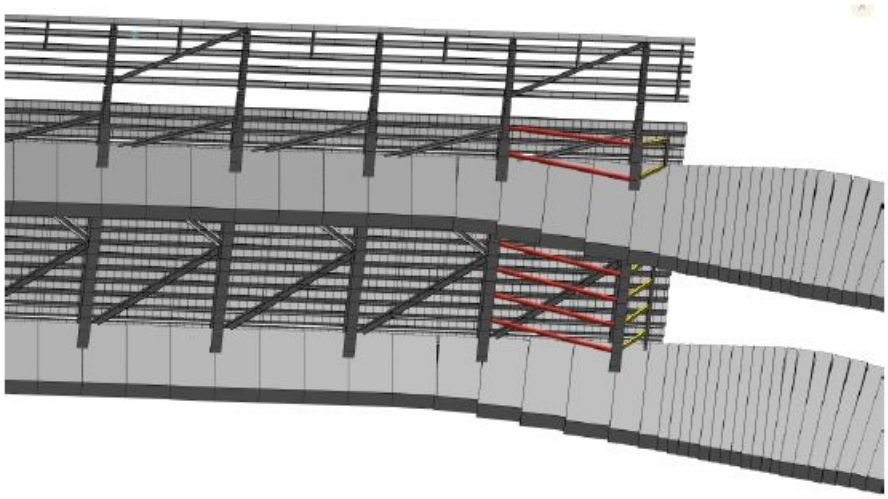

Figure B.24: Back post (Arup bv)

The cross girder closest to the counterweight, is braced by a back post (or: "achterhar"), to support the cantilevering part of the bridge deck. Figure B.24 shows these bracing elements. The yellow highlighted elements are in reality a plate that connects to the web of the cross girder. In the model it is simplified to a T-section girder (Figure B.25), that connects to the support girder. The red highlighted bracing elements are tubular sections connecting the 7th and 8th cross girder. These cross- sectional properties are given in figure B.26.

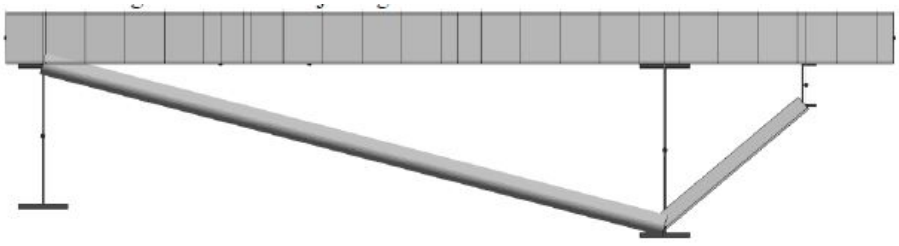

Figure B.25: Back post elements (Arup bv)

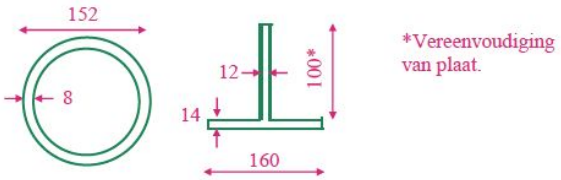

Figure B.26: Cross sectional properties of back post elements (Arup bv)

B.1.7 Support girder (SG)

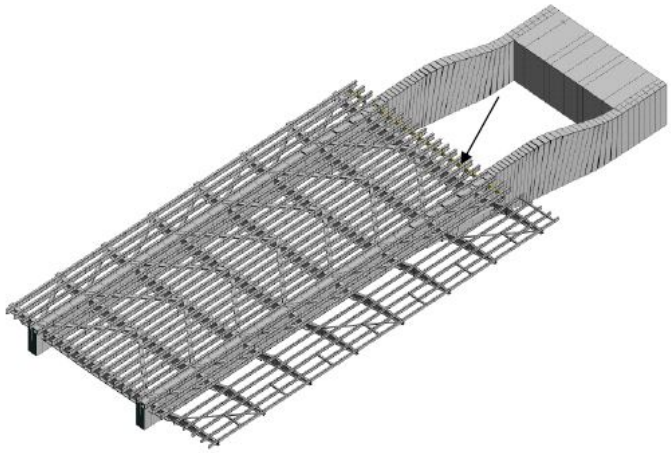

Figure B.27: Support girders (Arup bv)

Figure B.27 shows the support girder at the cantilevering part of the deck that connects to the back post elements. Its cross- sectional properties are given in figure B.28.

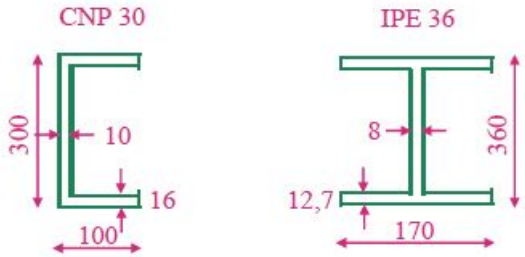

Figure B.28: Cross sectional properties of support girders (Arup bv)

B.1.8 Deck boards (DB)

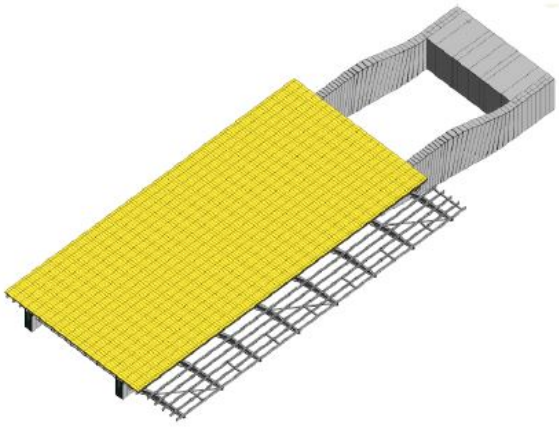

Figure B.29: Timber deck (Arup bv)

The timber boards that create the deck, are shown in figure B.29. All deck boards have the same rectangular cross- section: 280 mm width x 110 mm thickness.

B.2 Connections

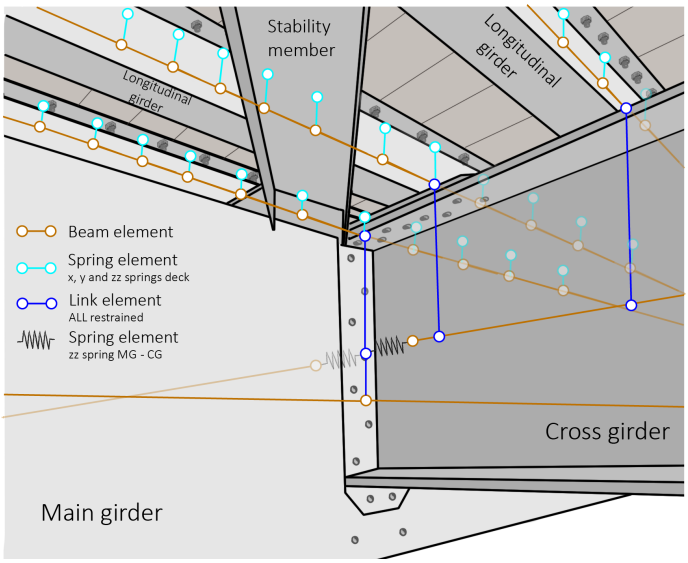

Figure B.30: Type of connection between elements in the model (3D view under the bridge). The deck bracing connections and beam elements for deck boards were not shown for the sake of clarity in the figure.

As for how all joint in the model are connected, an explanation will be given in this section. The most obvious connections regarding this model are shown in figure B.30, but

linkage of elements like the deck bracing and back post, should also be discussed. Therefore, figure B.31 shows a table containing information on all six linkage directions for all types of connections in the traffic bridge leaf model. The links are based upon the type and the geometry of the connections. The types of connections are given in figure B.32.

	x	y	z	xx	yy	zz
MG-CCG						S
MG-CL						S
MG-CR						S
MG-LG						
CCG-LG						
CL-LG						
CR-LG						
BR-CCG			S			
BR-CL&CR			S			
BR-LG				R	R	R
CG-BP						R
BP-SG						R
LG-DB	S	S				S

MG = Main girder, CCG = Center Cross Girder, CL = Console Left, CR = Console Right, LG = Longitudinal Girders, BR = BRacing deck, CG = Cross Girders, BP = Back Post, DB = Deck Boards

S = Spring stiffness, R = beam Release

Figure B.31: Rigid links between elements with the exception of assigned spring stiffnesses (S) and beam releases (R)

	Type
MG-CG	Rivets
MG-CW	Rivets
MG-LG	Welds
MG-BR	Welds
CG-BR	Welds
CG-LG	Rivets, welds, bolts
LG-BR	Welds, bolts
SG-MG	Rivets
BR-CG	Welds
BR-SG	Welds

MG = Main girder, CCG = Center Cross Girder, CL = Console Left, CR = Console Right, LG = Longitudinal Girders, BR = BRacing deck, CG = Cross Girders, BP = Back Post, DB = Deck Boards, CW = Counter Weight

Figure B.32: Connection types for the traffic bridge leaf

The rotational spring stiffness of the main girder- to- cross girder connections is not infinite around its weak axis z. The riveted connection is therefore separately analysed in a linear local shell model. This shell model consists of 2D shell elements) and link elements for the rivets (figure B.33).

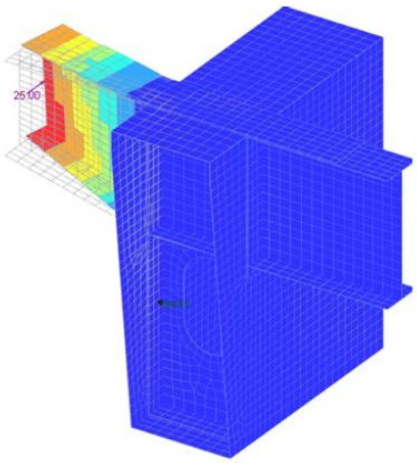

Figure B.33: Local shell model of main girder- to- cross girder connection (Arup bv)

To identify the rotational spring stiffness for the beam model, a horizontal force of 25 kN was put at 1.125 m from the connection. The deformation due to bending of the cantilever and rotation of the connection is 1.052mm. Based on several linear and non-linear local models, a rotation spring stiffness of 41.000 kNm/rad was determined.

Figure B.34 shows the result of the spring stiffness in the GSA global beam model.

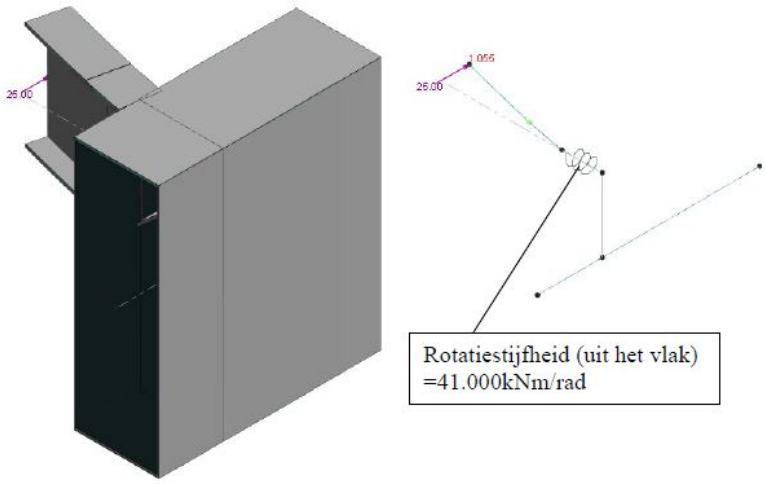

Figure B.34: Detail of rotation spring in global GSA beam model (Arup bv)

The deck bracing to longitudinal girder connections are all assumed to be pinned. As for the back post plate connection to the cross girder and the support girder, it is assumed to be released in its weak axis rotation (around the global z-axis).

The springs for the x, y and zz direction for the longitudinal girder- to- deck connection are thoroughly discussed in this thesis and its properties are altered during the iterations of the model.

B.3 Supports

This research only focuses on a closed situation of the bridge, so only the closed situation for the support at the counterweight is considered to be relevant. The support at the front end is shown in figure B.35 and the main girder is only restrained in vertical direction. Figure B.36 shows the support at the counterweight in the closed situation

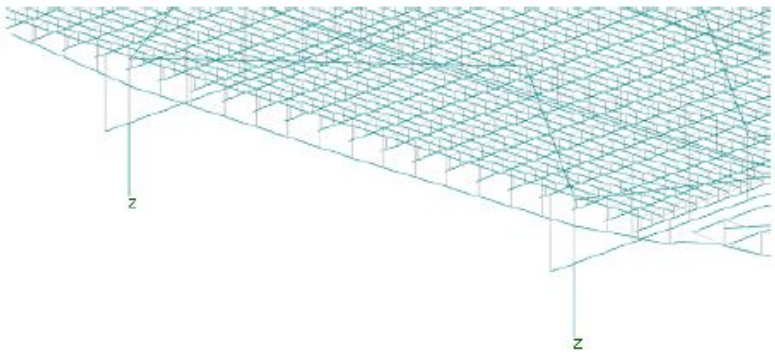

Figure B.35: Support at the front end in closed situation (Arup bv)

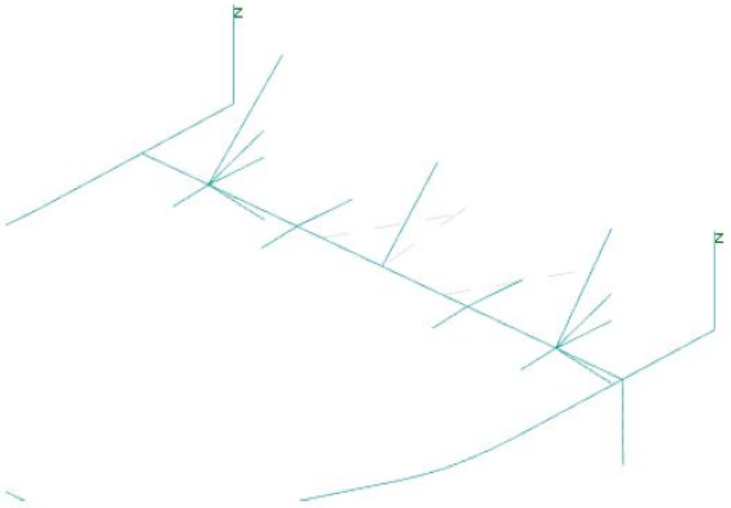

Figure B.36: Support at the counterweight in closed situation (Arup bv)

B.4 Material properties

The material properties for steel and timber beam elements used in the model are given in figure B.37. The density of the timber is set to zero, since the self weight is added separately as a surface load in the analysis.

	Staal	**Hout**
Elasticiteitsmodulus [N/mm2]	210.000	20.000
Poisson's ratio [-]	0,3	0
glijdingsmodulus [N/mm2]	81.000	1.250
Dichtheid [t/m3]	7,85	0
Thermische uitzettingscoëfficiënt [/°C]	$1{,}2 \cdot 10^{-5}$	$0{,}28 \cdot 10^{-5}$

Figure B.37: Material properties of the structural steel- and timber beam elements in the model (Arup bv)

Appendix C

Failure modes

Determining failure mode, loaded ***parallel*** to grain direction

The contribution of the withdrawal effect are unknown and are assumed to be zero for the failure mode calculation.

$d := 20mm$

$k_{90} := 0.9 + 0.015 \frac{d}{mm} = 1.2$

$\rho_k := 900$

$t_1 := 110mm - 22mm = 88 \cdot mm$

$t_{steel} := 0.012 \cdot m$

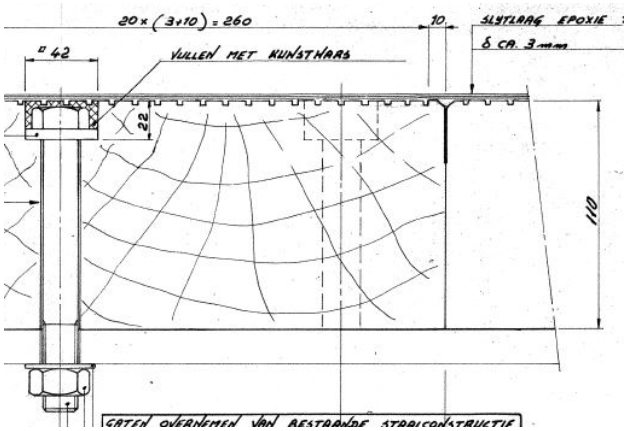

Bolt yield strength M20 8.8:

$f_{yb} := 640 \frac{N}{mm^2}$

Ultimate bolt strength M20 8.8:

$f_{ub} := 800 \frac{N}{mm^2}$

$f_{h.0.k} := 0.082 \frac{N}{mm^2} \cdot \left(1 - 0.01 \frac{d}{mm}\right) \cdot \rho_k = 59.04 \cdot MPa$ For fasteners with predrilled holes

Yield moment fasteners:

$M_{y.Rk} := 0.3 \cdot mm^{0.4} \cdot f_{ub} \cdot d^{2.6} = 0.579 \cdot kN \cdot m$ For round steel bolts

Thin plates

Failure Mode A

$$F_{V.Rk.A} := f_{h.0.k} \cdot 0.4 \cdot d \cdot t_1 = 41.564 \cdot kN$$

Failure Mode B

$$F_{V.Rk.B} := 1.15 \cdot \sqrt{2 \cdot M_{y.Rk} \cdot f_{h.0.k} \cdot d} = 42.535 \cdot kN$$

Thick plates

Failure Mode C

$$F_{V.Rk.C} := f_{h.0.k} \cdot t_1 \cdot d = 103.91 \cdot kN$$

Failure Mode D

$$F_{V.Rk.D} := f_{h.0.k} \cdot t_1 \cdot d \cdot \left(\sqrt{2 + \frac{4 \cdot M_{y.Rk}}{f_{h.0.k} \cdot d \cdot t_1^{\,2}}} - 1 \right) = 52.073 \cdot kN$$

Failure Mode E

$$F_{V.Rk.E} := 2.3 \cdot \sqrt{M_{y.Rk} \cdot f_{h.0.k} \cdot d} = 60.153 \cdot kN$$

Failure load:

$$F_{V.Rk} := \min\left(F_{V.Rk.A}, F_{V.Rk.B}, F_{V.Rk.C}, F_{V.Rk.D}, F_{V.Rk.E}\right) = 41.564 \cdot kN$$

So: failure mode A is governing

a

Determining failure mode, loaded *perpendicular* to grain direction

The contribution of the withdrawal effect are unknown and are assumed to be zero for the failure mode calculation.

$d := 20\,mm$

$k_{90} := 0.9 + 0.015\frac{d}{mm} = 1.2$

$\rho_k := 900$

$t_1 := 110\,mm - 22\,mm = 88\,mm$

$t_{steel} := 0.012\,m$

$\alpha := 90$

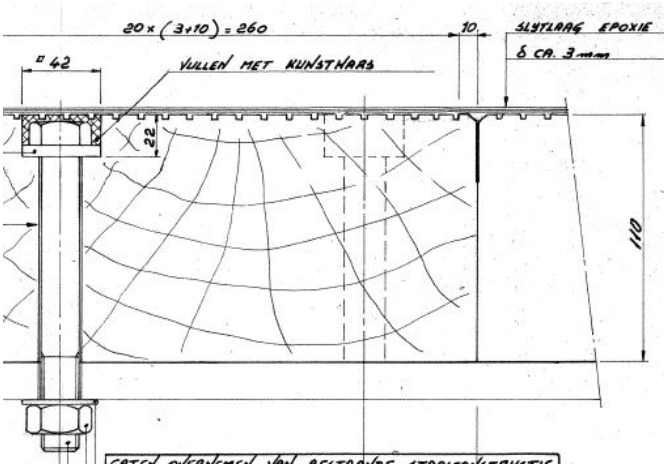

Bolt yield strength M20 8.8:

$f_{yb} := 640\frac{N}{mm^2}$

Ultimate bolt strength M20 8.8:

$f_{ub} := 800\frac{N}{mm^2}$

$f_{h.0.k} := 0.082\frac{N}{mm^2}\cdot\left(1 - 0.01\frac{d}{mm}\right)\cdot\rho_k = 59.04\,MPa$ For fasteners with predrilled holes

$f_{h.\alpha.k} := \frac{f_{h.0.k}}{k_{90}\sin(\alpha)^2 + \cos(\alpha)^2} = 50.903\,MPa$

Yield moment fasteners:

$M_{y.Rk} := 0.3\cdot mm^{0.4}\cdot f_{ub}\cdot d^{2.6} = 0.579\,kN\cdot m$ For round steel bolts

Thin plates

Failure Mode A

$$F_{V.Rk.A} := f_{h.\alpha.k} \cdot 0.4 \cdot d \cdot t_1 = 35.836 \cdot kN$$

Failure Mode B

$$F_{V.Rk.B} := 1.15 \cdot \sqrt{2 \cdot M_{y.Rk} \cdot f_{h.\alpha.k} \cdot d} = 39.495 \cdot kN$$

Thick plates

Failure Mode C

$$F_{V.Rk.C} := f_{h.\alpha.k} \cdot t_1 \cdot d = 89.59\,kN$$

Failure Mode D

$$F_{V.Rk.D} := f_{h.\alpha.k} \cdot t_1 \cdot d \cdot \left(\sqrt{2 + \frac{4 \cdot M_{y.Rk}}{f_{h.\alpha.k} \cdot d \cdot {t_1}^2}} - 1 \right) = 46.1\,kN$$

Failure Mode E

$$F_{V.Rk.E} := 2.3 \cdot \sqrt{M_{y.Rk} \cdot f_{h.\alpha.k} \cdot d} = 55.855\,kN$$

Failure load:

$$F_{V.Rk} := \min\left(F_{V.Rk.A}, F_{V.Rk.B}, F_{V.Rk.C}, F_{V.Rk.D}, F_{V.Rk.E}\right) = 35.836\,kN$$

So: failure mode A is governing

a

Appendix D

Determining the stiffness matrix for the bolted deck joint

The stiffness matrix for a rigid body restrained by four springs, can be determined using the displacement method. Figure D.1 displays a schematic of the rigid body, its restraints and the relevant dimensions.

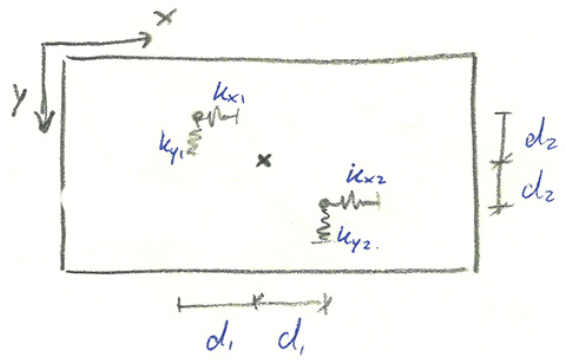

Figure D.1: Schematic display of the local joint model to determine the stiffness matrix according to the displacement method

According to the displacement method, the body should be moved with a displacement x, a displacement y and a rotation around the z-axis (u_x, u_y and ϕ_{xy} respectively). These displacements and rotation result in forces exerted by the springs on the rigid body, as the bolts would do on the timber deck board. According to Newton's second law (F = ma), equations can be found as in figure D.2. These three equations will then translate in the system of equations (equation D.1, D.2 and D.3) that are better described by using a matrix form.

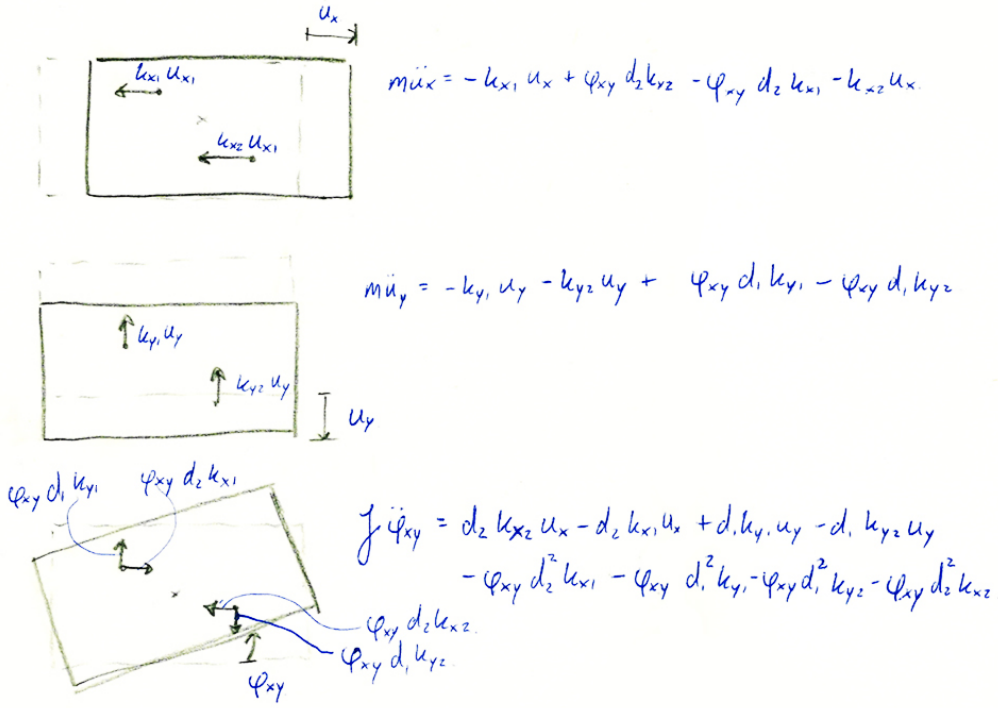

Figure D.2: Determining the equations of motion to determine the stiffness matrix

$$m\frac{d^2u_x}{dt^2} = u_x(-k_{x1} - k_{x2}) + \phi_{xy}d_2(k_{x2} - k_{x1}) \tag{D.1}$$

$$m\frac{d^2u_y}{dt^2} = u_y(-k_{y1} - k_{y2}) + \phi_{xy}d_1(k_{y1} - k_{y2}) \tag{D.2}$$

$$J\frac{d^2\phi_{xy}}{dt^2} = u_x d_2(k_{x2} - k_{x1}) + u_y d_1(k_{y1} - k_{y2}) + \phi_{xy}(d_1^2(-k_{y1} - k_{y2}) + d_2^2(-k_{x1} - k_{x2})) \tag{D.3}$$

So, the stiffness matrix is equal to:

$$\begin{bmatrix} k_{xx} & k_{xy} & k_{xzz} \\ k_{yx} & k_{yy} & k_{yzz} \\ k_{zzx} & k_{zzy} & k_{zzzz} \end{bmatrix} = \begin{bmatrix} k_{x1} + k_{x2} & 0 & d_2(k_{x1} - k_{x2}) \\ 0 & k_{y1} + k_{y2} & d_1(k_{y2} - k_{y1}) \\ d_2(k_{x1} - k_{x2}) & d_1(k_{y2} - k_{y1}) & d_2^2(k_{x1} + k_{x2}) + d_1^2(k_{y1} + k_{y2}) \end{bmatrix}$$

Appendix E

Vertical load spread among longitudinal girders

One of the most simple cases to consider is one deck beam loaded by a vertical concentrated force 'F' on top of three longitudinal girders. These three longitudinal girders each span from cross girder to cross girder. Figure E.1 shows a sketch of this considered structure.

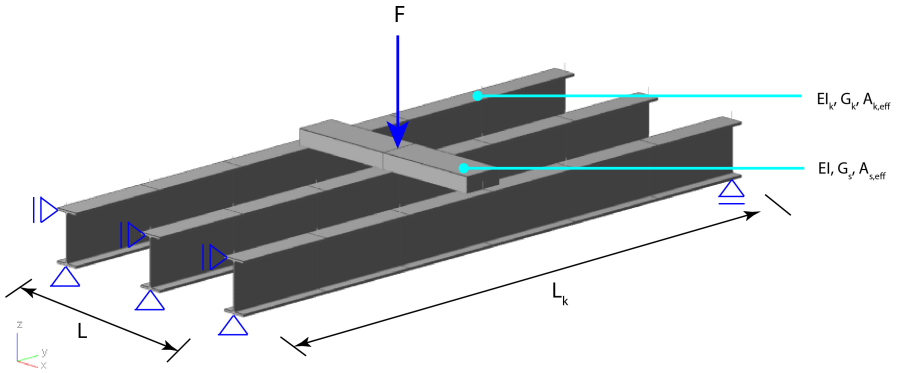

Figure E.1: Sketch of three longitudinal girders with one deck beam loaded by a concentrated force 'F'

To properly assess the distribution of forces to each of the girders, the displacements in the 'springs' (see figure E.2) due to bending and shear have to be considered. From the spring stiffnesses, the reaction forces can then be derived.

Bending deformation

The displacement fields of the deck beam can both be described by the Bernoulli beam fourth order differential equation for bending displacements:

$$EI\frac{d^4w}{dx^4} = -q \tag{E.1}$$

Solving this equation, will deliver a general solution:

$$w_{bending} = C_1 + C_2 x + C3x^2 + C_4 x^3 \tag{E.2}$$

For two fields, each having four unknown constants, eight boundary (or interface) conditions are needed to be specified. In figure E.2, the schematization of the deck beam and the eight conditions are shown.

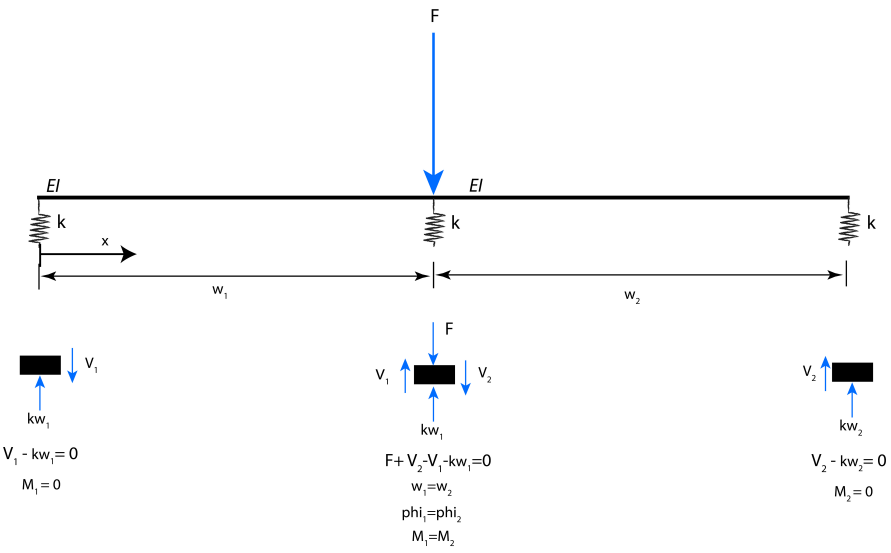

Figure E.2: Mechanical schematization of three longitudinal girders with one deck beam for bending deformations

The spring support stiffness (k) is equal to the bending stiffness of the longitudinal girder at the location of the deck beam (in this case at mid- span of the longitudinal girder): $k = \frac{48EI}{L^3}$

Shear deformation

For shear displacement, the second order differential equations for Timoshenko beams will be used:

$$GA_{eff}\frac{d^2w}{dx^2} = -q \tag{E.3}$$

Equation E.3 will yield a general solution for the shear displacement:

$$w_{shear} = D_1 + D_2 x \tag{E.4}$$

Figure E.3 shows the displacement fields and the corresponding boundary- and interface conditions. Only 2 boundary- and 2 interface conditions are required to solve the system of two second order differential equations.

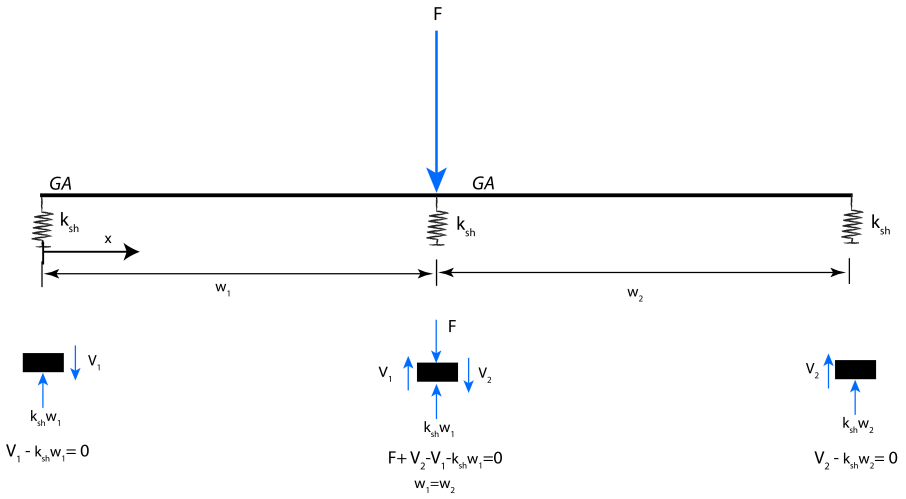

Figure E.3: Mechanical schematization of three longitudinal girders with one deck beam for shear deformations

The stiffness of the spring support for shear deflection is equal to the shear stiffness of the longitudinal girder at the location of the deck beam (in this case at mid-span): $k_{sh} = \frac{4G_k A_k}{L_k}$.

Total displacements

In table E.1, the parameters that were used for obtaining the load spread among three longitudinal girders, are given. The calculation of the total displacements were done by solving the previously mentioned differential equations. This was done by using a solver (e.g. Maple) and the full calculation is attached in appendix F.

General data		
F	100 kN	Vertical concentrated load
L_k	4.400 mm	Center to center distance between cross girders
L	1.500 mm	Total length of deck beam spanning across three longitudinal girders
Deck beam		
b	280 mm	Deck beam width
h	110 mm	Deck beam height
E	20.000 MPa	Elastic modulus of D70 graded timber
I	3.106 cm^4	Second moment of inertia of the deck beam
G	1.250 MPa	Shear modulus of D70 graded timber
A	30.800 mm^2	Cross sectional area of the deck beam
Longitudinal girders		
E_k	210.000 MPa	Elastic modulus of longitudinal girders
I_k	16.270 cm^4	Second moment of inertia for bending around strong axis
G_k	80,77 GPa	Shear modulus of longitudinal girders
A_k	2.668 mm^2	Effective shear area of the longitudinal girders

Table E.1: Standard parameters used to determine load spread among three longitudinal girders

For more complex cases, it might be useful to plot displacement and bending moment graphs in an engineering program (like Oasys GSA). But are these results accurate or do they account for other processes as well?

In figures E.4a and E.4b, the results for both the analytical (Maple) and the computed model (GSA) are shown in terms of beam deflections at spring locations. The results match very well, since for the bending and shear deformation, the longitudinal girders act as 'perfect' springs, their stiffness is easily predictable. In this case that means they do not deform out of plane and they have a constant cross section over their length. By comparison, it shows that the computed model in GSA accurately predicts the distribution of vertical force from the deck to the longitudinal girder.

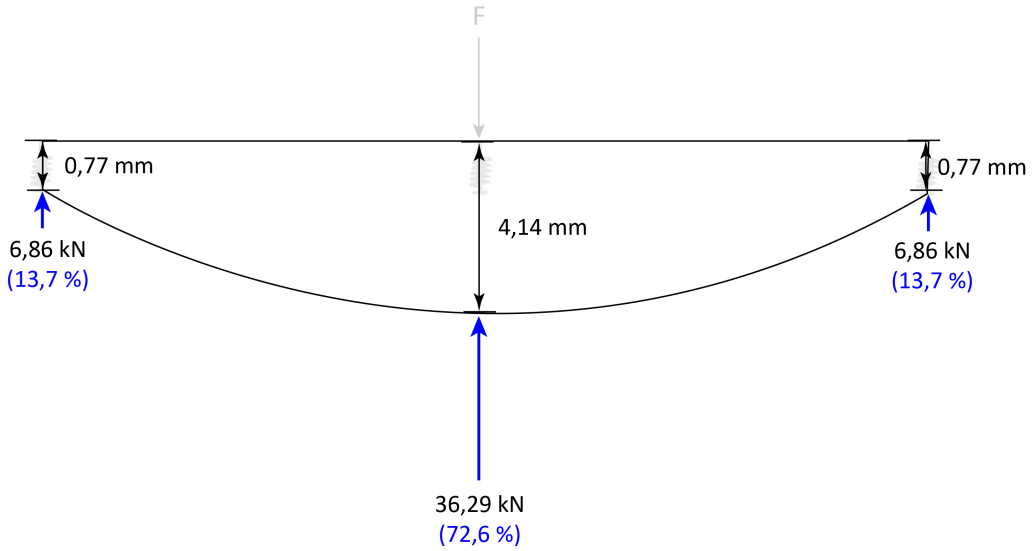

(a) Solving differential equations in Maple

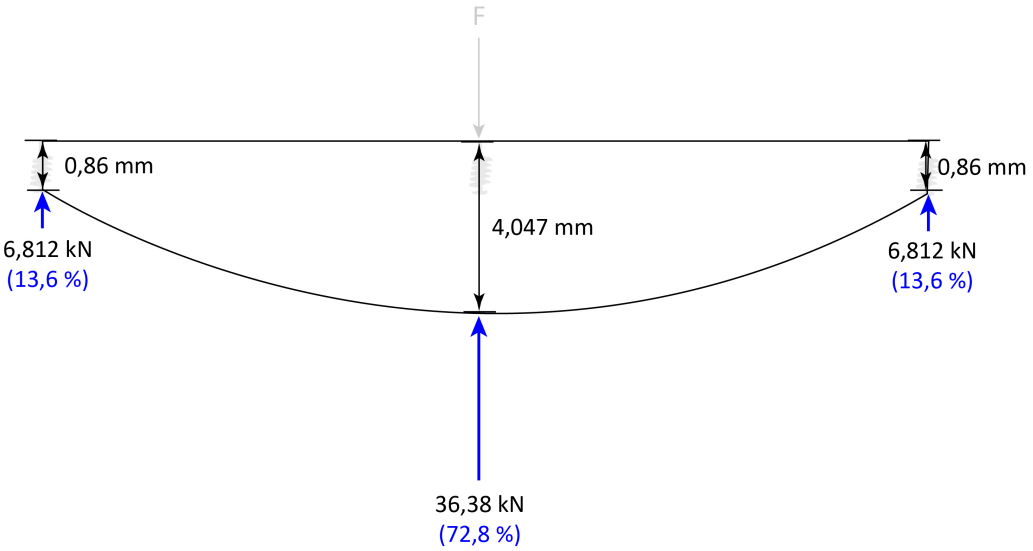

(b) Computed in GSA

Figure E.4: Total deflection for vertical force of 100 kN spreading to 3 longitudinal girders

To transform the deflection at the middle spring into a reaction force, an equivalent spring for the bending and shear stiffness had to be used (see figure E.5). Equation E.5 states the formula for the equivalent that is used to obtain the reaction force that is carried along to one of the cross girders. Note that this equivalent stiffness equation is only valid when the considered deck board is at the center of the longitudinal girder span.

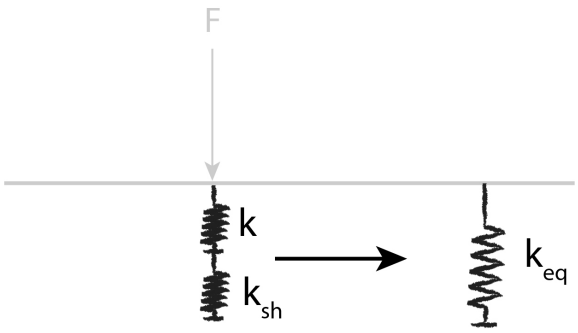

Figure E.5: Equivalent spring for bending and shear stiffness

$$k_{eq} = \frac{1}{\frac{1}{\frac{4G_k A_k}{L_k}} + \frac{1}{\frac{48EI}{L_k^3}}} \tag{E.5}$$

Multiplication of the deflection at the spring locations with the equivalent spring stiffness, results in reaction forces, as are presented in figure E.6.

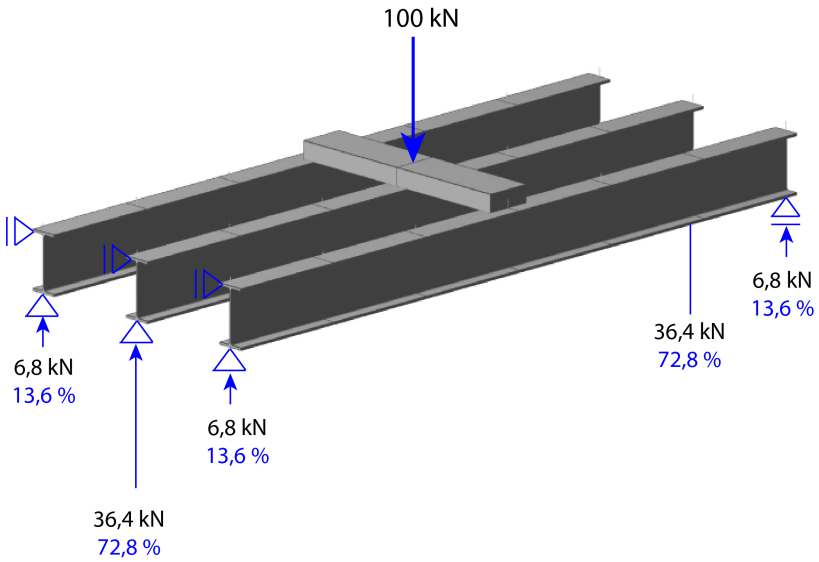

Figure E.6: Resulting load spread

The influence of stiffnesses and spans

Increasing the spring stiffness of the longitudinal girders (either by decreasing the span or using a higher steel grade), will result in a different load spread. When these three support springs get more stiff, a larger portion of the applied vertical load will distribute to the center girder. Figure E.7 presents a graph relating the percentage of load distributed to the center girder to the longitudinal girder span (c.t.c. distance of the cross girders).

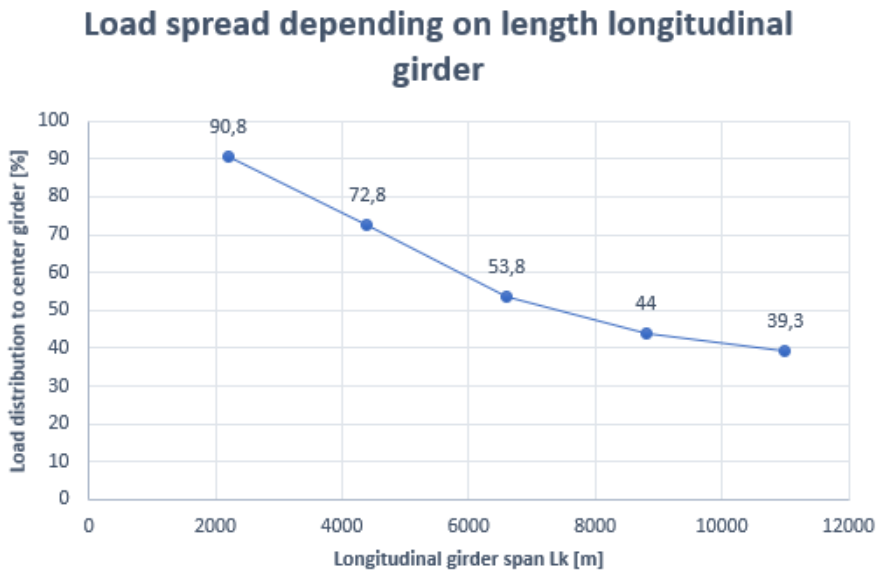

Figure E.7: Relation between longitudinal girder span and portion of the load taken by the center girder

Similarly, if the loaded deck board is closer to one of the cross girders, the bending stiffness of the longitudinal girder increases and thus a larger portion of the load will distribute to the center girder. Up to the point where the deck board is directly above the cross girder and the full vertical force is then taken by the center girder.

For the stiffness of the timber deck beams the opposite principle applies. For increasing stiffness of the deck beams, the load is spread more equally among the three girders. If one imagines the deck beam to be infinitely stiff, the beam would remain straight and all springs would deflect equally, resulting in equal reaction forces distributed to all three girders.

Load spread over six girders

Considering one deck beam, in actual effect, means a spread over six longitudinal girders. Figure E.8 shows the load spread among the girders, when the vertical concentrated load is applied at mid span. Naturally the largest part of the load (similar to considering three girders) is carried by the girders closest to the load.Some of the girders that are further away from the load, do not contribute significantly or they can even be pulled upwards.

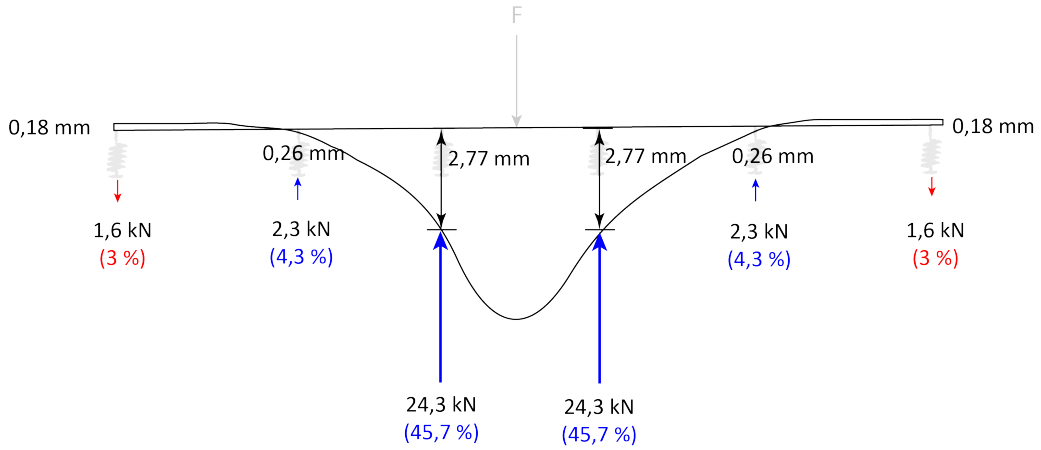

Figure E.8: Resulting load spread for a deck beam across 6 girders

Vertical distributed load

When a wheel load is applied to the deck, it is usually modelled as if it spreads over an area of 600 mm. For simplification, a three girder system will be considered to analyse whether a distributed load, will create a more equal load spread among the girders, which would be expected.

Figure E.9 displays the result of applying the same 100 kN load, but spread over a distance of 600 mm right above the center girder. This model was verified by solving differential equations in Maple (Appendix **??**) and computing it in GSA. The results were identical in terms of deflections and reaction forces.

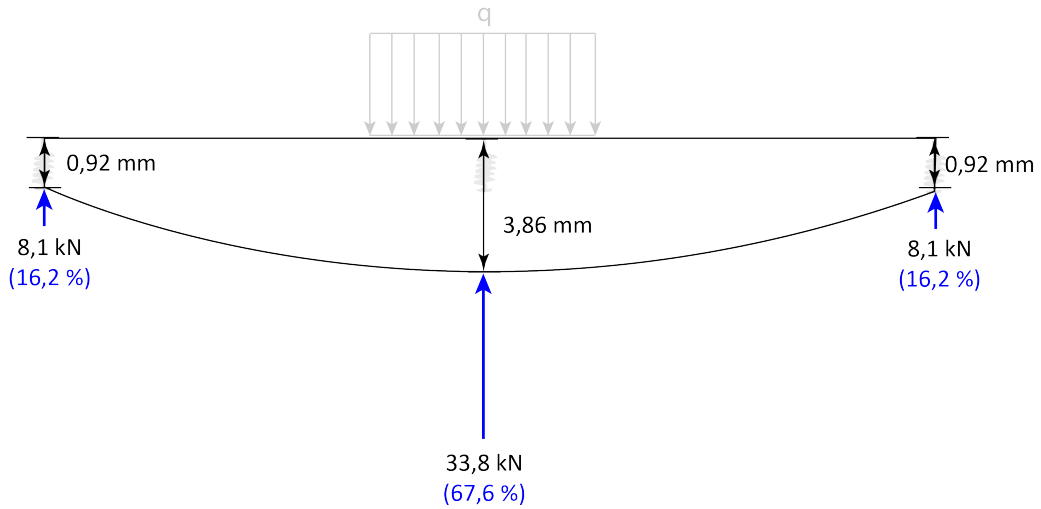

Figure E.9: Resulting load spread for a deck beam across 3 girders with a distributed wheel load

Multiplication by the equivalent spring stiffness, will result in the vertical reaction forces as are visualised in figure E.10.

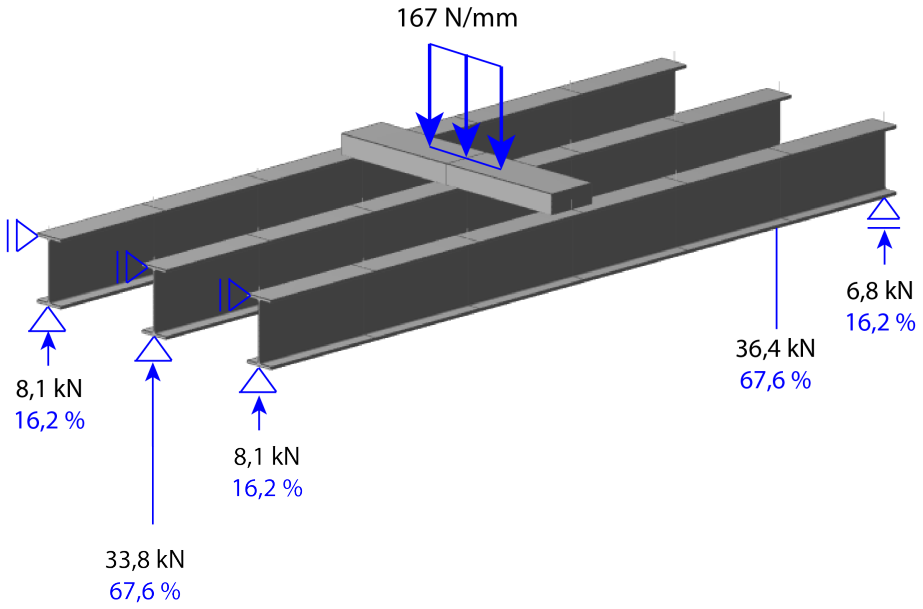

Figure E.10: Reaction forces for a deck beam across 3 girders with a distributed wheel load

Modelling response girders to wheel loads on one deck field

One deck field is in this case bounded by two cross- girders and the length of the deck beams (3750 mm). Before, the cross girder- to- longitudinal girder connection was assumed to be a pinned connection, but in reality, their respective flanges have been welded together and their connection is thus assumed to be fairly rigid.

This boundary condition will influence the load spread to the girders as was mentioned before. These clamped boundary conditions will increase the spring stiffness of the individual girders. As a result, the center girder will take more load. However, since there are now two loads applied and distributed, the center four girders all carry a substantial amount of load.

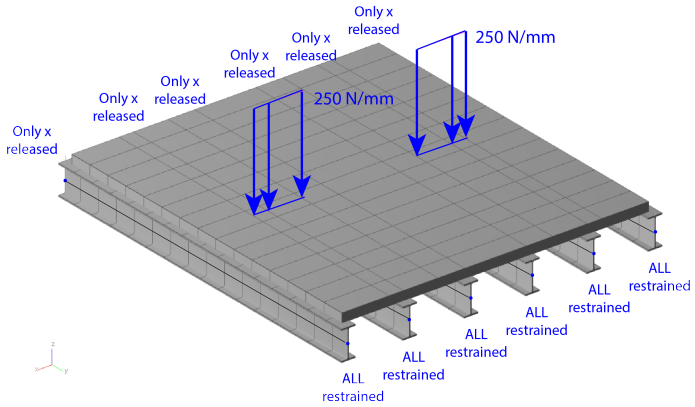

Figure E.11: Loaded situation of one deck field with clamped connections to the cross girders

Figure E.11 illustrates the loaded situation of one deck field and in figure E.12, the response is shown in terms of reaction forces and deflection.

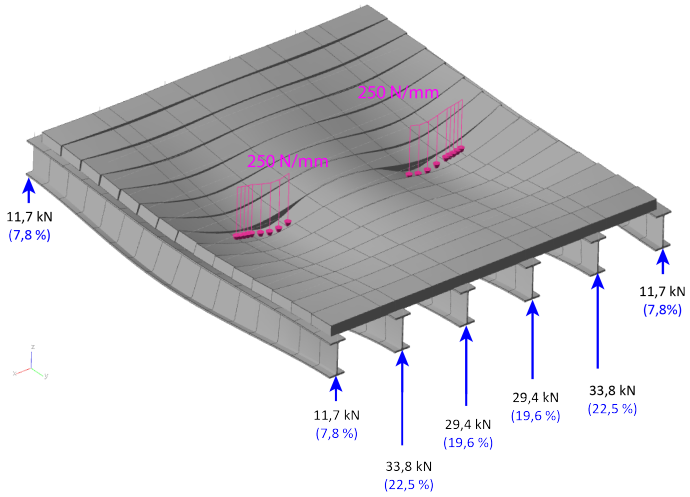

Figure E.12: Response of one deck field to one heavy loaded axle (Q_{1k}, Load model 1, Eurocode 1992-1 [31])

Appendix F

Calculations vertical load spread from deck to longitudinal girders (Maple)

Concentrated load F on 3 girders

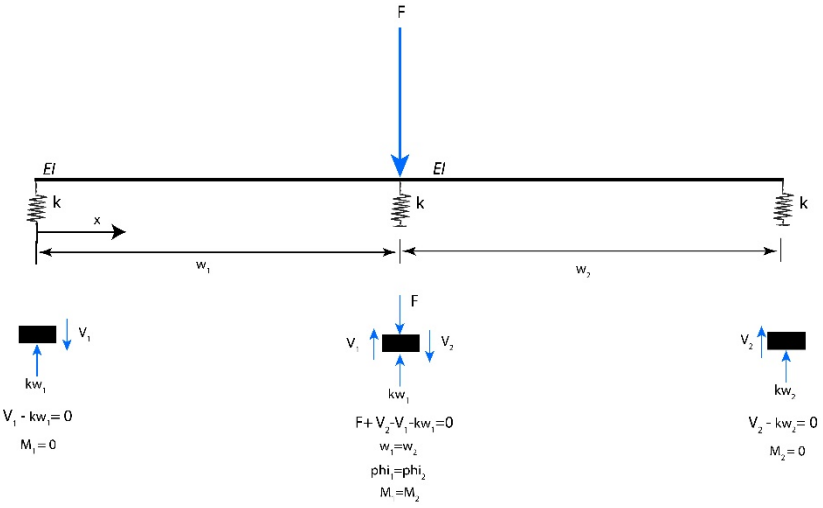


```
> restart;
> w1 := C1 + C2·x + C3·x^2 + C4·x^3 :
> w2 := D1 + D2·x + D3·x^2 + D4·x^3 :
> phi1 := -diff(w1, x) : kappa1 := diff(phi1, x) : M1 := EI·kappa1 : V1 := diff(M1, x) :
> phi2 := -diff(w2, x) : kappa2 := diff(phi2, x) : M2 := EI·kappa2 : V2 := diff(M2, x) :
>
> x := 0 : eq1 := k·w1 = V1 : eq2 := M1 = 0 :
> x := L/2 : eq3 := F + V2 - V1 - k·w1 = 0 : eq4 := w1 = w2 : eq5 := phi1 = phi2 : eq6 := M1 = M2 :
> x := L : eq7 := k·w2 = -V2 : eq8 := M2 = 0 :
>
> b := 280 : h := 110 : Iy := 1/12·b·h^3 :
> E := 20000 : EI := E·Iy :
> F := 100000 :
> L := 1500 :
>
> Ek := 210000 : Ik := 162700000 : EIk := Ek·Ik : Lk := 4400 :
> k := 48·EIk/Lk^3 :
>
> sol := solve({eq1, eq2, eq3, eq4, eq5, eq6, eq7, eq8}, {C1, C2, C3, C4, D1, D2, D3, D4}) : assign(sol) :
>
>
>
> x :='x':
> with(plots) :
> AA := plot(-w1, x = 0..L/2, title = "Bending displacement w(x)") :
> BB := plot(-w2, x = L/2..L) :
```

```
> display({AA, BB});
```

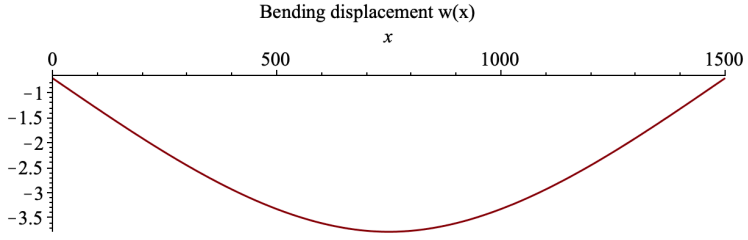

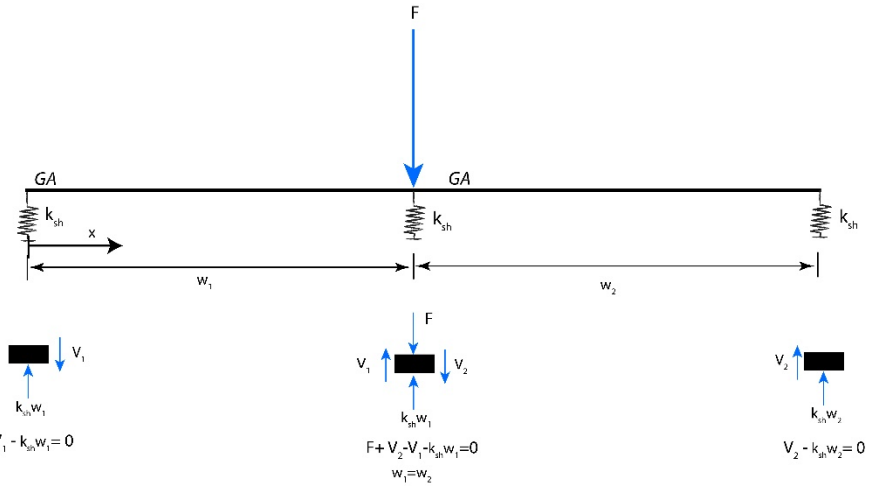


```
> Shear deformation :
> with(plots) :
> w1s := E1s + E2s·xs : w2s := E3s + E4s·xs :
> gamma1s := diff(w1s, xs) : V1s := ks·gamma1s : gamma2s := diff(w2s, xs) : V2s := ks·gamma2s :
> xs := 0 : eq1s := ksh·w1s − V1s = 0 :
> xs := L/2 : eq2s := ksh·w1s + V1s − V2s − F = 0 : eq3s := w1s = w2s :
> xs := L : eq4s := ksh·w2s + V2s = 0 :
> sol := solve({eq1s, eq2s, eq3s, eq4s}, {E1s, E2s, E3s, E4s}) : assign(sol) :
> Lk := 4400 : Gk := 80769.2 : Ak := 7273·0.3669 : L := 1500 : F := 100000 : Gs := 1250 : As := 30800 :
> ksh := 4·Gk·Ak/Lk : ks := Gs·As :
> with(plots) :
> xs :='xs':
> AAs := plot(-w1s, xs = 0 .. L/2, title = "Shear displacement ws(x)") :
> BBs := plot(-w2s, xs = L/2 .. L) :
> display({AAs, BBs});
```

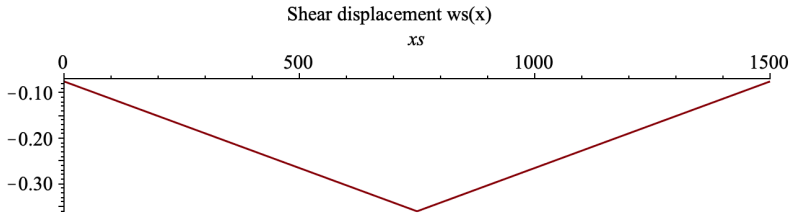


```
> w1t := w1s + w1 :
> xs := 0 : x := 0 : w1t;
```

0.7807018416

```
> xs := L/2 : x := L/2 : w1t;
```

4.143062532

```
> xs := L : x := L : w2s + w2;
```

0.7807018417

```
>
>
>
> keq := 1/(1/ksh + 1/k) :
> keq;
```

17530.12398

Concentrated load F on 6 girders

```
> restart;
> with(plots) :
> w1 := C1 + C2·x + C3·x^2 + C4·x^3 :
> w2 := D1 + D2·x + D3·x^2 + D4·x^3 :
> w3 := E1 + E2·x + E3·x^2 + E4·x^3 :
> w4 := F1 + F2·x + F3·x^2 + F4·x^3 :
> w5 := G1 + G2·x + G3·x^2 + G4·x^3 :
> w6 := H1 + H2·x + H3·x^2 + H4·x^3 :
>
>
> phi1 := -diff(w1, x) : kappa1 := diff(phi1, x) : M1 := EI·kappa1 : V1 := diff(M1, x) :
> phi2 := -diff(w2, x) : kappa2 := diff(phi2, x) : M2 := EI·kappa2 : V2 := diff(M2, x) :
> phi3 := -diff(w3, x) : kappa3 := diff(phi3, x) : M3 := EI·kappa3 : V3 := diff(M3, x) :
> phi4 := -diff(w4, x) : kappa4 := diff(phi4, x) : M4 := EI·kappa4 : V4 := diff(M4, x) :
> phi5 := -diff(w5, x) : kappa5 := diff(phi5, x) : M5 := EI·kappa5 : V5 := diff(M5, x) :
> phi6 := -diff(w6, x) : kappa6 := diff(phi6, x) : M6 := EI·kappa6 : V6 := diff(M6, x) :
>
>
> x := 0 : eq1 := k·w1 = V1 : eq2 := M1 = 0 :
> x := L1 : eq3 := w1 = w2 : eq4 := phi1 = phi2 : eq5 := M1 = M2 : eq6 := k·w1 - V2 + V1 = 0 :
> x := L2 : eq7 := w2 = w3 : eq8 := phi2 = phi3 : eq9 := M2 = M3 : eq10 := k·w2 - V3 + V2 = 0 :
> x := L3 : eq11 := w3 = w4 : eq12 := phi3 = phi4 : eq13 := M3 = M4 : eq14 := -F + V3 - V4 = 0 :
> x := L4 : eq15 := w4 = w5 : eq16 := phi4 = phi5 : eq17 := M4 = M5 : eq18 := k·w4 - V5 + V4 = 0 :
> x := L5 : eq19 := w5 = w6 : eq20 := phi5 = phi6 : eq21 := M5 = M6 : eq22 := k·w5 - V6 + V5 = 0 :
> x := L6 : eq23 := k·w6 = -V6 : eq24 := M6 = 0 :
>
>
> bw := 280 : h := 110 : Iy := 1/12·bw·h^3 :
> E := 20000 : EI := E·Iy :
> F := 100000 :
> L1 := 750 : L2 := 1500 : L3 := 1875 : L4 := 2250 : L5 := 3000 : L6 := 3750 :
>
> Ek := 210000 : Ik := 162700000 : EIk := Ek·Ik : Lk := 4400 :
> k := 48·EIk/Lk^3 :
> sol := solve({eq1, eq2, eq3, eq4, eq5, eq6, eq7, eq8, eq9, eq10, eq11, eq12, eq13, eq14, eq15, eq16, eq17, eq18, eq19, eq20, eq21, eq22, eq23, eq24}, {C1, C2, C3, C4, D1, D2, D3, D4, E1, E2, E3, E4, F1, F2, F3, F4, G1, G2, G3, G4, H1, H2,
      H3, H4}) : assign(sol) :
>
> x :='x':
> with(plots) :
> AA := plot(-w1, x = 0..L1, title = "Displacement w(x)") :
> BB := plot(-w2, x = L1..L2) :
> CC := plot(-w3, x = L2..L3) :
> DD := plot(-w4, x = L3..L4) :
> EE := plot(-w5, x = L4..L5) :
> FF := plot(-w6, x = L5..L6) :
>
> display({AA, BB, CC, DD, EE, FF});
```

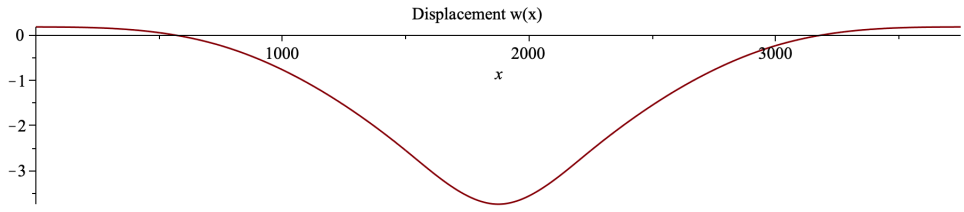

```
> Shear deformation
```

Shear deformation

```
> w1s := E1s + E2s·xs : w2s := E3s + E4s·xs : w3s := E5s + E6s·xs : w4s := E7s + E8s·xs : w5s := E9s + E10s·xs : w6s := E11s + E12s·xs :
> gamma1s := diff(w1s, xs) : V1s := ks·gamma1s : gamma2s := diff(w2s, xs) : V2s := ks·gamma2s : gamma3s := diff(w3s, xs) : V3s := ks·gamma3s : gamma4s := diff(w4s, xs) : V4s := ks·gamma4s : gamma5s := diff(w5s, xs) : V5s := ks·gamma5s : gamma6s := diff(w6s, xs) : V6s := ks·gamma6s :
> xs := 0 : eq1s := ksh·w1s − V1s = 0 :
> xs := L1 : eq2s := w1s = w2s : eq3s := ksh·w2s + V1s − V2s = 0 :
> xs := L2 : eq4s := w2s = w3s : eq5s := ksh·w3s + V2s − V3s = 0 :
> xs := L3 : eq6s := w3s = w4s : eq7s := F + V4s − V3s = 0 :
> xs := L4 : eq8s := w4s = w5s : eq9s := ksh·w5s + V4s − V5s = 0 :
> xs := L5 : eq10s := w5s = w6s : eq11s := ksh·w6s + V5s − V6s = 0 :
> xs := L6 : eq12s := ksh·w6s + V6s = 0 :
>
> sol := solve({eq1s, eq2s, eq3s, eq4s, eq5s, eq6s, eq7s, eq8s, eq9s, eq10s, eq11s, eq12s}, {E1s, E2s, E3s, E4s, E5s, E6s, E7s, E8s, E9s, E10s, E11s, E12s}) : assign(sol) :
> Lk := 4400 : G := 80769.2 : As := 7273·0.3669 : G1 := 1250 : As1 := 30800·0.833 :
>
> ksh := 4·G·As / Lk : ks := G1·As1 :
> with(plots) :
> xs := 'xs':
> AA := plot(−w1s, xs = 0..L1, title = "Displacement w(x)") :
> BB := plot(−w2s, xs = L1..L2) :
> CC := plot(−w3s, xs = L2..L3) :
> DD := plot(−w4s, xs = L3..L4) :
> EE := plot(−w5s, xs = L4..L5) :
> FF := plot(−w6s, xs = L5..L6) :
> display({AA, BB, CC, DD, EE, FF});
```

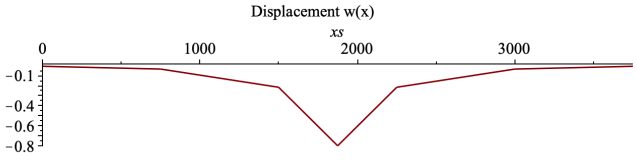


```
> x := 0 : xs := 0 : w1 + w1s;
```

−0.1782072663

```
> x := L1 : xs := L1 : w1 + w1s;
```

0.2626279065

```
> x := L2 : xs := L2 : w2 + w2s;
```

2.767812467

```
> x := L3 : xs := L3 : w3 + w3s;
```

4.539444143

Distributed wheel load q on 3 girders

```
> restart;
> w1 := C1 + C2·x + C3·x^2 + C4·x^3 :
> w2 := D1 + D2·x + D3·x^2 + D4·x^3 + q·x^4/(24·EI) :
> w3 := E1 + E2·x + E3·x^2 + E4·x^3 + q·x^4/(24·EI) :
> w4 := F1 + F2·x + F3·x^2 + F4·x^3 :
>
>
> phi1 := -diff(w1, x) : kappa1 := diff(phi1, x) : M1 := EI·kappa1 : V1 := diff(M1, x) :
> phi2 := -diff(w2, x) : kappa2 := diff(phi2, x) : M2 := EI·kappa2 : V2 := diff(M2, x) :
> phi3 := -diff(w3, x) : kappa3 := diff(phi3, x) : M3 := EI·kappa3 : V3 := diff(M3, x) :
> phi4 := -diff(w4, x) : kappa4 := diff(phi4, x) : M4 := EI·kappa4 : V4 := diff(M4, x) :
>
>
>
> x := 0 : eq1 := k·w1 = V1 : eq2 := M1 = 0 :
> x := L4 : eq3 := k·w4 = -V4 : eq4 := M4 = 0 :
> x := L1 : eq5 := w1 = w2 : eq6 := V1 = V2 : eq7 := phi1 = phi2 : eq8 := M1 = M2 :
> x := L2 : eq9 := k·w2 + V2 - V3 = 0 : eq10 := w2 = w3 : eq11 := phi2 = phi3 : eq12 := M2 = M3 :
> x := L3 : eq13 := V3 = V4 : eq14 := w3 = w4 : eq15 := phi3 = phi4 : eq16 := M3 = M4 :
>
> b := 280 : h := 110 : Iy := 1/12·b·h^3 :
> E := 20000 : EI := E·Iy :
> q := 100000/600 :
> L1 := 450 : L2 := 750 : L3 := 1050 : L4 := 1500 :
>
> Ek := 210000 : Ik := 162700000 : EIk := Ek·Ik : Lk := 4400 :
> k := 48·EIk/Lk^3 :
>
> sol := solve({eq1, eq2, eq3, eq4, eq5, eq6, eq7, eq8, eq9, eq10, eq11, eq12, eq13, eq14, eq15, eq16}, {C1, C2, C3, C4, D1, D2, D3, D4, E1, E2, E3, E4, F1, F2, F3, F4}) : assign(sol) :
> x :='x':
> with(plots) :

> AA := plot(-w1, x = 0..L1, title = "Displacement w(x)") :
> BB := plot(-w2, x = L1..L2) :
> CC := plot(-w3, x = L2..L3) :
> DD := plot(-w4, x = L3..L4) :
>
>
> display({AA, BB, CC, DD});
```

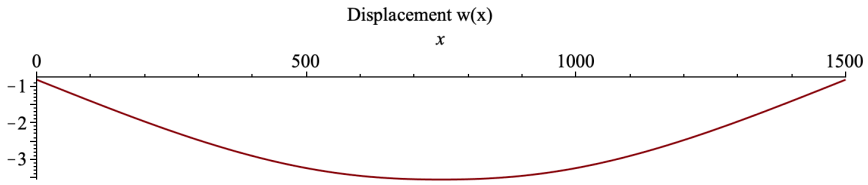


```
>
> with(plots) :
> w1s := E1s + E2s·xs : w2s := 1/ks·(E3s + E4s·xs - q·xs^2/2) : w3s := 1/ks·(E5s + E6s·xs - q·xs^2/2) : w4s := E7s + E8s·xs :
> gamma1s := diff(w1s, xs) : V1s := ks·gamma1s : gamma2s := diff(w2s, xs) : V2s := ks·gamma2s : gamma3s := diff(w3s, xs) : V3s := ks·gamma3s : gamma4s := diff(w4s, xs) : V4s := ks·gamma4s :
> xs := 0 : eq1s := ksh·w1s - V1s = 0 :
> xs := L1 : eq2s := w1s = w2s : eq3s := V1s = V2s :
> xs := L2 : eq4s := w2s = w3s : eq5s := ksh·w2s + V2s - V3s :
> xs := L3 : eq6s := w3s = w4s : eq7s := V3s = V4s :
> xs := L4 : eq8s := ksh·w4s + V4s = 0 :
> sol := solve({eq1s, eq2s, eq3s, eq4s, eq5s, eq6s, eq7s, eq8s}, {E1s, E2s, E3s, E4s, E5s, E6s, E7s, E8s}) : assign(sol) :
> Lk := 4400 : G := 80769.2 : As := 7273·0.3669 : L1 := 450 : L2 := 750 : L3 := 1050 : L4 := 1500 : q := 100000/600 : G1 := 1250 : As1 := 30800 :
> ksh := 4·G·As/Lk : ks := G1·As1 :
```

```
> with(plots) :
> xs :='xs':
> AAs := plot( -w1s, xs = 0 ..L1, title = "Displacement w(x)") :
> BBs := plot( -w2s, xs = L1 ..L2) :
> CCs := plot( -w3s, xs = L2 ..L3) :
> DDs := plot( -w4s, xs = L3 ..L4) :
>
> display( {AAs, BBs, CCs, DDs} );
```

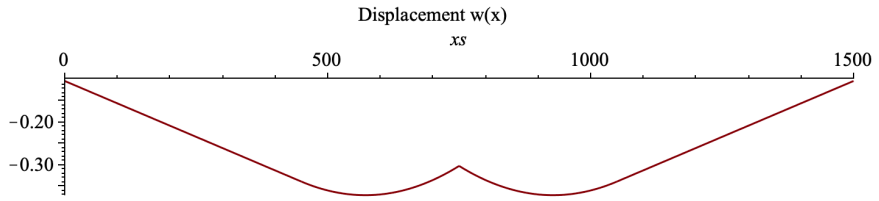


```
> x := 0 : xs := 0 : w1 + w1s;
```

0.9200358813

```
> x := L1 : xs := L1 : w1 + w1s;
```

3.432595952

```
> x := L2 : xs := L2 : w2 + w2s;
```

3.864394454

Appendix G

Force-, bending- and moment diagrams

Most bending moment-, shear force-, axial force- and deflection diagrams are similar in shape for the upper- and lower bound situation, only their magnitudes changed. For the exceptions to this, the figures have been split into a lower- and upper bound situation diagram.

G.1 Vertical load case

Table G.1 displays a comparison between the values for different structural elements in the upper- and lower bound situation.

Structural elements	Lower bound max.	Upper bound max.	Gain / penalty of interaction
Deck boards			
Axial force compression (local x)	-0.059 kN	-19.87 kN	+ 33600%
Axial force tension (local x)	0.076 kN	13.84 kN	+ 18111%
Horizontal shear force (local y)	0.041 kN	21.13 kN	+ 51437%
Vertical shear force (local z)	3.04 kN	2.09 kN	- 32%
Board- to- board compression (global x)	0 kN	-81.59 kN	+ ∞%
Board- to- board tension (global x)	0 kN	50.33 kN	+ ∞%
Deck connections			
Shear force (local x)	0 kN	7.89 kN	+ ∞%
Shear force (local y)	0 kN	37.25 kN	+ ∞%
Bending (local zz)	0.2 kNm	1.2 kNm	+ 500%
Longitudinal girders			
Axial force (local x) compression	-224.56 kN	-153.39 kN	- 32 %
Axial force (local x) tension	157.39 kN	187.29 kN	+ 19%
Horizontal shear force (local y)	5.11 kN	20.66 kN	+ 300%
Vertical shear force (local z)	41.86 kN	40.10 kN	- 4%
Bending (local xx)	0.21 kNm	0.67 kNm	+ 219%
Bending (local yy)	18.32 kNm	12.81 kNm	- 30%
Bending (local zz)	2.96 kNm	2.57 kNm	- 13%
Cross girders			
Axial force (local x)	45.68 kN	91.04 kN	+ 99%
Horizontal shear force (local y)	-55.17 kN	-16.17 kN	- 71%
Vertical shear force (local z)	82.40 kN	66.88 kN	- 19%
Bending (local xx)	-0.72 kNm	-0.72	0%
Bending (local yy)	88.21 kNm	40.37 kNm	- 54%
Bending (local zz)	18.69 kNm	7.67 kN	- 59%
Deflection (global z)	10.95 mm	8.46 mm	- 23%
Stability members			
Axial force (local x)	-78.95 kN	-28.56 kN	- 64%
Horizontal shear force (local y)	17.08 kN	3.1 kN	- 82%
Vertical shear force (local z)	1.34 kN	1.23 kN	- 8%
Bending (local xx)	5.53 kNm	0.0027 kNm	- 100%
Bending (local yy)	14.04 kNm	2.00 kNm	- 86%
Bending (local zz)	-0.69 kNm	-0.62 kNm	- 10%
Main girders			
Axial force (local x)	745.04 kN	1333.68 kN	+ 79%
Horizontal shear force (local y)	12.98 kN	6.06 kN	- 53%
Vertical shear force (local z)	658.27 kN	635.60 kN	- 3%
Bending (local xx)	-82.46 kNm	-31.75 kNm	- 61%
Bending (local yy)	6044.00 kNm	5390.93 kNm	- 11%
Bending (local zz)	29.62 kNm	10.5285	- 64%
Deflection (global z)	10.43 mm	8.20 mm	- 21%

Table G.1: Vertical load case: maximum/minimum forces, moments and deflections for structural elements in the upper- and lower bound situations

G.1.1 Deck boards (DB)

The comparison between the upper- and lower bound situation for forces in the deck boards, requires an explanation regarding the two different elements used. In figure G.1 it is explained how the forces are defined for a deck board element, using the top view.

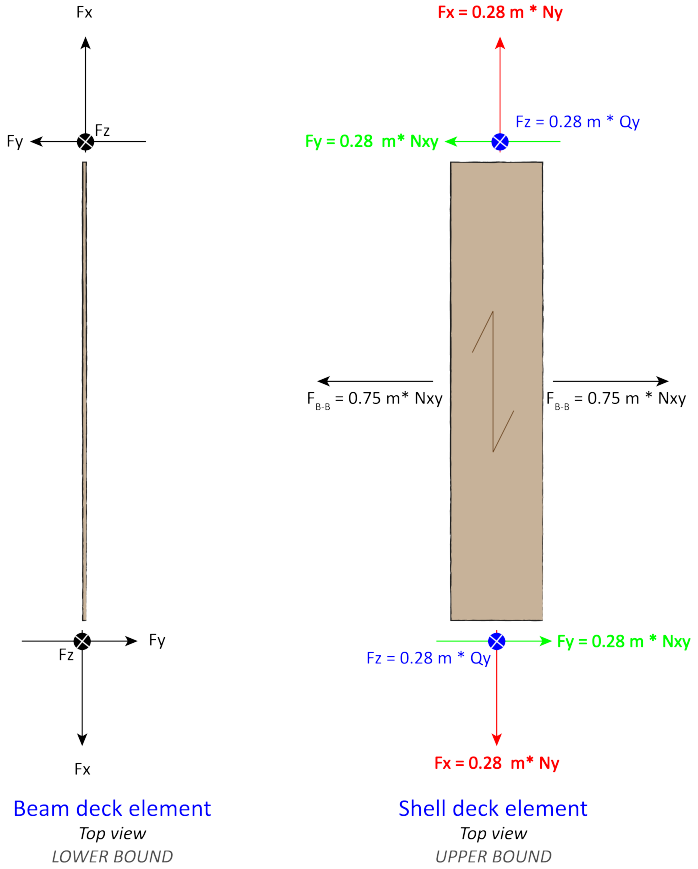

Figure G.1: Definition of forces for deck boards modelled by two different elements

The forces acting on the deck board elements for both the lower- and upper bound situations are given in figures G.2, G.3, G.4 and G.5.

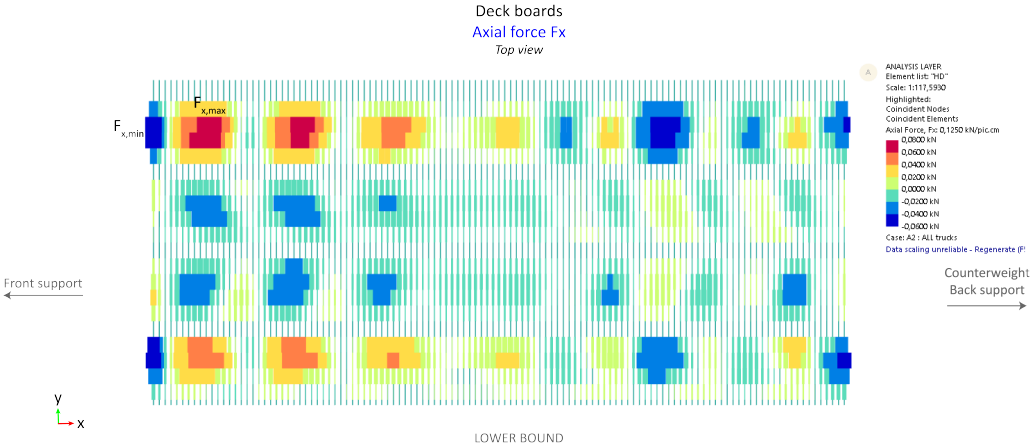

(a) Deck boards - lower bound - vertical load case - axial force

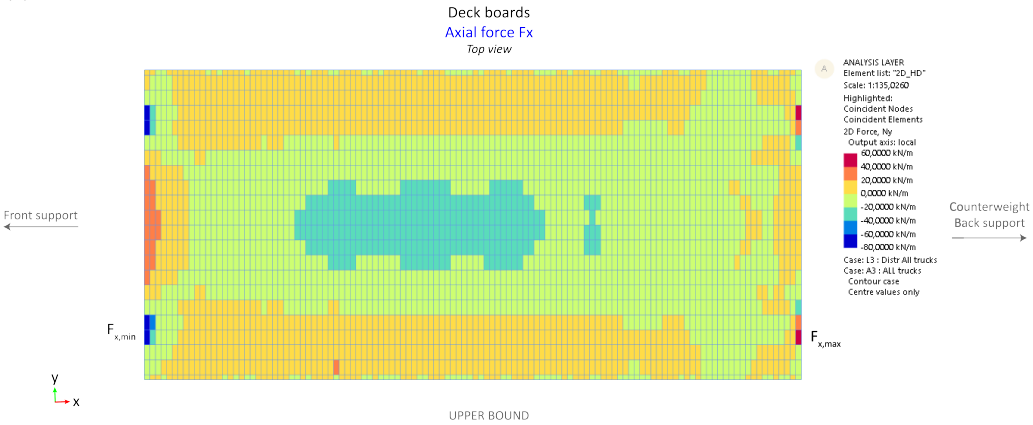

(b) Deck boards - upper bound - vertical load case - axial force

Figure G.2

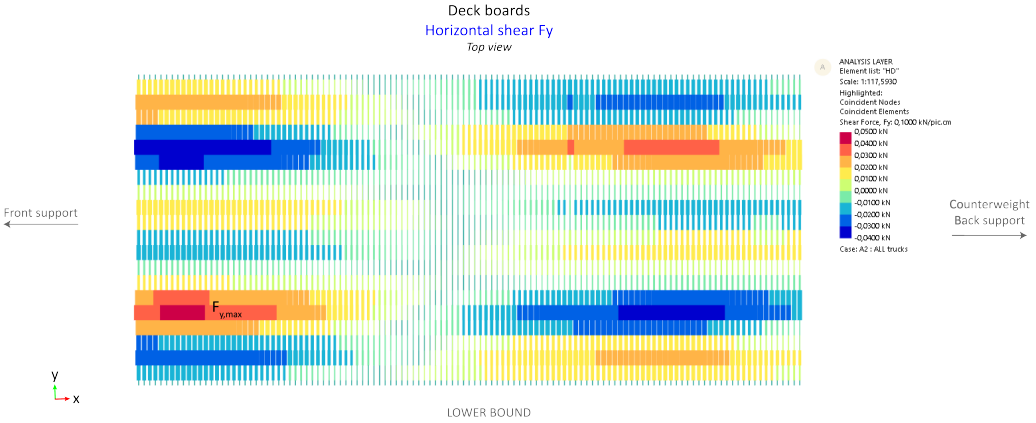

(a) Deck boards - lower bound - vertical load case - horizontal shear force

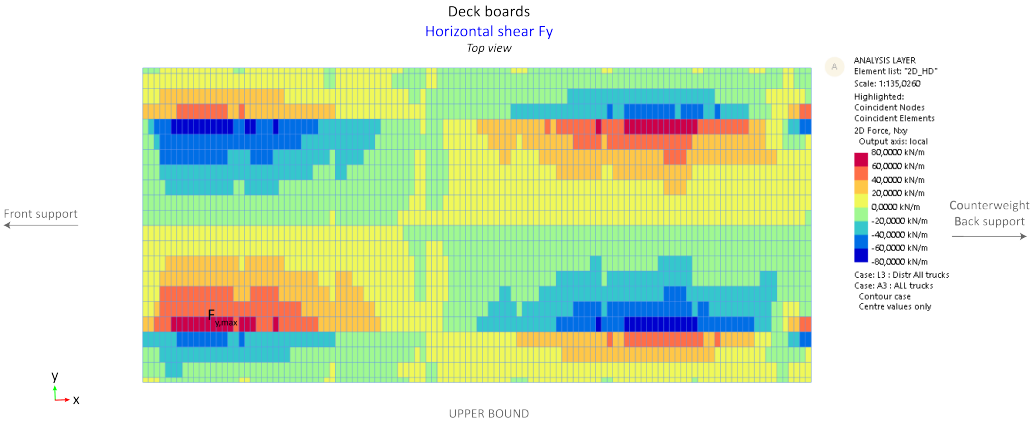

(b) Deck boards - upper bound - vertical load case - horizontal shear force

Figure G.3

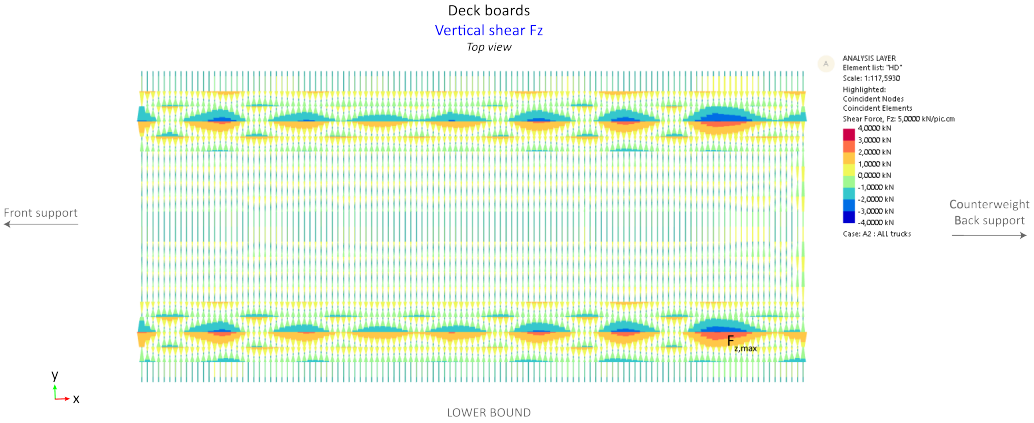

(a) Deck boards - lower bound - vertical load case - vertical shear force

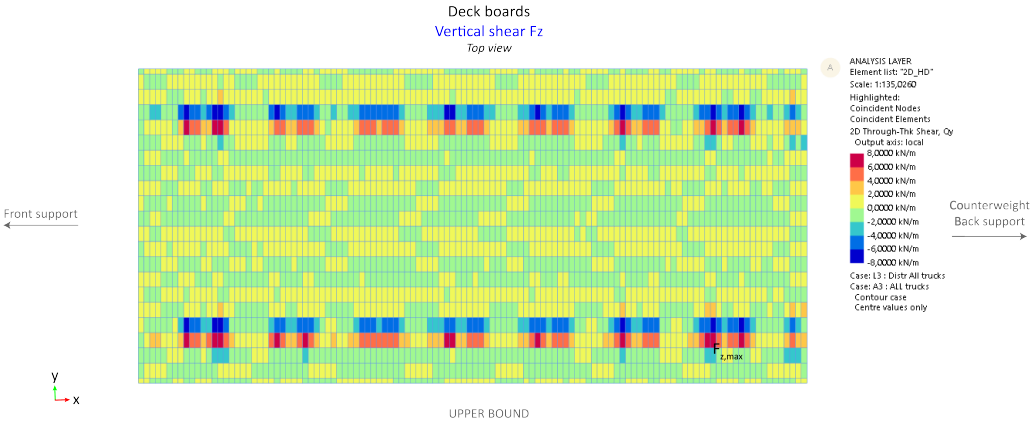

(b) Deck boards - upper bound - vertical load case - vertical shear force

Figure G.4

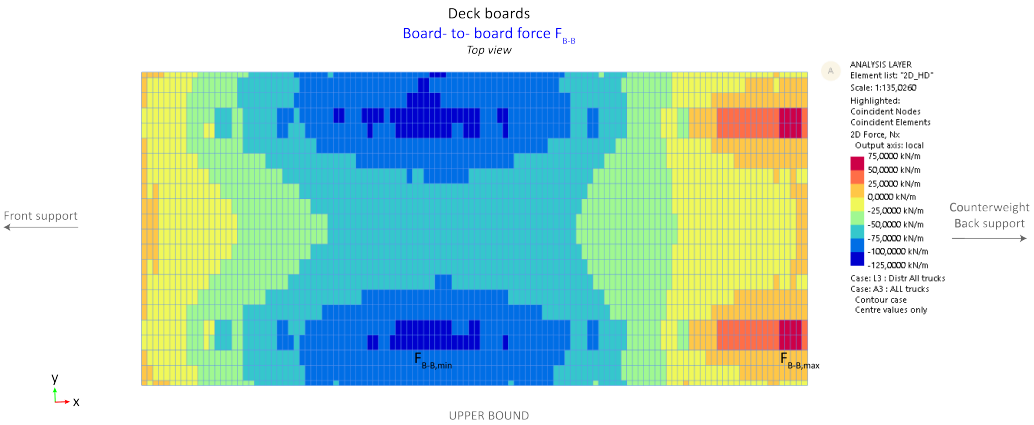

Figure G.5: Deck boards - upper bound - vertical load case - board- to- board forces

G.1.2 Longitudinal girders (LG)

Forces and bending moments acting on the steel longitudinal girders are given in figure G.6, G.7, G.8, G.9, G.10 and G.11.

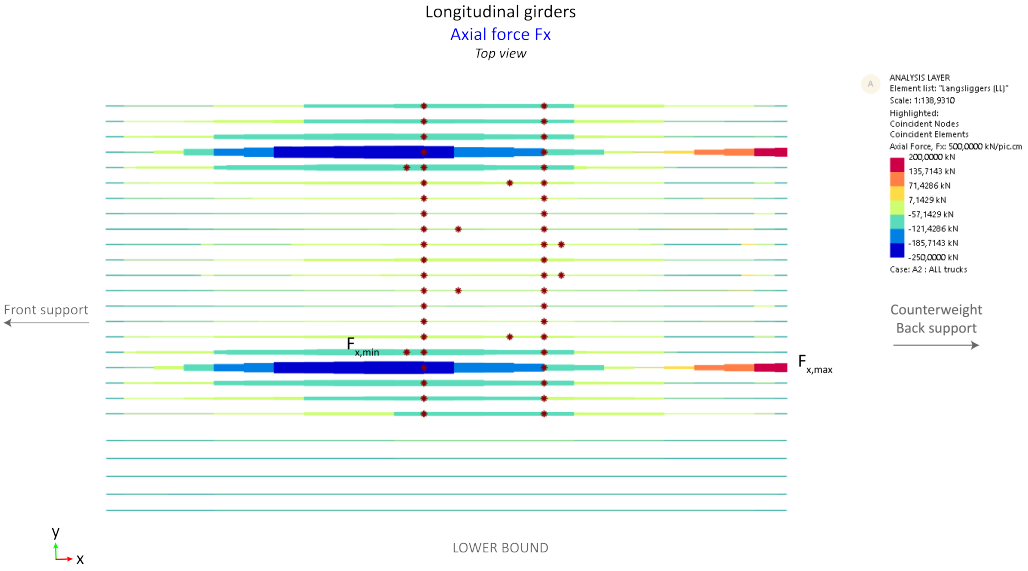

(a) Longitudinal girders - lower bound - vertical load case - axial force

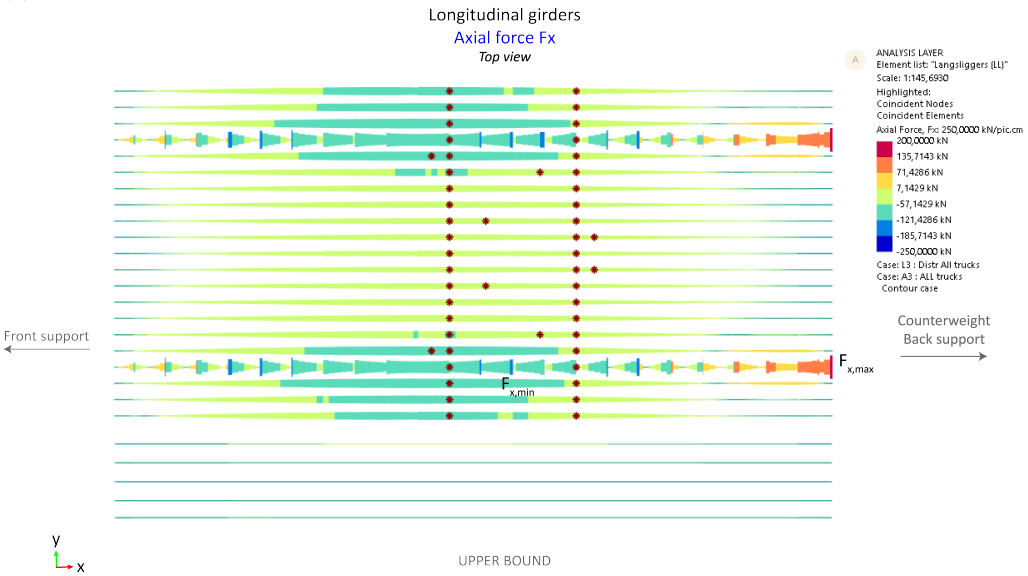

(b) Longitudinal girders - upper bound - vertical load case - axial force

Figure G.6

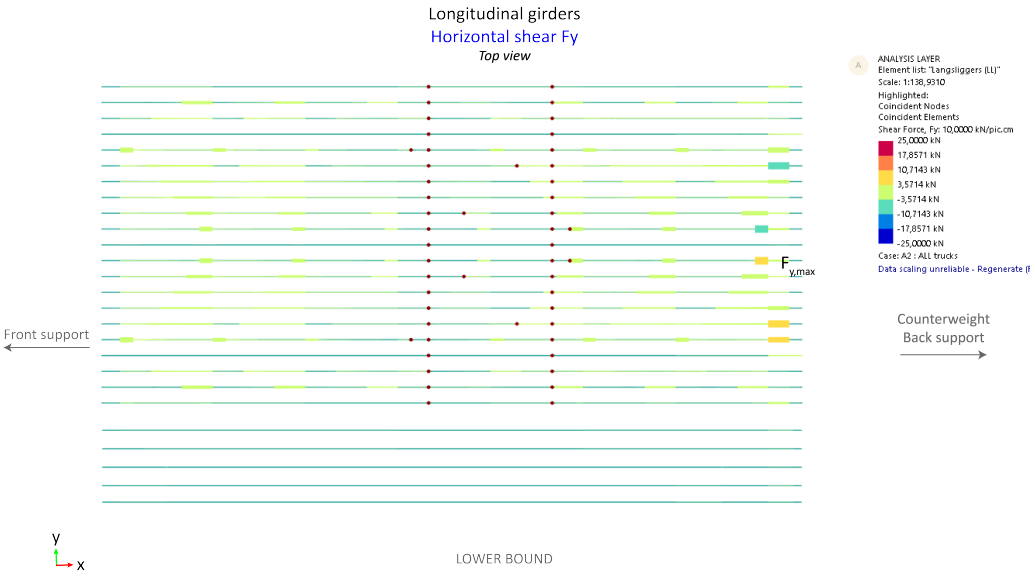

(a) Longitudinal girders - lower bound - vertical load case - horizontal shear force

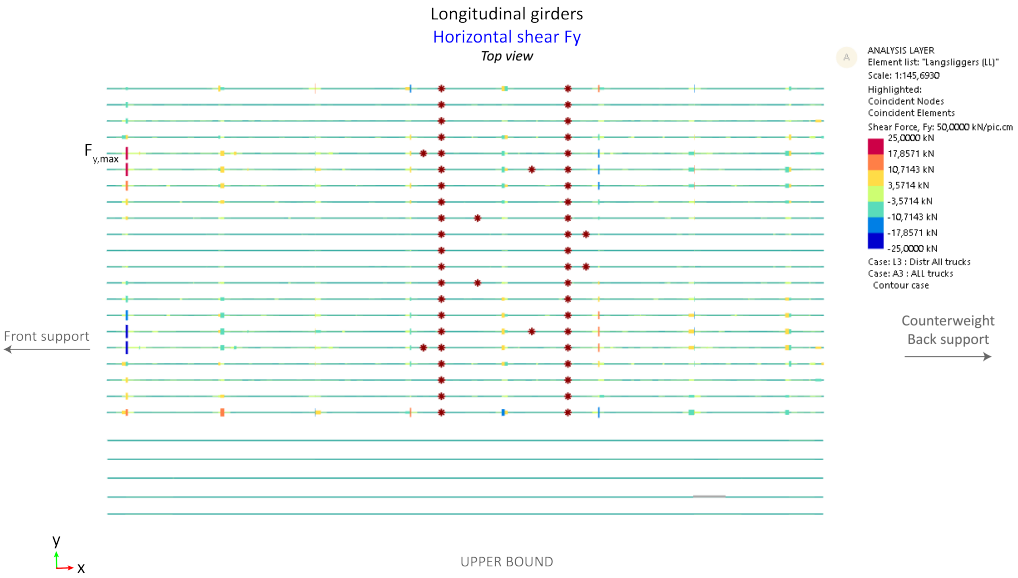

(b) Longitudinal girders - upper bound - vertical load case - horizontal shear force

Figure G.7

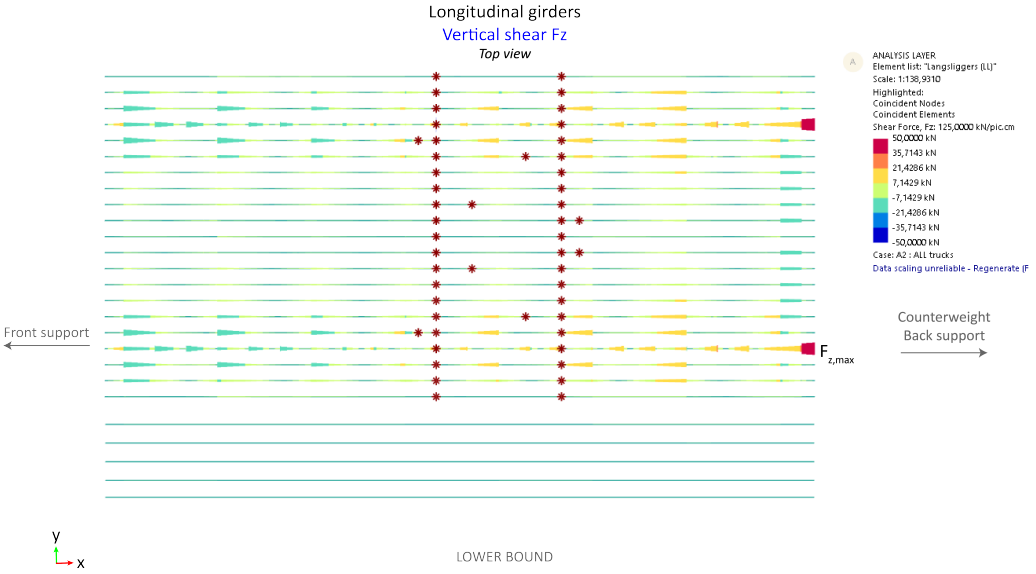

(a) Longitudinal girders - lower bound - vertical load case - Vertical shear force

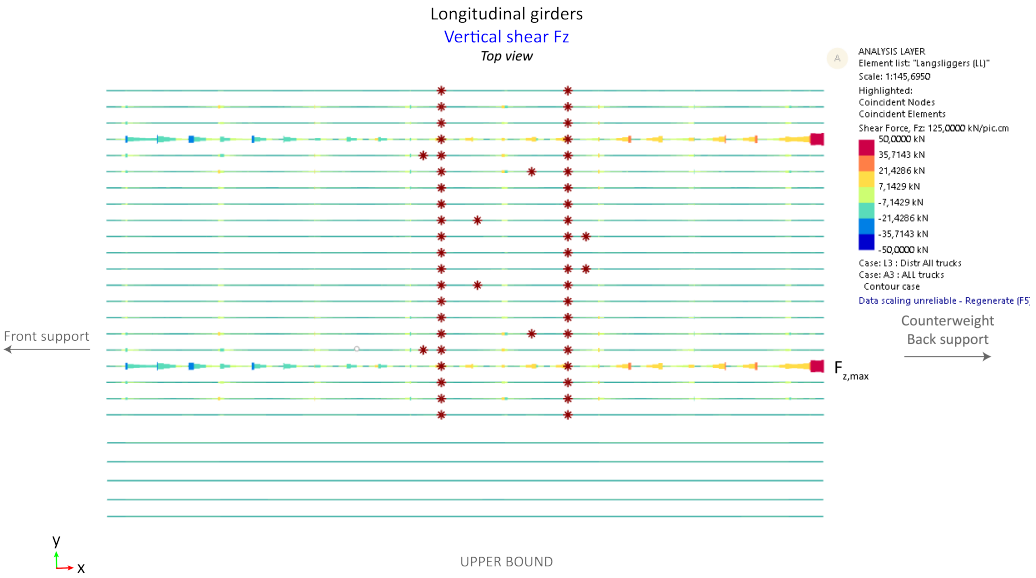

(b) Longitudinal girders - upper bound - vertical load case - vertical shear force

Figure G.8

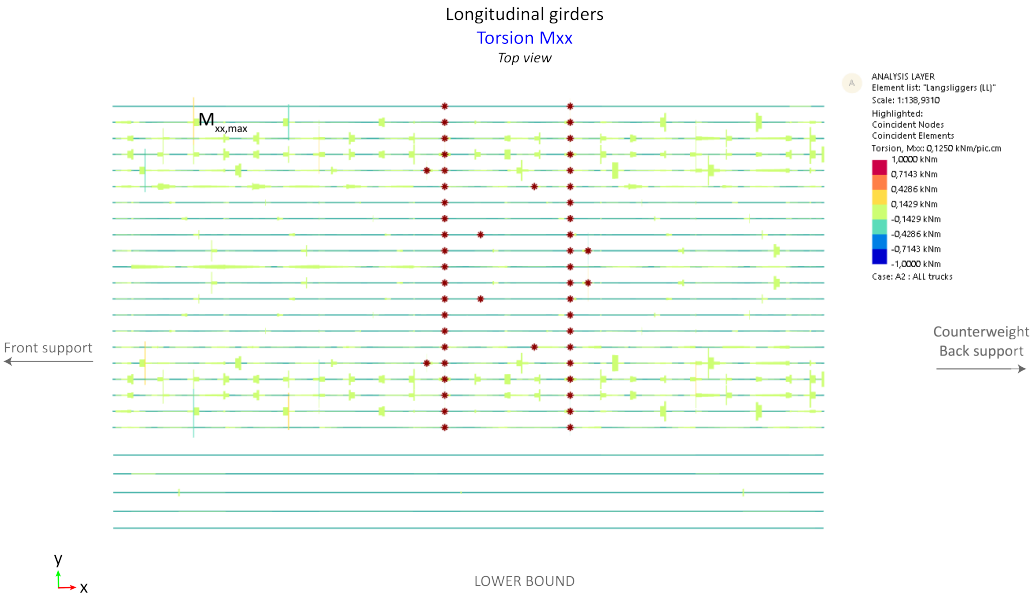

(a) Longitudinal girders - lower bound - vertical load case - torsion

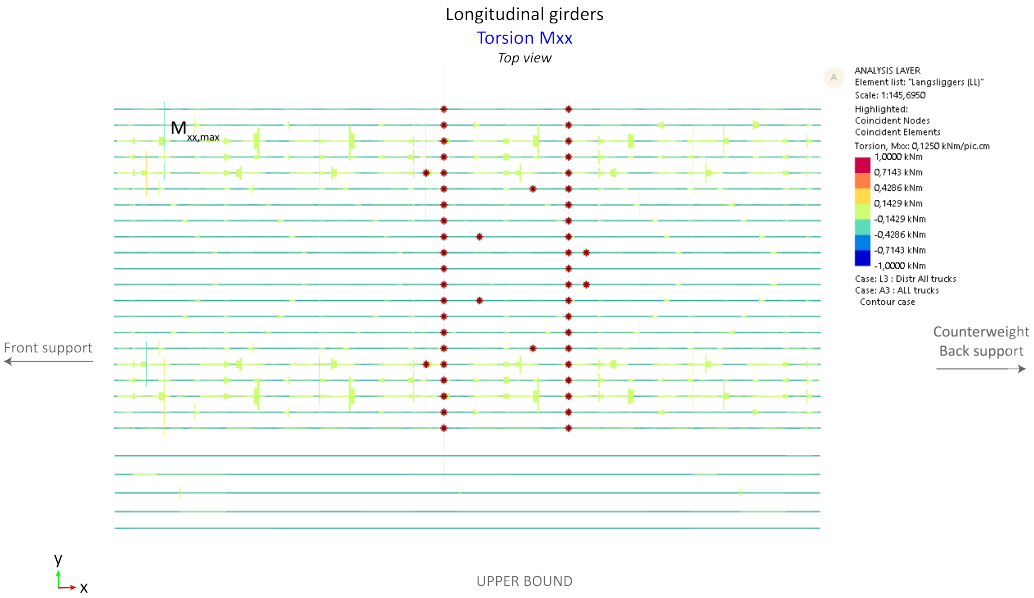

(b) Longitudinal girders - upper bound - vertical load case - torsion

Figure G.9

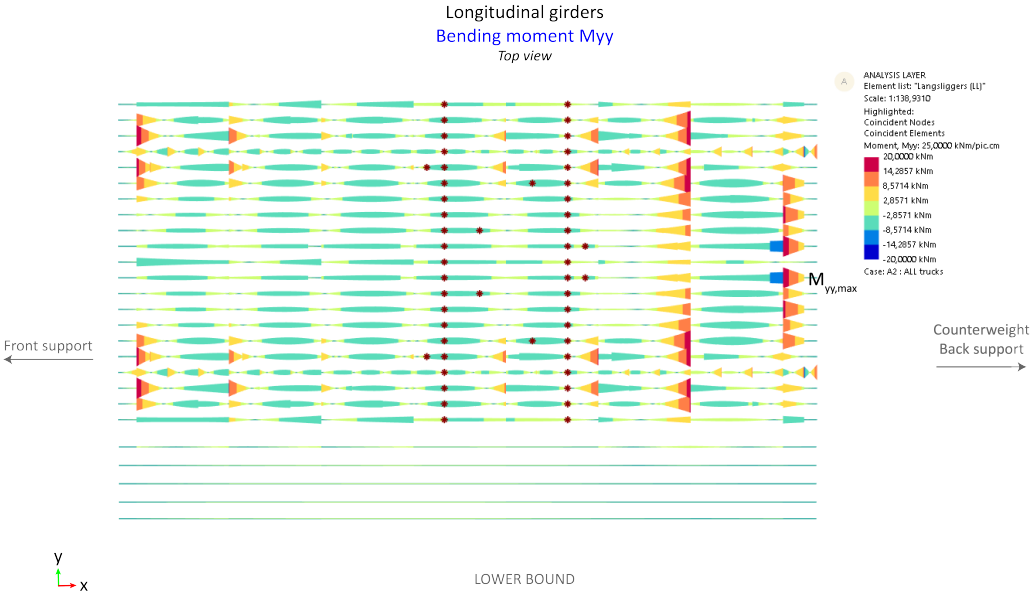

(a) Longitudinal girders - lower bound - vertical load case - bending moment around global y-axis

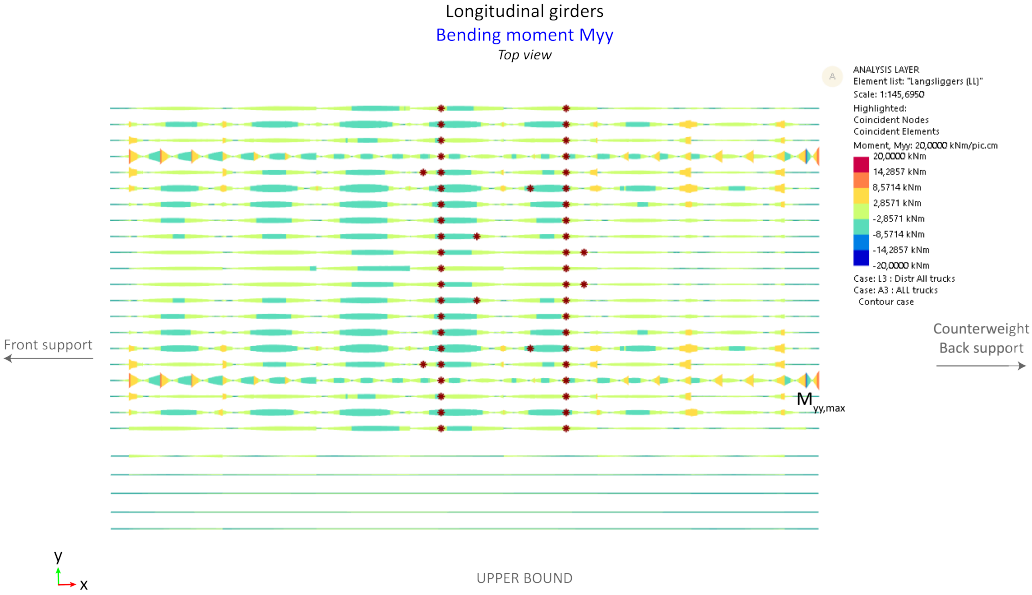

(b) Longitudinal girders - upper bound - vertical load case - bending moment around global y-axis

Figure G.10

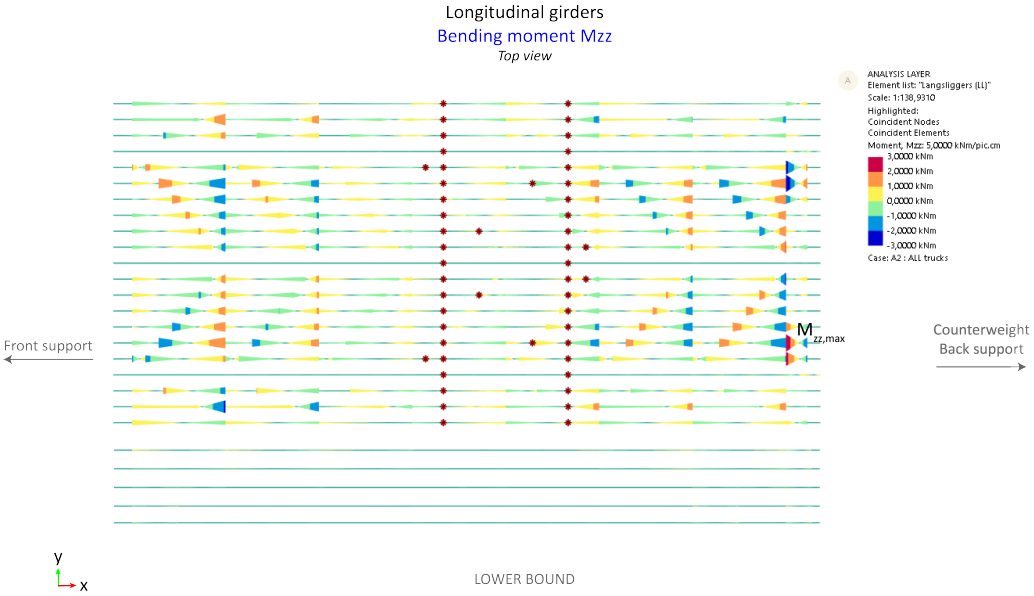

(a) Longitudinal girders - lower bound - vertical load case - bending moment around global z-axis

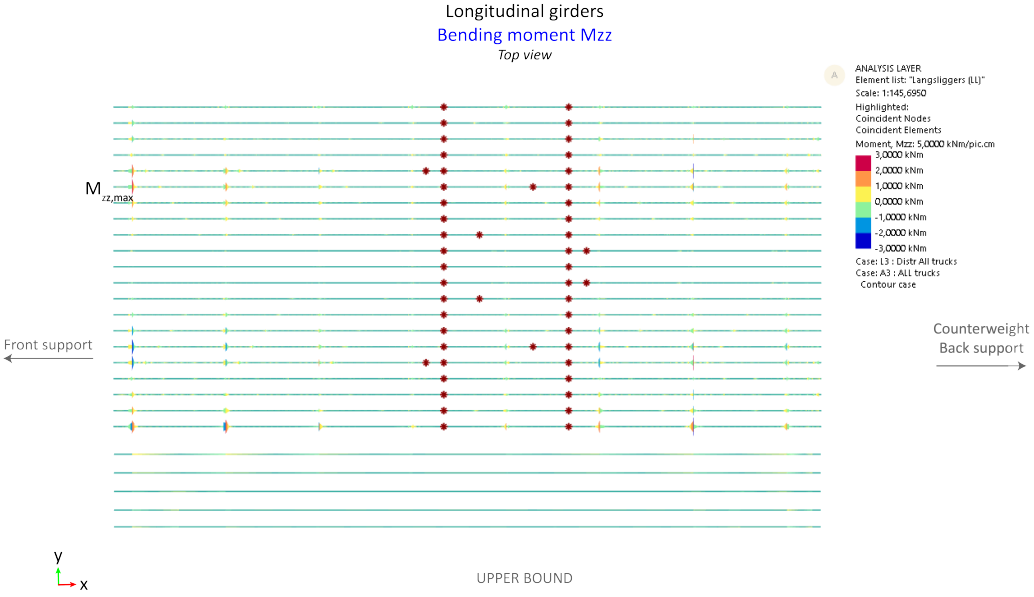

(b) Longitudinal girders - upper bound - vertical load case - bending moment around global z-axis

Figure G.11

G.1.3 Bracing elements (BR)

Forces and bending moments on bracing elements are given in figures G.12, G.13, G.14, G.15, G.16 and G.17.

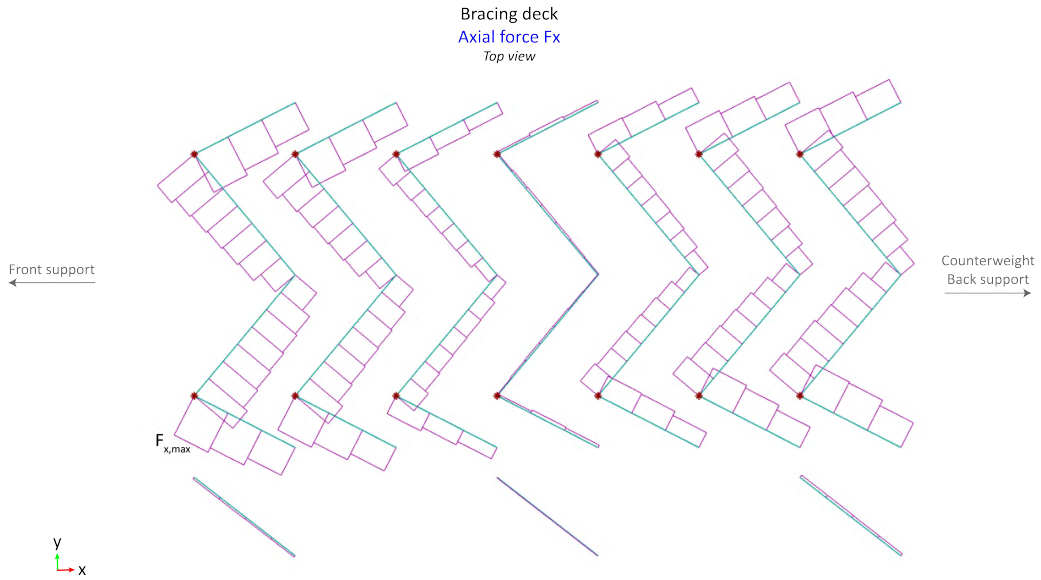

Figure G.12: Bracing elements - vertical load case - axial force

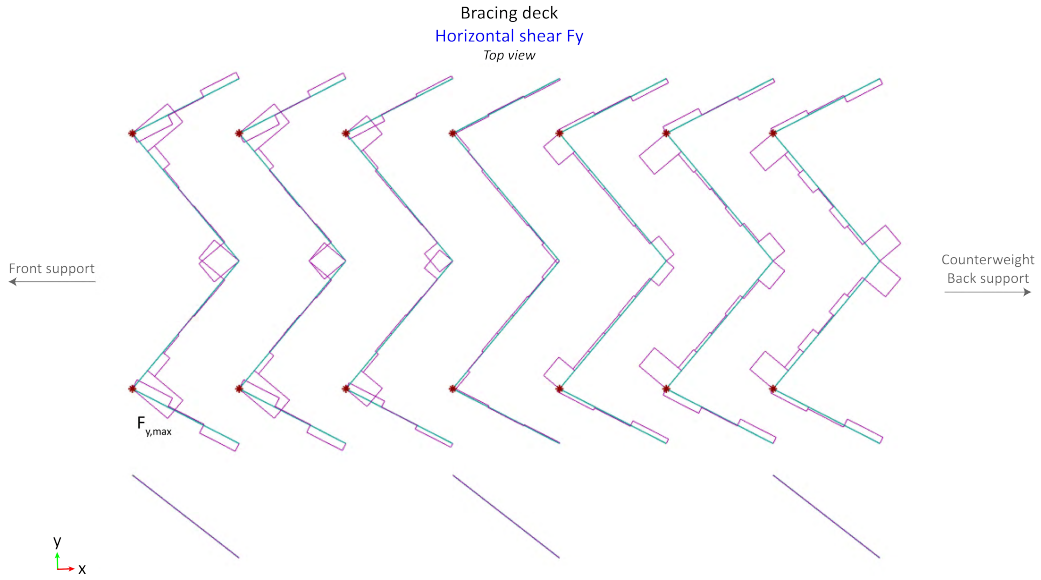

Figure G.13: Bracing elements - vertical load case - horizontal shear force

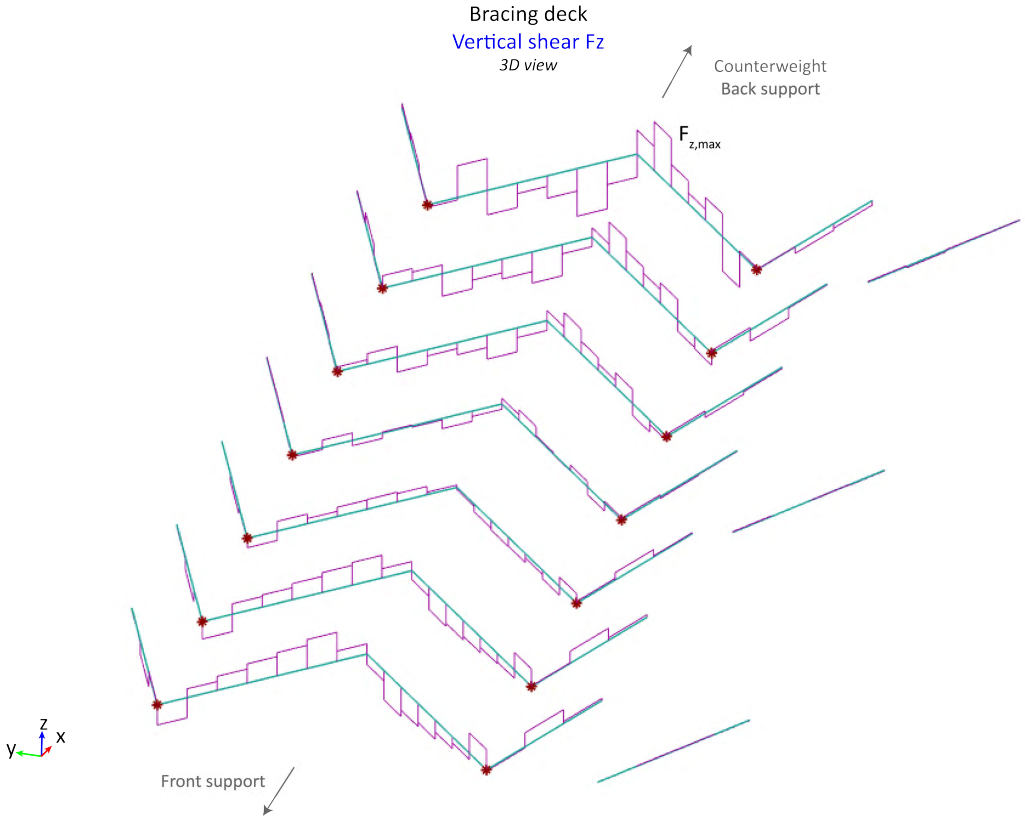

Figure G.14: Bracing elements - vertical load case - vertical shear force

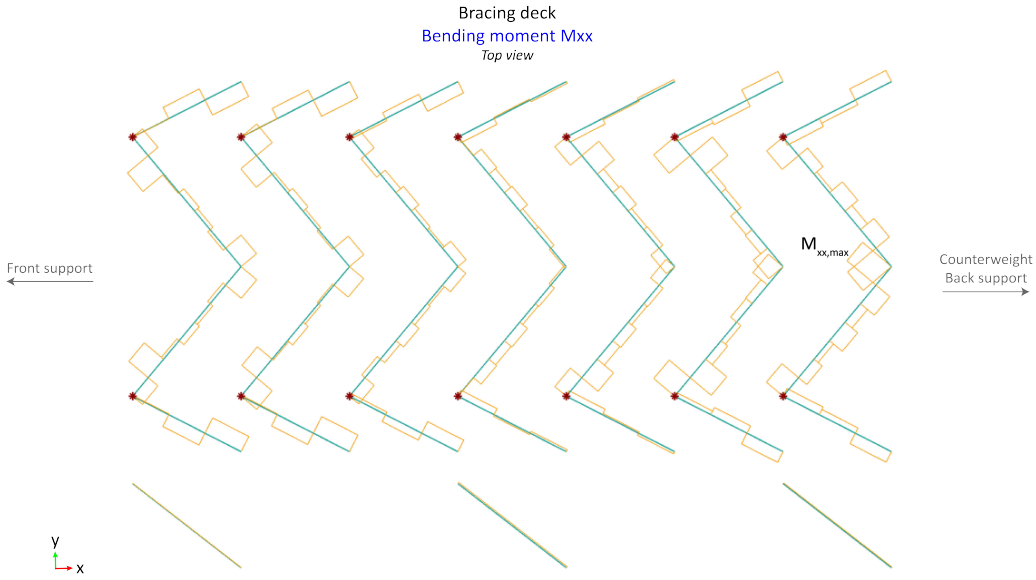

Figure G.15: Bracing elements - vertical load case - torsion

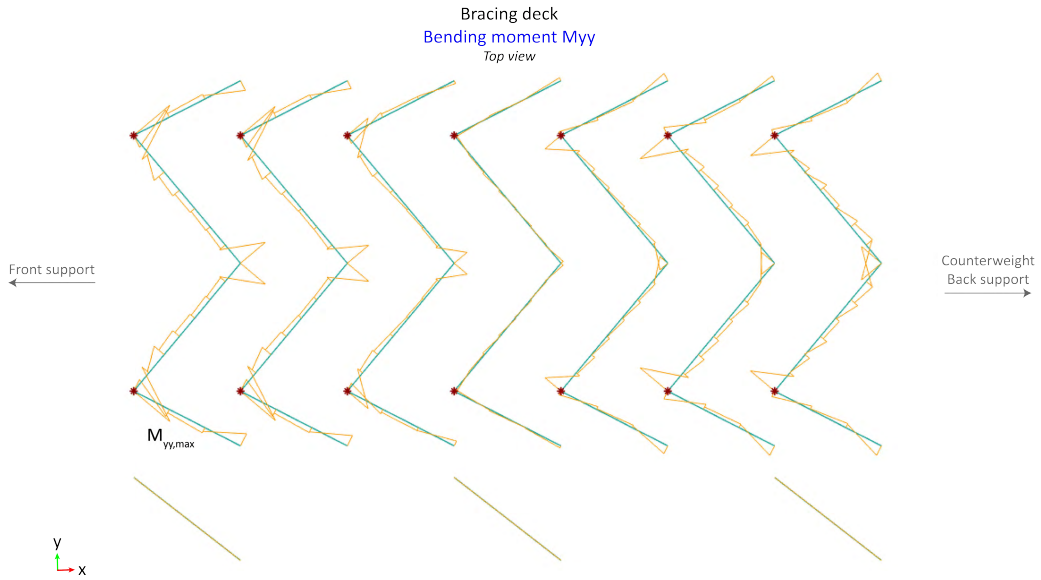

Figure G.16: Bracing elements - vertical load case - bending moment around element y-axis

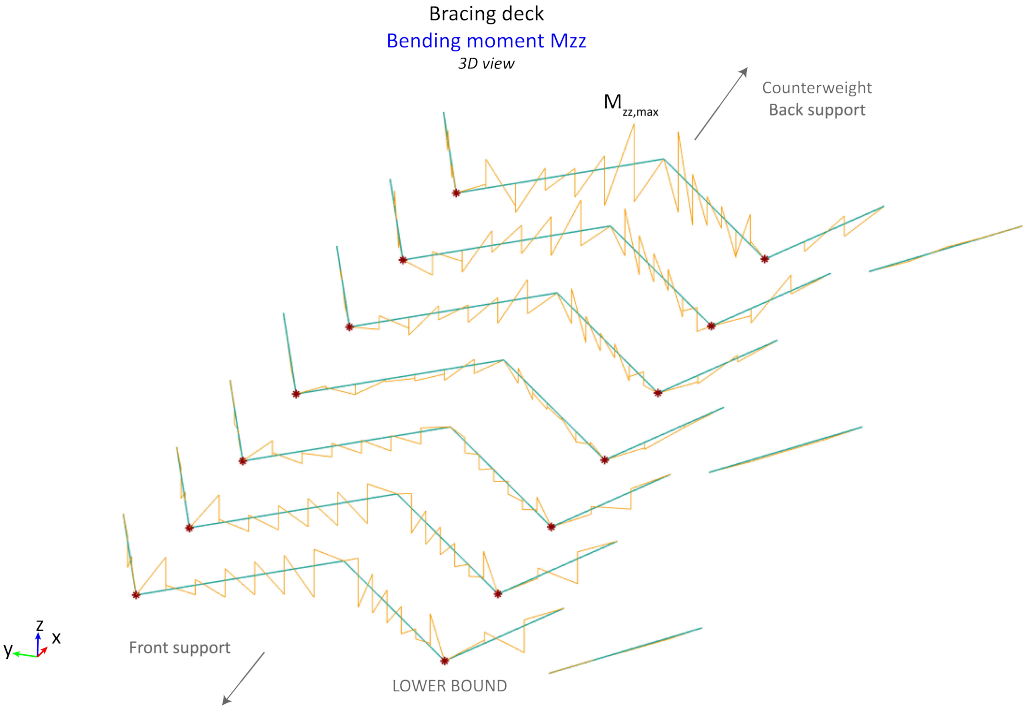

(a) Bracing elements - lower bound - vertical load case - bending moment around global z-axis

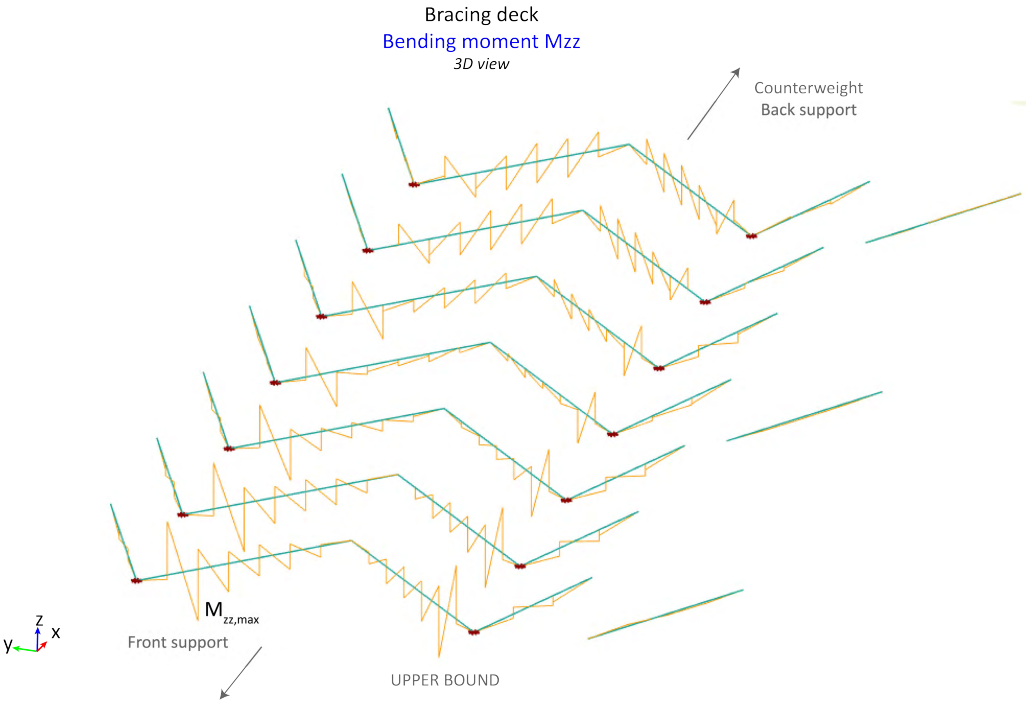

(b) Bracing elements - upper bound - vertical load case - bending moment around global z-axis

Figure G.17

G.1.4 Cross girders (CG)

Acting forces, bending moments and deflections are given in figures G.18, G.19, G.20, G.21, G.22, G.23 and G.24.

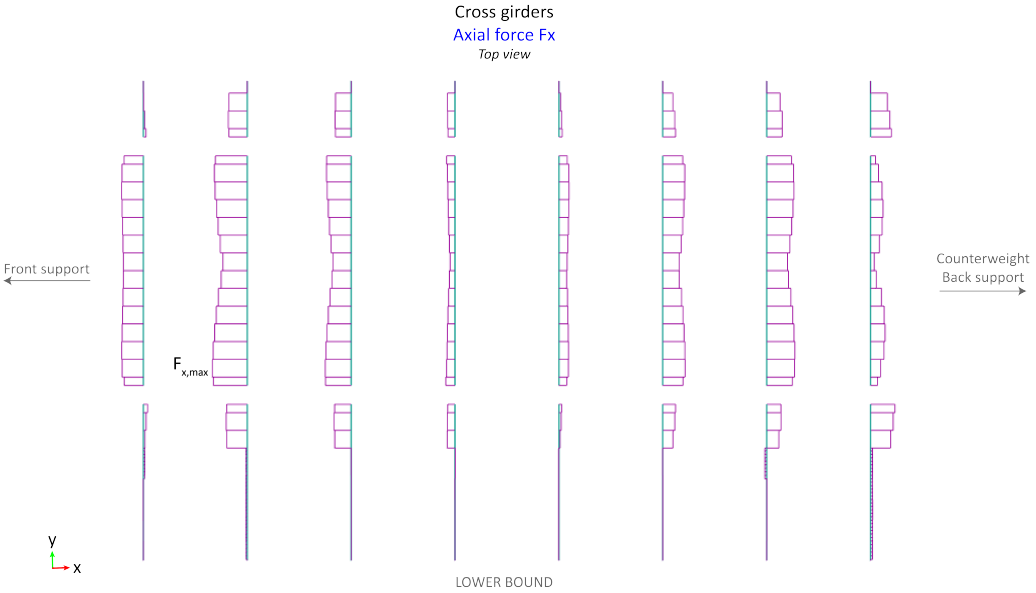

(a) Cross girders - lower bound - vertical load case - Axial force

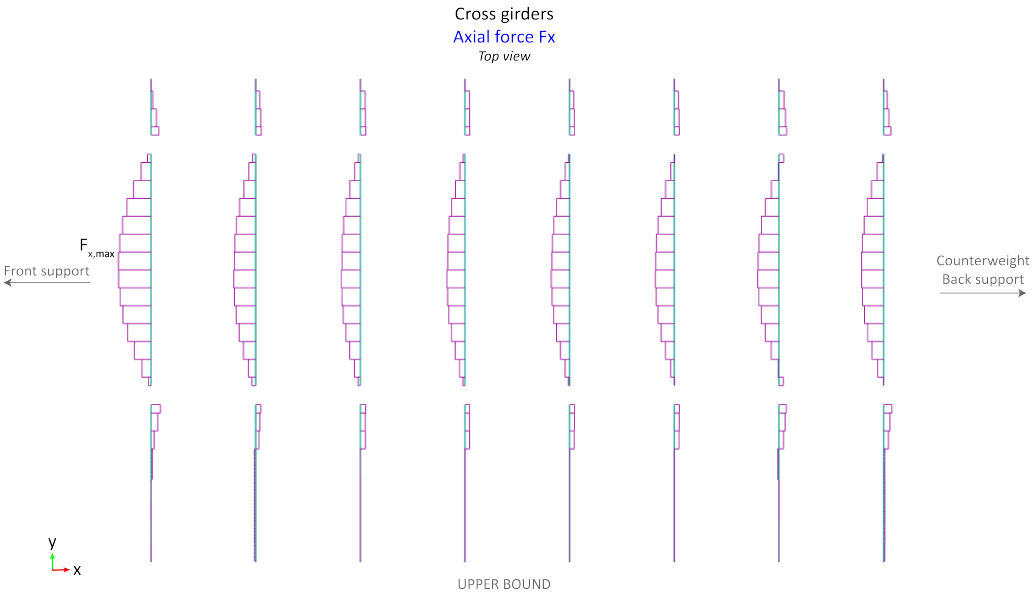

(b) Cross girders - upper bound - vertical load case - Axial force

Figure G.18

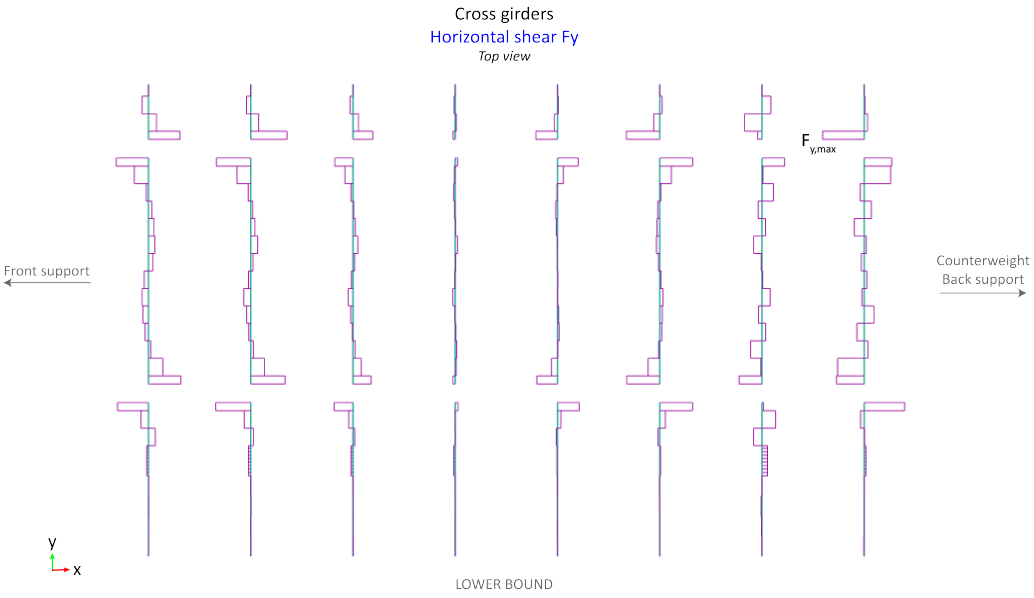

(a) Cross girders - lower bound - vertical load case - horizontal shear force

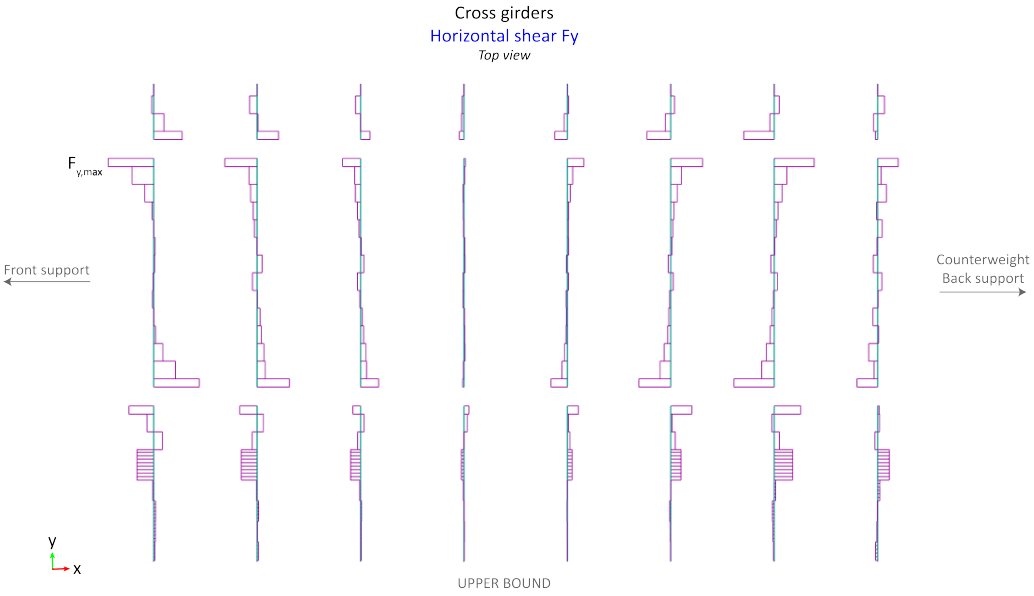

(b) Cross girders - upper bound - vertical load case - horizontal shear force

Figure G.19

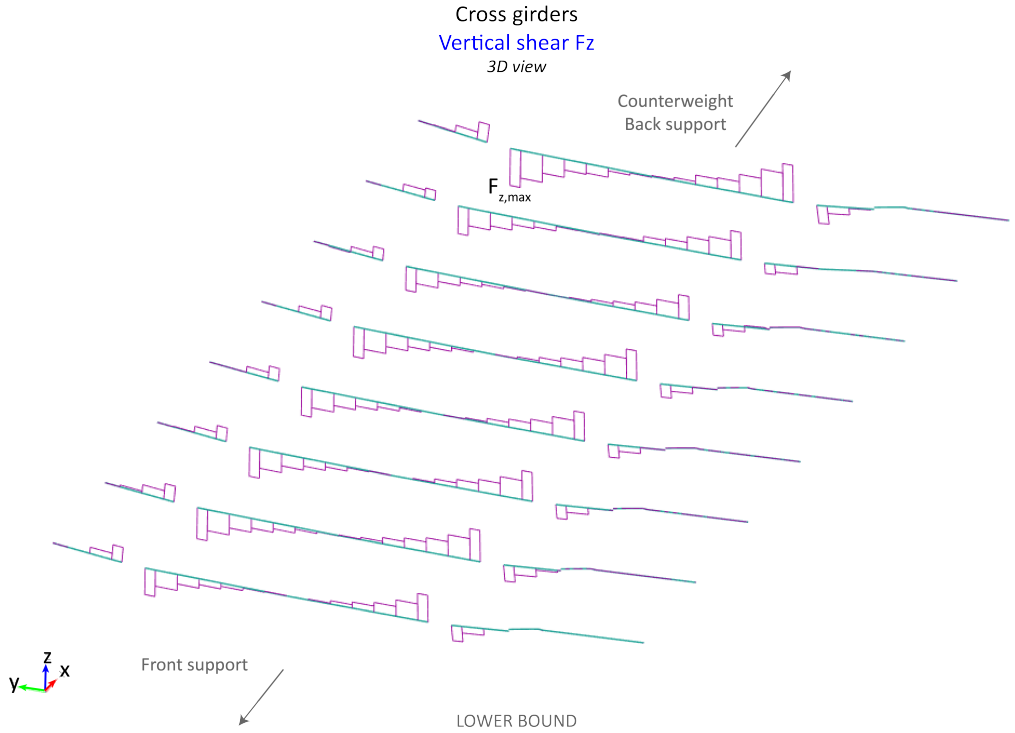

(a) Cross girders - lower bound - vertical load case - vertical shear force

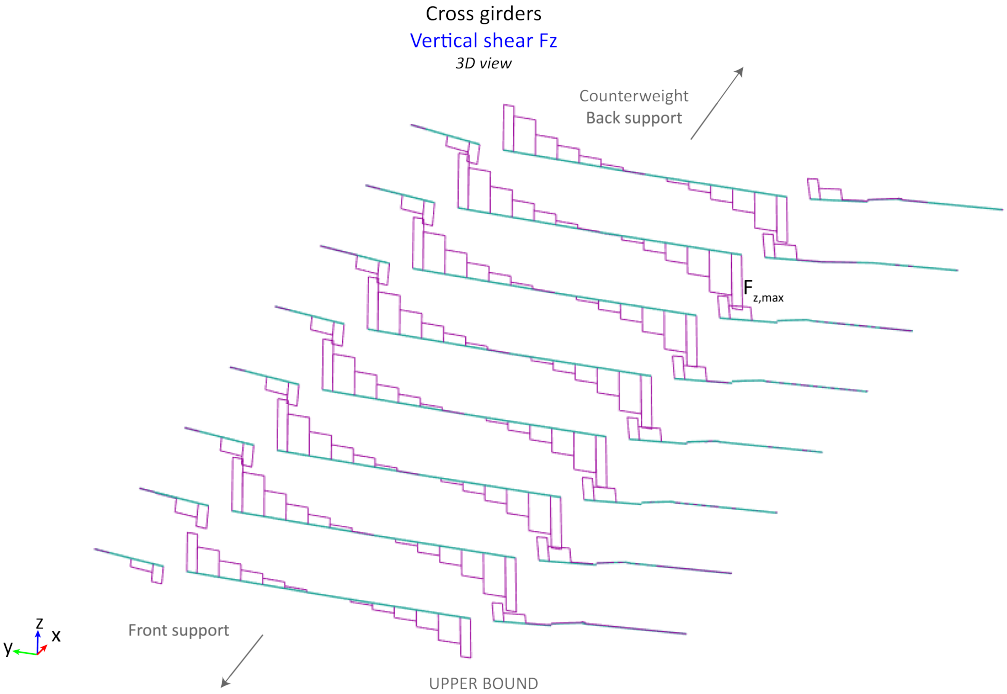

(b) Cross girders - upper bound - vertical load case - vertical shear force

Figure G.20

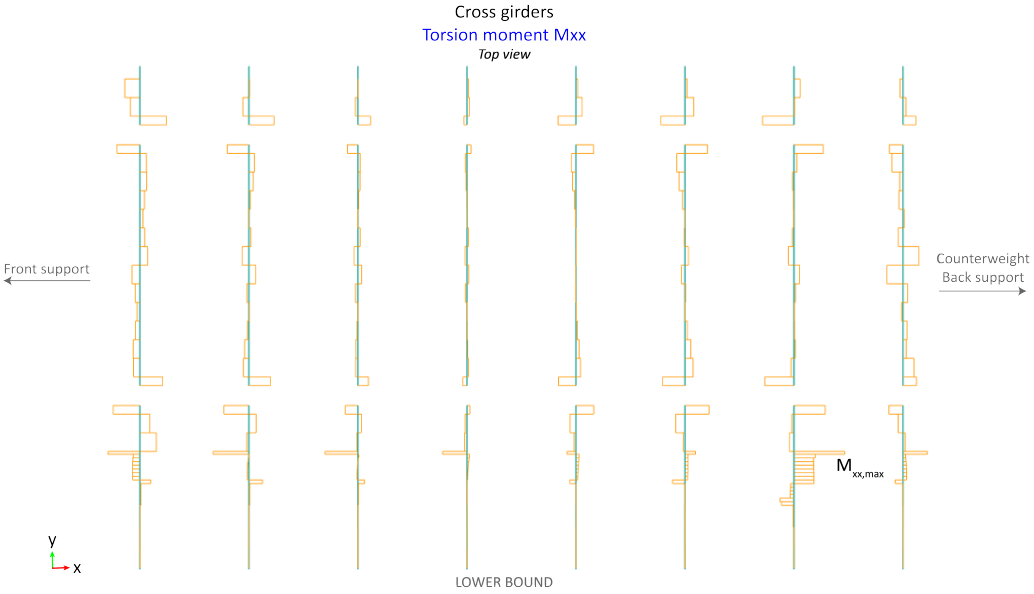

(a) Cross girders - lower bound - vertical load case - torsion

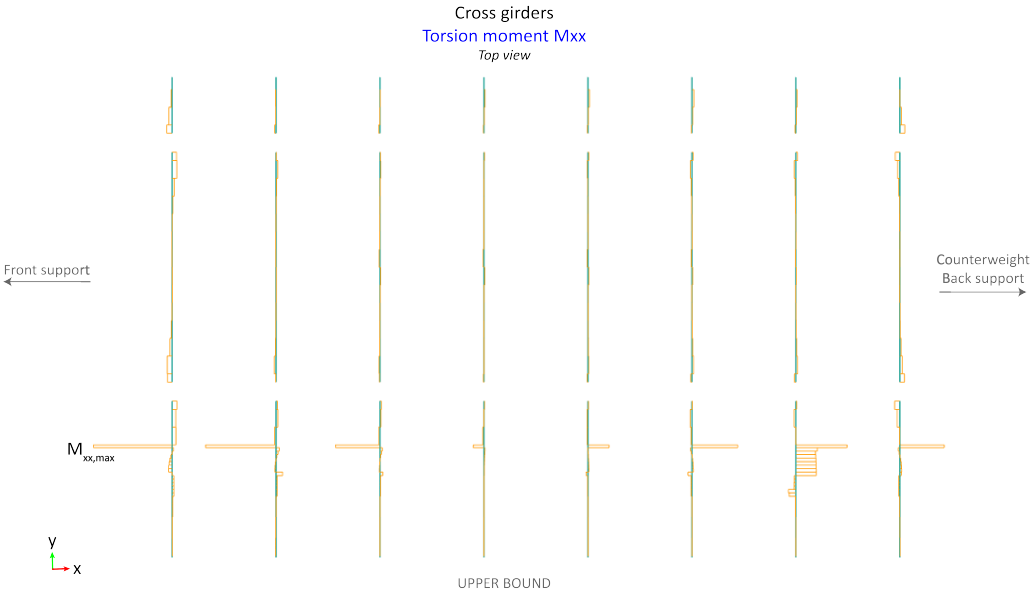

(b) Cross girders - upper bound - vertical load case - torsion

Figure G.21

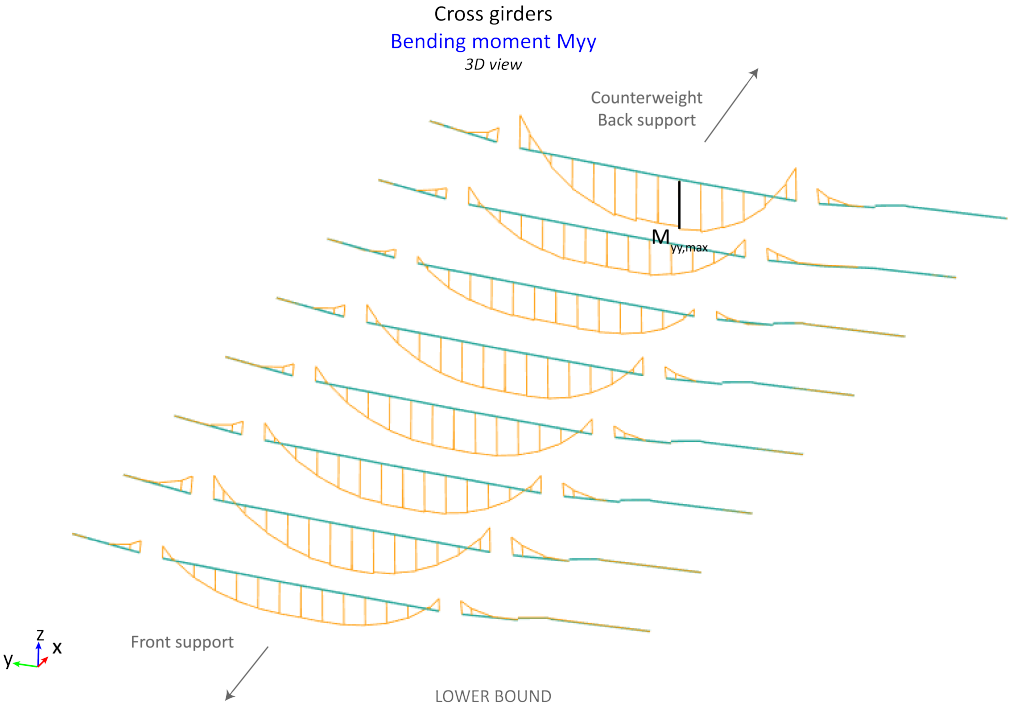

(a) Cross girders - lower bound - vertical load case - bending moment around element y-axis

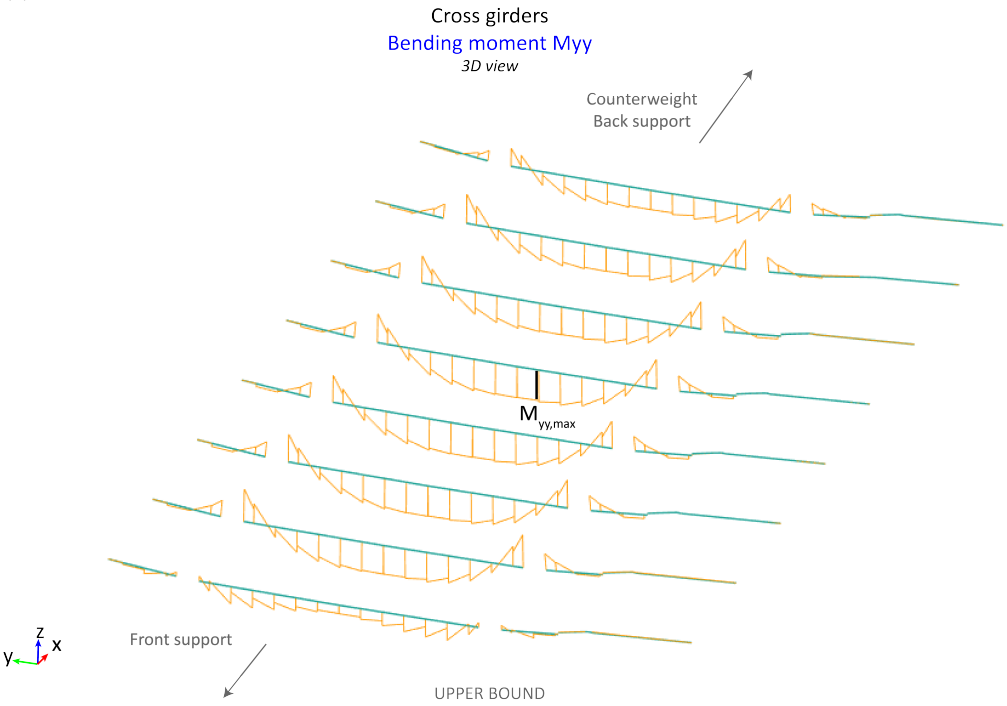

(b) Cross girders - upper bound - vertical load case - bending moment around element y-axis

Figure G.22

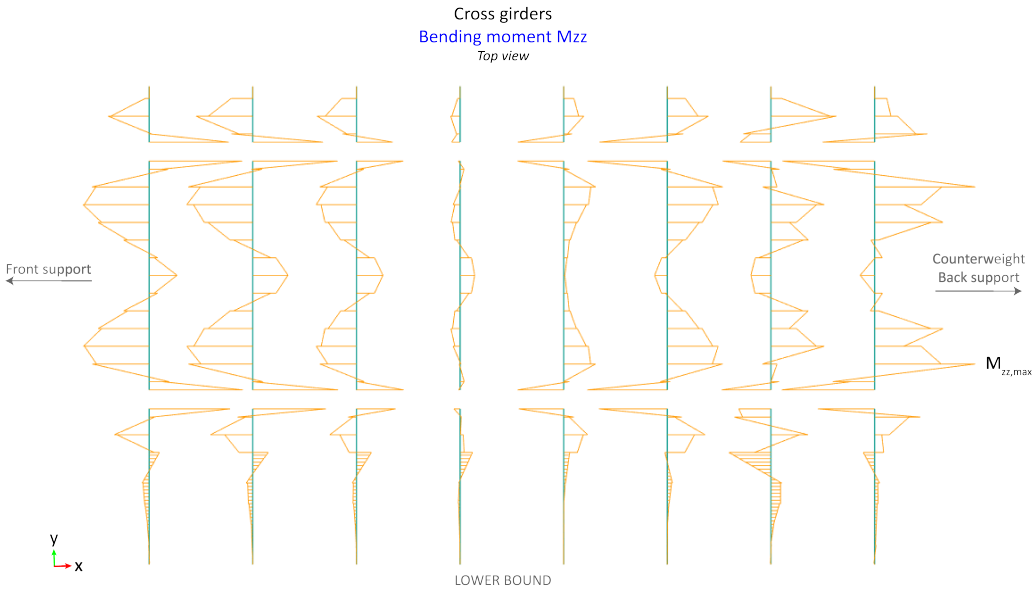

(a) Cross girders - lower bound - vertical load case - bending moment around global z-axis

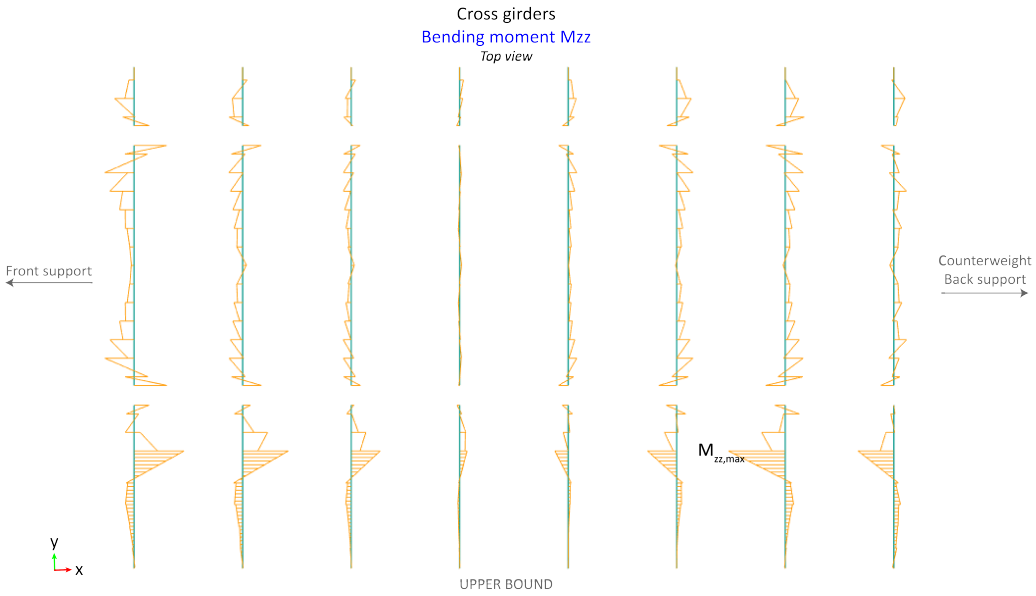

(b) Cross girders - upper bound - vertical load case - bending moment around global z-axis

Figure G.23

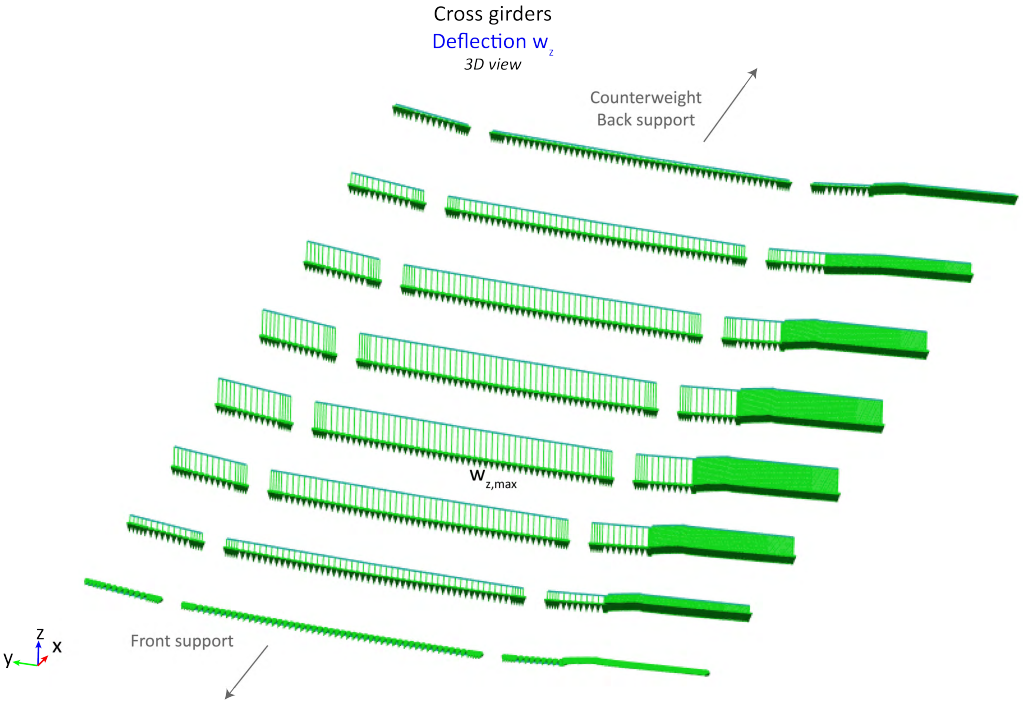

Figure G.24: Cross girders deflection for upper- and lower bound situation

G.1.5 Main girders (MG)

Forces and bending moments on one of the main girders (right) are given in figures G.25, G.26, G.27, G.28, G.29 and G.30.

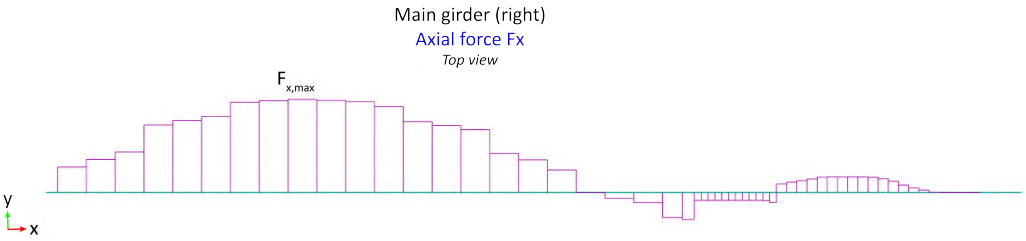

Figure G.25: Main girder - vertical load case - axial force

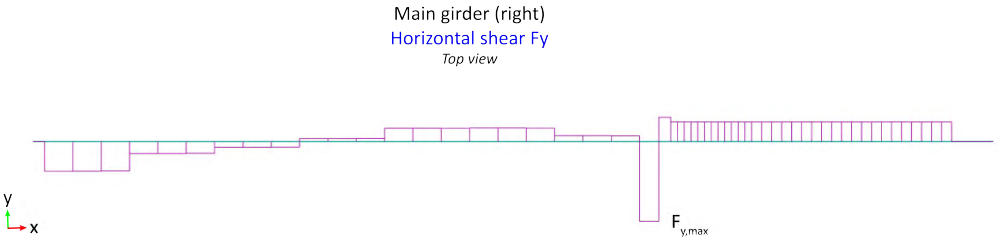

Figure G.26: Main girder - vertical load case - horizontal shear force

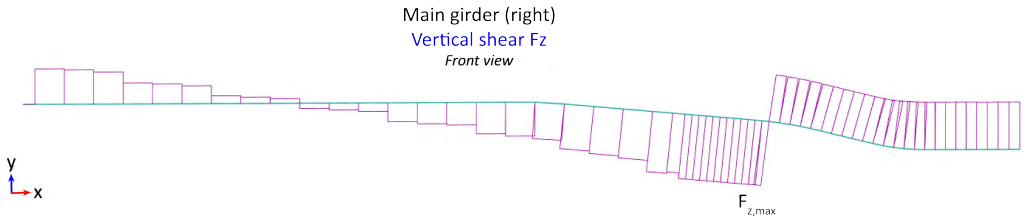

Figure G.27: Main girder - vertical load case - vertical shear force

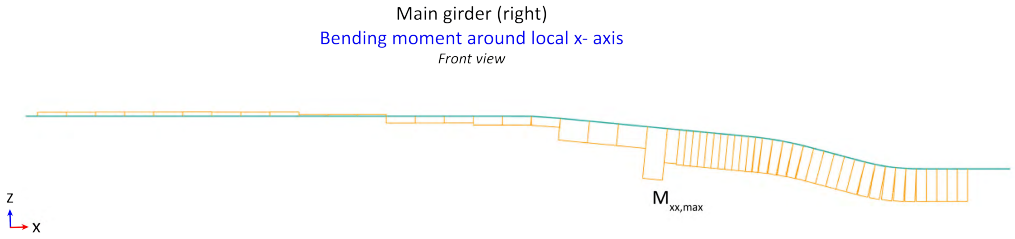

Figure G.28: Main girder - vertical load case - torsion

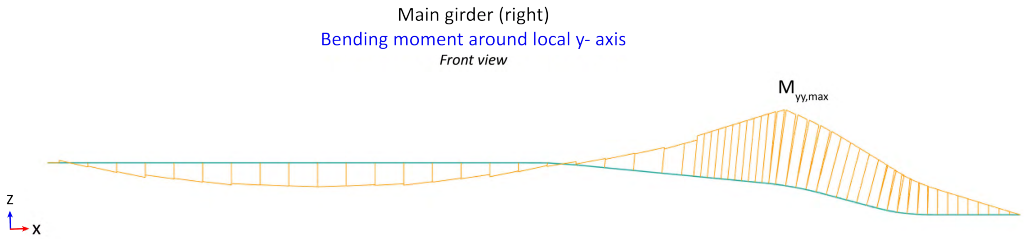

Figure G.29: Main girder - vertical load case - bending moment around element y-axis

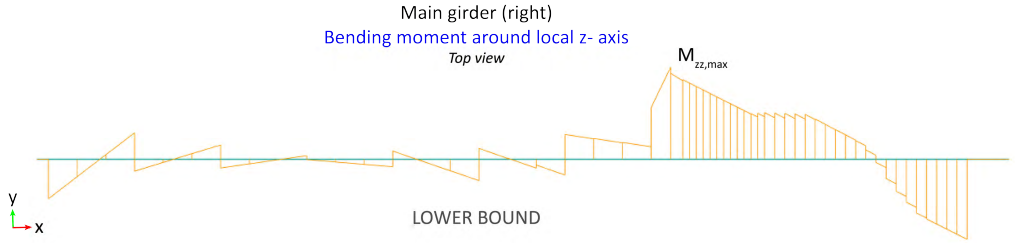

(a) Main girder - lower bound - vertical load case - bending moment around global z-axis

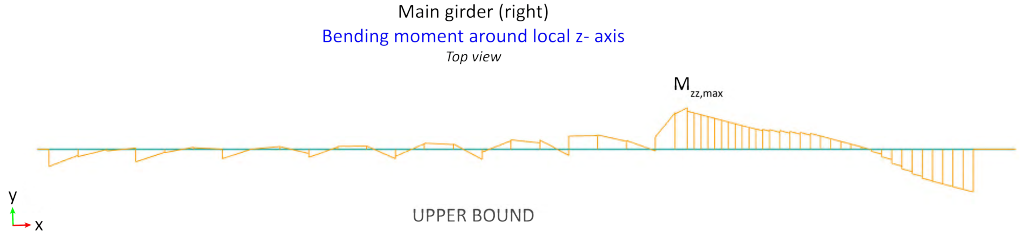

(b) Main girder - upper bound - vertical load case - bending moment around global z-axis

Figure G.30

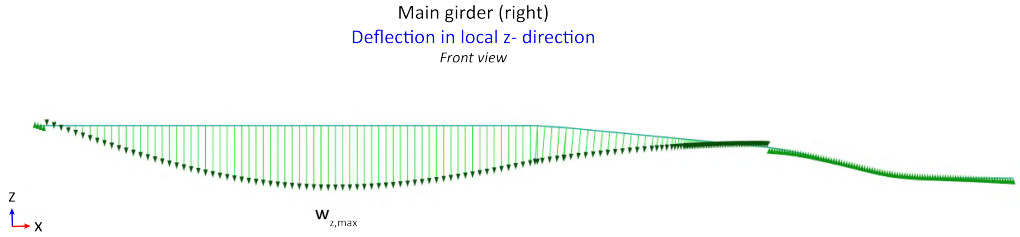

Figure G.31: Main girder deflection for upper- and lower bound situation

G.2 Horizontal load case

Structural elements	Lower bound max.	Upper bound max.	Gain / penalty of interaction
Deck boards			
Axial force compression (local x)	-0.09 kN	-93.57 kN	+ 103867%
Axial force tension (local x)	0.09 kN	153.88 kN	+ 170878%
Horizontal shear force (local y)	0.08 kN	39.79 kN	+ 49638%
Vertical shear force (local z)	2.73 kN	30.76 kN	+ 1027%
Board- to- board compression (global x)	0 kN	-122.61 kN	+ ∞%
Board- to- board tension (global x)	0 kN	166.58 kN	+ ∞%
Deck connections			
Shear force (local x)	0 kN	130.39 kN	+ ∞%
Shear force (local y)	0 kN	88.48 kN	+ ∞%
Bending (local zz)	2.0 kNm	10.7 kNm	+ 400%
Longitudinal girders			
Axial force (local x)	194.72 kN	280.27 kN	+ 44%
Horizontal shear force (local y)	32.28 kN	194.40 kN	+ 502%
Vertical shear force (local z)	18.62 kN	54.93 kN	+ 195%
Bending (local yy)	1.27 kNm	21.25 kNm	+ 1573%
Bending (local zz)	25.86 kNm	21.02 kNm	- 19%
Cross girders			
Axial force (local x)	837.27 kN	713.18 kN	- 15%
Horizontal shear force (local y)	99.36 kN	59.67 kN	- 40%
Vertical shear force (local z)	96.69 kN	-147.93 kN	+ 53%
Bending (local xx)	1.39 kNm	0.41 kNm	- 71%
Bending (local yy)	-463.46 kNm	-549.14 kNm	+ 18%
Bending (local zz)	64.70 kNm	29.71 kNm	- 54%
Stability members			
Axial force (local x)	-824.90 kN	-68.56 kN	- 92%
Horizontal shear force (local y)	31.27 kN	7.83 kN	- 75%
Vertical shear force (local z)	7.06 kN	2.10 kN	- 70%
Main girders			
Axial force (local x)	2971.05 kN	3113.83 kN	+ 5%
Horizontal shear force (local y)	800.35 kN	815.65 kN	+ 2%
Vertical shear force (local z)	-358.38 kN	-261.96 kN	- 27%
Bending (local xx)	858.20 kNm	1525.23 kNm	+ 78%
Bending (local yy)	3421.06 kNm	2322.75 kNm	- 32%
Bending (local zz)	2801.68 kNm	2063.55 kNm	- 26%
Deflection (global y)	70.70 mm	38.22 mm	- 46%

Table G.2: Horizontal load case: maximum/minimum forces, moments and deflections for structural elements in the upper- and lower bound situations

G.2.1 Deck boards (DB)

The forces acting on the deck board elements for both the lower- and upper bound situations are given in figures G.32, G.33, G.34 and G.35.

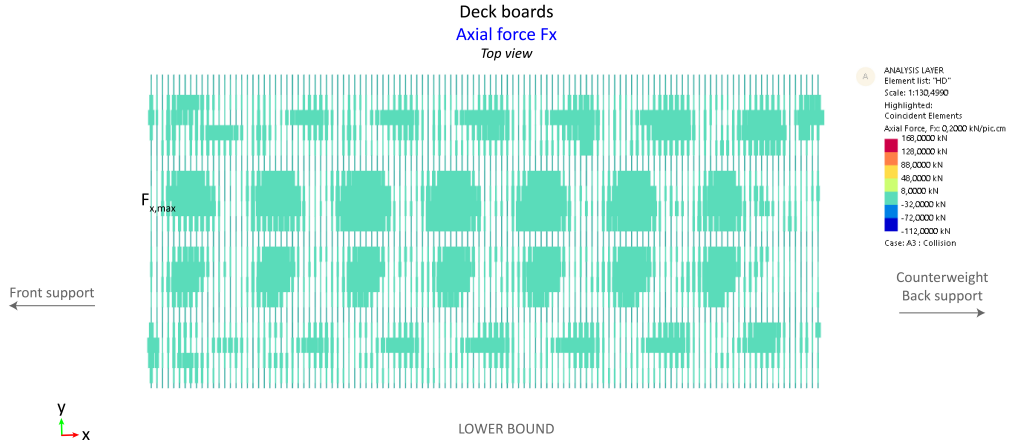

(a) Deck boards - lower bound - horizontal load case - axial force

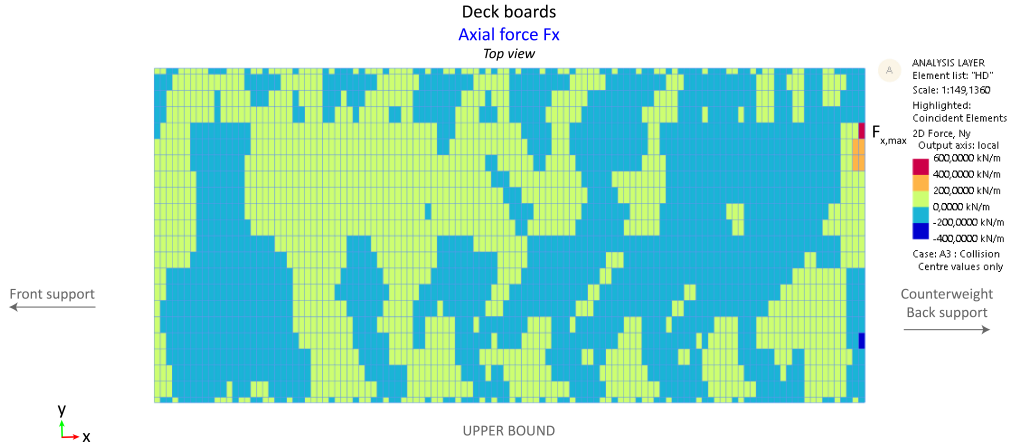

(b) Deck boards - upper bound - horizontal load case - axial force

Figure G.32

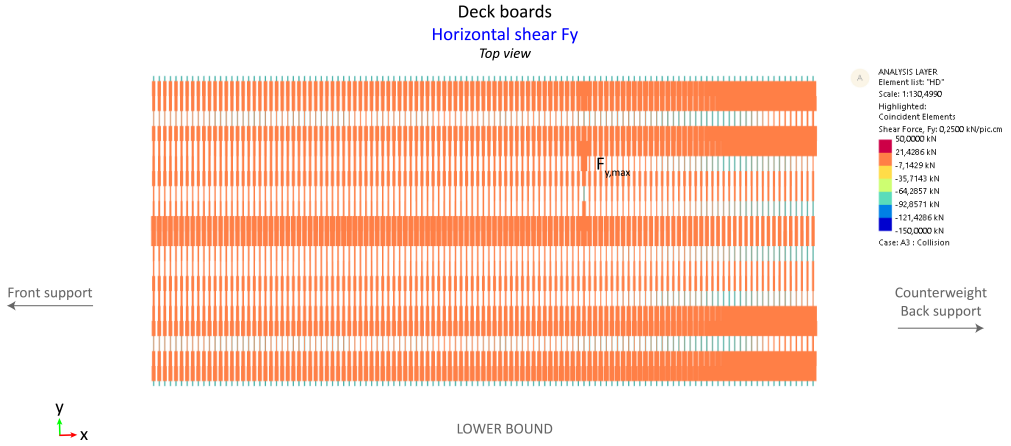

(a) Deck boards - lower bound - horizontal load case - horizontal shear force

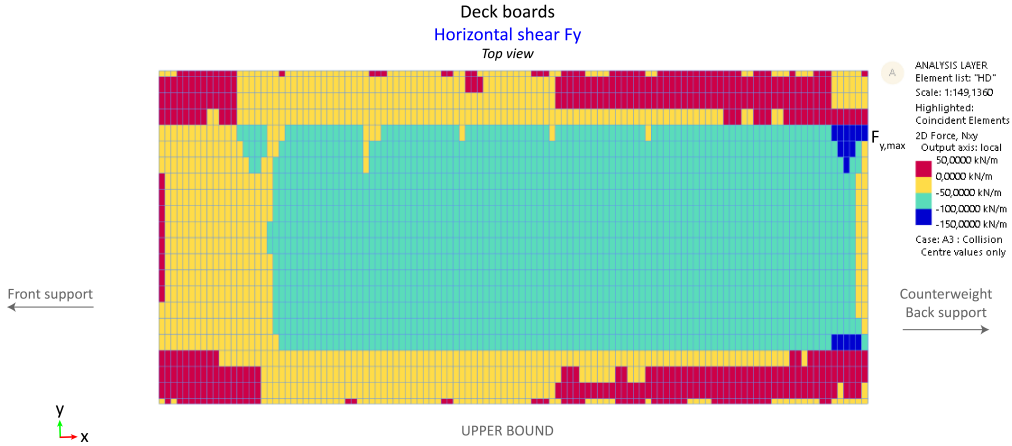

(b) Deck boards - upper bound - horizontal load case - horizontal shear force

Figure G.33

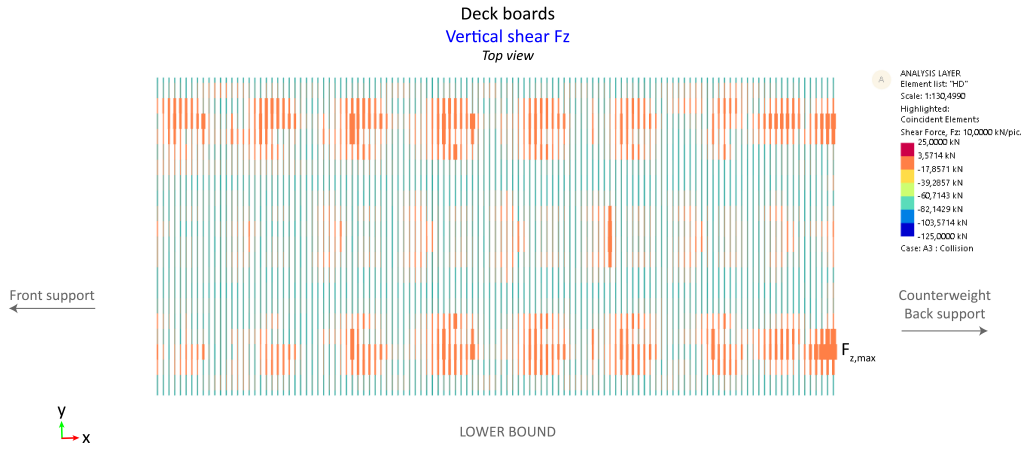

(a) Deck boards - lower bound - horizontal load case - vertical shear force

(b) Deck boards - upper bound - horizontal load case - vertical shear force

Figure G.34

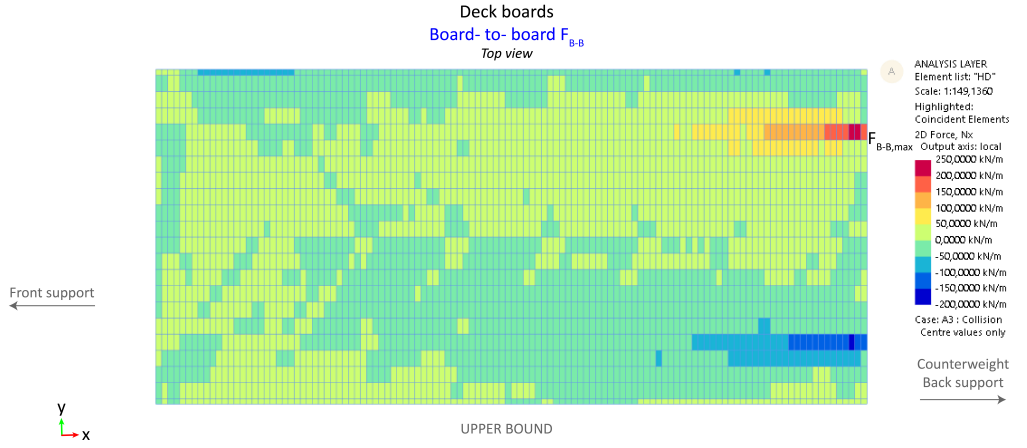

Figure G.35: Deck boards - upper bound - horizontal load case - board- to- board forces

G.2.2 Longitudinal girders (LG)

Forces and bending moments acting on the steel longitudinal girders are given in figure G.36, G.37, G.38, G.39 and G.40. The torsional moment (Mxx) diagrams are not given, since its values are negligibly small and do not increase for the upper bound situation.

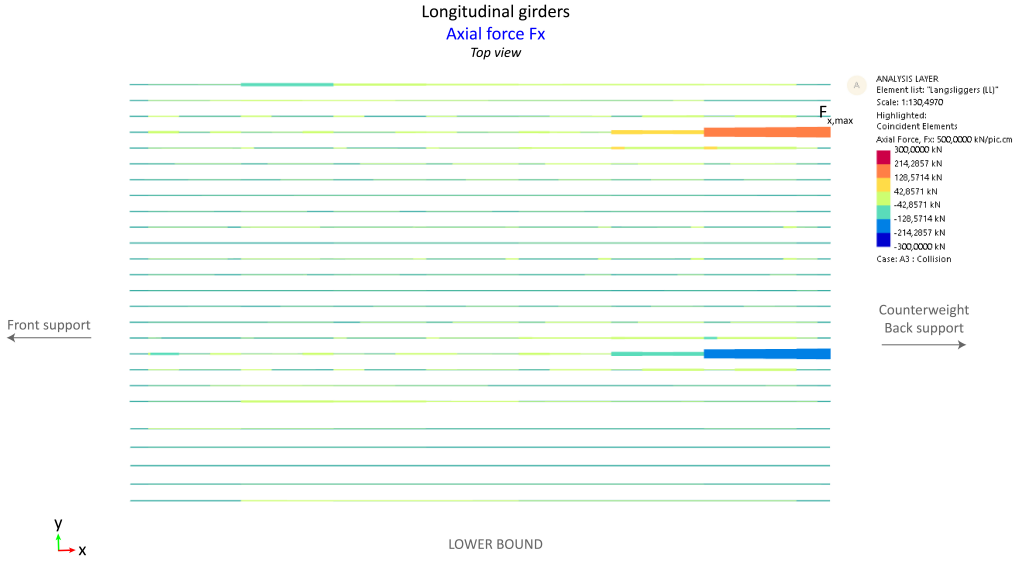

(a) Longitudinal girders - lower bound - horizontal load case - axial force

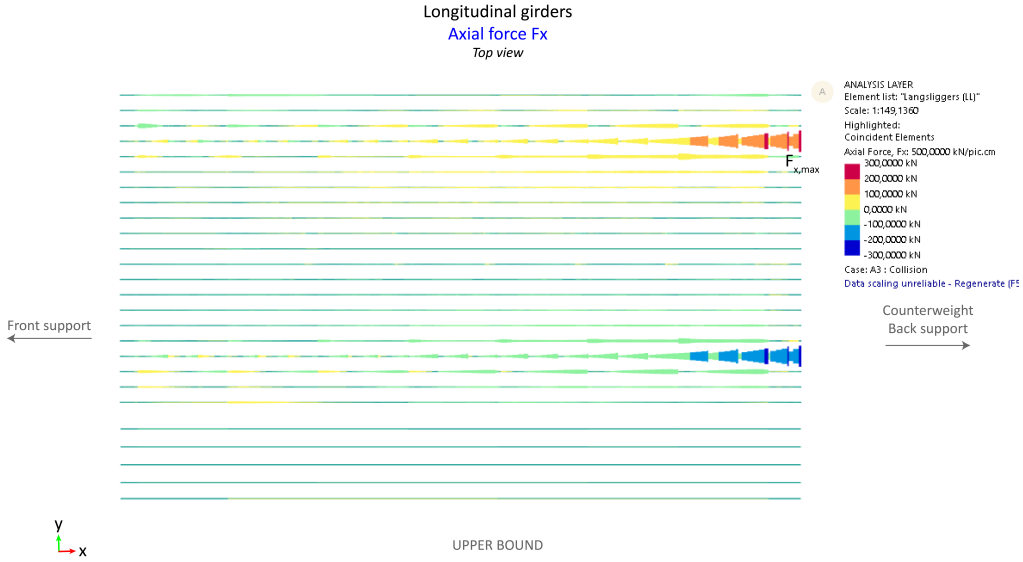

(b) Longitudinal girders - upper bound - horizontal load case - axial force

Figure G.36

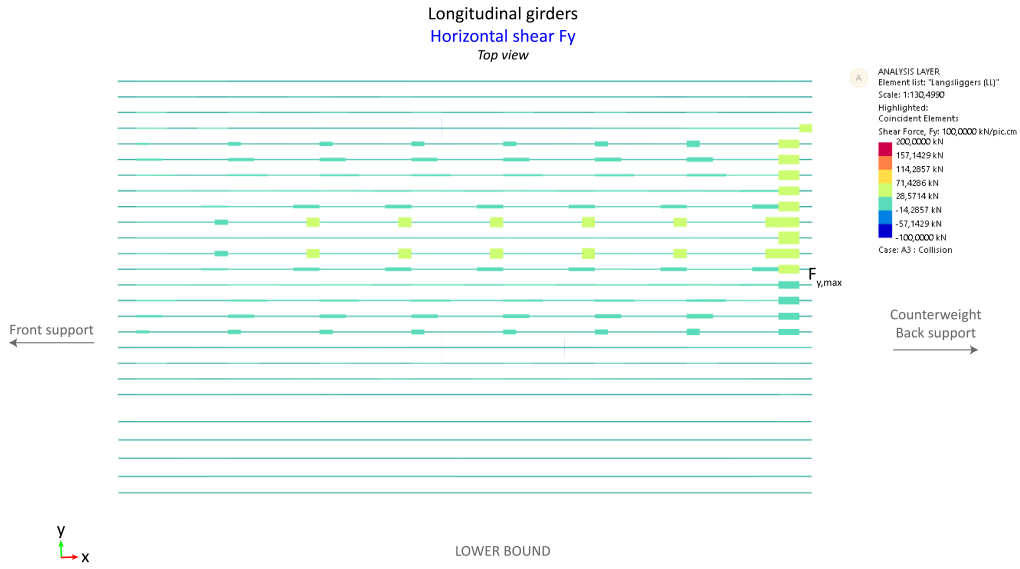

(a) Longitudinal girders - lower bound - horizontal load case - horizontal shear force

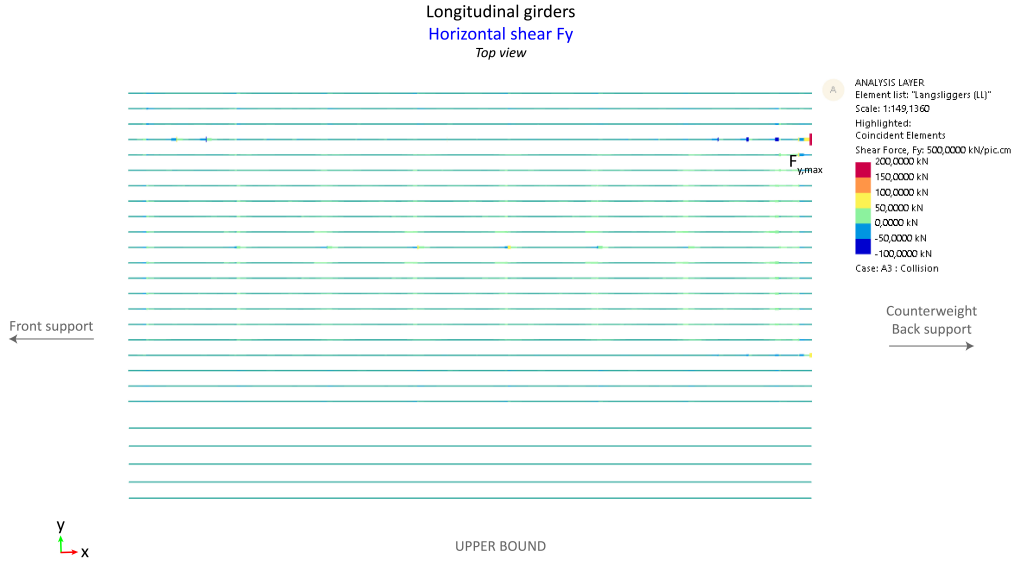

(b) Longitudinal girders - upper bound - horizontal load case - horizontal shear force

Figure G.37

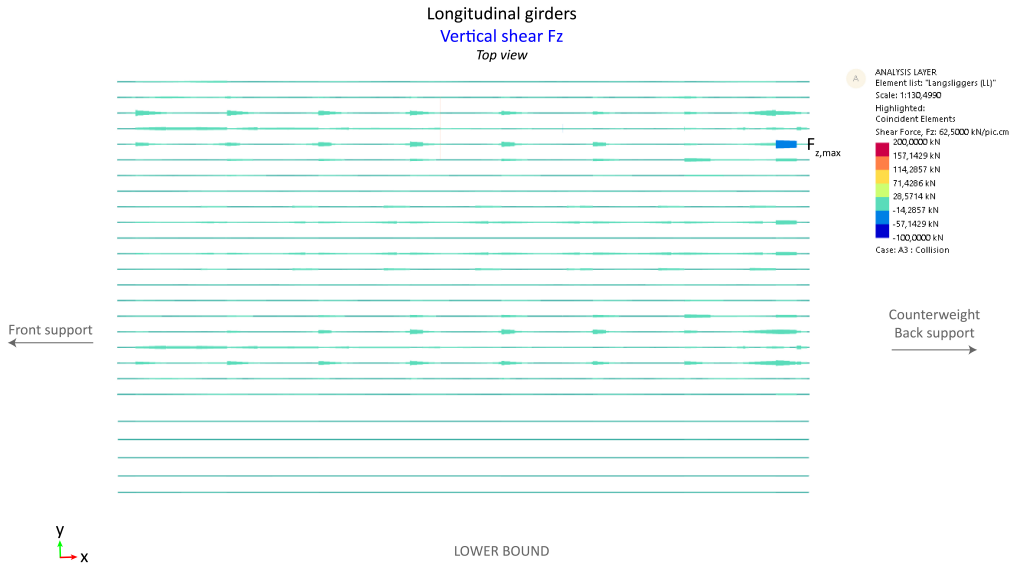

(a) Longitudinal girders - lower bound - horizontal load case - Vertical shear force

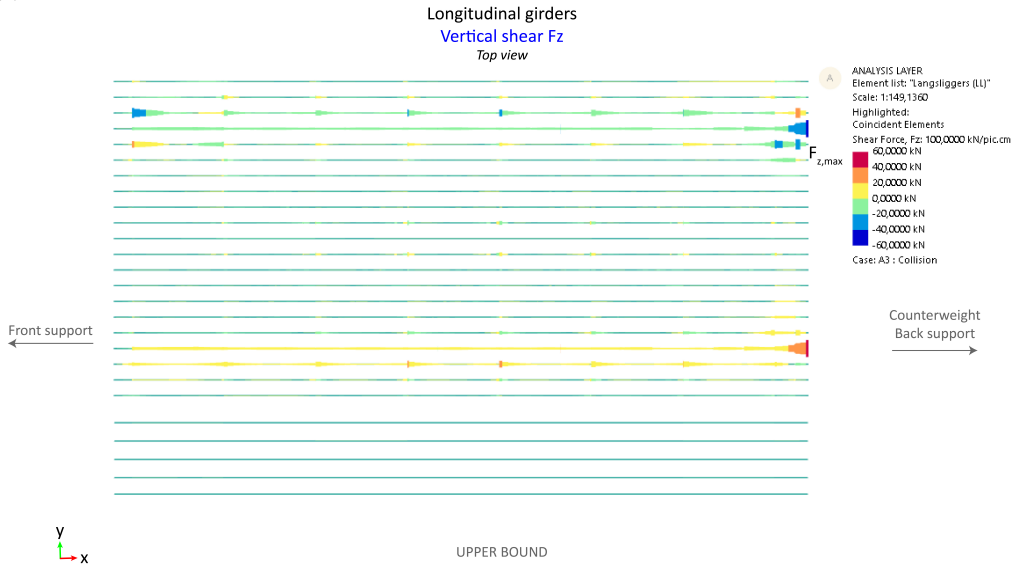

(b) Longitudinal girders - upper bound - horizontal load case - vertical shear force

Figure G.38

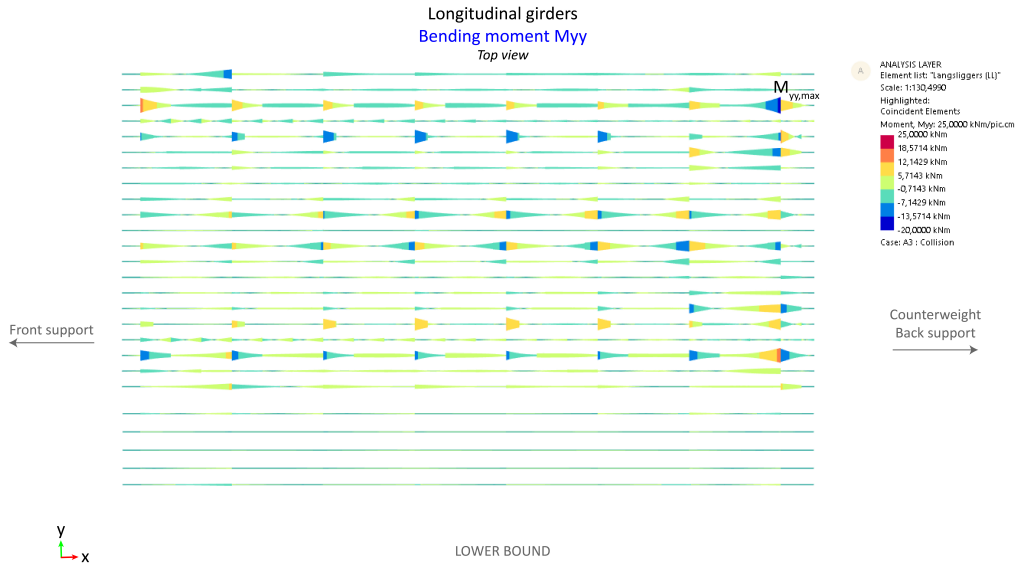

(a) Longitudinal girders - lower bound - horizontal load case - bending moment around global y-axis

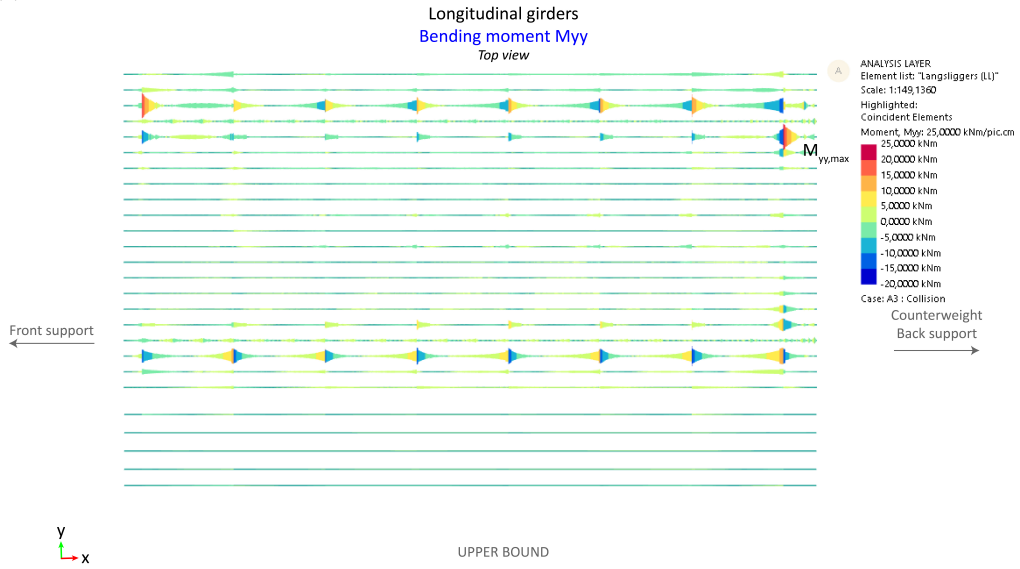

(b) Longitudinal girders - upper bound - horizontal load case - bending moment around global y-axis

Figure G.39

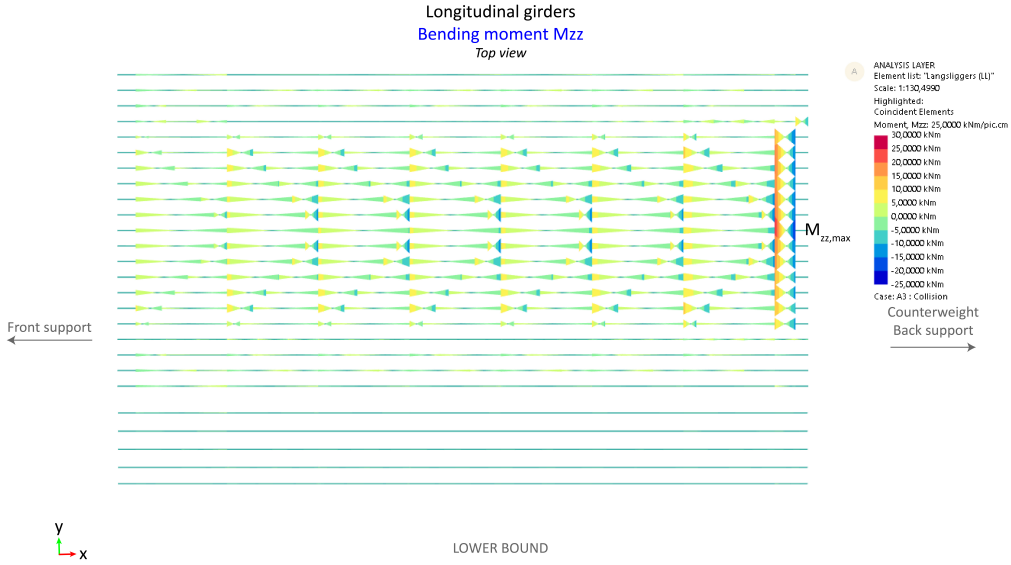

(a) Longitudinal girders - lower bound - horizontal load case - bending moment around global z-axis

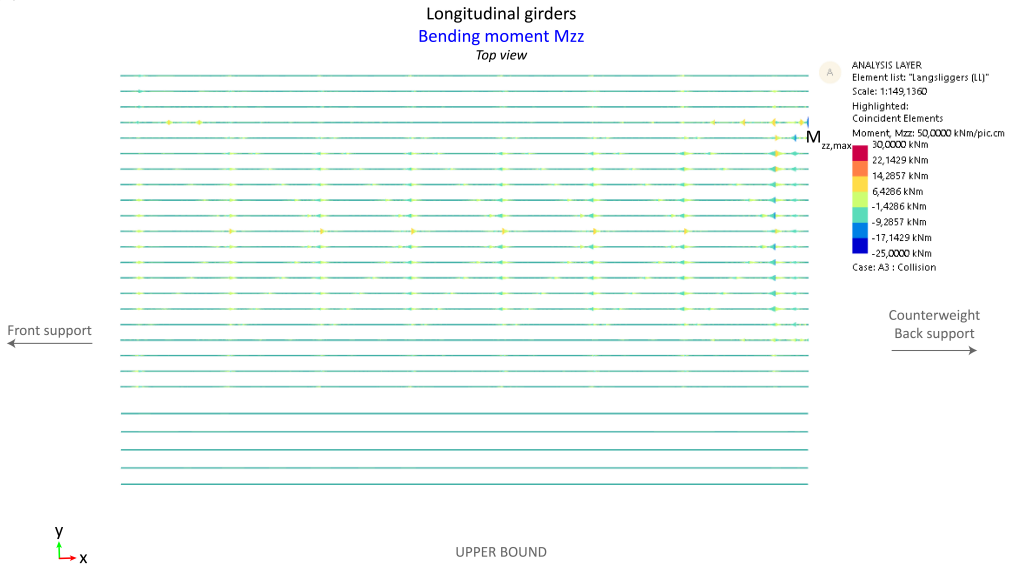

(b) Longitudinal girders - upper bound - horizontal load case - bending moment around global z-axis

Figure G.40

G.2.3 Bracing elements (BR)

The bracing elements (or: stability members) mainly transfer axial and shear forces, bending moments are insignificant and therefore not shown as diagrams in this section. Forces and bending moments on bracing elements are given in figures G.41, G.42 and G.43.

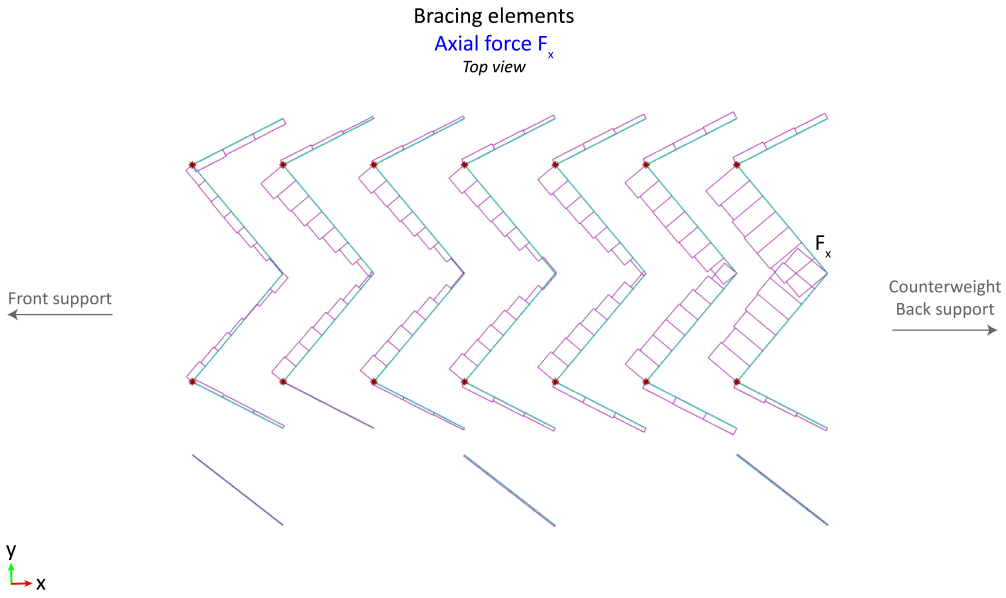

Figure G.41: Bracing elements - horizontal load case - axial force

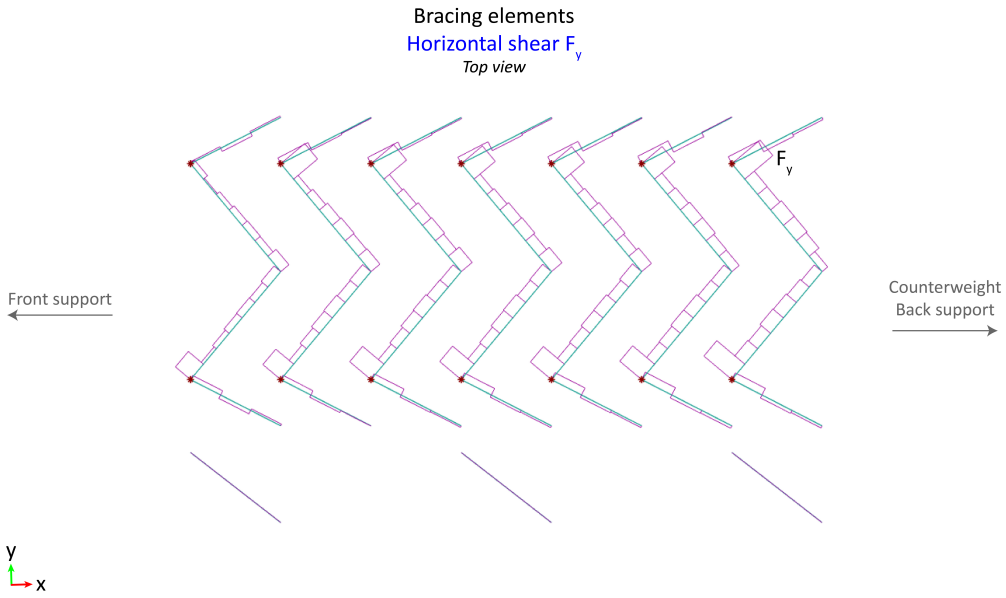

Figure G.42: Bracing elements - horizontal load case - horizontal shear force

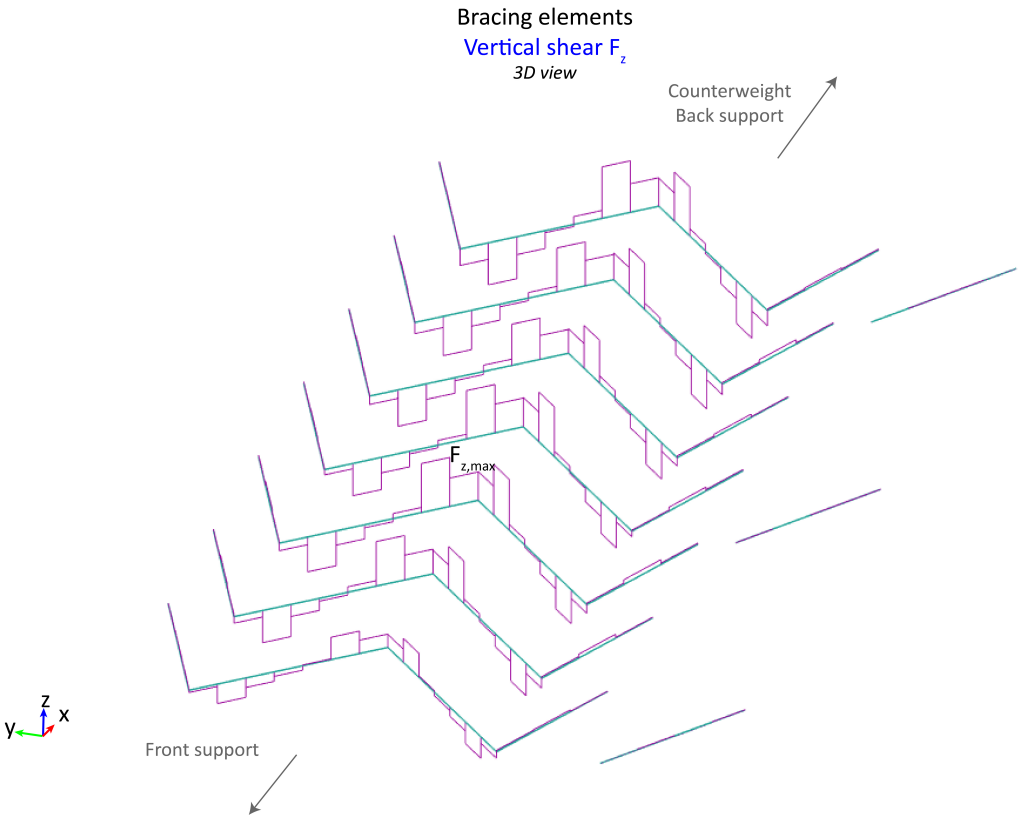

Figure G.43: Bracing elements - horizontal load case - vertical shear force

G.2.4 Cross girders (CG)

Acting forces and bending moments are given in figures G.44, G.45, G.46, G.47, G.48 and G.49.

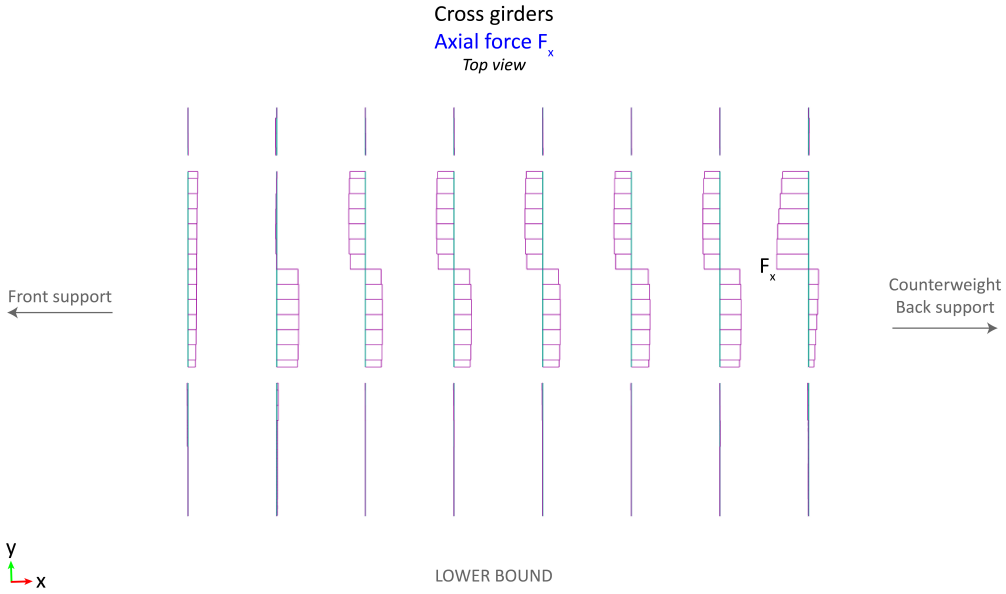

(a) Cross girders - lower bound - horizontal load case - Axial force

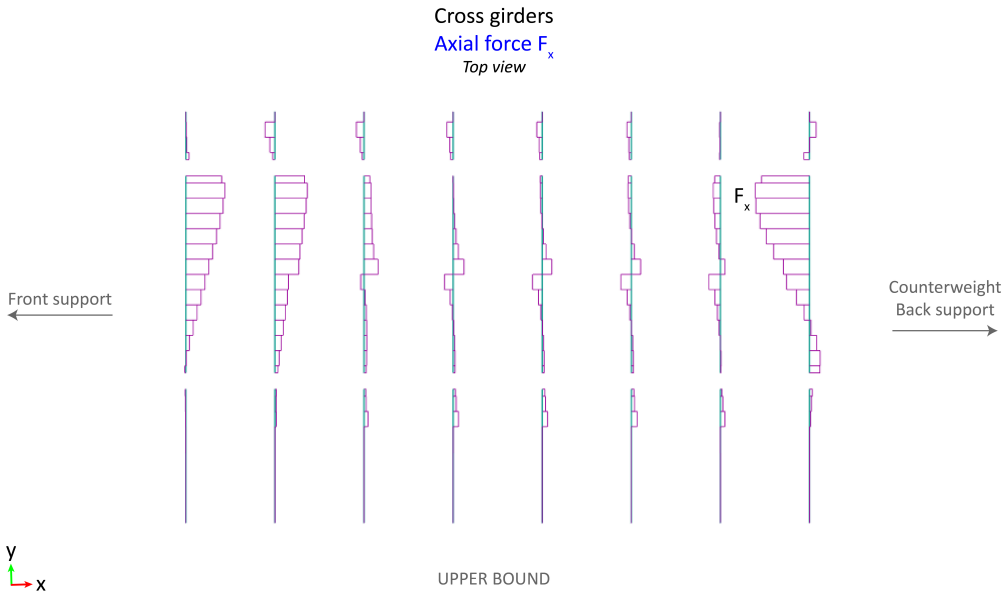

(b) Cross girders - upper bound - horizontal load case - Axial force

Figure G.44

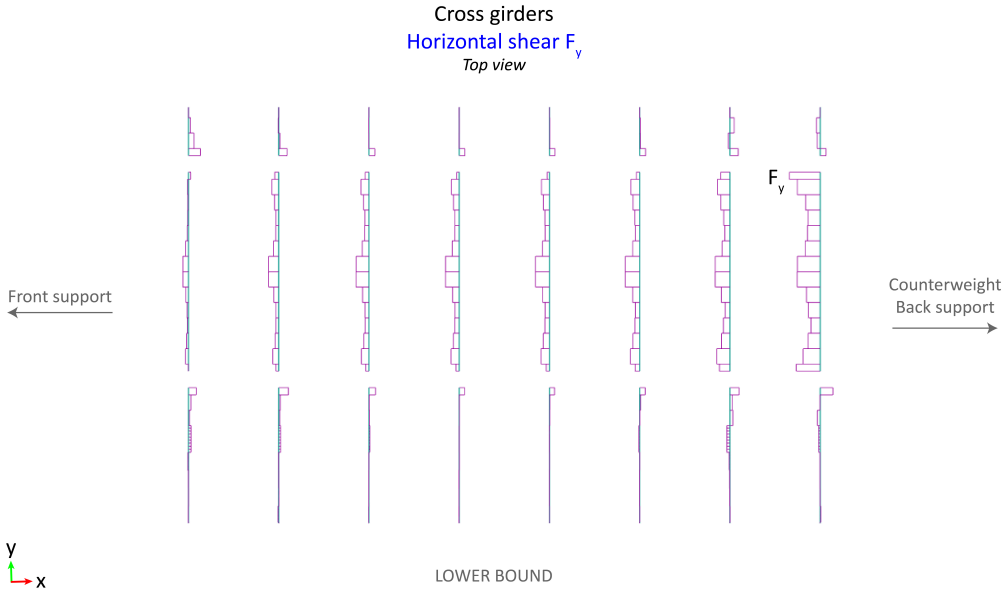

(a) Cross girders - lower bound - horizontal load case - horizontal shear force

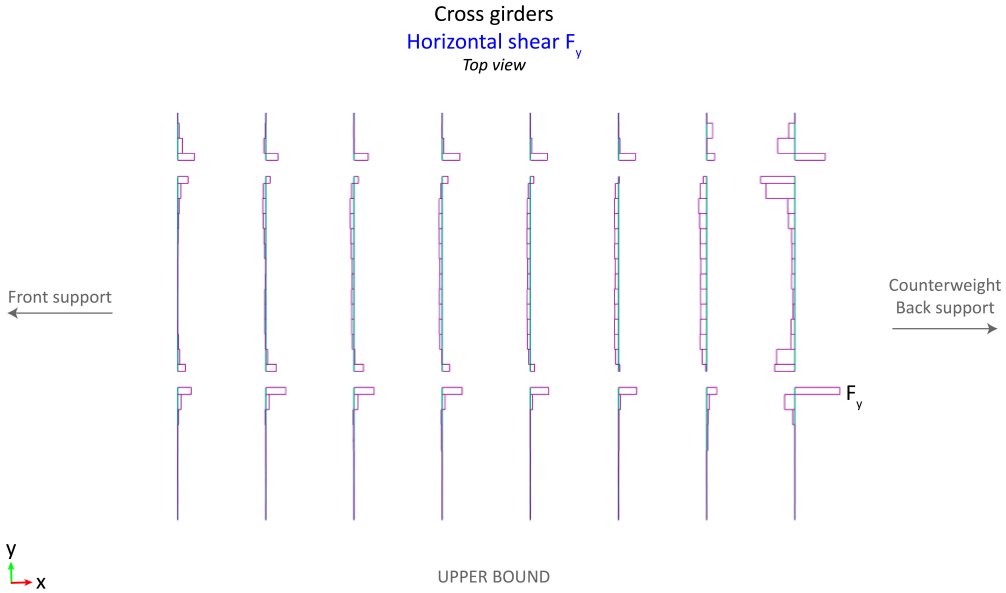

(b) Cross girders - upper bound - horizontal load case - horizontal shear force

Figure G.45

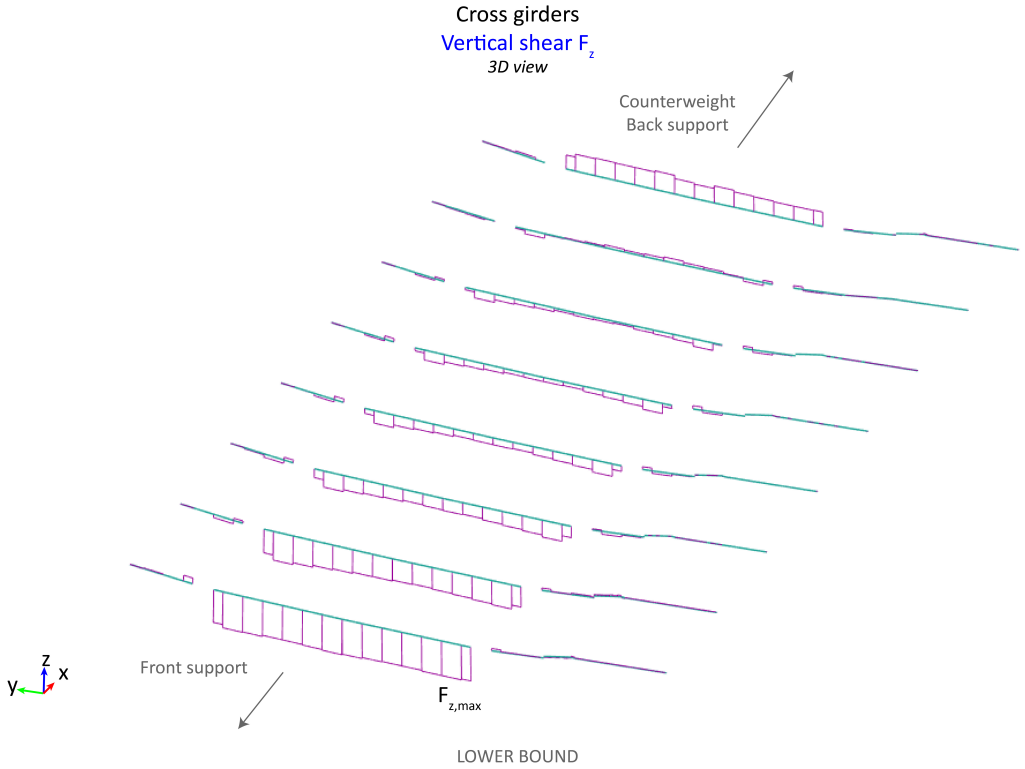

(a) Cross girders - lower bound - horizontal load case - vertical shear force

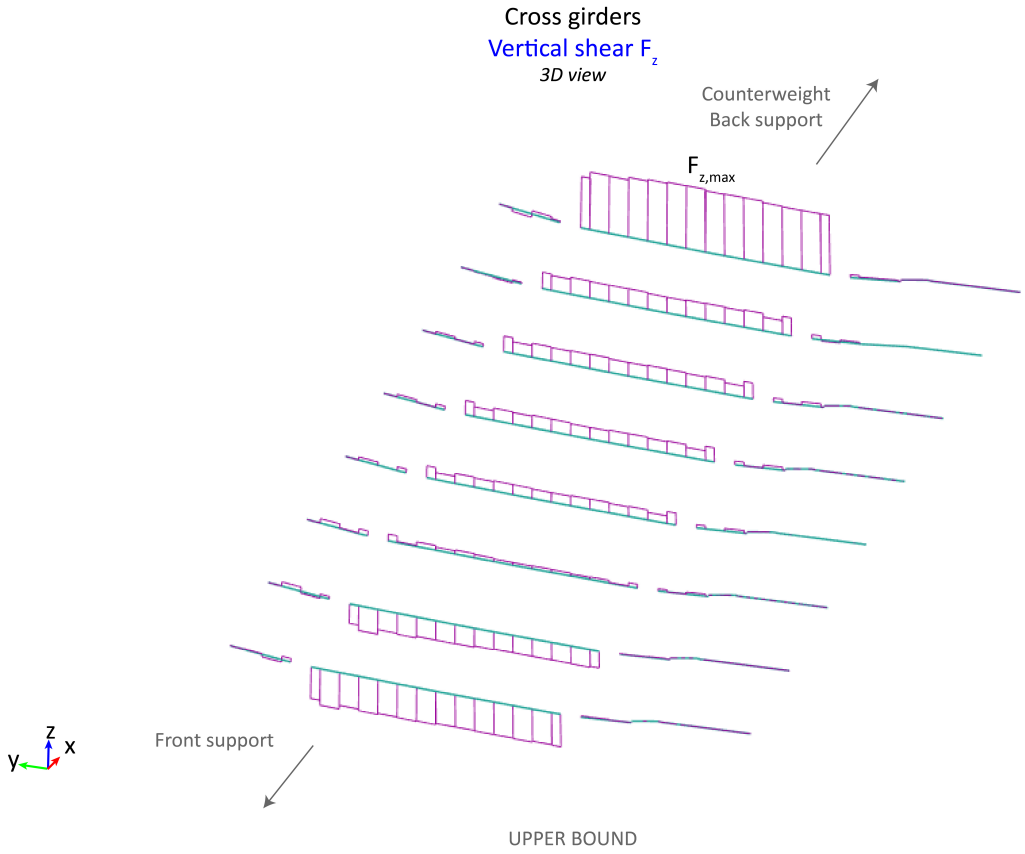

(b) Cross girders - upper bound - horizontal load case - vertical shear force

Figure G.46

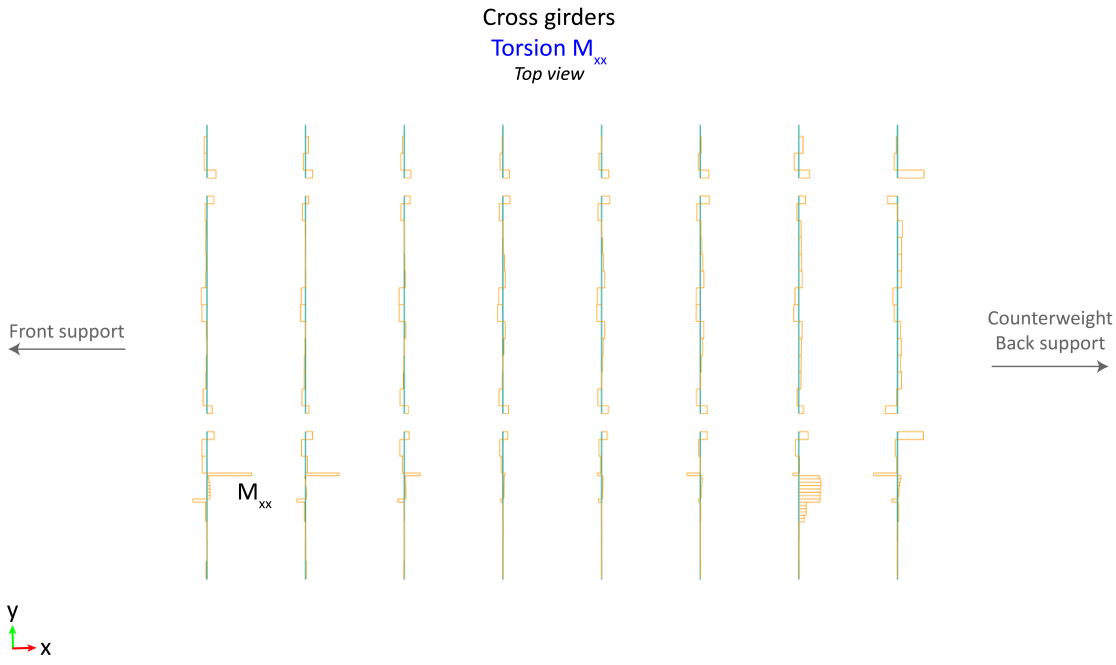

Figure G.47: Cross girders - vertical load case - torsion

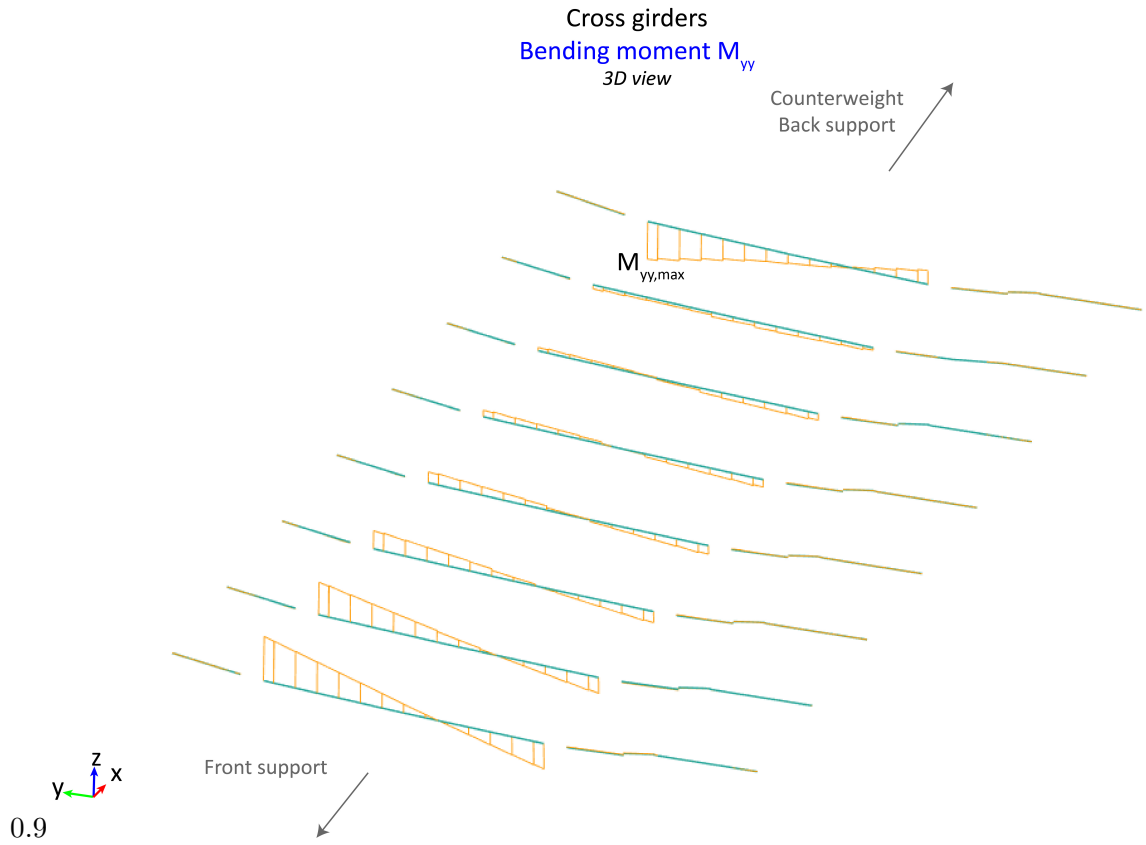

Figure G.48: Cross girders - vertical load case - bending around local y- axis

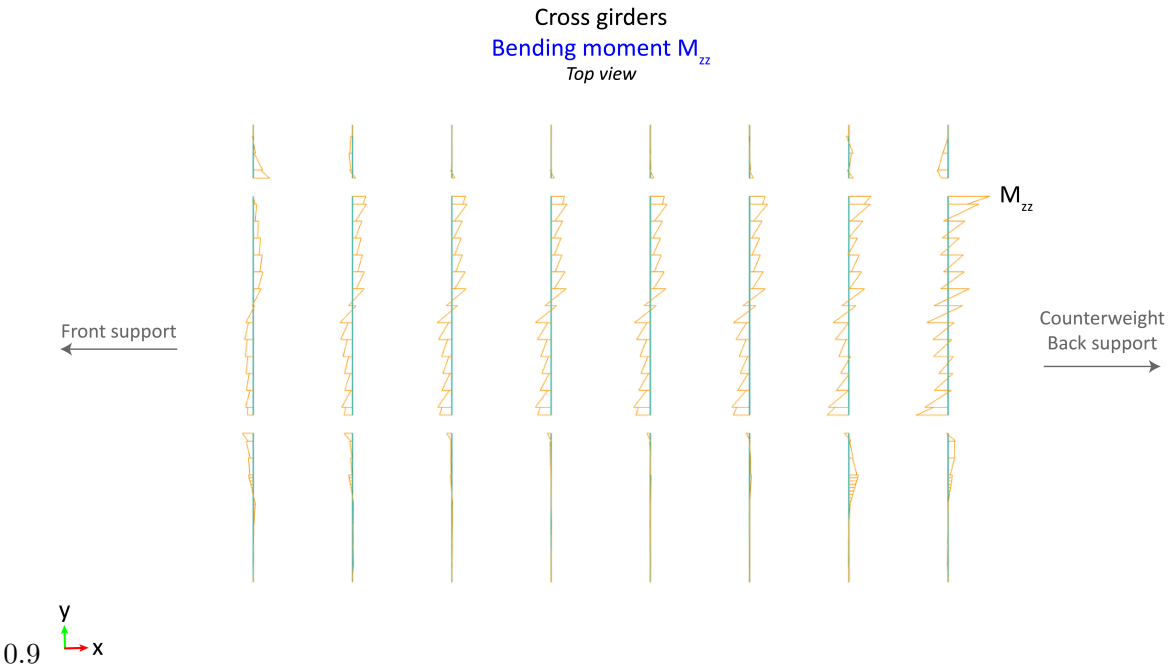

Figure G.49: Cross girders - vertical load case - bending around local z- axis

G.2.5 Main girders (MG)

Forces and bending moments on one of the main girders (right) are given in figures G.50, G.51, G.52, G.53, G.54 and G.55.

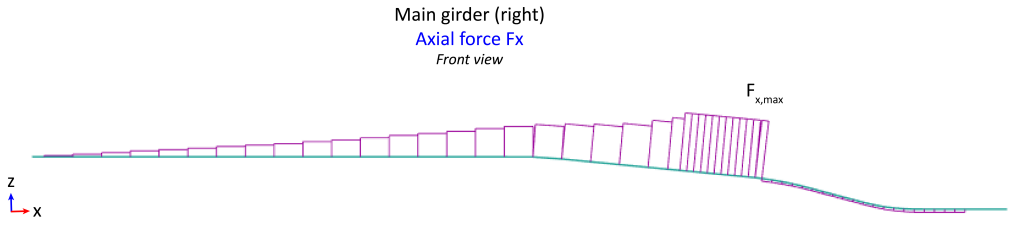

Figure G.50: Main girder - horizontal load case - axial force

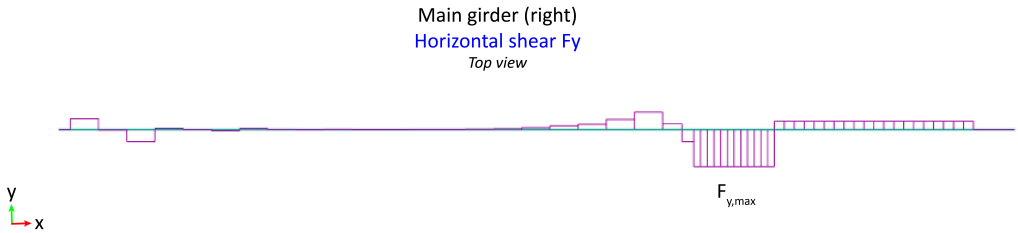

Figure G.51: Main girder - horizontal load case - horizontal shear force

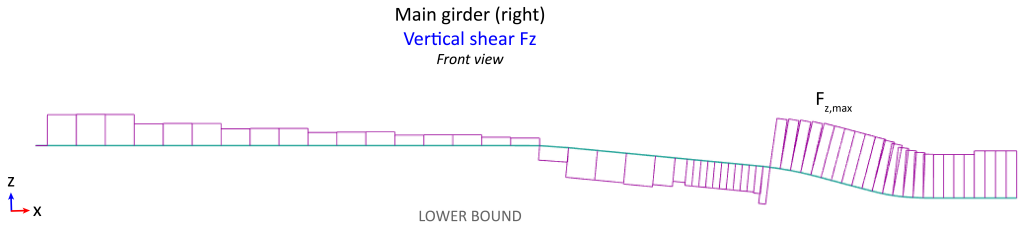

(a) Main girder - lower bound - horizontal load case - vertical shear force

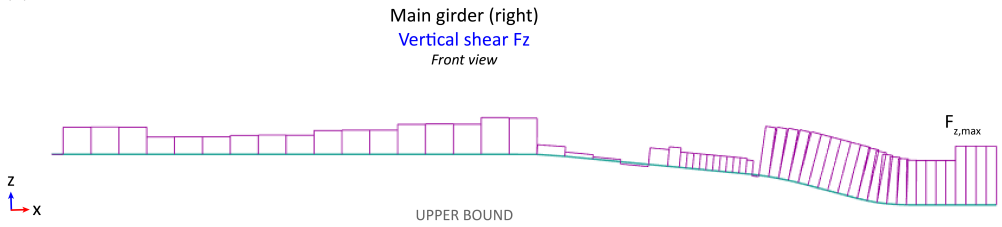

(b) Main girder - upper bound - horizontal load case - vertical shear force

Figure G.52

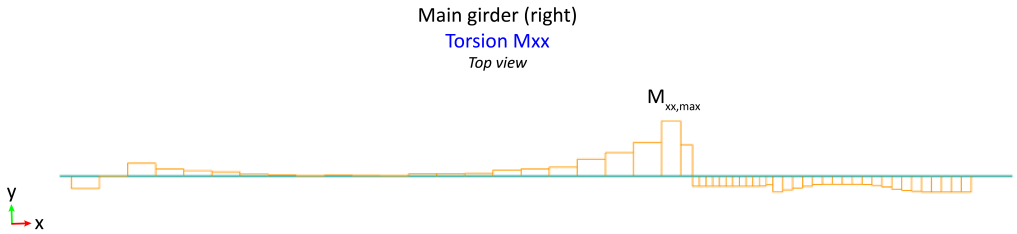

Figure G.53: Main girder - horizontal load case - torsion

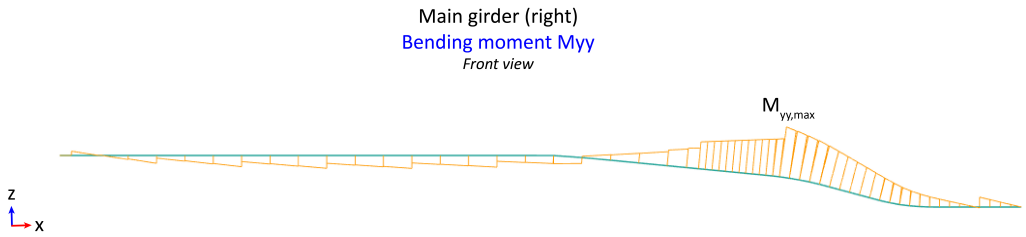

Figure G.54: Main girder - horizontal load case - bending moment around element y-axis

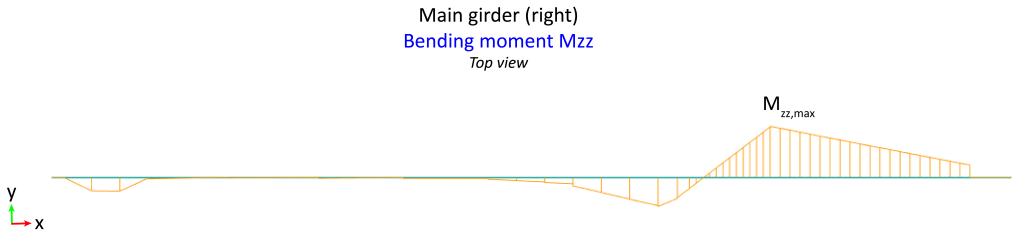

Figure G.55: Main girder - horizontal load case - bending moment around global z-axis

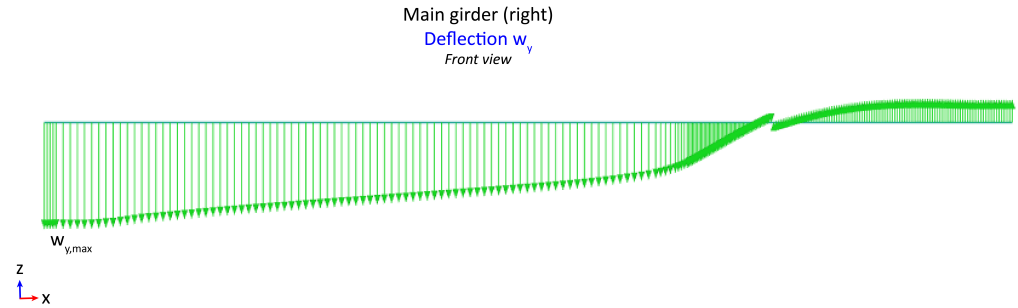

Figure G.56: Main girder deflection for upper- and lower bound situation

Appendix H

Validation iterative secant stiffness method

To validate whether the used iterative secant stiffness method is an accurate method to simulate hybrid interaction between girders, a simple model was created to run both a non-linear and SSM analysis on.

The geometry and elements in the verification model are fairly straight- forward. A simply supported hybrid beam, consisting of two steel (S235) IPE330 girders, spanning 10 meters, with a shear connector between the girders every single meter (figure H.1). The shear connectors are assigned with a non-linear stiffness and modelled as a spring. This verification model can be analyzed in a non-linear way, or by using the iterative secant stiffness method with a static linear analysis. Both methods require a GSA model and the SSM model requires the use of a GSApy script to sequentially assign a new linear spring stiffness.

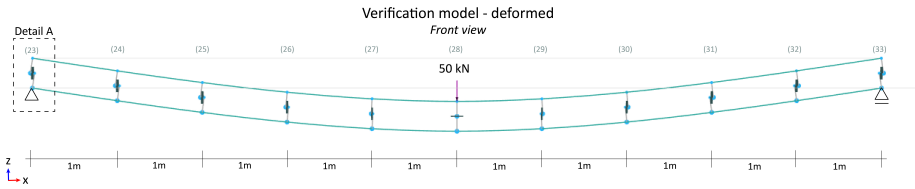

Figure H.1: Geometry and elements of the verification model including spring element IDs

The shear connectors are modelled at the interface between the flanges of the bottom and top- girder. Links (restrained in all directions) have been made to that interface location (175 mm from each neutral axis, see figure H.2). Hereafter, nodes at the interface have been connected to each other by a spring. This spring can be assigned with linear (SSM method, figure H.4) or non-linear (non-linear method, figure H.3) spring properties for the elongation of the spring in its axial direction.

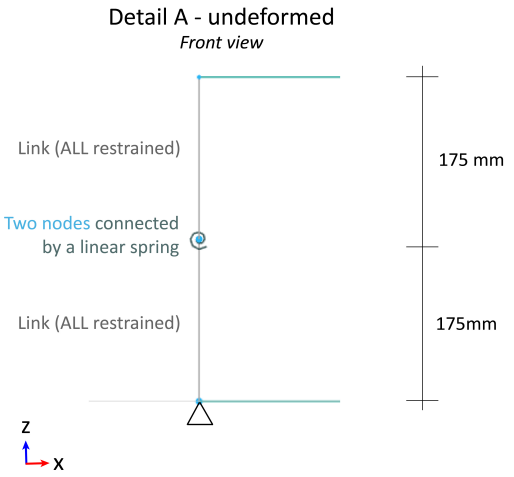

Figure H.2: Geometry and elements of detail A in the verification model

Property	Name	Colour	Type	x		y		z		xx		yy		zz	
				Spring Curve	Stiffness	Spring Curve	Stiffness	Spring Curve	Stiffness	Spring Curve	Stiffness	Spring Curve	Stiffness	Spring Curve	Stiffness
					[N/mm]		[N/mm]		[N/mm]		[Nmm/rad]		[Nmm/rad]		[Nmm/rad]
Defaults	Spring prop. #		Axial	Linear	0	Linear	0	Linear	0	Linear	0	Linear	0	Linear	0
1	Joint	...	General	1 : Material C	0	Linear	1e+09	Linear	1e+09	Linear	1e+09	Linear	1e+09	Linear	1e+09

Figure H.3: Spring property input for non-linear model

Property	Name	Colour	Type	x		y		z		xx		yy		zz	
				Spring Curve	Stiffness	Spring Curve	Stiffness	Spring Curve	Stiffness	Spring Curve	Stiffness	Spring Curve	Stiffness	Spring Curve	Stiffness
					[N/mm]		[N/mm]		[N/mm]		[Nmm/rad]		[Nmm/rad]		[Nmm/rad]
Defaults	Spring prop. #		Axial	Linear	0	Linear	0	Linear	0	Linear	0	Linear	0	Linear	0
1	1	...	General	Linear	4e+04	Linear	1e+09	Linear	1e+09	Linear	1e+09	Linear	1e+09	Linear	1e+09
2	2	...	General	Linear	4e+04	Linear	1e+09	Linear	1e+09	Linear	1e+09	Linear	1e+09	Linear	1e+09
3	3	...	General	Linear	4e+04	Linear	1e+09	Linear	1e+09	Linear	1e+09	Linear	1e+09	Linear	1e+09
4	4	...	General	Linear	4e+04	Linear	1e+09	Linear	1e+09	Linear	1e+09	Linear	1e+09	Linear	1e+09
5	5	...	General	Linear	4e+04	Linear	1e+09	Linear	1e+09	Linear	1e+09	Linear	1e+09	Linear	1e+09
6	6	...	General	Linear	4e+04	Linear	1e+09	Linear	1e+09	Linear	1e+09	Linear	1e+09	Linear	1e+09
7	7	...	General	Linear	4e+04	Linear	1e+09	Linear	1e+09	Linear	1e+09	Linear	1e+09	Linear	1e+09
8	8	...	General	Linear	4e+04	Linear	1e+09	Linear	1e+09	Linear	1e+09	Linear	1e+09	Linear	1e+09
9	9	...	General	Linear	4e+04	Linear	1e+09	Linear	1e+09	Linear	1e+09	Linear	1e+09	Linear	1e+09
10	10	...	General	Linear	4e+04	Linear	1e+09	Linear	1e+09	Linear	1e+09	Linear	1e+09	Linear	1e+09
11	11	...	General	Linear	4e+04	Linear	1e+09	Linear	1e+09	Linear	1e+09	Linear	1e+09	Linear	1e+09

Figure H.4: Spring property input for SSM model

The geometry and material properties of the top- and bottom girder, have been specified respectively in figures H.5 and H.6.

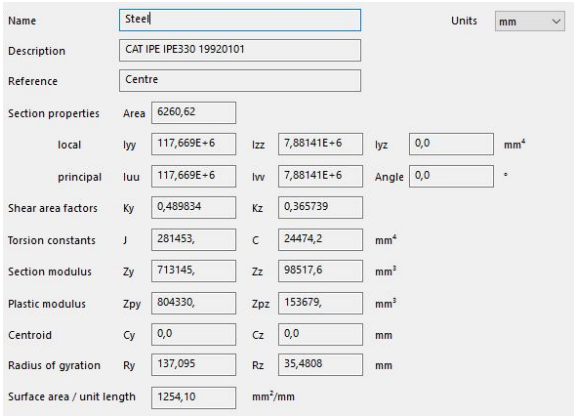

Name	Steel				Units	mm	
Description	CAT IPE IPE330 19920101						
Reference	Centre						
Section properties	Area	6260,62					
local	Iyy	117,669E+6	Izz	7,88141E+6	Iyz	0,0	mm⁴
principal	Iuu	117,669E+6	Ivv	7,88141E+6	Angle	0,0	°
Shear area factors	Ky	0,489834	Kz	0,365739			
Torsion constants	J	281453,	C	24474,2	mm⁴		
Section modulus	Zy	713145,	Zz	98517,6	mm³		
Plastic modulus	Zpy	804330,	Zpz	153679,	mm³		
Centroid	Cy	0,0	Cz	0,0	mm		
Radius of gyration	Ry	137,095	Rz	35,4808	mm		
Surface area / unit length	1254,10	mm²/mm					

Figure H.5: Steel girder cross- sectional properties

Parameter	Unit	Value
Strength (fy)	MPa	235,000
Material partial safety factor (γm)		1,00000
Strength (fu)	MPa	360,000
Failure strain (εmax)		0,0500000
Elastic modulus (E)	MPa	210000,
Shear modulus (G)	MPa	80769,2
Density (ρ)	kg/mm³	7,85000E-6
Thermal expansivity (α)	/°C	12,0000E-6
Poisson's ratio (ν)		0,300000

Figure H.6: Steel girder material properties

For the verification model, a non-linear curve for the axial spring stiffness had to be assumed in order to simulate both the slipping stage and the embedding stage. In the model for the non-linear analysis, the material curve in figure H.7 has been used as input for the non-linear spring stiffness of the connector in GSA. When running the analysis, the load increases in automatic load steps to 50 kN on the structure. Simultaneously at every load step, the forces and displacements in every connector will also increase and follow the specified material curve (or: load-, slip curve).

For the secant stiffness method (SSM), the same material curve is specified, but is not directly used as input for the spring stiffness. The same assumed curve (as used for the non-linear model) i.e. the free slip of 1mm, the slip stiffness (K_{slip} = 100 N/mm) and the embedding stiffness (K_{ser} = 4900 N/mm), are used in python to project results of a previous analysis to. From this projected result, a new secant stiffness can be used in the next iteration of the SSM analysis.

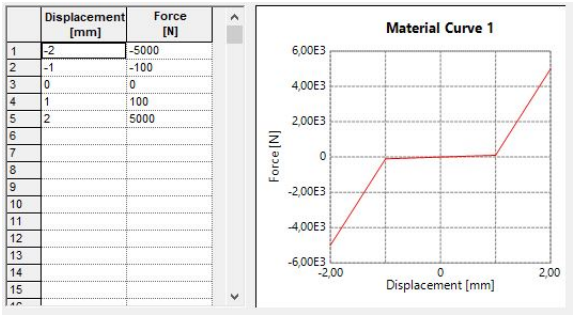

Figure H.7: Material curve for verification model

Figures H.8 and H.9 respectively show the deformation of the structure and a joint near the support.

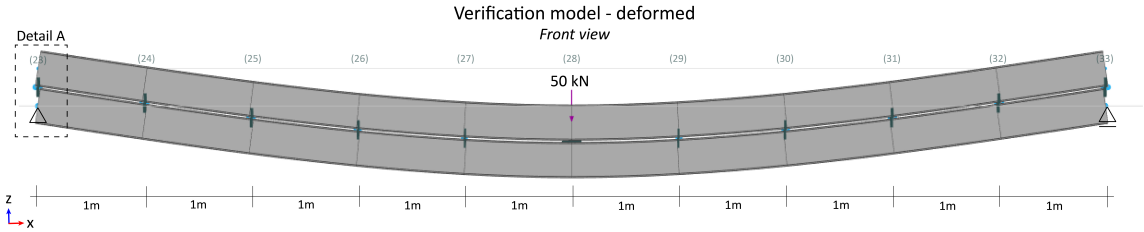

Figure H.8: Verification model showing deformed girders under a concentrated load of 50 kN

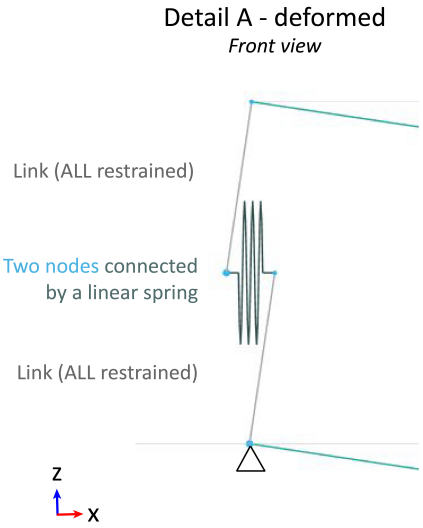

Figure H.9: Deformation of modelled connection near support (Detail A)

A comparison for both methods in terms of connection slip, connection shear force and deflection of the girders, is shown in figures H.10, H.11 and H.12.

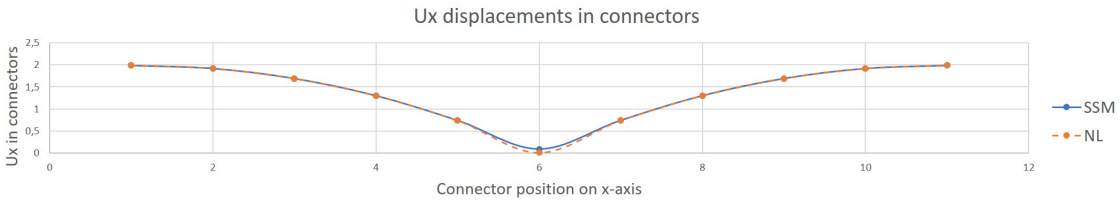

Figure H.10: Comparison of non-linear- and SSM analysis results for elongation of shear connections (U_x)

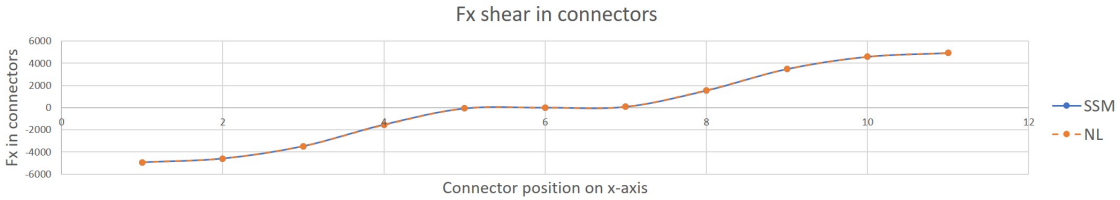

Figure H.11: Comparison of non-linear- and SSM analysis results for shear force in connections (F_x)

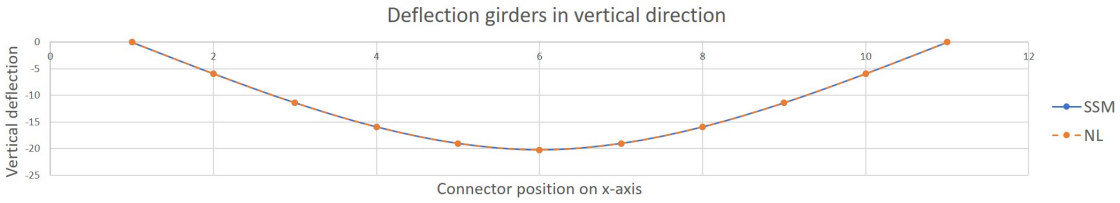

Figure H.12: Comparison of non-linear- and SSM analysis results for total deflection of girders

These graphs are based on the results from exported .CSV files (tables) on displacements and forces for both analysis types (figures H.13, H.14, H.15 and H.16).

Beam and Spring Displacements

Displacements reported are Beam and Spring element displacements; end values may differ from nodal displacements when the element has end releases or is offset.
Output axes: local
Element list: "Bolts"
Case list: 1 : Analysis Case 1

Elem	Case	Pos	Ux [mm]	Uy [mm]	Uz [mm]	|U| [mm]	Rxx [rad]	Ryy [rad]	Rzz [rad]	|R| [rad]
23	A1	45	1,037	0,0	-0,003071	1,037	0,0	0,005924	0,0	0,005924
		34	-0,9504	0,0	-0,003083	0,9504	0,0	0,005924	0,0	0,005924
24	A1	47	0,9848	0,0	-5,927	6,009	0,0	0,005706	0,0	0,005706
		36	-0,9333	0,0	-5,927	6,000	0,0	0,005705	0,0	0,005705
25	A1	48	0,8561	0,0	-11,40	11,43	0,0	0,005014	0,0	0,005014
		37	-0,8344	0,0	-11,40	11,43	0,0	0,005013	0,0	0,005013
26	A1	49	0,6505	0,0	-15,93	15,95	0,0	0,003842	0,0	0,003842
		38	-0,6492	0,0	-15,93	15,95	0,0	0,003840	0,0	0,003840
27	A1	50	0,3649	0,0	-19,05	19,05	0,0	0,002174	0,0	0,002174
		39	-0,3733	0,0	-19,05	19,05	0,0	0,002172	0,0	0,002172
28	A1	51	-0,005032	0,0	-20,25	20,25	0,0	190,0E-12	0,0	190,0E-12
		40	-0,005032	0,0	-20,25	20,25	0,0	189,2E-12	0,0	189,2E-12
29	A1	52	-0,3750	0,0	-19,05	19,05	0,0	-0,002174	0,0	0,002174
		41	0,3633	0,0	-19,05	19,05	0,0	-0,002172	0,0	0,002172
30	A1	53	-0,6606	0,0	-15,93	15,95	0,0	-0,003842	0,0	0,003842
		42	0,6392	0,0	-15,93	15,95	0,0	-0,003840	0,0	0,003840
31	A1	54	-0,8662	0,0	-11,40	11,43	0,0	-0,005014	0,0	0,005014
		43	0,8243	0,0	-11,40	11,43	0,0	-0,005013	0,0	0,005013
32	A1	55	-0,9948	0,0	-5,927	6,010	0,0	-0,005706	0,0	0,005706
		44	0,9233	0,0	-5,927	5,999	0,0	-0,005705	0,0	0,005705
33	A1	46	-1,047	0,0	-0,003071	1,047	0,0	-0,005924	0,0	0,005924
		35	0,9403	0,0	-0,003083	0,9403	0,0	-0,005924	0,0	0,005924

Figure H.13: Output of displacements for connectors in case of running the non-linear analysis

Beam and Spring Displacements

Displacements reported are Beam and Spring element displacements; end values may differ from nodal displacements when the element has end releases or is offset.
Output axes: local
Element list: "Bolts"
Case list: 1 : Analysis case 1

Elem	Case	Pos	Ux [mm]	Uy [mm]	Uz [mm]	|U| [mm]	Rxx [rad]	Ryy [rad]	Rzz [rad]	|R| [rad]
23	A1	45	1,036	0,0	0,0	1,036	0,0	0,005922	0,0	0,005922
		34	-0,9502	0,0	-12,50E-6	0,9502	0,0	0,005922	0,0	0,005922
24	A1	47	1,002	0,0	-5,923	6,007	0,0	0,005704	0,0	0,005704
		36	-0,9158	0,0	-5,923	5,993	0,0	0,005704	0,0	0,005704
25	A1	48	0,8882	0,0	-11,39	11,43	0,0	0,005013	0,0	0,005013
		37	-0,8020	0,0	-11,39	11,42	0,0	0,005013	0,0	0,005013
26	A1	49	0,6929	0,0	-15,93	15,94	0,0	0,003840	0,0	0,003840
		38	-0,6068	0,0	-15,93	15,94	0,0	0,003840	0,0	0,003840
27	A1	50	0,4122	0,0	-19,04	19,05	0,0	0,002173	0,0	0,002173
		39	-0,3260	0,0	-19,04	19,05	0,0	0,002173	0,0	0,002173
28	A1	51	0,04309	0,0	-20,24	20,24	0,0	0,0	0,0	0,0
		40	0,04309	0,0	-20,24	20,24	0,0	0,0	0,0	0,0
29	A1	52	-0,3260	0,0	-19,04	19,05	0,0	-0,002173	0,0	0,002173
		41	0,4122	0,0	-19,04	19,05	0,0	-0,002173	0,0	0,002173
30	A1	53	-0,6068	0,0	-15,93	15,94	0,0	-0,003840	0,0	0,003840
		42	0,6929	0,0	-15,93	15,94	0,0	-0,003840	0,0	0,003840
31	A1	54	-0,8020	0,0	-11,39	11,42	0,0	-0,005013	0,0	0,005013
		43	0,8882	0,0	-11,39	11,43	0,0	-0,005013	0,0	0,005013
32	A1	55	-0,9158	0,0	-5,923	5,993	0,0	-0,005704	0,0	0,005704
		44	1,002	0,0	-5,923	6,007	0,0	-0,005704	0,0	0,005704
33	A1	46	-0,9502	0,0	0,0	0,9502	0,0	-0,005922	0,0	0,005922
		35	1,036	0,0	-12,50E-6	1,036	0,0	-0,005922	0,0	0,005922

Figure H.14: Output of displacements for connectors in case of running the secant stiffness analysis

Beam and Spring Forces and Moments

The force in an element at any point is the force required to maintain
equilibrium if the element is cut at that point and the end 2 part of the
element is discarded. Thus: +ve axial forces are tensile
Forces and moments are output in element axis directions
i.e. Fx: axial force; Fy & Fz: shear forces; Mxx: torsion; Myy & Mzz: moments
Element axes for springs are as defined by the spring property axis no.
Element list: "Bolts"
Case list: 1 : Analysis Case 1

Elem	Case	Pos	Fx [N]	Fy [N]	Fz [N]	Mxx [Nmm]	Myy [Nmm]	Mzz [Nmm]	|Fyz| [N]	|Myz| [Nmm]
23	A1	45	-4937,	0,0	-12480,	0,0	-370,2	0,0	12480,	370,2
		34	-4937,	0,0	-12480,	0,0	-370,2	0,0	12480,	370,2
24	A1	47	-4599,	0,0	37,92	0,0	-788,3	0,0	37,92	788,3
		36	-4599,	0,0	37,92	0,0	-788,3	0,0	37,92	788,3
25	A1	48	-3483,	0,0	10,17	0,0	-1453,	0,0	10,17	1453,
		37	-3483,	0,0	10,17	0,0	-1453,	0,0	10,17	1453,
26	A1	49	-1569,	0,0	-9,547	0,0	-1692,	0,0	9,547	1692,
		38	-1569,	0,0	-9,547	0,0	-1692,	0,0	9,547	1692,
27	A1	50	-73,83	0,0	-31,64	0,0	-1227,	0,0	31,64	1227,
		39	-73,83	0,0	-31,64	0,0	-1227,	0,0	31,64	1227,
28	A1	51	6,887E-6	0,0	-25050,	0,0	-749,1E-6	0,0	25050,	749,1E-6
		40	6,887E-6	0,0	-25050,	0,0	-749,1E-6	0,0	25050,	749,1E-6
29	A1	52	73,83	0,0	-31,64	0,0	1227,	0,0	31,64	1227,
		41	73,83	0,0	-31,64	0,0	1227,	0,0	31,64	1227,
30	A1	53	1569,	0,0	-9,547	0,0	1692,	0,0	9,547	1692,
		42	1569,	0,0	-9,547	0,0	1692,	0,0	9,547	1692,
31	A1	54	3483,	0,0	10,17	0,0	1453,	0,0	10,17	1453,
		43	3483,	0,0	10,17	0,0	1453,	0,0	10,17	1453,
32	A1	55	4599,	0,0	37,92	0,0	788,3	0,0	37,92	788,3
		44	4599,	0,0	37,92	0,0	788,3	0,0	37,92	788,3
33	A1	46	4937,	0,0	-12480,	0,0	370,2	0,0	12480,	370,2
		35	4937,	0,0	-12480,	0,0	370,2	0,0	12480,	370,2

Figure H.15: Output of forces for connectors in case of running the non-linear analysis

Beam and Spring Forces and Moments

The force in an element at any point is the force required to maintain
equilibrium if the element is cut at that point and the end 2 part of the
element is discarded. Thus: +ve axial forces are tensile
Forces and moments are output in element axis directions
i.e. Fx: axial force; Fy & Fz: shear forces; Mxx: torsion; Myy & Mzz: moments
Element axes for springs are as defined by the spring property axis no.
Element list: "Bolts"
Case list: 1 : Analysis case 1

Elem	Case	Pos	Fx [N]	Fy [N]	Fz [N]	Mxx [Nmm]	Myy [Nmm]	Mzz [Nmm]	|Fyz| [N]	|Myz| [Nmm]
23	A1	45	-4934,	0,0	-12500,	0,0	-12,57	0,0	12500,	12,57
		34	-4934,	0,0	-12500,	0,0	-12,57	0,0	12500,	12,57
24	A1	47	-4597,	0,0	0,0	0,0	-6,054	0,0	0,0	6,054
		36	-4597,	0,0	0,0	0,0	-6,054	0,0	0,0	6,054
25	A1	48	-3483,	0,0	0,0	0,0	0,4657	0,0	0,0	0,4657
		37	-3483,	0,0	0,0	0,0	0,4657	0,0	0,0	0,4657
26	A1	49	-1536,	0,0	0,0	0,0	-0,4657	0,0	0,0	0,4657
		38	-1536,	0,0	0,0	0,0	-0,4657	0,0	0,0	0,4657
27	A1	50	-73,82	0,0	0,0	0,0	13,04	0,0	0,0	13,04
		39	-73,82	0,0	0,0	0,0	13,04	0,0	0,0	13,04
28	A1	51	0,0	0,0	-26080,	0,0	-1,701E-9	0,0	26080,	1,701E-9
		40	0,0	0,0	-26080,	0,0	-1,701E-9	0,0	26080,	1,701E-9
29	A1	52	73,82	0,0	0,0	0,0	-13,04	0,0	0,0	13,04
		41	73,82	0,0	0,0	0,0	-13,04	0,0	0,0	13,04
30	A1	53	1536,	0,0	0,0	0,0	0,4657	0,0	0,0	0,4657
		42	1536,	0,0	0,0	0,0	0,4657	0,0	0,0	0,4657
31	A1	54	3483,	0,0	0,0	0,0	-0,4657	0,0	0,0	0,4657
		43	3483,	0,0	0,0	0,0	-0,4657	0,0	0,0	0,4657
32	A1	55	4597,	0,0	0,0	0,0	6,054	0,0	0,0	6,054
		44	4597,	0,0	0,0	0,0	6,054	0,0	0,0	6,054
33	A1	46	4934,	0,0	-12500,	0,0	12,57	0,0	12500,	12,57
		35	4934,	0,0	-12500,	0,0	12,57	0,0	12500,	12,57

Figure H.16: Output of forces for connectors in case of running the secant stiffness analysis

On the next pages, a python script is given on how the iterative secant stiffness analysis has been performed by repetitively, opening the verification model, changing the model, generating and processing output files. This iterative analysis method is described in detail in section 11.1.

```
# -*- coding: utf-8 -*-
"""
Created on Wed Apr 29 16:10:55 2020

@author: Maureen.Klomp
"""


from gsapy import GSA
import matplotlib.pyplot as plt
import pandas as pd


# ========================================================================
# Parameters
# ========================================================================
```

String for the spring stiffness properties in 6 directions: x, y, z, xx, yy, zz.

```
#Spring property string
string = "SET, PROP_SPR.3, 1, 1, , GLOBAL, GENERAL, 0, 40000, 0, 1000000000, 0, 1000000000, 0, 1000000000, 0, 1000000000, 0, 1000000000"

# N - Number of bolts in the model
N = 11

#Bolt distance
d1 = 55 #mm
d2 = 80 #mm

# Kslip - Frictionless bolt slip
Kslip = 100 #N/mm Close to zero

Kser = 4900 #N/mm

#Marker size
size_marker = 4

print('------------------------------------------------------------')
print('Run dummy (0) iteration -  stiffness Kslip')
print('------------------------------------------------------------')


print(' ')
print('> Replacing stiffness by Kslip...')
print(' ')


print('Splitting the strings...')
d = string.split()

c0 = []
for i in range(N):
    c1 = string.split()
    c0.append(c1)
```

Stiffnesses as input for the material curve that is the same as given as input for the Non-linear model.

Splitting, adapting and joining each string for the spring properties (11 in total for the number of connectors)

```
#Changing values
print('Changing the values...')
for j in range(N):
    for i in range(len(d)):
        if c0[j][i] == "1,":
            c0[j][i] = str(j+1) + ","
        if c0[j][i] == "40000,":
            c0[j][i] = str(Kslip) + ","



#Re-joining strings
print('Joining strings...')
for j in range(N):
    c0[j] = ' '.join(c0[j])









print(' ')
```

```
print('> Run model with distributed Kslip values...')
print(' ')


gsa_path = r"C:\Users\Maureen.klomp\Desktop\API\Thesis_models\Verification_Method\Verification_Method_SSM_final.gwb"

#open model
print("Opening model..")
try:
    model0 = GSA(r"C:\Users\Maureen.klomp\Desktop\API\Thesis_models\Verification_Method\Verification_Method_SSM_final.gwb", version="10.1
    model0.set_locale(2)
except Exception as e:
    print(e)

# modify spring properties
print("Modifying spring properties...")

try:
    for i in range(N):
        r0 = model0.gwa_command(c0[i])
except Exception as e:
    print(e)
print(r0)
```

Adapting the input strings for the spring properties in the GSA model

```
#run analysis
print("Running analysis tasks...")
a0 = model0.analyse()
print(a0)



nr_views0 = model0.get_highest_view(option="SOV")
views0 = model0.get_views("SOV")


#print("number of views = "+str(nr_views0))

print("Saving all output views to file...")
try:
    for i in range(nr_views0):
        view0 = views0[i]
        view_name0 = view0[1]
        sv = model0.save_view_to_file(view_name=view_name0, file_type="csv")
except Exception as e:
        print(e)

#Elements
elements = model0.get_elements()
nodes = model0.get_nodes()

class loc:
    for p in range(33, 53):
        def deck_node(p=p):
            return elements[p].topo[1]
        def x(p=p):
            index = loc.deck_node(p)
            return nodes[index].coords[0]
        def y(p=p):
            index = loc.deck_node(p)
            return nodes[index].coords[1]



print("Closing model...")
model0.close()









#Number of iterations:
n = 20

#Number of connectors:
```

```
N = 11

print('------------------------------------------------------------')
print('Automation of ', n, ' iterations')
print('------------------------------------------------------------')

                    The free slip value as input for the
#Load slip curve:   material curve
u_slip = 1 #mm
F_slip = u_slip * Kslip
u_elastic = u_slip + 3 #mm
F_elastic = F_slip + (3*Kser)

F_x = [[]] * n
u_x_0 = [[]] * n

df_F = [[]] * n
df_u = [[]] * n
u_x = [[]] * n
u_star_x = [[]] * n
K_star_x = [[]] * n


for i in range(n):

    u_x_a = []
    u_star_x_a = []
    K_star_x_a = []

    c = [[]]*n
    d = string.split()


    df_F[i] = pd.read_csv('Verification_Method_SSM_final_Bolts_Forces('+str(i)+').csv', skipfooter = 20, engine='python', sep= ";", heade
    df_F[i] = df_F[i].dropna()
    df_F[i] = df_F[i].reset_index()
    F_x[i] = df_F[i]['Fx'].tolist()

    df_u[i] = pd.read_csv('Verification_Method_SSM_final_Bolts_Displ('+str(i)+').csv', skipfooter = 20, engine='python', sep= ";", header
    df_u[i] = df_u[i].reset_index()
    u_x_0[i] = df_u[i]['Ux'].tolist()

    for j in range(N*2):
        if (j % 2) == 0:
            x1 = float(max(u_x_0[i][j+1], u_x_0[i][j]) - min(u_x_0[i][j+1], u_x_0[i][j]))
            if F_x[i][int(j/2)] > 0:
                u_x_a.append(x1)
            else:
                u_x_a.append(-x1)

    u_x[i] = u_x_a

    for j in range(N):
        if -F_slip < F_x[i][j] < F_slip:
            u_star_x_0 = F_x[i][j]/Kslip
            u_star_x_a.append(u_star_x_0)
        if F_x[i][j] < - F_slip:                                  If previous result is in the
            u_star_x_1 = ((F_x[i][j]+F_slip)/Kser) - u_slip       embedding stage, project the result
            u_star_x_a.append(u_star_x_1)                         horizontally to the assumed load-,
        if F_x[i][j] > F_slip:                                    slip curve (or: material curve)
            u_star_x_2 = ((F_x[i][j]-F_slip)/Kser) + u_slip
            u_star_x_a.append(u_star_x_2)

    u_star_x[i] = u_star_x_a

    for j in range(N):
        if abs(F_x[i][j]) < abs(F_slip):                          Check whether the previous result is
            K_star_x_0 = Kslip                                    in the slip or embedding stage. If
            K_star_x_a.append(K_star_x_0)                         it is in the embedding stage, assign
        else:                                                     adapted stiffness K*. Otherwise,
            K_star_x_1 = F_x[i][j]/u_star_x[i][j]                 keep K_slip
            K_star_x_a.append(K_star_x_1)

    K_star_x[i] = K_star_x_a

    #Splitting strings:
    for j in range(N):
        c0 = string.split()
        c[i].append(c0)


    for j in range(N):
        for k in range(len(d)):
            if c[i][j][k] == "1,":
                c[i][j][k] = str(j+1) + ","
            if c[i][j][k] == "40000,":
                c[i][j][k] = str(K_star_x[i][j]) + ","
```

```
for j in range(N):
    c[i][j] = ' '.join(c[i][j])

#Running model:
model = GSA(r"C:\Users\Maureen.klomp\Desktop\API\Thesis_models\Verification_Method\Verification_Method_SSM_final.gwb", version="10.1"
model.set_locale(2)

for j in range(N):
    r = model.gwa_command(c[i][j])

a = model.analyse()

nr_views = model.get_highest_view(option="SOV")
views = model.get_views("SOV")
for l in range(nr_views):
    view = views[l]
    view_name_ = view[1]
    save_view = model.save_view_to_file(view_name=view_name_, file_type="csv")

s = model.save_as(r"C:\Users\Maureen.klomp\Desktop\API\Thesis_models\Verification_Method\Verification_Method_SSM_final_results.gwb")

model.close()


print("Iteration", i+1, "succeeded")
```

Appendix I

Results

This appendix presents figures on the obtained results from SSM analyses for both the vertical and horizontal load case. First, the results for the current deck boards will be given. Later, the results for a deck as a monolithic plate will be shown. For more information on the results and the discussion, check chapters 12 and 13.

Vertical load case

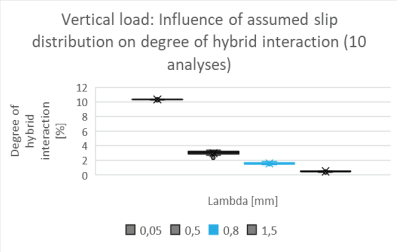

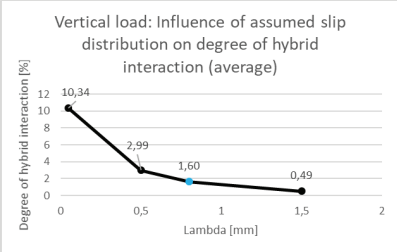

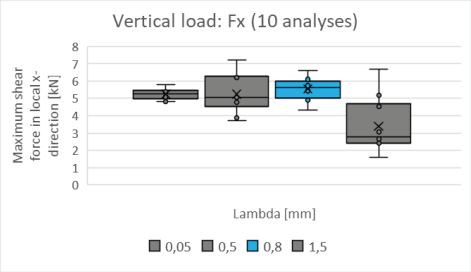

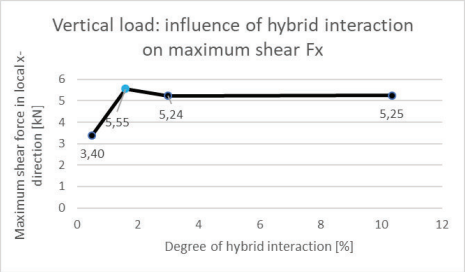

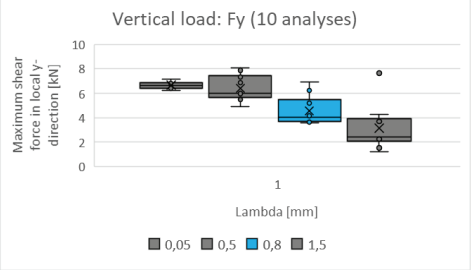

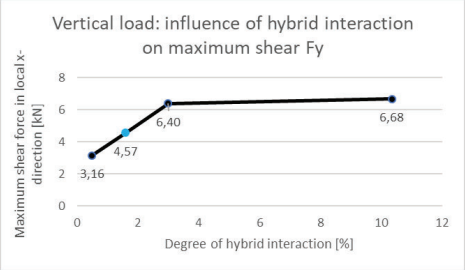

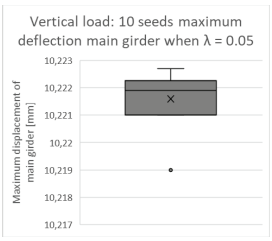
Vertical load: 10 seeds maximum deflection main girder when λ = 0.05
Maximum displacement of main girder [mm]
10,223
10,222
10,221
10,22
10,219
10,218
10,217

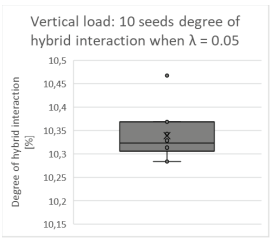
Vertical load: 10 seeds degree of hybrid interaction when λ = 0.05
Degree of hybrid interaction [%]
10,5
10,45
10,4
10,35
10,3
10,25
10,2
10,15

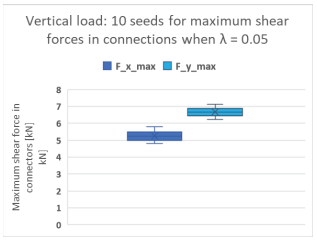
Vertical load: 10 seeds for maximum shear forces in connections when λ = 0.05
F_x_max
F_y_max
Maximum shear force in connectors [kN]
8
7
6
5
4
3
2
1
0

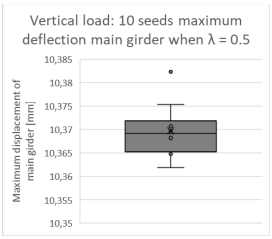
Vertical load: 10 seeds maximum deflection main girder when λ = 0.5
Maximum displacement of main girder [mm]
10,385
10,38
10,375
10,37
10,365
10,36
10,355
10,35

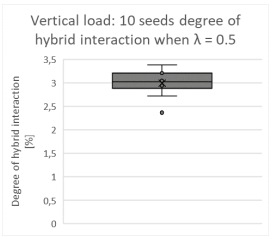
Vertical load: 10 seeds degree of hybrid interaction when λ = 0.5
Degree of hybrid interaction [%]
3,5
3
2,5
2
1,5
1
0,5
0

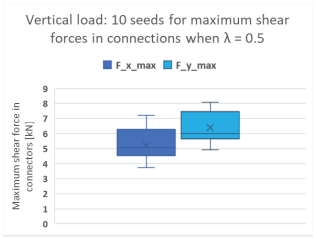
Vertical load: 10 seeds for maximum shear forces in connections when λ = 0.5
F_x_max
F_y_max
Maximum shear force in connectors [kN]
9
8
7
6
5
4
3
2
1
0

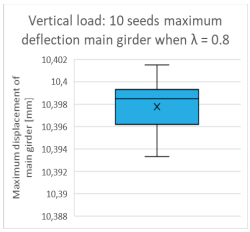
Vertical load: 10 seeds maximum deflection main girder when λ = 0.8
Maximum displacement of main girder [mm]
10,402
10,4
10,398
10,396
10,394
10,392
10,39
10,388

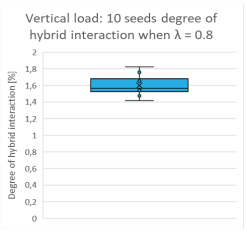
Vertical load: 10 seeds degree of hybrid interaction when λ = 0.8
Degree of hybrid interaction [%]
2
1,8
1,6
1,4
1,2
1
0,8
0,6
0,4
0,2
0

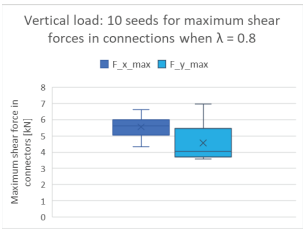
Vertical load: 10 seeds for maximum shear forces in connections when λ = 0.8
F_x_max
F_y_max
Maximum shear force in connectors [kN]
8
7
6
5
4
3
2
1
0

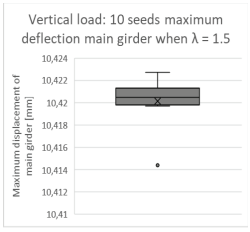
Vertical load: 10 seeds maximum deflection main girder when λ = 1.5
Maximum displacement of main girder [mm]
10,424
10,422
10,42
10,418
10,416
10,414
10,412
10,41

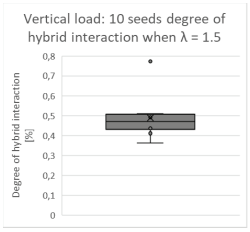
Vertical load: 10 seeds degree of hybrid interaction when λ = 1.5
Degree of hybrid interaction [%]
0,8
0,7
0,6
0,5
0,4
0,3
0,2
0,1
0

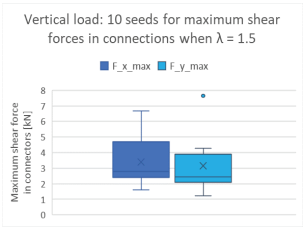
Vertical load: 10 seeds for maximum shear forces in connections when λ = 1.5
F_x_max
F_y_max
Maximum shear force in connectors [kN]
8
7
6
5
4
3
2
1
0

Kser- influence – Vertical load

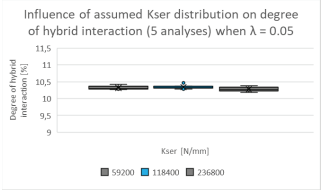

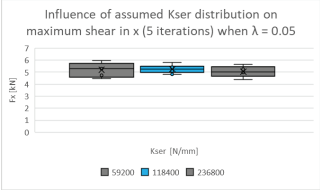

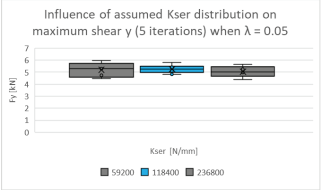

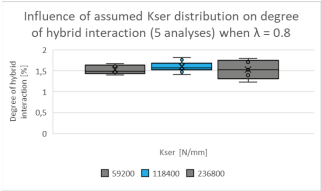

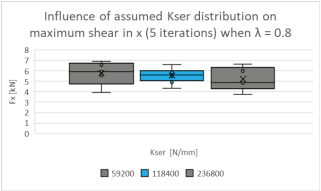

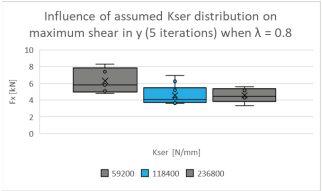

Horizontal load case

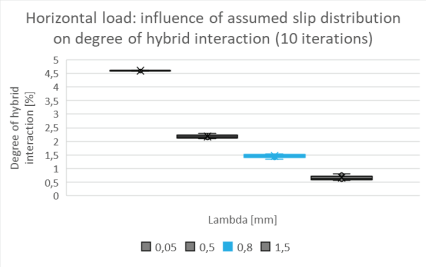

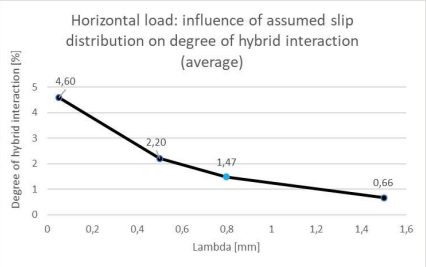

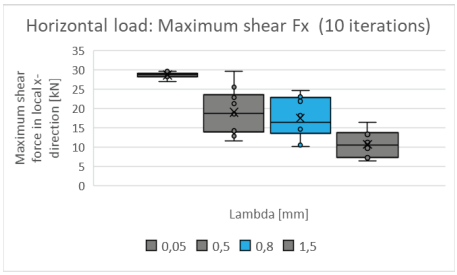
Horizontal load: Maximum shear Fx (10 iterations)
Maximum shear force in local x-direction [kN]
35
30
25
20
15
10
5
0
Lambda [mm]
0,05
0,5
0,8
1,5

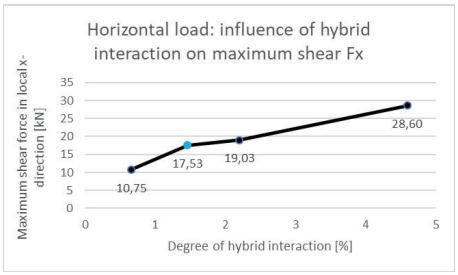
Horizontal load: influence of hybrid interaction on maximum shear Fx
Maximum shear force in local x-direction [kN]
35
30
25
20
15
10
5
0
10,75
17,53
19,03
28,60
0
1
2
3
4
5
Degree of hybrid interaction [%]

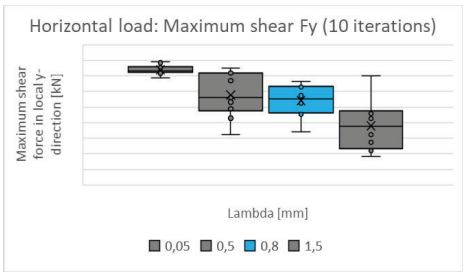
Horizontal load: Maximum shear Fy (10 iterations)
Maximum shear force in local y-direction [kN]
Lambda [mm]
0,05
0,5
0,8
1,5

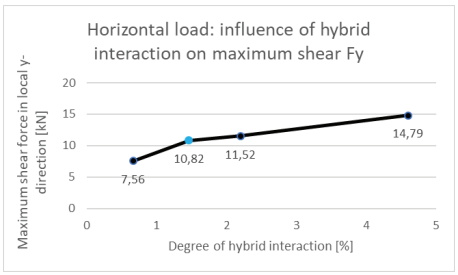
Horizontal load: influence of hybrid interaction on maximum shear Fy
Maximum shear force in local y-direction [kN]
20
15
10
5
0
7,56
10,82
11,52
14,79
0
1
2
3
4
5
Degree of hybrid interaction [%]

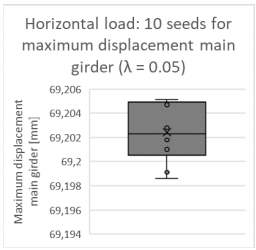
Horizontal load: 10 seeds for maximum displacement main girder (λ = 0.05)
Maximum displacement main girder [mm]
69,206
69,204
69,202
69,2
69,198
69,196
69,194

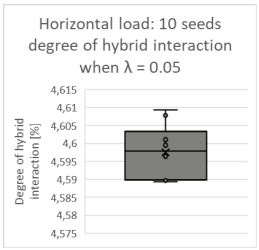
Horizontal load: 10 seeds degree of hybrid interaction when λ = 0.05
Degree of hybrid interaction [%]
4,615
4,61
4,605
4,6
4,595
4,59
4,585
4,58
4,575

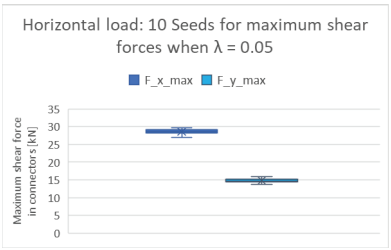
Horizontal load: 10 Seeds for maximum shear forces when λ = 0.05
F_x_max
F_y_max
Maximum shear force in connectors [kN]
35
30
25
20
15
10
5
0

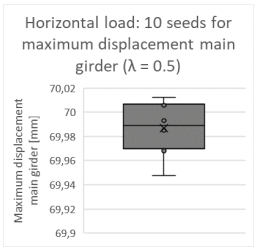
Horizontal load: 10 seeds for maximum displacement main girder (λ = 0.5)
Maximum displacement main girder [mm]
70,02
70
69,98
69,96
69,94
69,92
69,9

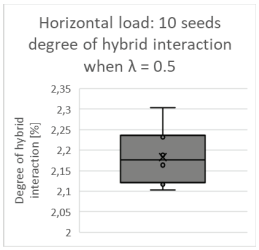
Horizontal load: 10 seeds degree of hybrid interaction when λ = 0.5
Degree of hybrid interaction [%]
2,35
2,3
2,25
2,2
2,15
2,1
2,05
2

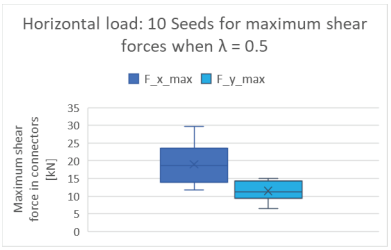
Horizontal load: 10 Seeds for maximum shear forces when λ = 0.5
F_x_max
F_y_max
Maximum shear force in connectors [kN]
35
30
25
20
15
10
5
0

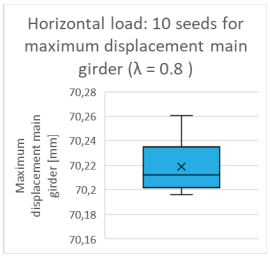

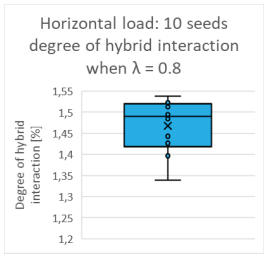

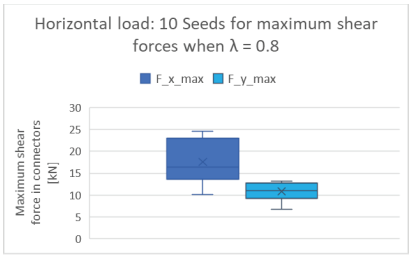

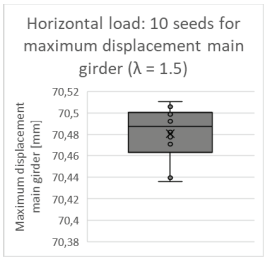

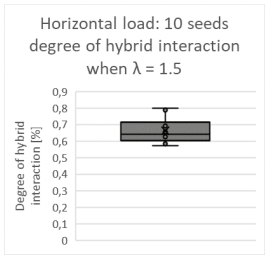

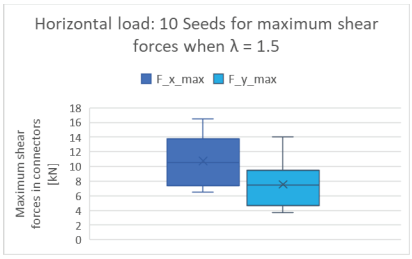

Mono-plate vertical

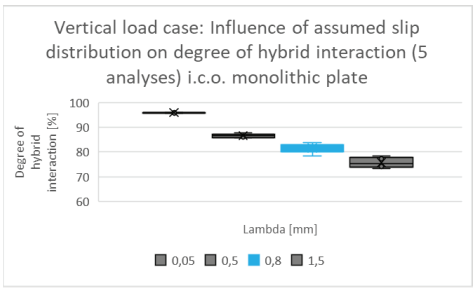

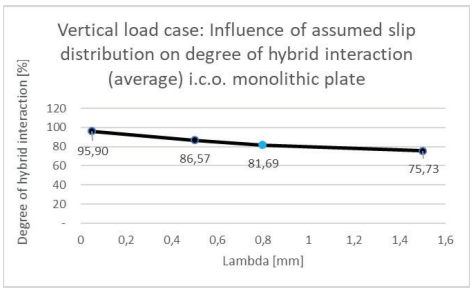

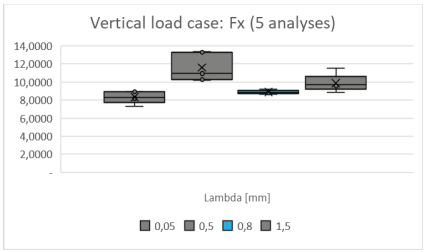

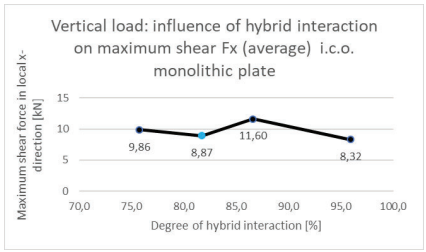

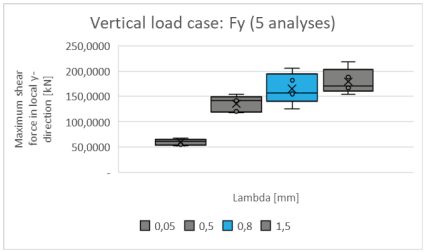

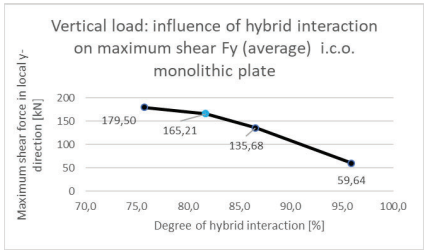

Mono-plate horizontal

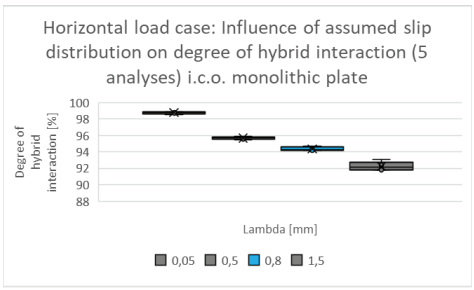

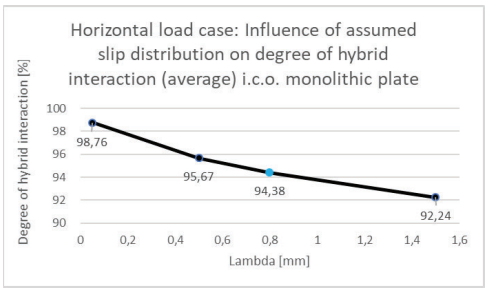

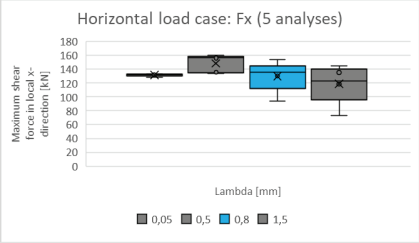
Horizontal load case: Fx (5 analyses)
Maximum shear force in local x-direction [kN]
180
160
140
120
100
80
60
40
20
0
Lambda [mm]
0,05 0,5 0,8 1,5

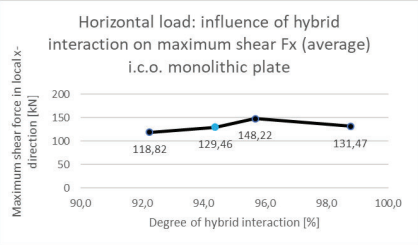
Horizontal load: influence of hybrid interaction on maximum shear Fx (average) i.c.o. monolithic plate
Maximum shear force in local x-direction [kN]
200
150
100
50
0
118,82
129,46
148,22
131,47
90,0
92,0
94,0
96,0
98,0
100,0
Degree of hybrid interaction [%]

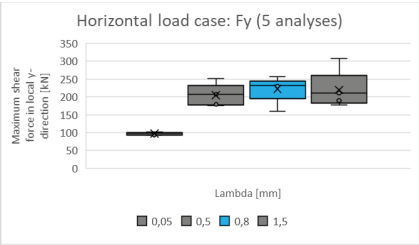
Horizontal load case: Fy (5 analyses)
Maximum shear force in local y-direction [kN]
350
300
250
200
150
100
50
0
Lambda [mm]
0,05 0,5 0,8 1,5

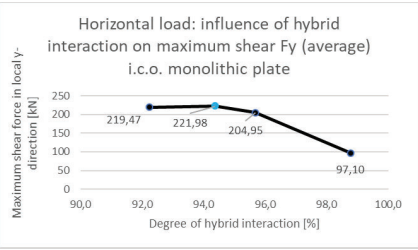
Horizontal load: influence of hybrid interaction on maximum shear Fy (average) i.c.o. monolithic plate
Maximum shear force in local y-direction [kN]
250
200
150
100
50
0
219,47
221,98
204,95
97,10
90,0
92,0
94,0
96,0
98,0
100,0
Degree of hybrid interaction [%]

Appendix J

Script SSM

On the next pages, a python script is given on how the iterative secant stiffness analysis has been performed by repetitively, opening the verification model, changing the model, generating and processing output files. This iterative analysis method is described in detail in section 11.1.

```
# -*- coding: utf-8 -*-
"""

One iteration, Linear analysis, only x- direction.

Created on Mon Mar  2 09:37:21 2020

@author: Maureen.Klomp
"""
from gsapy import GSA
#from gsapy import Node
import numpy as np
#import scipy.stats
import pandas as pd
from math import pi

# ============================================================================
# Parameters
# ============================================================================

#Elements
el_start = 25022
el_end = 27520
```

String for the spring stiffness properties in 6 directions: x, y, z, xx, yy and zz

```
#Spring property string
string = "SET, PROP_SPR.3, 5, 1, , GLOBAL, GENERAL, 0, 10000000, 0, 40000, 0, 46600,0, 439, 0, 10000000, 0, 10000000"

# N - Number of bolts in the model
N = 2499

#Number of iterations:
n = 40

#Bolt distance
d1 = 55 #mm
d2 = 80 #mm

# Kslip - Frictionless bolt slip
Kslip = 0.100 #kN/mm Close to zero
Kslip_r = 10 #kNm/rad
```

Slip stiffness for the first iteration and characteristic for the slipping stage of the connections

```
# Kser - Slip modulus
rho_m = 1050 #kg/m3
d = 20

Kser_mean = 2*2* ((rho_m**1.5)*d)/23 #N/mm
Kser_std = 0.2 * Kser_mean #N/mm

Kser = np.random.normal(Kser_mean, Kser_std, N)


# Slip - Hole clearance (u_slip) Weibull
labdaw2 = 0.8 #Scale
kweib2 = 2 #Shape

wb = np.random.weibull(kweib2,N)
R = wb*labdaw2
theta = np.random.uniform(0, 0.5*pi, N)




print('------------------------------------------------------------')
print('Run dummy (0) iteration -  stiffness Kslip')
print('------------------------------------------------------------')
```

Running a first "dummy" iteration where the stiffnesses in all connections is equal to K_slip (or: K_slip_r for the rotational stiffness)

```
# ============================================================================
print(' ')
print('> Replacing stiffness by Kslip...')
print(' ')
```

Splitting, adapting and joining the strings for the stiffness in local x, y and zz direction

```
print('Splitting the strings...')
d = string.split()

c0 = []
for i in range(N):
    c1 = string.split()
    c0.append(c1)



#Changing values
print('Changing the values...')
for j in range(N):
    for i in range(len(d)):
```

```
        if c0[j][i] == "5,":
            c0[j][i] = str(j+5) + ","
        if c0[j][i] == "1,":
            c0[j][i] = str(j+1) + ","
        if c0[j][i] == "46600,":
            c0[j][i] = str(Kslip) + ","
        if c0[j][i] == "40000,":
            c0[j][i] = str(Kslip) + ","
        if c0[j][i] == "439,":
            c0[j][i] = str(Kslip_r) + ","


#Re-joining strings
print('Joining strings...')
for j in range(N):
    c0[j] = ' '.join(c0[j])




# ========================================================================
print(' ')
print('> Run model with distributed Kslip values...')   Opening, changing, analyzing, saving and
print(' ')                                               closing the GSA model through GSApy


gsa_path = r"C:\Users\Maureen.klomp\Desktop\API\Thesis_models\Iteration\BBM_1_spring_joint_Iteration.gwb"

#open model
print("Opening model..")
try:
    model0 = GSA(r"C:\Users\Maureen.klomp\Desktop\API\Thesis_models\Iteration\BBM_1_spring_joint_Iteration.gwb", version="10.0")
    model0.set_locale(2)
except Exception as e:
    print(e)

# modify spring properties
print("Modifying spring properties...")

try:
    for i in range(N):
        r0 = model0.gwa_command(c0[i])     gwa.command adapts the spring stiffness properties for
except Exception as e:                     all connections (N = 2449 times) in the GSA model
    print(e)
print(r0)



#run analysis
print("Running analysis tasks...")
a0 = model0.analyse()
print(a0)



nr_views0 = model0.get_highest_view(option="SOV")
views0 = model0.get_views("SOV")


#print("number of views = "+str(nr_views0))

print("Saving all output views to file...")
try:                                          Saving results as .csv files for the deflection of the main
    for i in range(nr_views0):                girder and displacements and forces in the connectors for both
        view0 = views0[i]                     load cases (nr_views = 6 .csv files)
        view_name0 = view0[1]
        sv = model0.save_view_to_file(view_name=view_name0, file_type="csv")
except Exception as e:
        print(e)
```

```
print("saving model...")
s = model0.save_as(r"C:\Users\Maureen.klomp\Desktop\API\Thesis_models\Iteration\BBM_1_spring_joint_Iteration_results(0).gwb")
```

```
print("Closing model...")
model0.close()
```

Saving the model to check for errors and closing the model in order to be able to run a next analysis using the same GSA model.

```
# ========================================================================
print(' ')
print('> Read csv file(0)...')
print(' ')
df = pd.read_csv('BBM_1_spring_joint_Iteration_Connectors_Forces(0).csv', skipfooter = 20, engine='python', sep= ";", header = 16,
names = ["Elem", "Case", "Pos", "Fx", "Fy", "Fz", "Mxx", "Myy", "Mzz", "|Fyz|", "|Myz|"])

df = df.dropna()
df = df.reset_index()
```

Reading resulting .csv file for the forces in connections.

```
#For rotational stiffness (zz) of the joint with one spring a distinction was made between an end- and intermediate joint
Elem = []
Kr = []
#print(len(df.Fz))
#print(N)
for i in range(N):
    Elem0 = int(df.Elem[i])
    Elem.append(Elem0)
    if Elem[i] < 26926:
        Kr0 = (4/3) * Kser[i] * (d1**2 +d2**2) / 1000000 #kNm/rad
        Kr.append(Kr0)
    else:
        Kr0 = ((4/3) * Kser[i] * (d2**2)) / 1000000 #kNm/rad
        Kr.append(Kr0)
```

Calculating the rotational stiffness respectively for the intermediate- and end deck joint

```
rd_index_x = []
for i in range(N):
        #Random index
        rd_index0 = np.random.randint(0,N)
        rd_index_x.append(rd_index0)
        #Displacement point of end slip
        def u_slip_x(i=i):
            return R[rd_index_x[i]] * np.cos(theta[rd_index_x[i]])
        def F_slip_x(i=i):
            return u_slip_x(i) * Kslip
        def u_elastic_x(i=i):
            return u_slip_x(i) + 3
        def F_elastic_x(i=i):
            return F_slip_x(i) + 3 * Kser[i]

rd_index_y = []
for i in range(N):
        #Random index
        rd_index0 = np.random.randint(0,N)
        rd_index_y.append(rd_index0)
        #Displacement point of end slip
        def u_slip_y(i=i):
            return R[rd_index_y[i]] * np.sin(theta[rd_index_y[i]])
        def F_slip_y(i=i):
            return u_slip_y(i) * Kslip
        def u_elastic_y(i=i):
            return u_slip_y(i) + 3
        def F_elastic_y(i=i):
            return F_slip_y(i) + 3 * Kser[i]
```

Creating a list of (N) assumed load-, slip curves for both the local x- and y- direction

```
# ============================================================================
print('------------------------------------------------------------')
print('Automation of ', n, ' iterations')
print('------------------------------------------------------------')

F_x = [[]] * n                                  Repeat the same steps but now "n" times (n = number
F_x_0 = [[]] * n                                of iterations) while the stiffness properties are
u_x = [[]] * n                                  adapted depending on the previously obtained result
u_x_0 = [[]] * n                                compared to the load-, slip curve


u_star_x = [[]] * n                             u_star is the projected displacement result and K_star
K_star_x = [[]] * n                             is the secant stiffness (from the origin to the
                                                projected result on the curve)

F_y = [[]] * n
F_y_0 = [[]] *n
u_y = [[]] * n
u_y_0 = [[]] * n

MG_y = [[]] * n
MG_z = [[]] * n

df_F = [[]] * n
df_u = [[]] * n
df_MG = [[]] * n

u_star_y = [[]] * n
K_star_y = [[]] * n

for i in range(n):

    u_x_a = []
    F_x_a = []
    u_star_x_a = []
    K_star_x_a = []

    u_y_a = []
    F_y_a = []
    u_star_y_a = []
    K_star_y_a = []

    c = [[]]*n
    d = string.split()

#X  df_F[i] = pd.read_csv('BBM_1_spring_joint_Iteration_Connectors_Forces('+str(i)+').csv', skipfooter = 20, engine='python', sep=
    ";", header = 16, names = ["Elem", "Case", "Pos", "Fx", "Fy", "Fz", "Mxx", "Myy", "Mzz", "|Fyz|", "|Myz|"])
    df_F[i] = df_F[i].dropna()
    df_F[i] = df_F[i].reset_index()             Read csv file for forces in connections
    F_x_0[i] = df_F[i]['Fy'].tolist()
    df_u[i] = pd.read_csv('BBM_1_spring_joint_Iteration_Connectors_Displ('+str(i)+').csv', skipfooter = 20, engine='python', sep=
    ";", header = 14, names = ["Elem", "Case", "Pos", "Ux", "Uy", "Uz", "|U|", "Rxx", "Ryy", "Rzz", "|R|"])
    df_u[i] = df_u[i].reset_index()
    u_x_0[i] = df_u[i]['Uy'].tolist()           Read csv file for displacements in connections

    for j in range(N):
        Fx1 = float(F_x_0[i][j])
        F_x_a.append(Fx1)
    F_x[i] = F_x_a

    for j in range(N*2):
        if (j % 2) == 0:
            x1 = float(max(u_x_0[i][j+1], u_x_0[i][j]) - min(u_x_0[i][j+1], u_x_0[i][j]))
            if F_x[i][int(j/2)] > 0:
                u_x_a.append(x1)
            else:
                u_x_a.append(-x1)

    u_x[i] = u_x_a

    for j in range(N):
        if -F_slip_x(j) < F_x[i][j] < F_slip_x(j):      Check whether resulting force is in the slip- or the
            u_star_x_0 = F_x[i][j]/Kslip                embedding stage for the x- direction
            u_star_x_a.append(u_star_x_0)
        if F_x[i][j] < - F_slip_x(j):
            u_star_x_1 = ((F_x[i][j]+F_slip_x(j))/Kser[i]) - u_slip_x(j)
            u_star_x_a.append(u_star_x_1)
        if F_x[i][j] > F_slip_x(j):
            u_star_x_2 = ((F_x[i][j]-F_slip_x(j))/Kser[i]) + u_slip_x(j)
            u_star_x_a.append(u_star_x_2)

    u_star_x[i] = u_star_x_a
```

Master thesis

Hybrid interaction of timber decks in movable bridges

M. D. Klomp

Delft University of Technology